T

CR 115524

STANFORD RSL FINAL REPORT NO. 71-6

The National Aeronautics and Space Administration
Research Contract NAS9-7313

Reproduced from best available copy.

"INFRARED SPECTROMETRY STUDIES"
Final Report (C) - Phase IV

"Emittance Spectra of Selected Targets from Mission 108 Airborne Data"

Period: October 1, 1970 to September 31, 1971

R. J. P. Lyon, Principal Investigator
School of Earth Sciences
Stanford University
Stanford, California 94305

Reproduced by
NATIONAL TECHNICAL
INFORMATION SERVICE
U S Department of Commerce
Springfield VA 22151

(NASA-CR-115524) INFRARED SPECTROMETRY STUDIES. PHASE 4: EMITTANCE SPECTRA OF SELECTED TARGETS FROM MISSION 108 AIRBORNE DATA Final R.J.P. Lyon (Stanford Univ.) 31 Oct. 1971 245 p CSCL 08G G3/13

N72-21356

Unclas 23848

APR 1972
RECEIVED

October 31, 1971

REMOTE SENSING LABORATORY
SCHOOL OF EARTH SCIENCES
STANFORD UNIVERSITY • STANFORD, CALIFORNIA

STANFORD RSL FINAL REPORT NO. 71-6

The National Aeronautics and Space Administration
Research Contract NAS9-7313

"Infrared Spectrometry Studies"
Final Report (C) - Phase IV

"SPECTRAL DATA FROM FLIGHTS 1 AND 3, MISSION 108"

Period: October 1, 1970 to September 30, 1971

The Phase IV Final Report is composed of three sections

(A) Software (Computer Programming) - RSL 71-2
(B) Digital Data Acquisition System - RSL 71-3
(C) Spectral Data from Flights 1 and 3, Mission 108 RSL 71-6

The report covers the last twelve month period of the contract. The research was supported also by equipment provided by a Facilities Contract from NASA/Ames Research Center NAS2-3402(F). These supports are gratefully acknowledged.

The three latest published papers, resulting from these studies are also reproduced in the Appendix of this Report.

Details of illustrations in this document may be better studied on microfiche

R. J. P. Lyon
Principal Investigator

October 31, 1971

TABLE OF CONTENTS

		Page No.
I.	INTRODUCTION	1
II.	OBJECTIVES	2
III.	RESULTS	2
	A. Summary	2
	B. Task 3.2 Final Evaluation of Aircraft Feasibility Experiments	4
	C. Task 3.3 Completion of Digital Data System	6
	D. Task 3.4 Collection of Field IR Spectra of Rock Types	6
IV.	MISSION 108 REPORT: AIRBORNE INFRARED SPECTRAL STUDY OF TEST SITES NO. 2 (PISGAH), AND NO. 22 (TONOPAH-CROWN SPRINGS)	11
	A. General Information	12
	B. Flight Records	12
	C. Data Analysis Steps	14
	1. Spectral Location	14
	2. Spectral Pre-processing	15
	3. Elimination of Noisy Spectra	19
	D. Stepwise Discriminant Analysis (BMDO7M)	21
	1. Training Group Selection	21
	2. BMDO7M-Results	26
	E. Color-Coding of Spectra Using I^2S Digicol Additive Viewer	45
	F. Direct Comparison of Spectral Groups with Emittance-Ratio Imagery	45
	1. Concept of Emittance-Ratio Imagery	45
	2. "Science" Manuscript	46
	3. Problem Areas	46
	G. Spectral Files	47
V.	DELIVERABLE ITEMS	105
	A (4.1) Report on Feasibility Study	105
	B (4.2) Technical Report on MSC Aircraft Mission	105
	C (4.3) Library Spectra Geological Materials	105
	D (4.4) Final Summary Report	105

Page No.

APPENDICIES

A.1	Calibration Steps	A1-0 to POLY 30B
A.2	Computed Spectral Groups from MX108, Flights 1 and 3 (October 8-10, 1969)	A2-1 to A2-104
B.1	7th Symposium Abstract (RSL 71-4)	B1
B.2	IEEE Paper	B2-131 to B2-138
B.3	Science Paper (RSL 71-5)	B3-1 to B3-12

STANFORD RSL TECHNICAL REPORT SERIES

67-1 "Field Infrared Analysis of Terrain-Spectral Correlation Program" Part I (by R.J.P. Lyon)

67-2 "Field Infrared Analysis of Terrain-Spectral Correlation Program" Part II and Part III (by R.J.P. Lyon)

67-3 "Statistical Analysis of IR Spectra--Stanford Programs Applied to USGS Spectra in Tech Letter #13" (by R.J.P. Lyon)

67-4 "Computer Reduction and Analysis of an Infrared Image" (by Keenan Lee)

68-1 "Infrared Exploration for Coastal and Shoreline Springs" (by Keenan Lee)

68-2 "Re-evaluation of the Normative Minerals of Sonora Pass Rock Standards-University of Nevada Reports #7 and #12" (by Attila Kilinc)

68-3 "Nearest Neighbor--A New Non-parametric Test Used for Classifying Spectral Data" (by Paul Switzer)

68-4 Final Report "Field Analysis of Terrain"--NGR-05-020-115 (contains all the drawings and logic diagrams for Stanford CVF Spectrometer and Digital Data Recording System (by R.J.P. Lyon)

69-1 "Mission 78--Flights 1 and 2 Ninety-Day Report" (by R.J.P. Lyon)

69-2 "Quantitative Geological Analysis of Multiband Photography from the Mono Craters Area, California" (by G.I. Ballew)

69-3 "The Stanford Infrared Spectra Processing Package" (by John Moore with subsequent modifications by Michael Heathman)

69-4 "Thermal Dynamics at the Earth-Air Interface: The Implications for Remote Sensing of the Geologic Environment" (by Rossman Smith)

69-5 "Infrared Spectrometry Studies: Final Report Phase I" (by R.J.P. Lyon)

69-6 "Infrared Spectrometry Studies: Final Report Phase II" (by R. J. P. Lyon and Attila Kilinc)

69-7 "Infrared Exploration for Shoreline Springs at Mono Lake, California, Test Site" (by Keenan Lee)

70-1 "Detailed Ground Study of 8-13 μm Infrared Imagery, Carrizo Plains, California" (by R. Campbell, Jr., L. D. Hoover and F. Querol-Suñé)

70-2 "Terms in Geologic Remote Sensing: A Condensed Glossary" (by R. J. P. Lyon)

70-3 "Geologic Interpretation of Airborne Infrared Thermal Imagery of Goldfield, Nevada" (by I. A. Kilinc and R. J. P. Lyon)

70-4 "Surface Heat Flow Studies for Remote Sensing of Geothermal Resources" (by H. Hase, Geological Survey of Japan)

70-5 "Geophysical Analysis of Thermal Infrared Imagery near Goldfield Nevada: Experimental and Correlation Analysis" (by W. B. Ervine)

70-6 "The Multiband Approach to Geologic Mapping from Orbiting Satellites: Is it Redundant or Vital?" (by R. J. P. Lyon), now published in Remote Sensing of Environment, 1, (4), 237-244

70-7 "Airborne Geological Mapping Using Infrared Emission Spectra" (by R. J. P. Lyon and J. Patterson), now published in Proc. of the 6th Symposium on Remote Sensing of Environment, 1, 527-552

70-8 "Pseudo-Radar: Very High Contrast Aerial Photography at Low Sun Angles" (by R. J. P. Lyon, Jose Mercado and Robert Campbell, Jr.), now published in Photogrammetric Engineering, 36, (12), 1257-1261

70-9 "Remote Sensing in Exploration for Mineral Deposits" (by R. J. P. Lyon and Keenan Lee), now published in Economic Geology, 65, 785-800

70-10 "Phenomena and Properties of Geologic Materials Affecting Microwaves - A Review" (by D. Oberste-Lehn)

70-11 "1969/70 Stanford Spectral Data Management System" (by Michael Heathman)

71-1 "Operational Calibration of an Airborne Infrared Spectrometer Over Geologically-Significant Terrains", (by R. J. P. Lyon and A. A. Marshall)

71-2 "1970/71 Stanford Spectral Data Management Programs" (by A. A. Marshall) Final Report (A) -- Phase IV (Software - Computer Programming).

71-3 "Stanford Digital Data System." Final Report (B) -- Phase IV.

71-4 "Comparison of Airborne Infrared Spectral Emittance and Radar Scatterometer Data from Pisgah Crater Lava Flows," (Abstr.) Paper presented at 7th Int. Symp. on Rem. Sens. of Environ., Ann Arbor, Mich., May 17, 1971.

71-5 "Infrared Spectral Emittance in Geological Mapping: Airborne Spectrometer Data from Pisgah Crater, California." Paper submitted to Science, August 1971. pp. 14.

71-6 "Spectral Data from Flights 1 and 3, Mission 108." Final Report (C) -- Phase IV (IR Spectral Emittance Data - Airborne).

I. INTRODUCTION

Under the general title of "Supporting Research and Technology Effort in Identification of Geological Materials by Remote Infrared Spectroscopy" the Remote Sensing Laboratory of School of Earth Sciences, Stanford University, has been carrying out infrared (IR) radiance measurements from geological materials. These involve laboratory and field spectroscopic measurements both on the ground and airborne. The net result of this work is a proven, feasible system for airborne use over terrains with minimal vegetation. The perturbing effect of a long atmospheric path has not been proven and this may be a great barrier to successful spacecraft usage. This in no way detracts from its highly successful operation from altitudes of several thousand feet.

In recent months parallel studies at University of Michigan based directly upon results of this work, but operating with image-forming airborne scanners, have shown that the spectral emittance concepts can be utilized in emittance-ratio imagery which broadly depicts the silicate composition of the terrain. This forms a fitting conclusion to the studies as the imaging mode of data presentation is much more meaningful to geological users. In addition the possibilities of analog processing the multichannel-imaged data are most attractive both in ease of data handling and cost. Considerable savings of time and funds can be made providing the requisite spectral resolution can be retained. A trade off exists between signal-to-noise (S/N) ratio and the spectral bandpass of each channel and channels which are too wide sacrifice spectral discrimination for high S/N ratios.

These aspects are explored in greater detail in the three publications included herein as Appendices.

II. OBJECTIVES

Stanford University proposed three main objectives in the concluding phases of this study effort,

A. To make a final evaluation of the aircraft feasibility experiments

B. To complete the digital data system for the ground mobile IR System

and C. To collect (in the field) IR spectra of rock types.

The central theses of the study have been that surface material compositions could be deduced from infrared emittance measurements, and that the spectra from various rock and soil types, as delineated by field geological mapping, were sufficiently different from each other as to make statistically significant populations. To explore the latter point ground measurements are necessary to define the optimum differentiation of materials before these data are perturbed by the atmospheric column, as when seen from high altitude aircraft or spacecraft. All these three tasks were continuing efforts commenced in earlier phases of the study. Stanford personnel, being principally geologists, have always been worried about the geological homogeneity of the terrains being overflown, and thus great emphasis was placed on the collection of field spectra under (geologically) controlled conditions.

III. RESULTS

A. Summary

Successful achievement of the objectives was attained in a majority sense, although severe and crippling problems in the spectrometer-data system linkage precluded much field work. This was a bitter disappointment but increased attention was directed to evaluation of the airborne data from

Mission 108. Several weeks of "field operations" were achieved however, gathering spectra of selected rock specimens, but by operating without the data system, the data have had to be hand reduced--a very tedious process.

The highlights of the work, however, have shown the great practicality of the airborne data. Two papers have been published (and one more is in press) relating airborne data to field operations. The titles are

1. "Airborne Geological Mapping using Infrared Emission Spectra: I", (R. J. P. Lyon and J. Patterson). Proc. 6th Symp. Remote Sensing of Environ., Ann Arbor, Mich., 1970, p. 527-550.
2. "Operational Calibration of an Airborne Infrared Spectrometer and Geologically Significant Terrains", (R. J. P. Lyon and A. A. Marshall) I. E. E. E. Transactions on Geoscience Electronics, Vol. GE-9(3), July 1971, 131-138.
3. "Infrared Spectral Emittance in Geological Mapping: Airborne Spectrometer Data from Pisgah Crater, California", (R. J. P. Lyon) submitted to Science, Aug. 28, 1971, pp. 12.

In addition, a fourth paper entitled "Comparison of Airborne Infrared Spectral Emittance and Radar Scatterometer Data from Pisgah Crater Lava Flows" was presented at the Seventh International Symposium in Remote Sensing of Environment. This paper reported the use of a color-bar generation system (Digicol-I^2S) to generate a given color for each input IR spectrum. Prior to this stage of the analysis, the BMDO7M stepwise discrimination program was used to identify the 3 wavelengths for best "separation" of the materials. These 3 radiance levels were quantized into 16-level steps, and used to pre-set the 16-level matricies for the red, blue and green color guns of a color TV monitor. The unit could handle 16 such matricies at once as vertical color bars across the TV tube. The

eye then could rapidly identify similarities and contrasts in the data sets. Due to the familiar problems (plates, costs, etc.) in color reproduction the paper was not printed in a final form for that Symposium volume, but the techniques remain an interesting way to compare spectral (line-trace) data. The key comparison was made with the presentation of scatterometer data (5th Symposium volume) by the University of Kansas group, and the contrasts of skin depth in the information identified (See the Abstract in the Appendix B).

B. Task 3.2 Final Evaluation of Aircraft Feasibility Experiments

Several aspects of this Task were completed and the material presented in publications. The most complete discussion to date is that published in the Sixth Symposium Volume of Remote Sensing of Environment (1970), pages 527-550, dealing with Mission 78 flight data. Although Mission 108 was plagued with malfunctions of all types over the Nevada target areas (Sites No. 22 and 75) success was achieved in evaluating the four flight lines of Day 1, over Site No. 2 (Pisgah Crater, Calif.). Publication No. 2 (above, presented in the Geoscience Electronics issue of IEEE, July 1971) contains a very complete account of the operational calibration steps and results for that mission. The excellent recovery of data and its subsequent good correlation with the ground geology has been one of the high points of the feasibility study. Positional recovery was possible to a few feet for each spectrum and similarity between spectra taken over the same materials is clear. The data taken more specifically over the geological targets themselves were used in Publication No. 3 which has been submitted to Science magazine for consideration and publication (See Appendix B).

The combination of these papers may be used to show that feasibility of the method has been proven. We have not had the opportunity yet for a higher altitude (RB57) flight to assess the effects of a longer airpath

although a detailed request for such a flight was submitted as part of our SKYLAB proposal (SU/UN-SO-191). In addition the P3 aircraft was not available during most of the study period, either due to down time for installation and wing repair, or to prior scheduling (or scheduling changes). Accordingly we were not able to perform any more Padre Island flights. The success of Mission 108 data over Pisgah Crater site, however, makes the detailed testing of Padre Island somewhat redundant, particularly as the noise levels (a problem area) in the Pisgah data are so low in the MX108 tapes.

The Mission 108 data are treated in greater detail in Section IV and the spectral curves appear in the Appendicies both as the original computer output (A) and in (B) in condensed form in Publication No. 4 (RSL71-5).

Shortage both of funding and time have precluded much more field evaluation. It is clear that the geological mapping system works, that it can define geological materials, but nagging details of precise correlations with rock species remain. Whether it is worthwhile (i.e. cost-effective) to chase these details further is quite debatable. Clearly future engineering research and development (R and D) effort should be devoted to the RB57 flight, although further scientific research on the geological-infrared emittance aspects would dictate a more careful analysis even of existing flight records.

C. Task 3.3 Completion of Digital Data System

A detailed report on the design integration and testing results of the Stanford Spectral Digital Data Acquisition System has been prepared under separate cover as Final Report (B) - Phase IV. This is RSL Technical Report 71-3, written by the Research Geophysicist, Lee Lu, a graduate in the Geophysics Department at Stanford. Lee has succeeded with a redesign of the system and tapes can now be made with this system which are compatible with the IBM 360-67 computer at Stanford.

The system is a 10-bit A/D unit in which each "word" has a leading identification-time block (ID) followed by formated data from the spectrometer and radiometer (interleaved), processed upon encoder commands from the spectrometer itself. (This external clock A/D aspect caused considerable problems with premature noise spikes but has now been made less sensitive with the new design.) Upon receipt of the completed spectrum the 6 additional channels of meteorological data (solar input, wind, soil temperature, etc.) are multiplexed in, and the digital computer word completed for tape read-in.

Complete schematics and output-results from the unit appear in the referenced report. Photographs of the unit in operation appear in Figs. 1-6 attached.

D. Task 3.4 Collection of Field IR Spectra of Rock Types

Considerable difficulty was experienced in the field collection of data. A decision was made to wait for completion of the data system before renting the Exotech 10 Spectrometer to gather field data. This proved to be a mistake as the digital system was only completed immediately in May, just prior to the end of the project funding. We did get the spectrometer and recorded field spectra in May using X-Y recorders and an

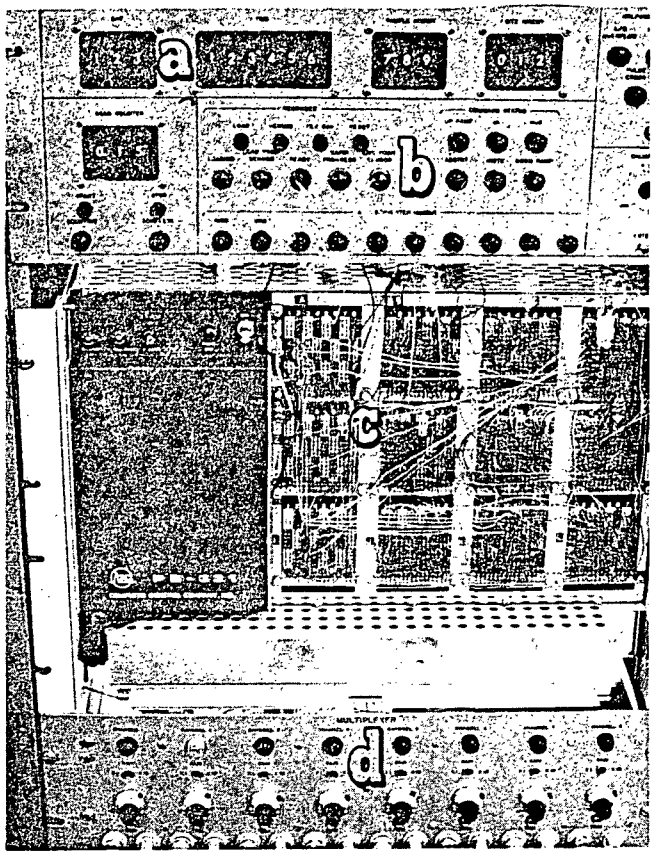

Fig. 1

Digital Data System showing:

A. Input for ID
B. Status lights
C. Wiring Board
D. Input and monitor channels (8 pairs)
   1. Spectrometer
   2. Radiometer
   3-8. Met. data

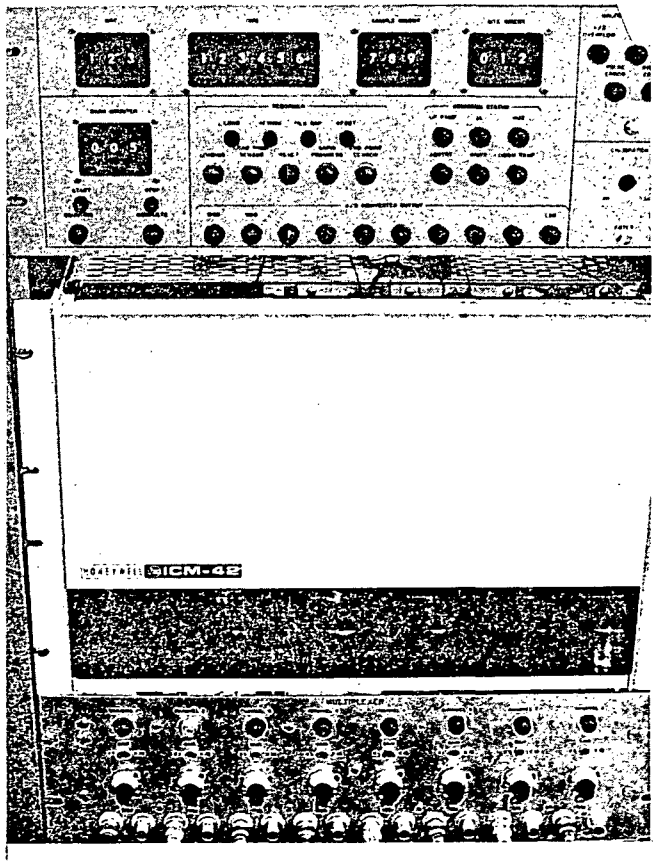

Fig. 2

Same with cover added. Notice status lights are different.

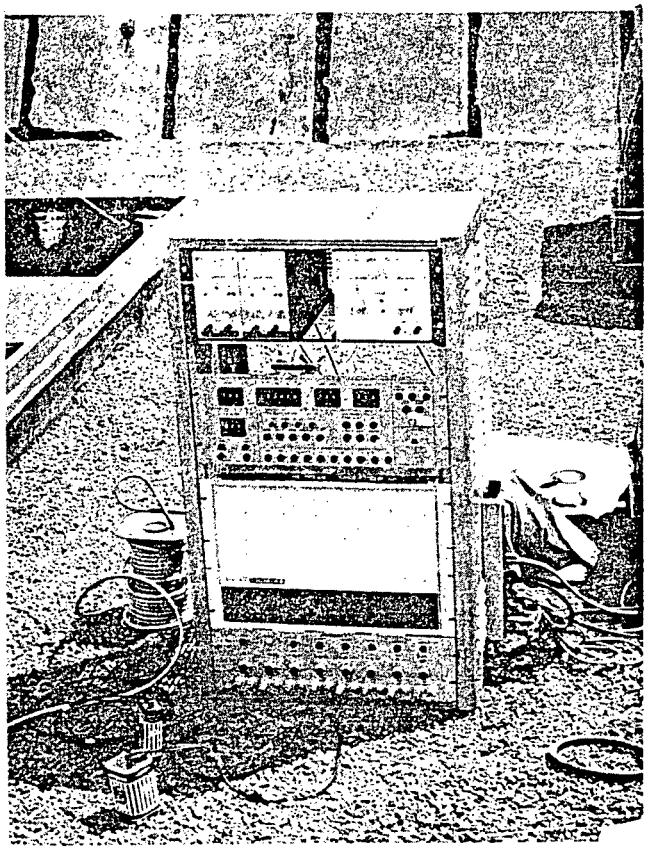

Fig. 3.

Data system operating on roof of Earth Science Lab. Digital recorder is hidden at rear.

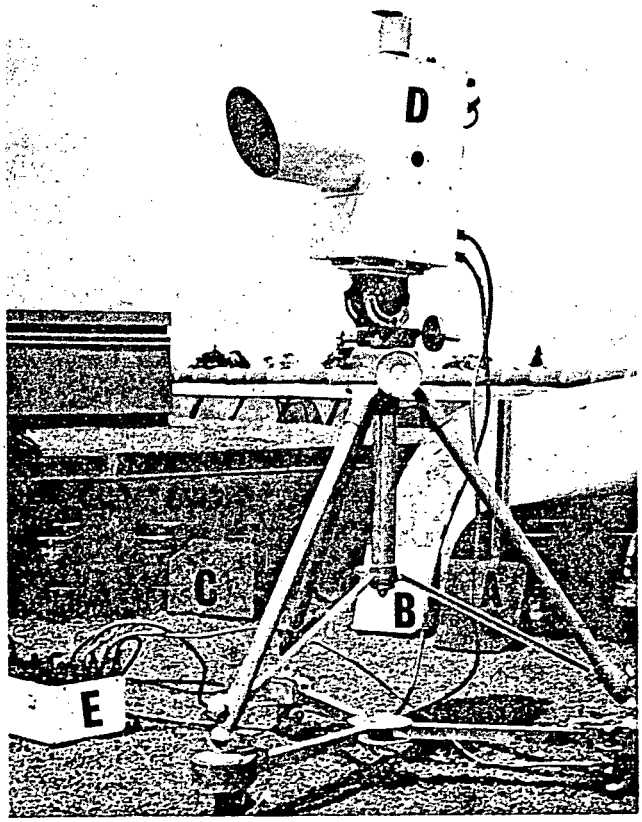

Fig. 4

Exotech Model 10 Spectroradiometer. Note polished rock slabs at rear for study.

Rock A - Std. Gabbro
B - Std. Quartz Diorite
C - Red granite

Optical Head - D
Electronic Box - E

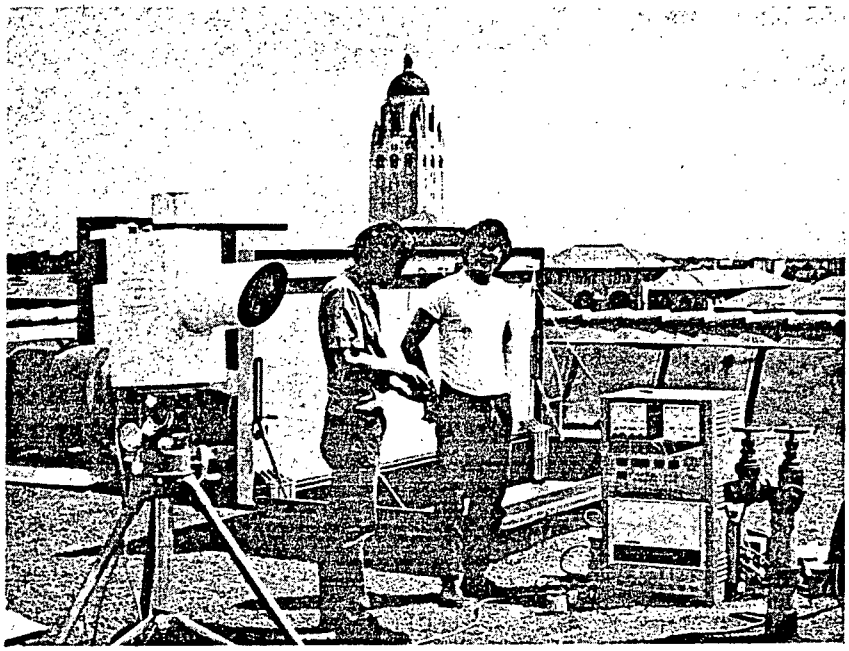

Fig. 5

System operating on roof taking sky spectra (near horizon

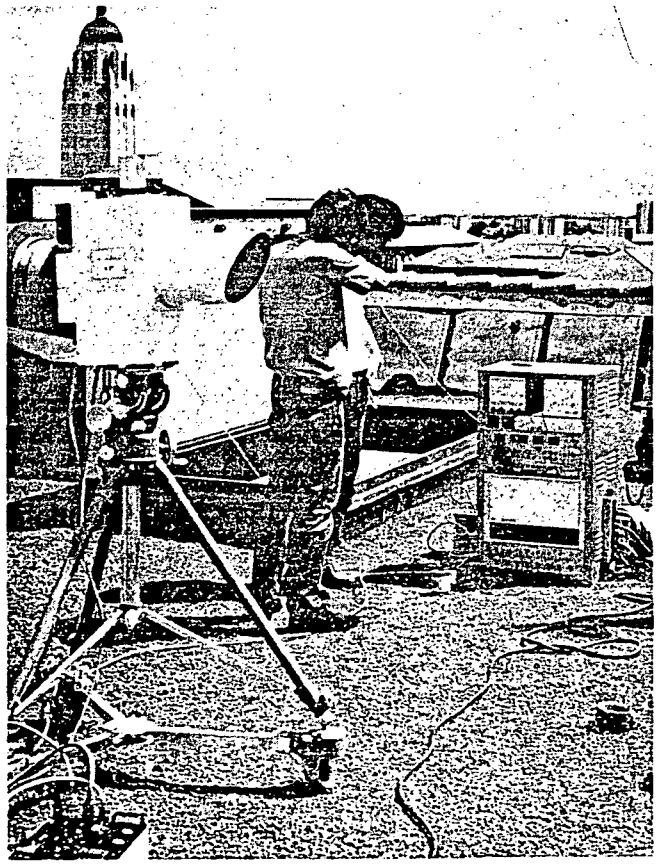

Fig. 6

Similar view. System counts up to a pre-set number of spectra and cuts off.

X-T recorder. These ground spectral sets, which number 25, were obtained at Stanford, with the total experiment set up outside the buildings, using field-collected samples from many sources in the western U.S.A. Because repetitive spectra on an X-Y record are superimposed we took the mean curve from the record and hand-digitized the curve at discrete intervals. After a few curves, we realized the magnitude of the task, and as we were in the final month of the project, left the completion of this task to concentrate our efforts on the aircraft spectra. The X-Y (and X-T) records must be digitized and corrected for (a) the optical functions of the Exotech unit, (b) the difference in target radiance and (ambient) blackbody internal reference. The original curves can be provided, if required, but obviously they are less useful than fully reduced data.

IV. MISSION 108 REPORT: AIRBORNE INFRARED SPECTRAL STUDY OF TEST SITES NO. 2 (PISGAH) AND NO. 22 (TONOPAH-CROW SPRINGS).

Sub-Table of Contents

A. General Introduction

B. Flight Records

C. Data Analysis Steps

1. Spectral Locations
2. Spectral Preprocessing
3. Elimination of Noisy Spectra

D. Stepwise Discriminant Analysis (BMDO7M)

1. Training Group Selection
2. BMDO7M - Results

E. Color-coding of Spectra using I^2S-Digicol Additive Color Unit

F. Direct Comparison of Spectral Groups with Emittance-Ratio Imagery

1. Concept of Emittance-Ratio Imagery
2. "Science" Manuscript
3. Problem Areas

G. Spectral files

A. General Introduction

Most of the results of Mission 108, Flights 1 and 3 have been prepared as two papers for publication. The raw data output has been preserved in tabular and graphical form in Appendix A herein, and the reduced results (normalized spectral emittance curves) are included in the rear of this section of the Report. The calibration steps which were published as a RSL paper (71-1) in IEEE Geoscience Transactions are included in the first part of Appendix A.

The readers' course of action should be, therefore, to read,

a. The "IEEE" paper (71-1) for the detailed calibration steps (see Appendix B2)

b. The "Science" paper (71-5) for the results of the flight analysis over the alluvial sands and lavas of Pisgah Crater and Lavic Lake (see Appendix B3)

c. Computer processing in greater detail in Tech. Report 71-2, as a separate report (Final Report IV (A)).

d. General background in the paper (70-7) in 6th Int. Symp. on Remote Sensing of Environ., Ann Arbor, Mich., p. 527-551 (1970), reproduced in Final Report III.

B. Flight Records

The flight records in the "Screening and Indexing Report - Mission 108, Oct. 8-10, 1969" are very brief, and have been included herein (following four pages, Tables Ia-b and IIa-b.

The selected data times used for calculation of the calibrations have been tabulated in Table III along with the statistics of the reduced data. The original spectral curves and tabulated details have been included as Appendix A1.

TABLE Ia

MISSION 108/SITE 2

FLIGHT 1

SENSOR COVERAGE PLOT LOG

MISSION	108/2		DATE	October 8, 1969	NOTES
SENSOR		RC-8/1			Twenty-percent overlap.
FILM		2402 Plus X			The RC-8 camera mounts were pinned down.
FILTER		AV W-15			
ROLL NO.		1			

LINE	RUN	ALT.	FRAMES	REMARKS
19	1	2000 ft	6386 6396	Calibration run over Lake Palmdale, Palmdale, Calif.
17	1	2000 ft	6398 6423	Pisgah Crater and Lavic Lake, California; heading 160°.
18	1	2000 ft	6424 6437	Lavic Lake, Calif.
18	2	2000 ft	6438 6454	
17	2	2000 ft	6455 6480	Heading 340°.
20	1	2000 ft	6481 6490	East of Lavic Lake, Calif.; the location is approximate.
20	2	2000 ft	6491 6497	
			6500 6514	Extra frames over Stanford University.

Palmdale
1701
1801
1802
1702
Shallow lake

-12A-
19

TABLE Ib

INFRARED SCANNER
IN-FLIGHT LOG

DATE: October 8, 1969
MISSION: 108/2
FLIGHT: 1

OPERATOR: C. Kenreck — Roll 1

SITE	LINE	RUN	TIME START	TIME STOP	GAIN CH-1	GAIN CH-2	Ground speed, knots	Radar alt, ft	OUTSIDE AIR °C		RS-14 SPATIAL RESOLUTION CH-1 mrad	RS-14 SPATIAL RESOLUTION CH-2 mrad	FILTER 3-5.5	FILTER 7-9	FILTER 9-13	FILTER 8-14	CAL TEMP IR-1	CAL TEMP IR-2	CAL TEMP UV	MARK V	REMARKS
2	19	1	17:12:00	17:13:30	6.0	6.0	180	2000	23		3	3	X			X	500	000		1	Added run. 3 mrad channel number 2. Tape reel number 1.
2	17	1	18:49:40	18:53:15	5.0	6.0	180	2000	25		3	3	X			X	193	000		2	No direct imagery.
2	18	1	18:56:40	18:58:34	5.5	6.5	180	2000	25		3	3	X			X	193	000		3	No direct imagery.
2	18	2	19:00:30	19:02:53	5.5	6.5	180	2000	25		3	3	X			X	193	000		4	No direct imagery.
2	17	2	19:06:10	19:09:45	5.5	6.5	180	2000	25		3	3	X			X	193	000		5	No direct imagery.
2	20	1	19:15:35	19:17:00	5.5	6.5	180	2000	27		3	3	X			X	193	000		6	No direct imagery.
2	20	2	19:18:38	19:19:36	5.5	6.5	180	2000	27		3	3	X			X	193	000		7	No direct imagery.

Palmdale
1701
1801
1802
1702
Shallow lake

-128-
20

MX 108/2
FLIGHT 1

TABLE IIa

MISSION 108/SITE 22

FLIGHT 3

SENSOR COVERAGE PLOT LOG

MISSION 108/22					DATE October 10, 1969						NOTES
SENSOR		RC-8/1	RC-8/2	—							Twenty-percent overlap on RC-8/1. The RC-8/1 camera clock malfunctioned.
FILM		2402	SO-117								
FILTER		AV W-15	(a)								
ROLL NO.		1	1								
LINE	RUN	ALT.	FRAMES	FRAMES	FRAMES	FRAMES	FRAMES	FRAMES	FRAMES	FRAMES	REMARKS
9	1	2000 ft	6517 6529	1565 1587							Mining area northwest of Tonopah, Nevada.
9	2	2000 ft	6530 6546								
9	3	2000 ft	6547 6565								
9	4	5000 ft	6566 6576	1589 1604							
9	5	5000 ft	6577 6586								
10	1	2000 ft	6587 6595								Mining area south of Tonopah, Nevada.
10	2	2000 ft	6596 6604								
			Roll 2								
10	4	2000 ft	6607 6614								
4	2	2000 ft	6615 6646								Calibration run over Mono Lake, California.

[a] The RC-8/2 camera has three filters, the 4600, cc 20 M, and W-15.

Mono ? 401

Mono 402

TABLE II b

MX 108/22

FLIGHT 3

INFRARED SCANNER
IN-FLIGHT LOG

DATE: October 10, 1969

MISSION: 108/22

FLIGHT: 3

OPERATOR: G. Kenreck — Roll 1

RS-14

SITE	LINE	RUN	TIME START	TIME STOP	GAIN CH-1	GAIN CH-2	Ground speed, knots	Radar alt, ft	OUTSIDE AIR °C		SPATIAL RESOLUTION CH-1 mrad	SPATIAL RESOLUTION CH-2 mrad	FILTER 2-5.6	FILTER 7-9	FILTER 9-12.5	FILTER 8-14	CAL IR-1	TEMP IR-2	TEMP UV	MARK ∇	REMARKS
22	9	1	17:05:35	17:07:33	8.0	8.0	160	2000	10		3	3	X			X	650	050		1	A 15-second late start.
22	9	2	17:13:00	17:15:35	8.0	8.0	160	2000	10		3	3	X			X	650	050		2	A 15-second late start.
22	9	3	17:21:20	17:24:05	8.0	8.0	160	2000	9		3	3	X			X	650	050		3	No direct imagery.
22	9	4	17:29:15	17:31:50	8.0	8.0	190	5000	4		3	3	X			X	650	050		4	No direct imagery.
22	9	5	17:35:40	17:38:45	8.0	8.0	180	5000	5		3	3	X			X	650	050		5	No direct imagery.
22	10	1	17:50:25	17:52:00	8.0	8.0	180	2000	9		3	3	X			X	650	050		6	Tape change. Reel number 6.
22	10	2	17:56:30	17:58:00	8.0	8.0	180	2000	9		3	3	X			X	650	050		7	No direct imagery.
22	10	3	18:03:45	18:05:00	8.0	8.0	180	2000	9		3	3	X			X	650	000		8	Abort.
22	10	4	18:09:20	18:10:40	8.0	8.0	180	2000	9		3	3	X			X	650	000		1	No direct imagery.

-120-

22

TABLE III

Tabulated Reduced Data

A. Stanford/MSC Mission-108, Flight 1 (Pisgah, Site 2), Oct. 8, 1969

GMT Time		N	Signal Mean (MV)	Std. Deviation* (MV)	Rel. Error**	Temperature by Spectrometer
	PRE-FLIGHT					
1518	40°C EXT BB	22	669	13	0.0043	40°C***
1516	Rock A	30	569	15	0.0048	43
1517	Rock B	30	595	15	0.0046	42
	IN-FLIGHT					
1712	Palmdale Lake	30	1010	15	0.0027	30°C
1915	Shallow Lake	30	1000	18	0.0033	30
	POST-FLIGHT					
2121	40°C EXT BB	25	693	19	0.0055	39°C
2120	Rock A	36	512	22	0.0072	45
2120	Rock B	28	568	24	0.0080	43

B. Stanford/MSC Mission-108, Flight 3 (Mono, Site 3), Oct. 10, 1969

GMT Time		N	Signal Mean (MV)	Std. Deviation (MV)	Rel. Error	Temperature by Spectrometer
	PRE-FLIGHT					
1423	40°C EXT BB	30	664	16	0.0042	40°C***
1422	Rock A	30	569	15	0.0048	43
1423	Rock B	30	593	15	0.0046	42
	IN-FLIGHT					
1642	Mono Lake Run 401	30	987	19	0.0034	30°C
1943	Mono Lake Run 402	30	1080	17	0.0029	27

* Standard Deviation (σ) is defined as

$$\sigma = \sqrt{\frac{(X-\bar{X})^2}{N-1}}$$

** Relative Error is defined as

$$E = \frac{\sigma}{\bar{X}.\sqrt{N}}$$

*** By definition, and used as a calibration point for temperature

C. Data Analysis Steps

1. Spectral Locations

(1) The RC-8 B/W films are inspected to locate (a) the priority of flight line study and (b) the few specific flight lines (of the many flown) on which detailed study will be made. Line segments are identified directly on the films (by pin scratches or by wax pencil) outlining areas of presumed homogeneity in the target. This analysis may be made from low altitude photographs or from prior geological experience in the area.

(2) Times for the RC-8 photo centers are obtained both (a) from the ADAS-head codes on the frame edge and (b) from the computer-generated listing of photo-"times". The RC-8 systems may (or may not) show an electrical pulse for actual shutter closure relative to the (earlier) intervalometer pulse itself--time differences up to 400 msec may occur here.

The (a) and (b) times should agree within 10 msec (aircraft moves 300 ft/sec).

(3) The B/W 35 mm boresight films are then selected to match the flight-lines on the RC-8 films, and B/S photo centers identified (by scratching diagonals) on every fifth frame. These centers are transferred to the RC-8 films by optically matching the images. The centers (or every fifth one) are pricked through to mark the flight line onto the RC-8 film. B/S frames are numbered (by hand, unless the data block is readable).

(4) Times for the B/S photo centers are compared (a) by identifying specific features (lakeshores, roads, canals, trails, rock outcrops, etc. on both the RC-8 and B/S films, and (b) by counting frame sequences off from the computer-generated listings.

(5) Times of characteristic events (line starts and stops, and roads, lakes, etc.), which have temperature changes can be independently derived from the analog paper traces of radiometer (or spectrometer) output and the IRIG timing pulses. From these events the B/S frame times can be

checked and from these then the RC-8 frames. (Timing was found to be accurate enough that a time difference may be seen between the RC-8 camera at the rear of the P3 and the B/S camera on the front. Near-coincidence of RC-8 and B/S photo centers will show a time difference roughly that of the aircraft length x velocity). However, marked divergences in timing also are present and caution should be exercised at all times. Non-imaging (numerical) radiance data can only be referenced to geological materials if the timing is correctly determined. The computer has no idea from where its data are derived.

(6) Perhaps the most useful data base of all is the analog paper trace which contains the IRIG timing, spectrometer and radiometer outputs, and the (intervalometer) pulse of the RC-8 and B/S shutter closure pulses. Detailed inspection of these records, together with viewing of the digitized equivalents settle many questions in specific event timings. In addition the standard deviation (variability) of the data can be reviewed by inspecting the curve shapes over the line segment being analyzed. Noisy data can be eliminated at this stage.

(7) Only after all these steps have been covered are you ready to commence the computer search for the stop- and start-times.

2. Spectral Pre-processing

(1) Using the start- and stop-times selected to cover the area, sub-areas or groups are determined which contain multiples of 20-40 spectra. A lower number does not allow any rejection of spectra in later processing, and hence retention of valid statistics for the sub-area. Greater than 40 spectra in a group averages too-divergent materials and lowers the geological sensitivity of the technique. Purely for processing ease only up-ramp (or down-ramp) spectra are used, that is every second spectrum is analyzed (RSL 69-1, p. 8).

(2) The spectra are read sequentially into the computer, and the 9 radiometer readings for each spectrum calculated to show RAD (LOW), RAD (HIGH), RAD (AVER) and DEL (RAD). Those spectra for which the DEL (RAD) exceeds the equivalent of 1° C are flagged and discarded from further processing (see page A of each spectral group listing in the Appendix A). The millivolt equivalent of this 1° C range is determined each day from the pre-flight radiometer calibrations. Key data points are the pre-flight logs, which (a) state the observed voltage from observing an external blackbody target at a fixed temperature (T_1) and (b) the specific temperature at which the internal blackbody reference (T_2) has been set for that day's operations. Similar calculations are made for the spectrometer calibrations, and both sets are repeated in post-flight calibration steps. Clearly the millivolt output/^{o}C should not change markedly for the same T_1 and T_2 values.

(3) For the remaining spectra in the group the Counter Point (CP) data values are averaged (AVER SPECTRUM) and standard deviation (S.D.) and REL ERROR (coefficient of variation) calculated for each CP and for the spectrum as a whole. For the whole group the mean radiance level ($\overline{R}$ in mV) can be equated to a brightness temperature, which over water for example, closely approximates the true surface temperature. The S.D. millivolt level can be used to express "noise" and approximates the RMS noise read in the aircraft (with the CVF wheel stopped) during flight. Again over water the RMS noise will be at a minimum value, and if the total aircraft system is functioning well, will closely approximate the S.D. of the data if the CVF wheel is turned on again. Table IV lists typical flight data over Mono Lake, Flight 3, which is large enough to secure both measurements consecutively.

TABLE IV

RMS Noise Measurements and S. D. of Lake Spectra

Time (GMT)	RMS (mV)	S. D. (mV)	
	a. Mono Lake, MX108, Flight 3, 10/10/69		
1642	24	19	(in-flight)
1943	24	17	(in-flight)
	b. Preflight, MX108, Flight 1, 10/8/69		
1517	20	15	(ground)
	c. In-flight, MX108, Flight 1, 10/8/69		
1915	25	18	(in-flight)

Listing of raw data (mV) and S. D. (mV) are made (see Sheet B in the Appendix A files).

Plots of raw data (Sheet C) and S. D. (Sheet D) are prepared for the group of spectra from that sub-area.

(4) A suitably-nearby lake or other water body is overflown both before and after the flight lines at the target. Spectral groupings from these water sub-areas are processed, as in (2) and (3) above, and used to develop "airborne blackbody spectra". This is based on the known (and high) emittance character of water by which radiance levels can be measured with the spectrometer in flight. (For further details see Ref. RSL 71-1, page 132, or RSL 69-1, 90 Day Report, MX 78, page 12.)

(5) Provided the S. D. level is acceptable, and that sufficient spectra remain to be statistically significant, then the raw data are divided by the airborne blackbody (the lake sub-area) to give spectral "emittance" values. To be correctly termed emittance the data should be recalculated from "observed millivolts" back to radiance in milliwatts/cm^2/ster, taking into account the (higher) T_2 level of the internal blackbody reference and the

target (T_1) temperature. As a short cut in calculations the "emittance" data from step 5 are simply inverted (FLIPPED) to compensate for the higher reference level. For greater detail see reference (IEEE). RSL 71-1 in Appendix B2, pages 133-4.

(6) The inverted emittance spectra are smoothed with a 9-point, high-level, smoothing routine (see RSL 69-1, p. 44) to lower their standard deviation. This particular routine was selected so as to minimize the peak shifting (common to most smoothing programs).

(7) Analysis of previous flight data has shown that about 18 data points may be removed off each end of the CVF spectrum (Table V), as the information contained therein is primarily that of the atmosphere between the ground and the target. This is further reinforced by inspection of the S. D. of the raw data spectrum (Sheet D) which always shows lower S. D. values in these bands, regardless of the style of target being overflow. Such consistency could only come from the greater opacity (smaller optical thickness) of the atmospheric path to the ground in those bands. The AIRPATH absorption ratio also has a higher value over these bands (see RSL 71-1, Appendix B2).

TABLE V

Data Points Clipped from the Spectra

Short Wavelength End		Long Wavelength End	
Cp No. 91-109	6.67-7.955 μm	Cp No. 161-178	12.12-13.285 μm

Remaining Data Band

Cp No. 110-160 8.105-12.04 μm

(8) The smoothed, ratioed inverted and clipped spectra are further transformed by setting their emittance mean $\bar{X}_\epsilon = 0.0$ and the standard deviation = 1.0. The transform prepares the group mean spectra for direct comparison in subsequent analytical (discriminant) programs. The spectral

curves from Mission 108, Flights 1 and 3 have been assembled in the following tables and figures. Each set of one table and one figure (labelled as sheets E and F) are derived from the sub-area groupings of Appendix B (Sheets A-D, respectively). These final 2 sheets of normalized spectra are the basic material for geological analysis of the flight line.

3. Elimination of Noisy Spectra

Noisy spectra are ones in which the usual, open smooth curves are replaced by numerous spiked values deviating markedly from the mean. These may be due to a variety of causes. In earlier flights (MX 56, 78, etc.) there was ample evidence of electronic interference (cross talk) between the several instruments in the aircraft and data system (see MX78 - 90 Day Report RSL No. 69-1, p. 15 et. seq.) In this mission these problems have been cleared up.

Other causes of "noise" relate to natural effects, particularly those of rapidly changing " true" surface temperatures (contact temperatures) induced by the rough surfaces of the black basaltic lavas. Our flights at 0900 local time covered rough ground which still had considerable shadow content. Accordingly both the spectrometer and the radiometer recorded high variability in radiance level. With the temperature discriminant in use spectra with associated radiometer readings showing excursions (1σ) of above 1° C were discarded. This helped to lower the S. D. of data points greatly, as seen either in their tabulated values (Sheet B) or in the S. D. plots (Sheet D). Later analysis using the BMDO7M stepwise discriminant program showed less scatter than with raw data (particularly smoothed rather than unsmoothed curves), but still "wild" spectra occurred in the training groups, as indicated by the divergence in plotted positions on the canonical variable plot, the final output sheet of that program. Careful identification of the specific spectra were made and a single spectrum plotted for each. Immediately it was clear that these had widely varying emittance values not at all relatable

to the average for that group. (At this time we have not specifically looked at the terrain we believe responsible for these "wild" curves, but that is a necessary future step).

We developed a simple discriminant function to remove these spectra. As a further preprocessing step we calculated, for each spectrum,

$$\text{SIGMA} = \sum_{i=1}^{i=N} (X_i - \bar{X})^2 \quad . \tag{1}$$

where i is the sequential emittance values at each counter point.

SIGMA was designed to emphasize those spectra with spikes and enable their removal. So far we have found that the alluvium and lake sediments, i.e., the smoother terrain have very low values (SIGMA = 10-20). Rough basaltic flows have SIGMA values above 35-40 and often 60-80. In an arbitrary assignment we selected a SIGMA rejection value of 35 for the basalts and 20 for the alluvials, which resulted in much better classification in the analysis. We do not yet have logic developed to set this level automatically but something set at 25-50% above the value for SIGMA of the group mean spectrum, would be suitable. Unfortunately, this means a double processing step at the moment so has been temporarily shelved.

The beneficial apsects of the noise rejection program may be seen in the following section.

D. Stepwise Discriminant Analysis (BMDO7M)

Most classification programs in use today rely upon an initial selection of "training groups". On the other hand "clustering" programs search within the data sets for maximum similarity, but are lengthy to run. Although we are intuitively drawn to the concept we have found our data to be too noisy for simple clustering systems. The several we have tried have given poor to fair results with a higher cost than the BMDO7M. No doubt this is due to the high number of data points in our spectra (53 points) but also the (still) appreciable levels of SD of the data points adds confusion. Consequently, we have concentrated on the BMDO7M program, with its initial selection of "training" curves.

1. Training Group Selection

The selection of the spectra for training groups is the single most important step in the geological analysis. The terrain contained in such a sub-area should be homogeneous, i.e., free from obvious material-changes which would cause wide S.D. changes. An excellent example of this problem can be seen in Fig. 7 , where the S.D. plot of three different sub-areas is presented. Curve A is a low noise, smooth S.D. curve ($\bar{\sigma}$ = 21 mV) with even temperature. Curve B shows high S.D. and noise which is most likely due to rapid oscillation in the surface temperatures over a rough basalt flow ($\bar{\sigma}$ = 39 mV). The interesting curve C shows a low S.D. curve at all wavelengths except where the compositional reststrahlen appear (stippled peak, centered at 9.5 μm). This directly indicates variability in composition in a target terrain at a constant, even temperature.

A total of 24 groups have been selected and plotted on Fig. 8. The mean spectrum for each groups is shown and the groups are arranged together if similar in pattern. Generally similar materials show similar

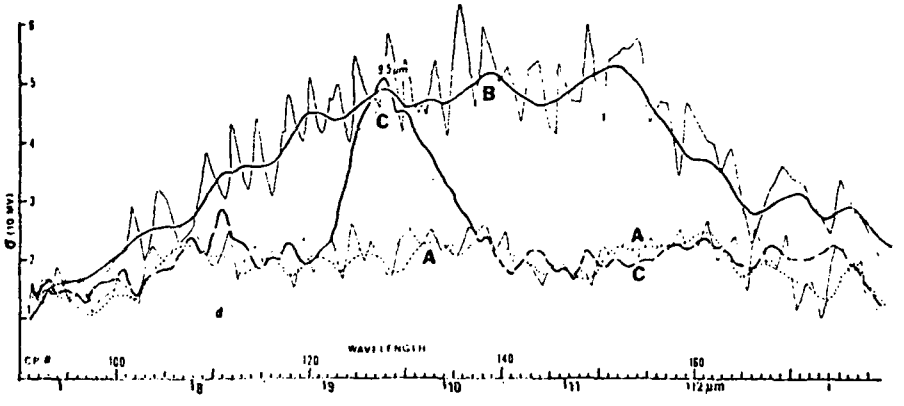

Fig. 7 A one-sided smoothed plot of standard deviation versus wavelength for 3 sub-areas. Ordinate is in 10 mv units. Curve A is "sand over basalt", sub-area II C, N = 11, $\bar{\sigma}$ = 21 mV; Curve B is a basalt lava flow, sub-area II B, N = 10, $\bar{\sigma}$ = 39 mV; curve C is dry lake sediment, sub-area A, N = 53, $\bar{\sigma}$ = 23 mV. Note that C shows an average flat curve with a single sharp peak (stippled) at 9.5 µm, indicative of variable surface compositions within that terrain area.

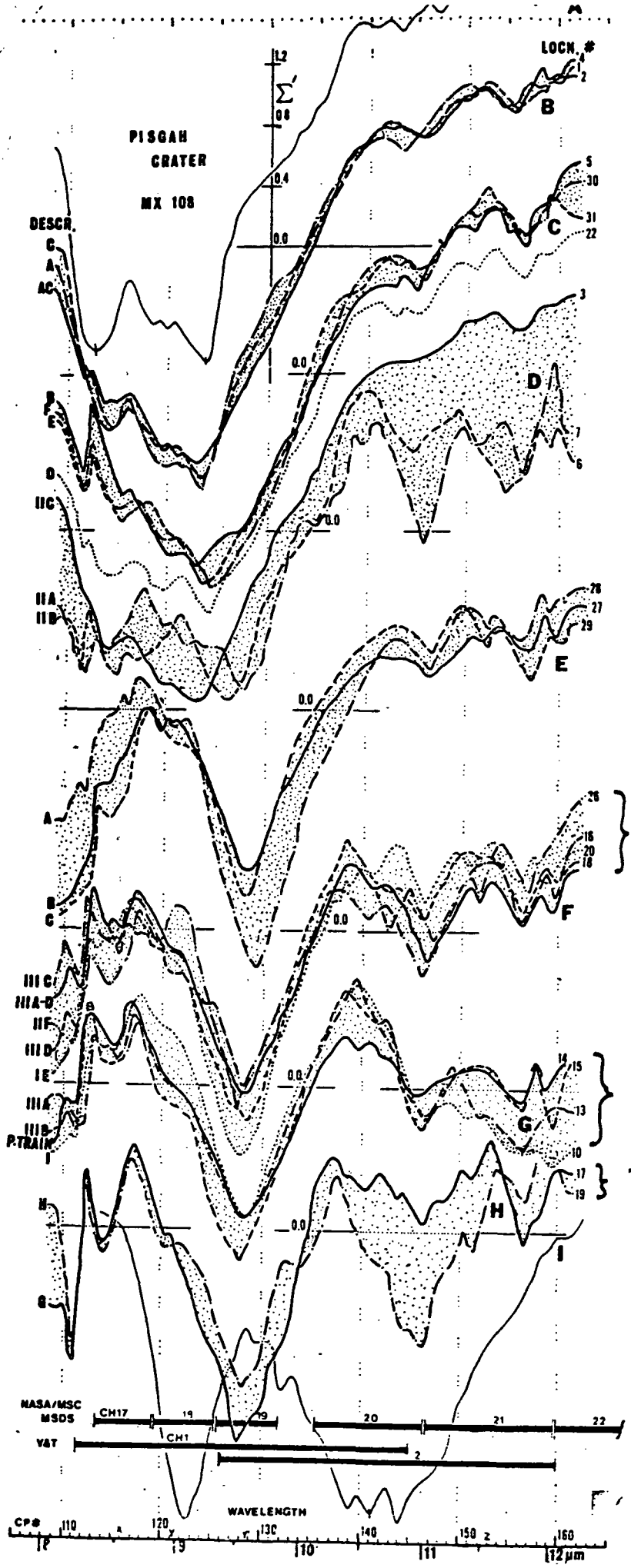

Fig. 8 Nine sets of normalized group mean spectral emittance curves, all with the same horizontal scale (wavelength from 8.0 to 12.0 μm). The vertical scale in all sets is constant, but the sets have been displaced vertically for ease in viewing. Normalized spectral emittance is plotted as the ordinate, with the mean = 0.0 as the central line on each spectrum. Spectral shapes thus may be directly compared.

spectra, e.g., younger alluviums, older alluviums, dry lake sediments. The basalt flows however, while showing broadly comparable spectra, differ sufficiently so as to make 3 sub-sets possible. No explanation for these differences is available at this time. It is certainly not simply relatable to flow phase history (Phases I, II and III), which forms the initial portion of the symbols on the spectra. Additionally it is not clearly their geographic sequence from north to south (numbered sub-areas 1-31) in Fig. 9.

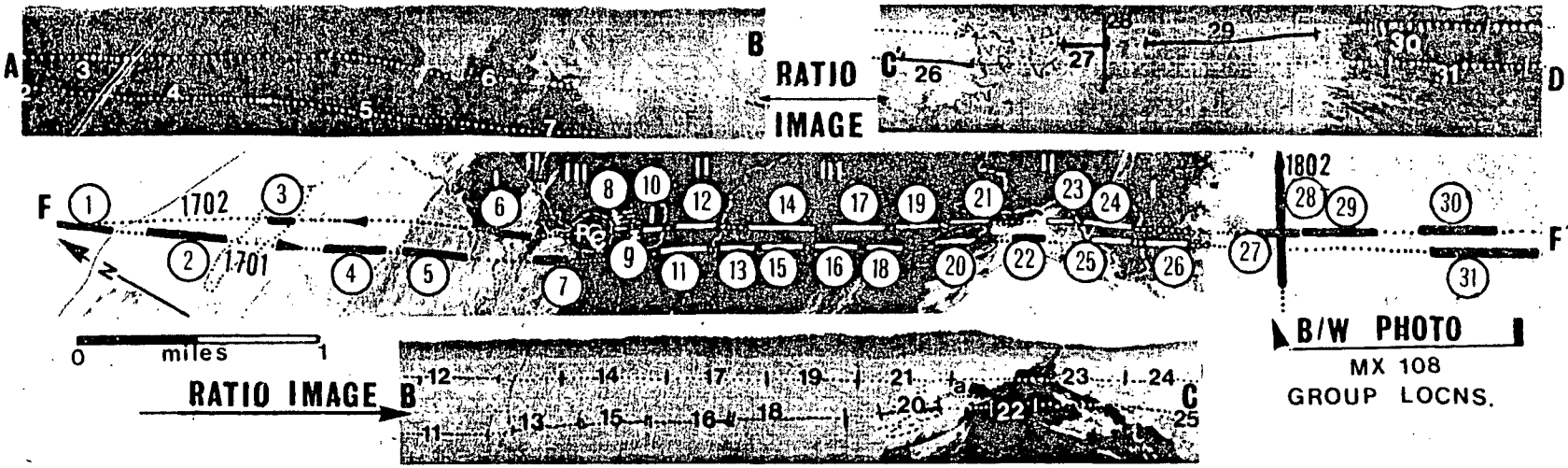

Fig. 9. Composite illustration from Pisgah Crater (PC) and associated flows (black areas), with alluvium (gray) and Lavic Lake (white). The central strip (F-F') is a section of the black and white photography, with the MX-108 flight lines (1701, 1702, 1802) as dotted lines. Spectral sub-group locations (#1-31) are indicated as bars along the flight lines. The three image strips (A-B, B'-C, C''-D) are consecutive sections of the ratio-imagery examples from (1a), with the group localities indicated for easy reference. The imagery tones are darker, when the ratio of radiance in the two channels (8.2 to 10.9/9.4 to 12.0 μm) is less than unity, medium gray if equal, and lighter if the ratio is greater than unity.

2. BMDO7M Results

The procedure for running this program has been described several times before and will not be further discussed (See Ref.: 4th Rem. Sens. Symp., p. 215-230, 6th Rem. Sens. Symp., p. 538-540 (RSL 70-7).

The end page of output of the program is a two-dimensional representation of the N-dimensions used for the discriminant process. Although the actual decisions are made in N-dimensional space (here N = 10), the linear combination of the 2-best dimensions are used for this plot, which shows the projection of the "clouds" of data points. Several groups of results have been summarized here in the following figures, by only using these canonical plots. As follows these are,

MX108, Flight 1, Pisgah Crater, Site 2

Figure 10: P-lava III, Dry Lake Sediments A, and Alluvial A

10A: Unsmoothed data, 99 spectra, 90% correct classification

10B: Smoothed data, 99 spectra, 90% correct classification

10C: Smoothed, but using ξ discriminant. 80 spectra left, 98% correct classification.

Figure 11: All Alluvials (A+AC+C), all Dry Lake Sediments (A+B+C), plus 4 lava types (IIA+D; IIB+C; IIIA+B+C+D; III G+H+J)

11A: Smoothed data, 6 categories, 325 spectra, 63% correct classification

11B: Smoothed data, only 4 categories (IIA+B+C+D lava and IIIA+B+C+D+G+H+J lava), 325 spectra, 69% correct classification.

Figure 12: Six (6) lava groups (IIIA; IIIB; IIC; IIID; I-E; IIF)

12A: Smoothed data, 6 categories, 108 spectra, 48% correct classification

12B: Smoothed, but using ξ discriminant (< 50) and $\Delta T (< 1^{\circ}C)$, 64 spectra left, 65% correct classification

MX108, Flight 3, Crow Springs, Site 22

Figure 13: Four (4) training groups (PEBL 1, QMP 1; TVA 1; OUT 1) and three (3) "unknowns" as test groups (QMP 2; TVA 2; PEBL 2).

13A: 4 categories plus 3 "unknowns" for Training sets, 149 spectra, 70% correct classification for Unknowns, 113 spectra, 40% correct classification.

13AA: Positional groupings for QMP 1 and 2 only

13AB: Positional groupings for PBL 1 and 2 and OUT 1 only

13AC: Positional groupings for TVA 1 and 2 only

13B: 4 categories only, 75 spectra (OUT 1; QMP 2; TRE 2; TRE 1) 97% correct classification

Sequence of Wavelengths Chosen

The program chooses values (CP's) in a step-wise manner, a single best value, best pair, trio, quartet, etc., until stopped by an option card value (here N = 10 steps). The choice is based upon finding the wavelength which shows the lowest within-group variance and the highest between-group variance, hence the wavelength with the greatest spread between groups). Table VI lists these sequences, and the group descriptions as similar materials or dissimilar materials.

It is interesting that 6 lavas, all somewhat similar, are differentiated using CP's much higher than the dissimilar materials of Figs. 10 and 11, indicating that the statistical significant information between these basaltic lavas lies in the region 10.0 to 11.5 μm. If we study the lavas mixed with alluviums and dry lake sediments then the information differentiating between these materials lies in the region 8.0 to 10.0 μm.

Summary-Airborne Data

Classifications show a much higher percentage correct if the following facts apply;

TABLE VI

WAVELENGTHS (CP NOS.) USED IN SEQUENCE IN BMDO7M DISCRIMINANT PROGRAM

A. Pisgah Crater, Site 2

1. Dissimilar materials - 3 categories
Dry Lake Seds, Alluvial and Lava

10A	120	128	124	112	109	(90%)
10B	121	128	133	153	137	(90%)
10C	116	151	121	127	157	(98%)

2. Similar materials - 6 categories
6 Lavas

12A	153	123	159	126	147	(48%)
12B	147	156	145	110	142	(65%)

3. Dissimilar materials (4-6) categories
(a) 4 Lavas, alluvial and Dry Lake Seds

11A	122	117	128	110	145	(63%)

(b) 2 Lavas, alluvial and Dry Lake Seds

11B	122	117	127	109	138	(69%)

B. Crow Springs - Site 22

1. (a) Dissimilar materials (4-7) categories

13A	153	116	126	110	133

(b) Dissimilar materials - 4 categories

13B	125	133	155	129	111

(1) If the spectra cluster together, if the wild spectra have been removed by use of either the ΔT or ξ discriminant in the pre-processing, e.g., Figs. 10A, 10B, 10C

(2) If markedly dissimilar spectral means are used, e.g., alluvials, lake sediments and a lava, e.g., Figs. 10A, B, C, and Fig. 13B.

If similar spectra are used, e.g., all lavas, then quite low success is achieved (30-40%)., e.g., Figs. 11A and 11B - 39% with 4 lavas.

(3) Three to five categories are best. Above that the "clouds" tend to merge together, e.g., Fig. 11A, Fig. 13A (4 lavas - 39%)

(NOTE: 15 pages of figures follow here)

FIGURE 10A

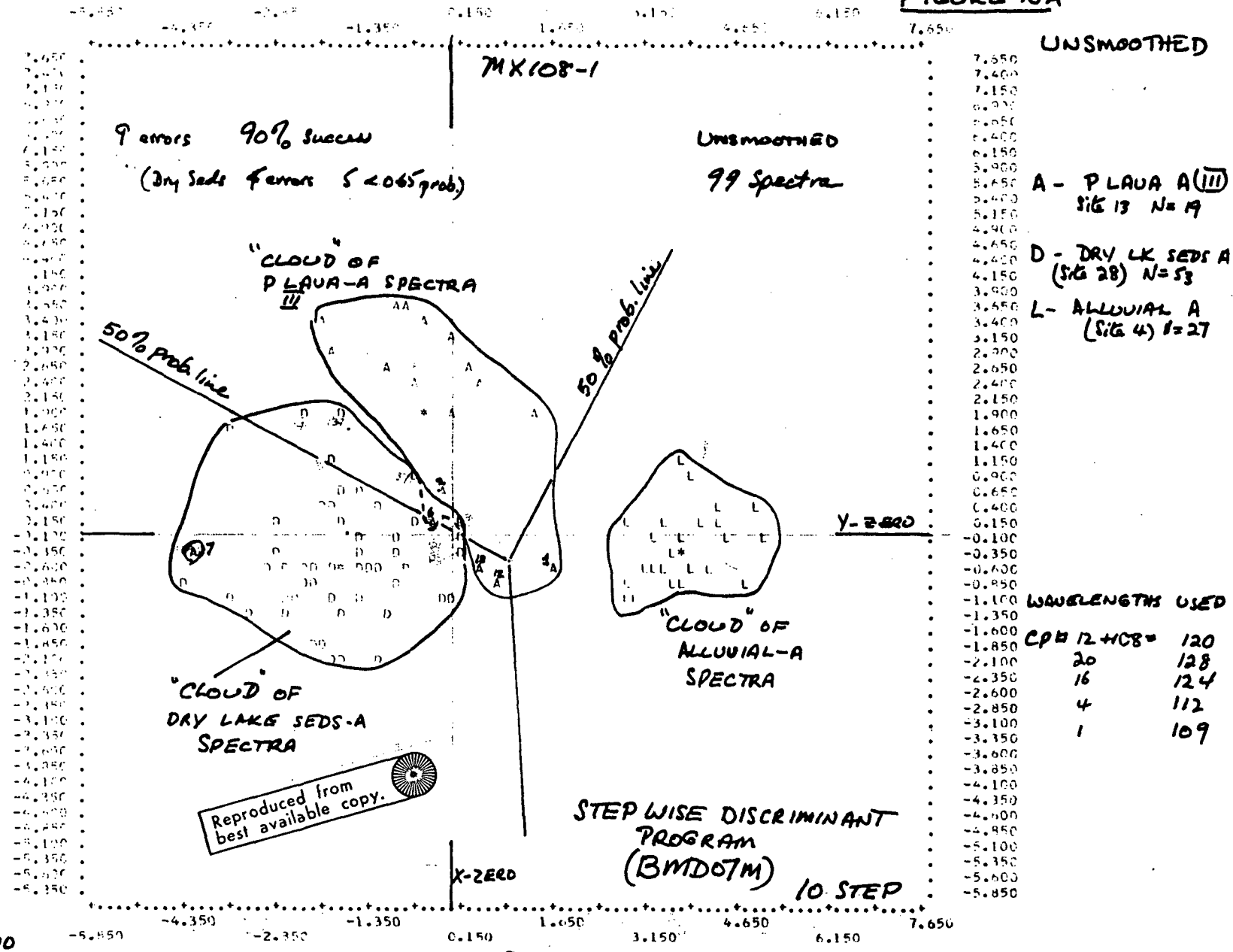

11/70

FIGURE 10B SMOOTHED

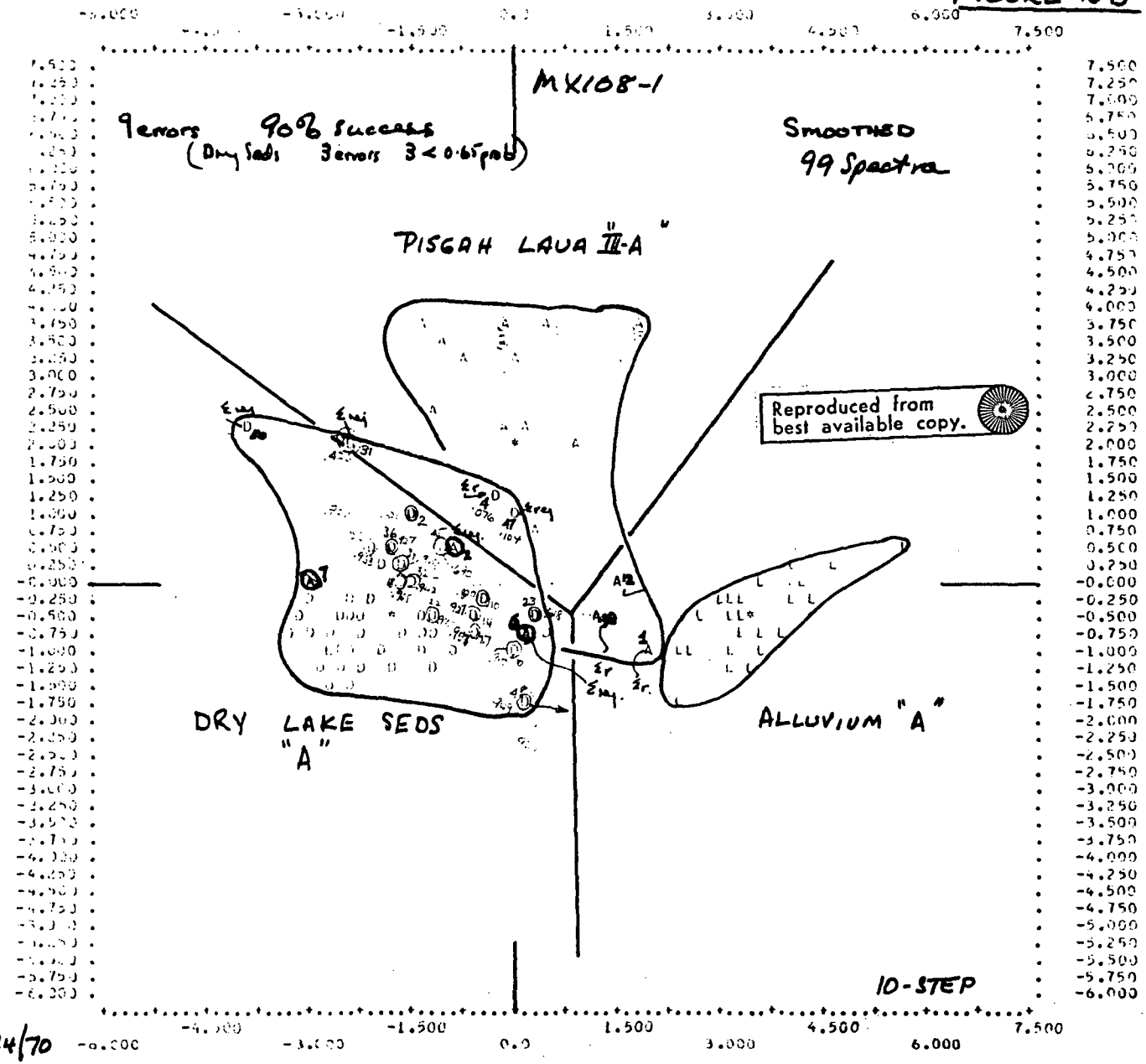

A = P LAVA-A (III) (Site 13) N=19

D = DRY LK SEDS A (Site 28) N=53

L ALLUVIAL A (Site 4) N=27

99

WAVELENGTHS USED

CP# 13 + 108 = 121
20 — 128
25 — 133
45 — 153
29 — 137

11/14/70

FIGURE 10C

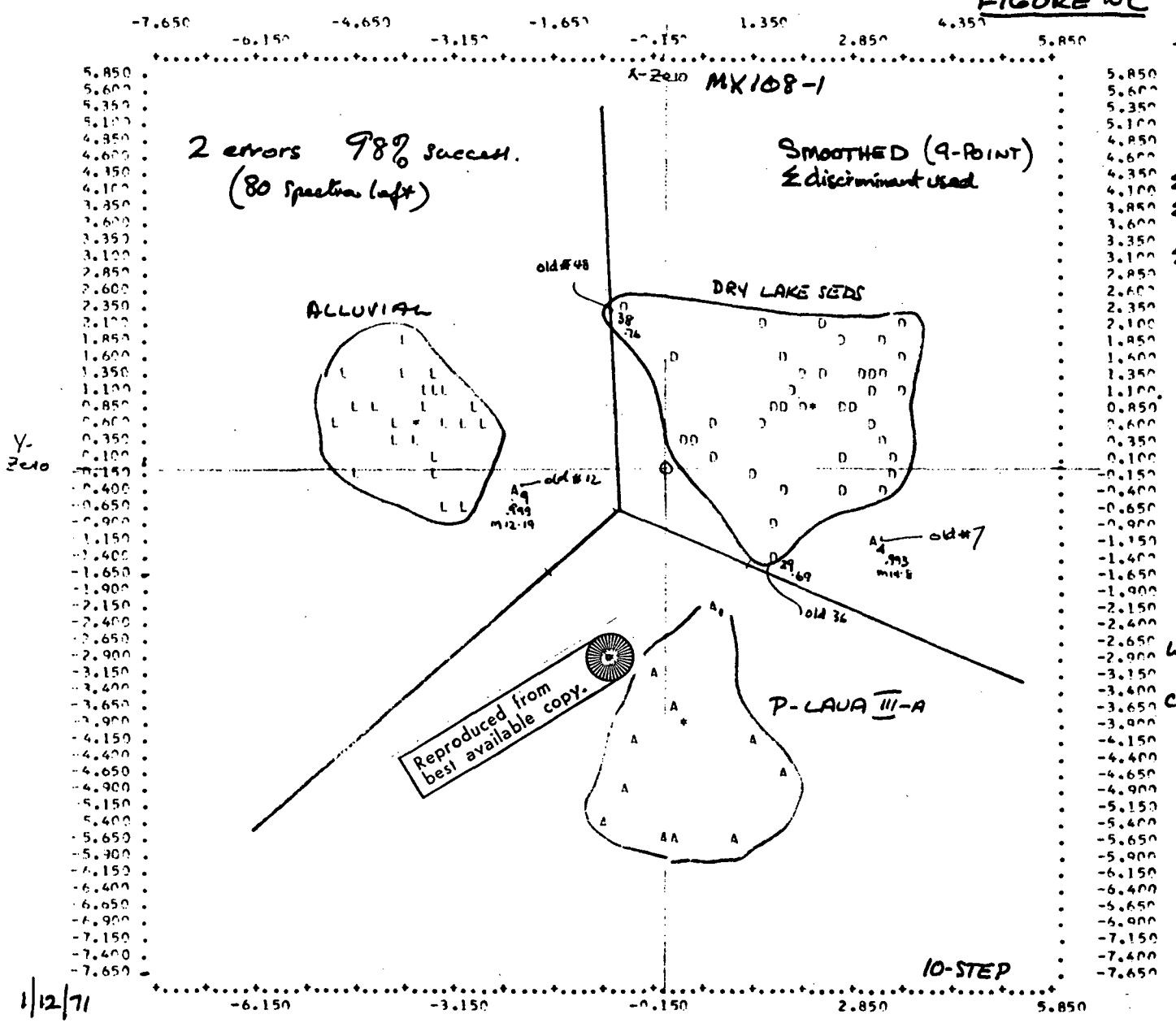

SMOOTHED + Σ used.

D.L.A

Σ Alluvium-A >8 (L)
Σ Dry Lk Beds A >40 (12 removed) (D)
Σ P Lava A >50 (6 removed) (A)

WAVELENGTHS USED

CP#	8	108
	45	153
	13	121
	19	127
	49	157

1/12/71

FIGURE 11 A

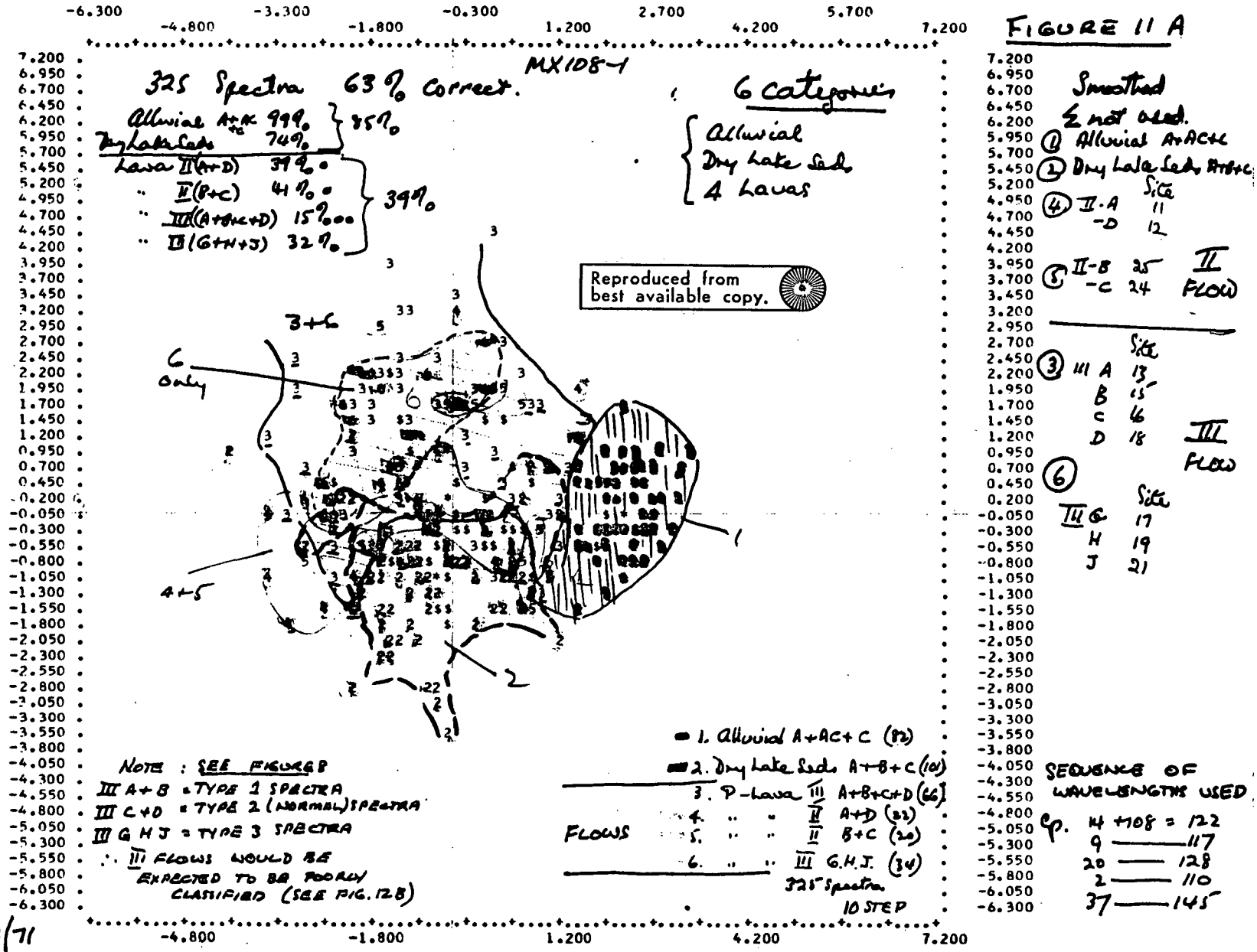

5/11/71

FIGURE 11 AA

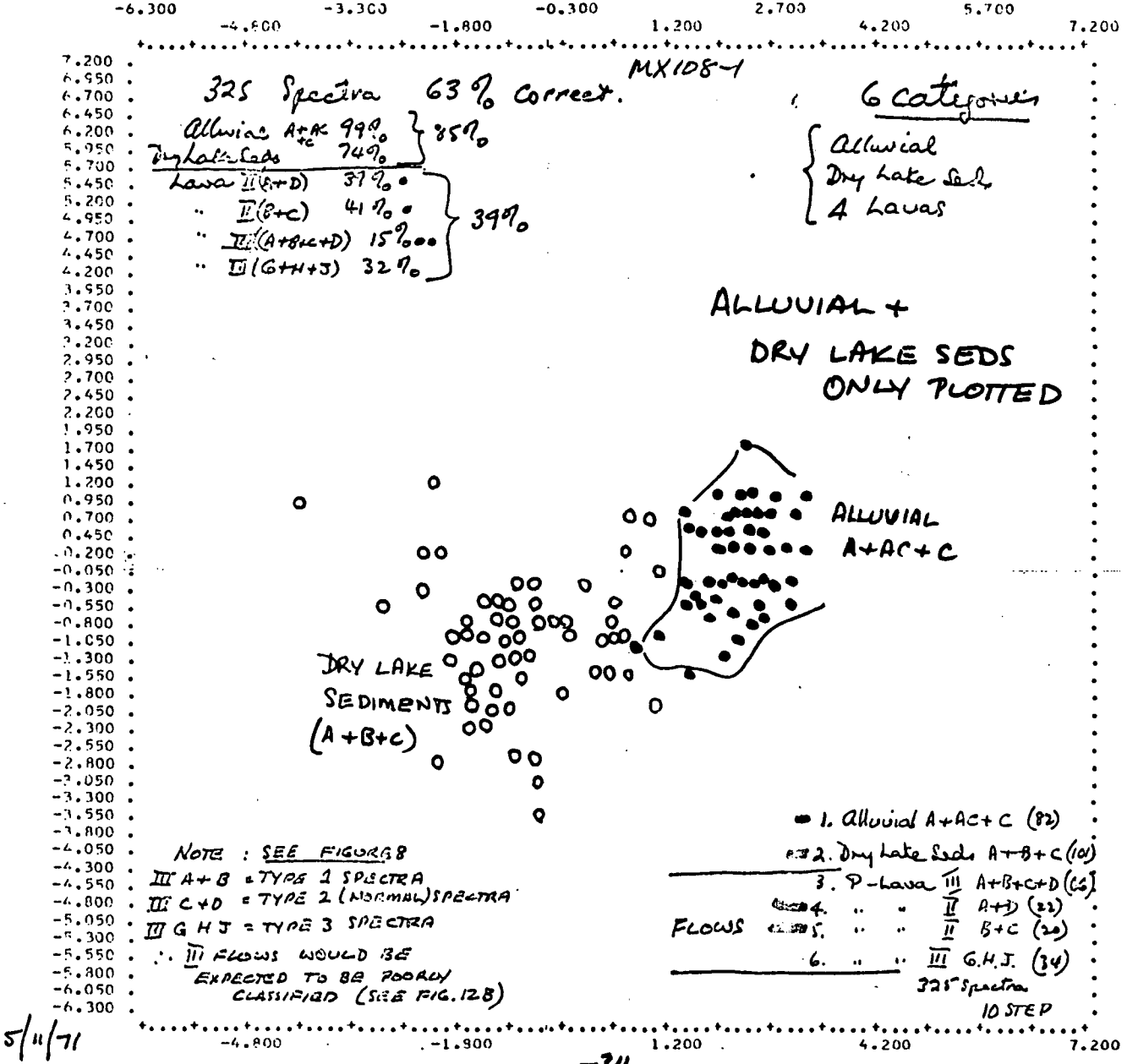

5/11/71

FIGURE 11 AB

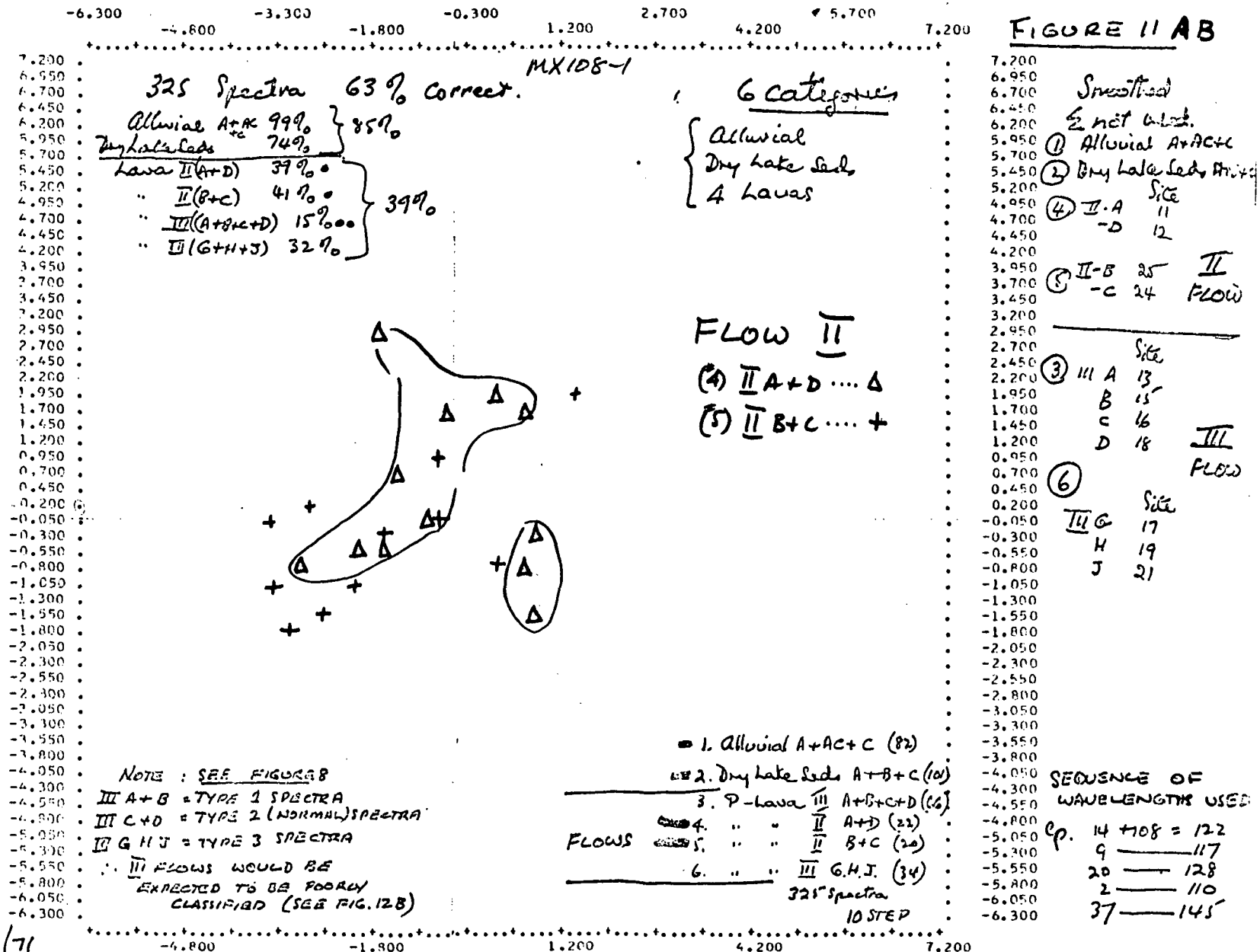

5/11/71

FIGURE 11 AC

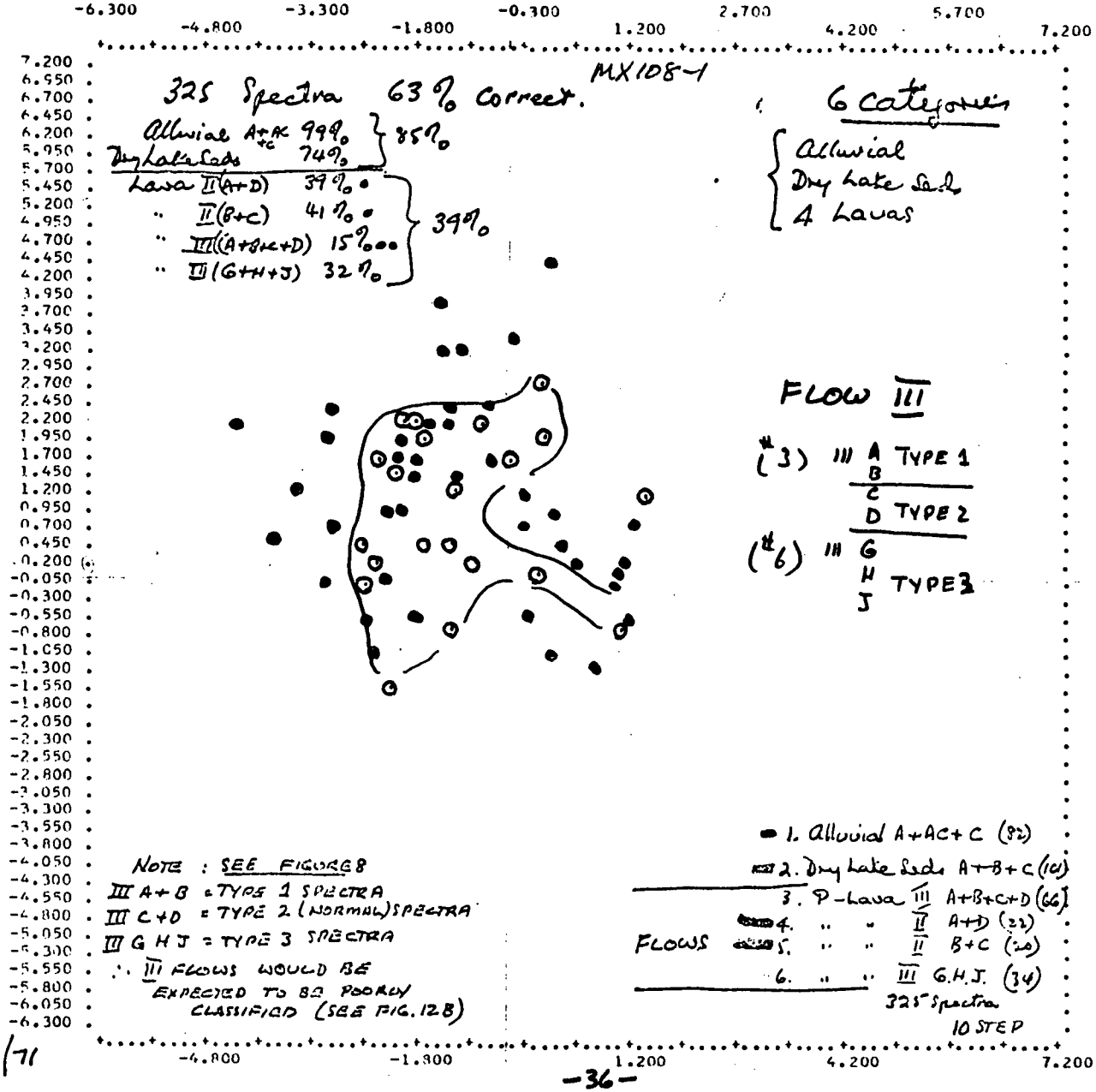

Smoothed
Σ not used.

① Alluvial A+AC+C
② Dry Lake Beds A+B+C

II FLOW

		Site
④	II-A	11
	-D	12
⑤	II-B	25
	-C	24

III FLOW

		Site
③	III A	13
	B	15
	C	16
	D	18

		Site
⑥	III G	17
	H	19
	J	21

SEQUENCE OF WAVELENGTHS USED

Cp. 14 +108 = 122
9 ——— 117
20 ——— 128
2 ——— 110
37 ——— 145

5/11/71

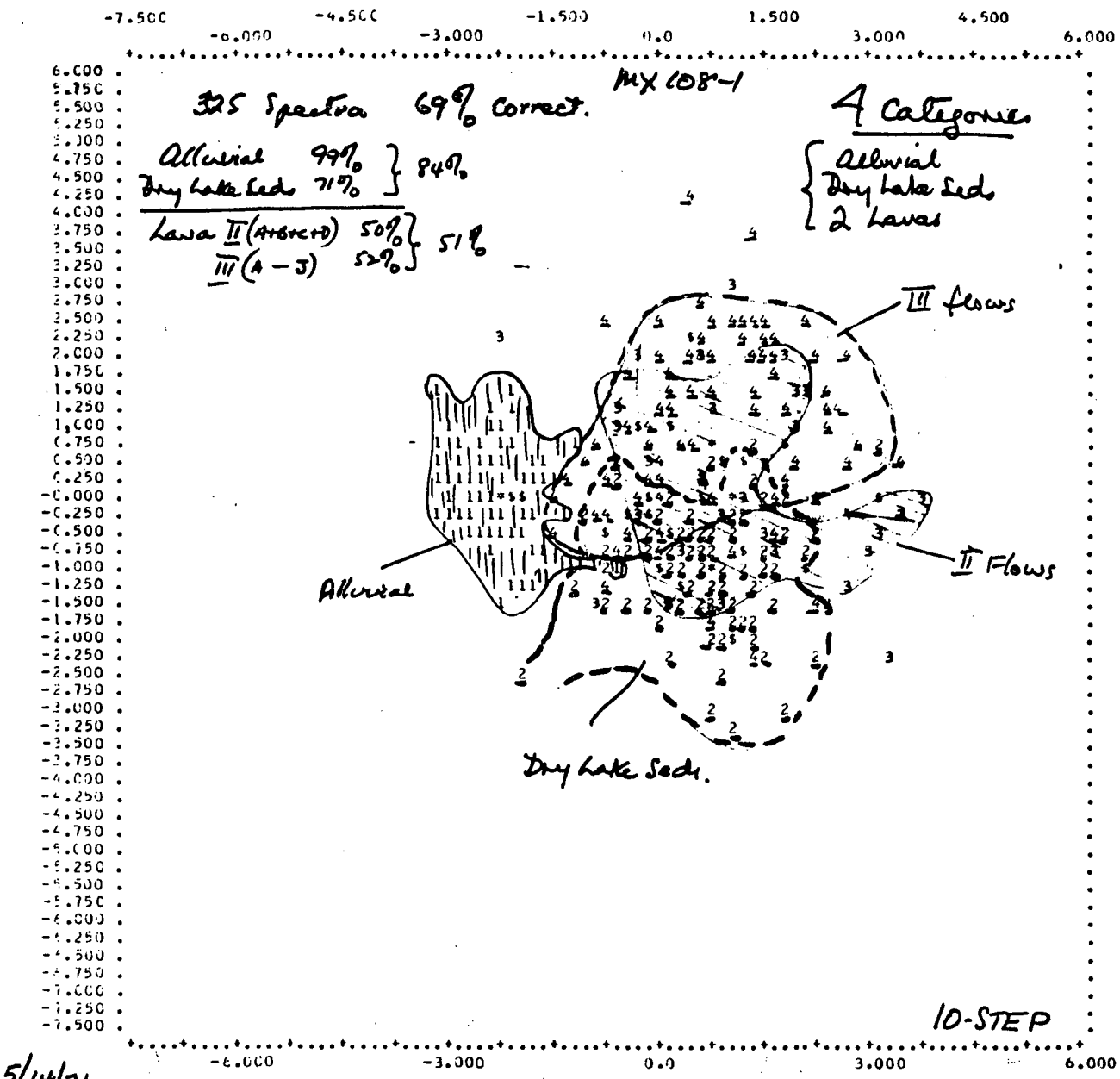

FIGURE 11B

	Site	
(1) Al	A	4
	AC	2
	C	1
(2) Dry Lake Sed		
	A	28 site
	B	27
	C	29

1 = Alluvial A+AC+C	(82)	
2 = Dry Lake Sed A+B+C	(101)	
3 = Lava-2(II)	(42)	
4 = Lava-3(III)	(100)	
	325	

3 = older 4+5 = II (A+D)+(B+C)

4 = older 3+6 = III (A+B+C+D)+(G+H+J) (11)(12)(13)(14)(15) (17)(19)(21)

(3) II A (11) II B (23) D (12) C (24)

(4)

Site		Site	
IIIA	13	III G	17
B	15	H	19
C	16	J	
D	18		

SEQUENCE OF WAVELENGTHS USED

Cp 14 +108 = 122
9 — 117
19 — 127
1 — 109
30 — 138

5/14/71

FIGURE 12A

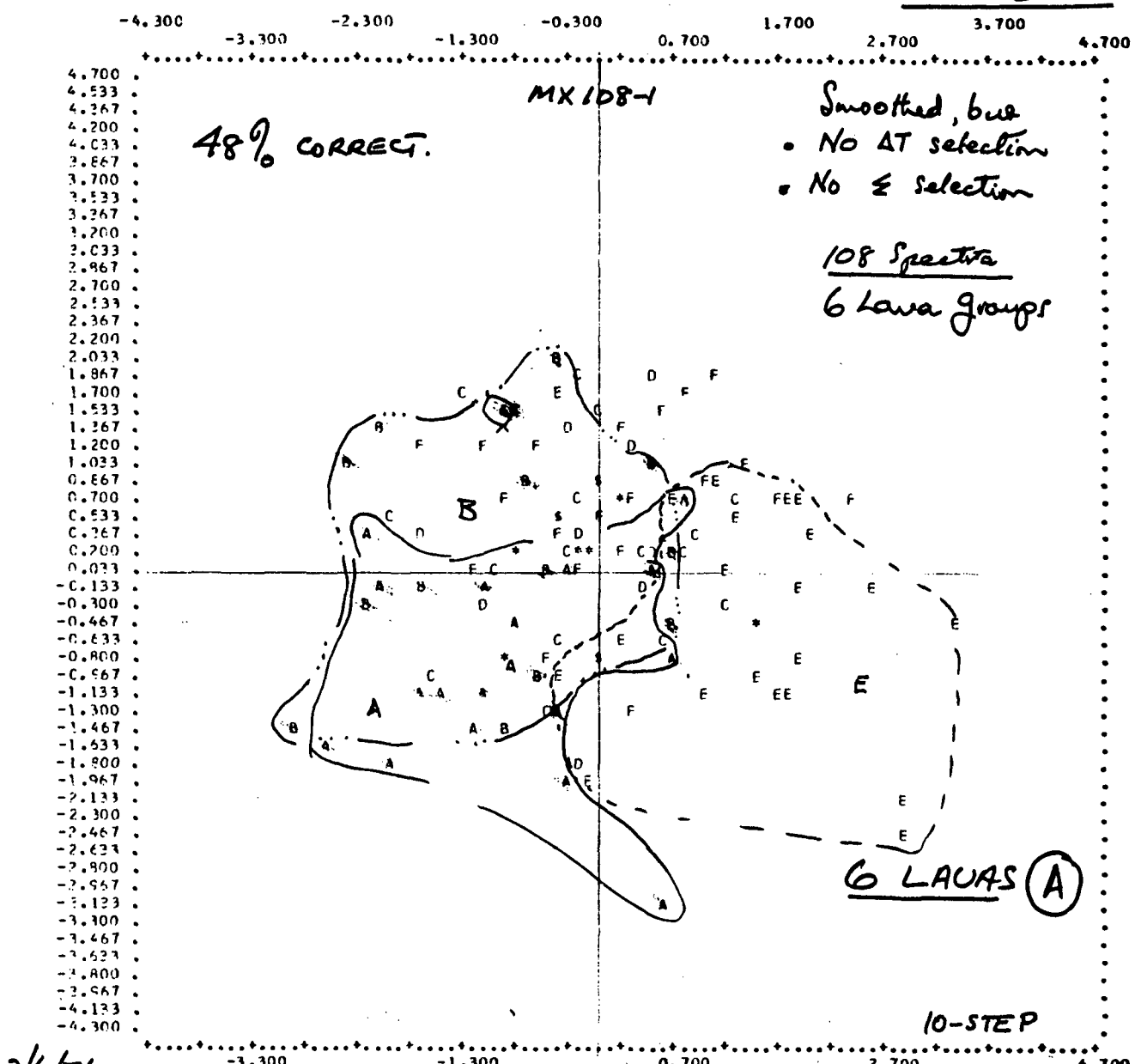

2/6/71
AN 6 LAVA
Groups.
10 steps
ΔT not used
ε not used.

48% Correct

52 out of 108

SEQUENCE OF WAVELENGTHS USED
Cp 45+108 — 153
15 — 123
51 — 159
18 — 126
39 — 147

2/6/71

FIGURE 12 B

2/11/71

MK108-1

65% CORRECT

Smoothed and
ΔT < PC
a Σ < 50 used
for selection

64 Spectra left
6 Lava groups

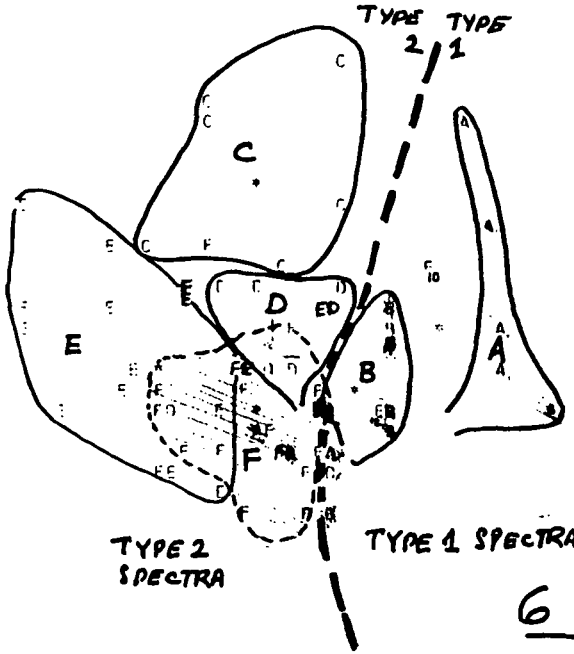

6 LAVAS (B)

NOTE:
RELATIVE TO FIG. 11 A HERE
WE ARE USING ONLY LAVAS
AND THEY ARE SEPARATED
BY SPECTRAL TYPE, NOT AGE!
A = III A ; B = III B TYPE 1 SPECTRA (III A IS MORE DIFFERENT THAN III B)
C = III C ; D = III D } TYPE 2 SPECTRA
E = Ie ; F = II F }

10-STEP

All 6 LAVA Groups.
65% correct at 10 Steps
a. ΔT < 1% decision
b. Σ < 50

65% Correct

42 B = 64
(discarded 44)
total 108

Type 2 Spectra
II-F 21
III-C 18
I-E 21
III-D 12
72

Type 1 Spectra
III-A 19
III-B 17
36
108

SEQUENCE OF WAVELENGTHS USED

Cp. 39 +108 — 147
48 — 156
37 — 145
2 — 110
34 — 142

MX 108-3

FIGURE 13A

CROW SPRINGS (Silc 22)

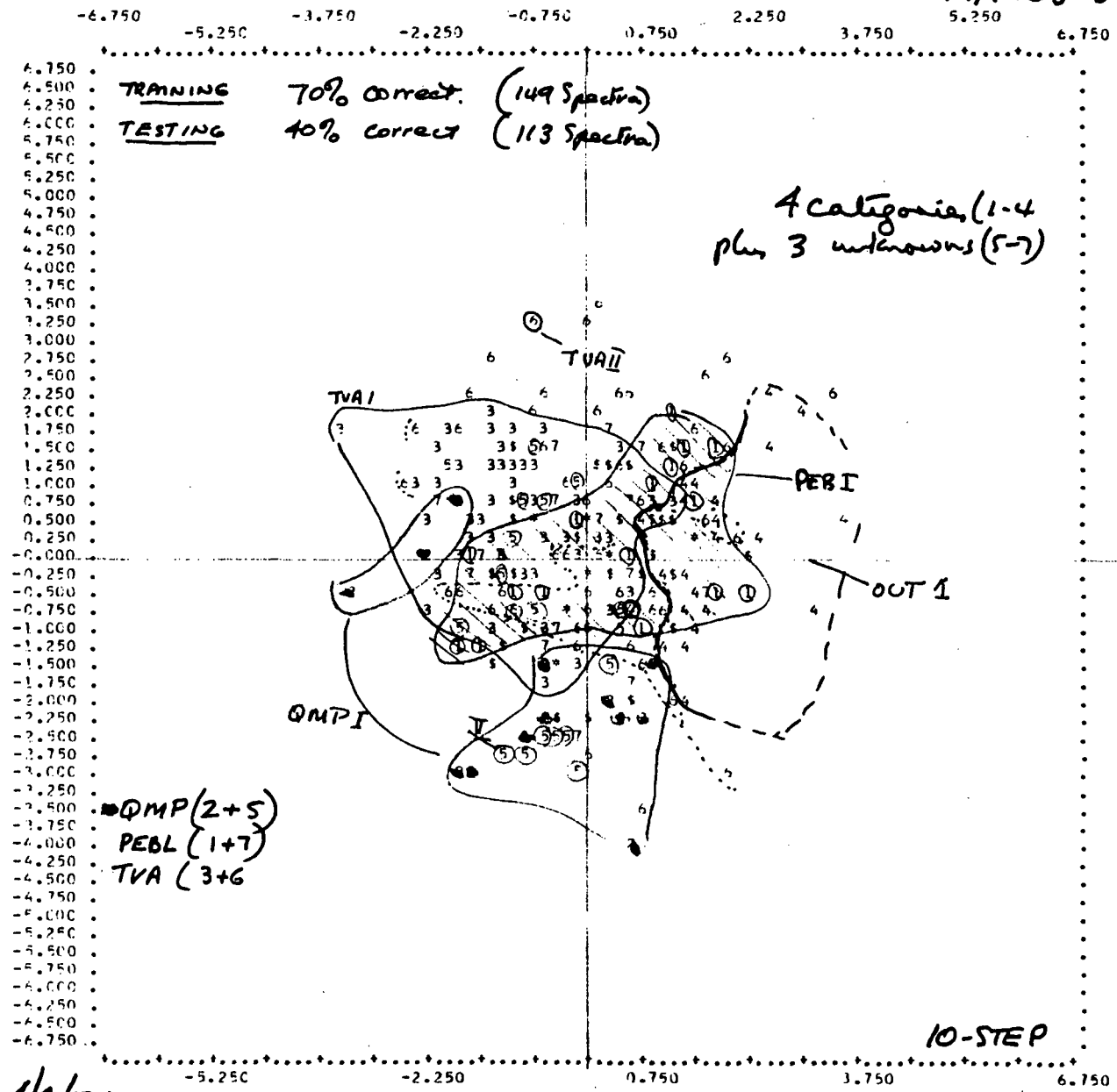

TRAINING GROUPS

1 = PEBL 1. (27)
2 = QMP 1 (33)
3 = TVA 1 (64)
4 = OUT 1 (35)

TEST GROUPS "UNKNOWNS"

5 = QMP 2 (23)
6 = TVA 2 (63)
7 = PEBL 2 (27)

SEQUENCE OF WAVELENGTHS USED

Cp 45' 408 = 153
6 — 116
18 — 126
2 — 110
25' — 133

4/4/71

50

MX 108-3

FIGURE 13AA

CROW SPRINGS (Sic 22)

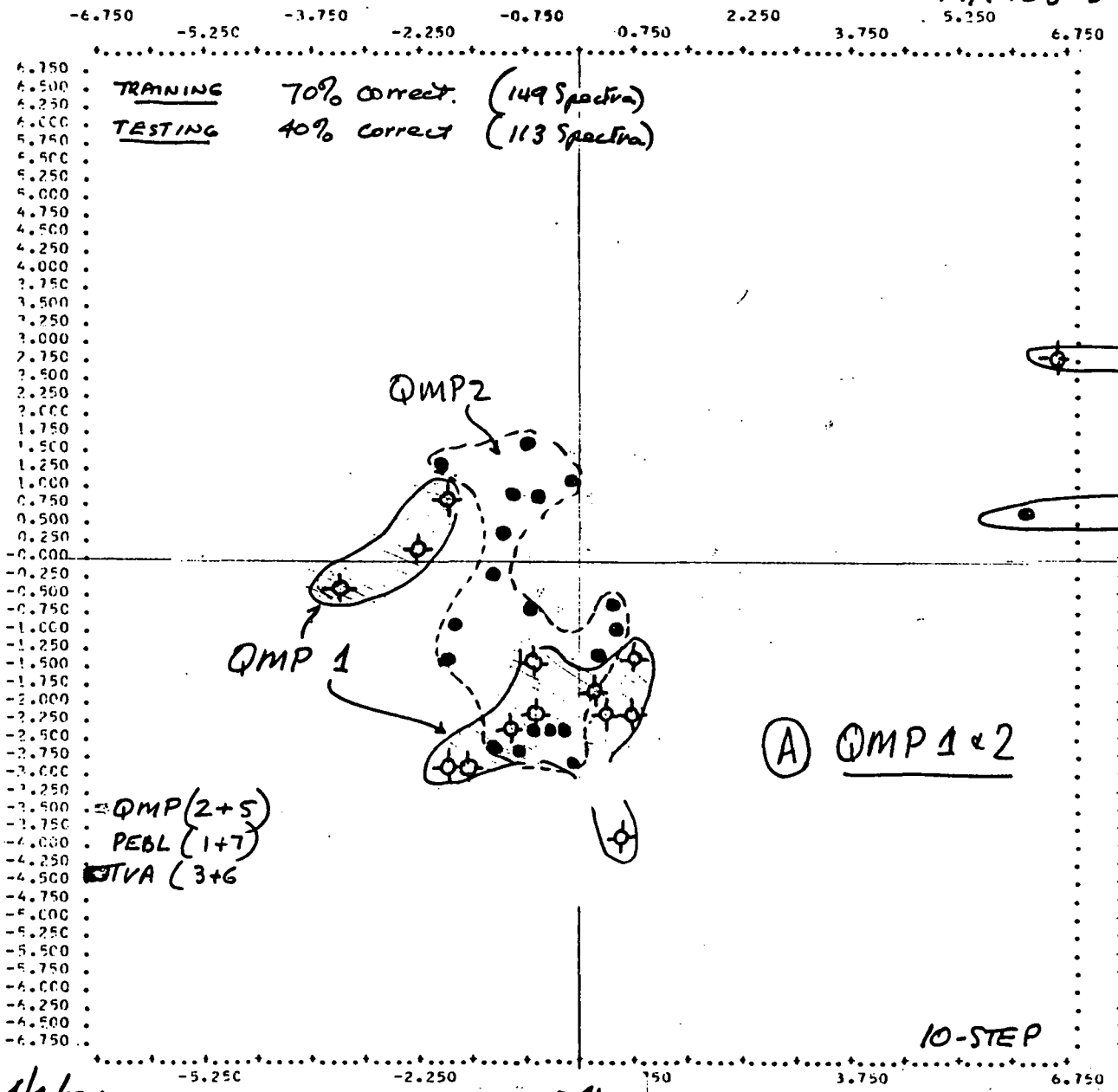

TRAINING GROUPS

1 = PEBL 1 (27)
2 = QMP 1 (33)
3 = TVA 1 (64)
4 = OUT 1 (31)

TEST GROUPS "UNKNOWNS"

5 = QMP 2 (23)
6 = TVA 2 (63)
7 = PEBL 2 (27)

SEQUENCE OF WAVELENGTHS USED

Ch 45 + 108 = 153	
8	116
18	126
2	110
25	137

4/4/71

51

MX 108-3 FIGURE 13 AC

CROW SPRINGS (Site 22)

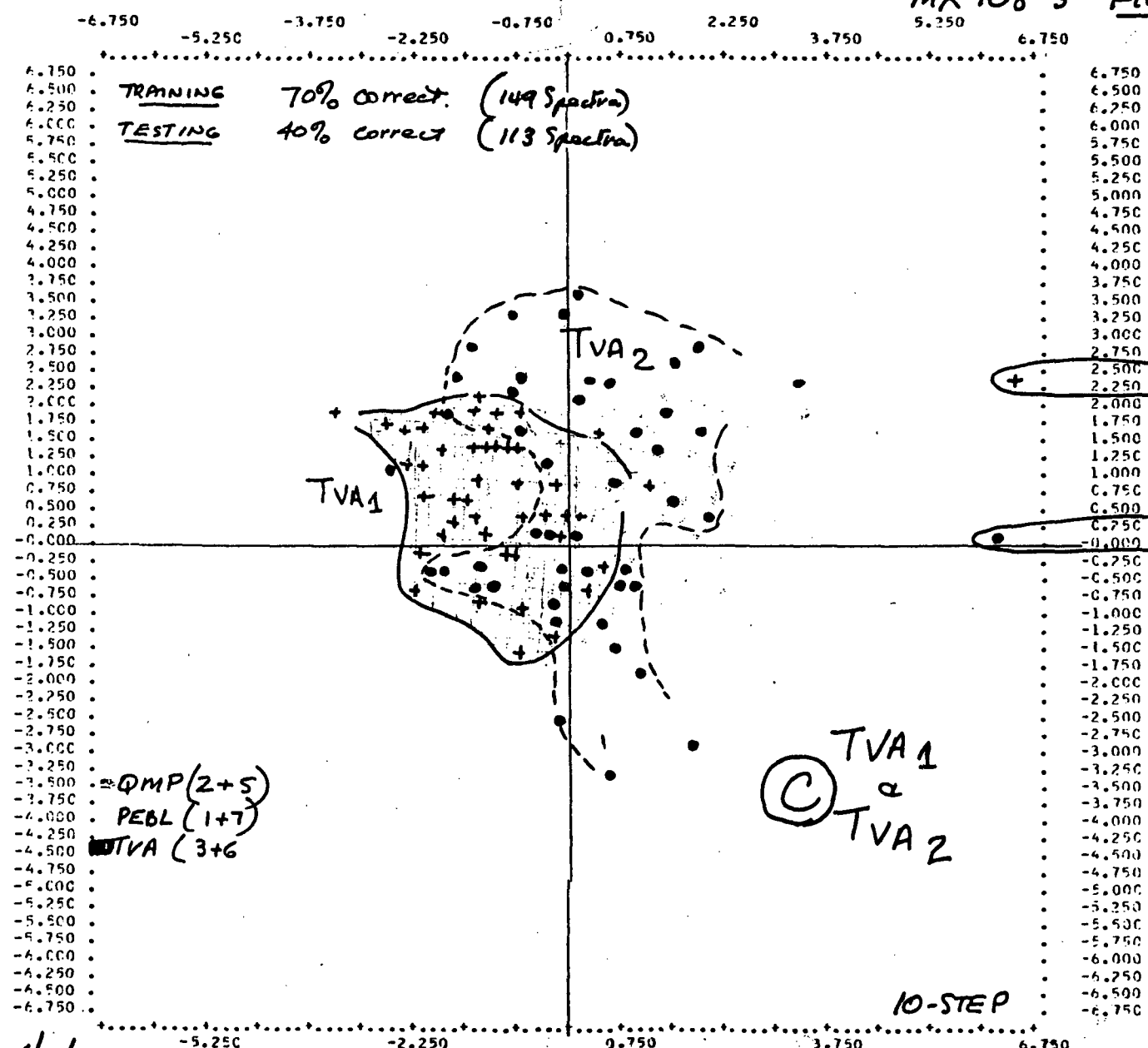

TRAINING GROUPS

1 = PEBL 1. (27)
2 = QMP 1 (23)
3 = TVA 1 (64)
4 = OUT 1 (35)

TEST GROUPS "UNKNOWNS"

5 = QMP 2 (23)
6 = TVA 2 (63)
7 = PEBL 2 (27)

SEQUENCE OF WAVELENGTHS USED

Cp 45 + 108	153
8	116
18	126
2	110
25	133

4/4/71

-42-

52

MX 108-3 FIGURE 13AB

CROW SPRINGS (Site 22)

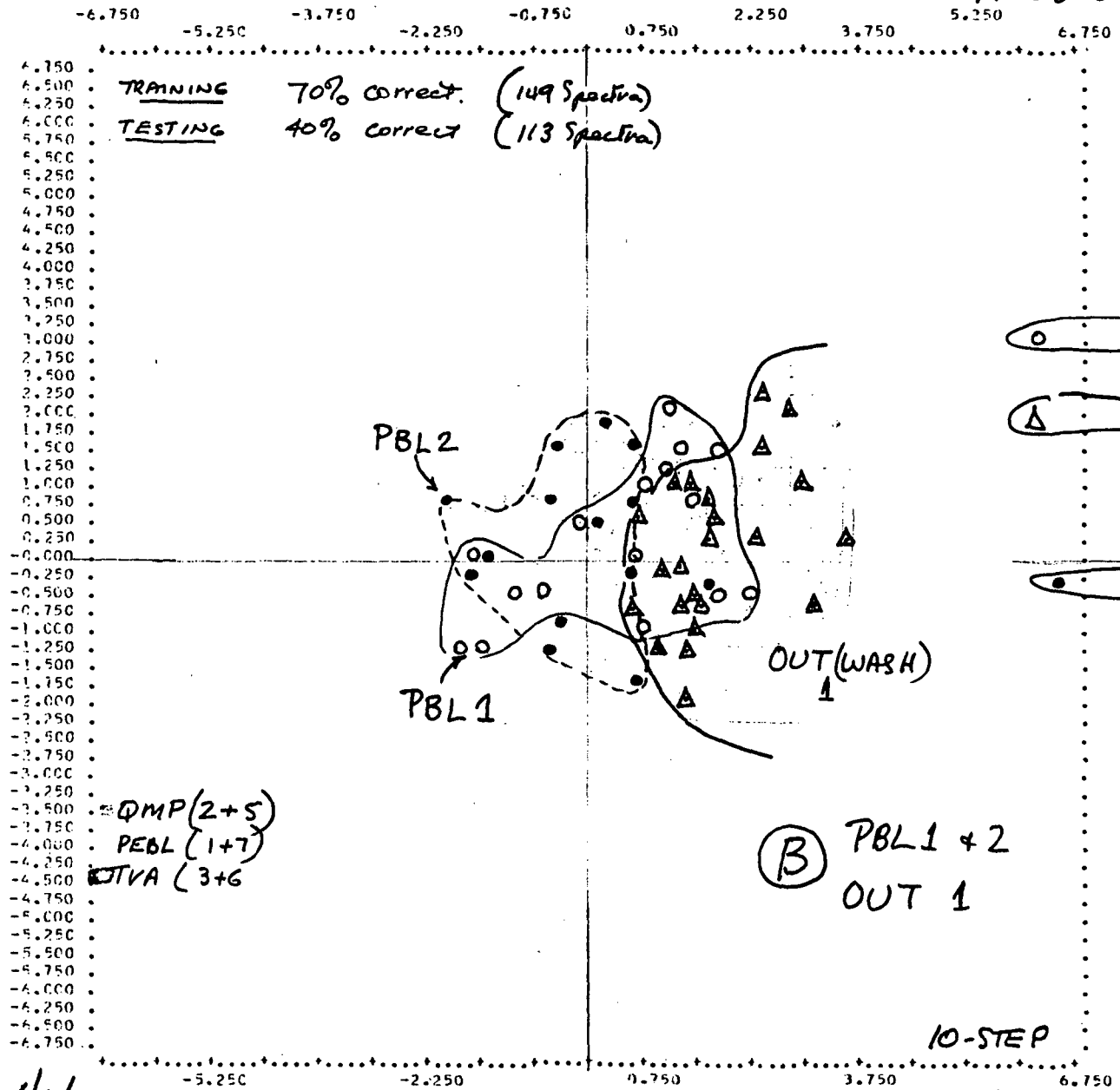

TRAINING GROUPS

1 = PEBL 1 (27)

2 = QMP 1 (23)

3 = TVA 1 (64)

4 = OUT 1 (35)

TEST GROUPS "UNKNOWNS"

5 = QMP 2 (23)

6 = TVA 2 (63)

7 = PEBL 2 (27)

SEQUENCE OF WAVELENGTHS USED

CP 45 HOR = 153

8	116
18	126
2	110
25	133

4/4/71

MX108-3 FIGURE 13B

CROW SPRINGS Site 22

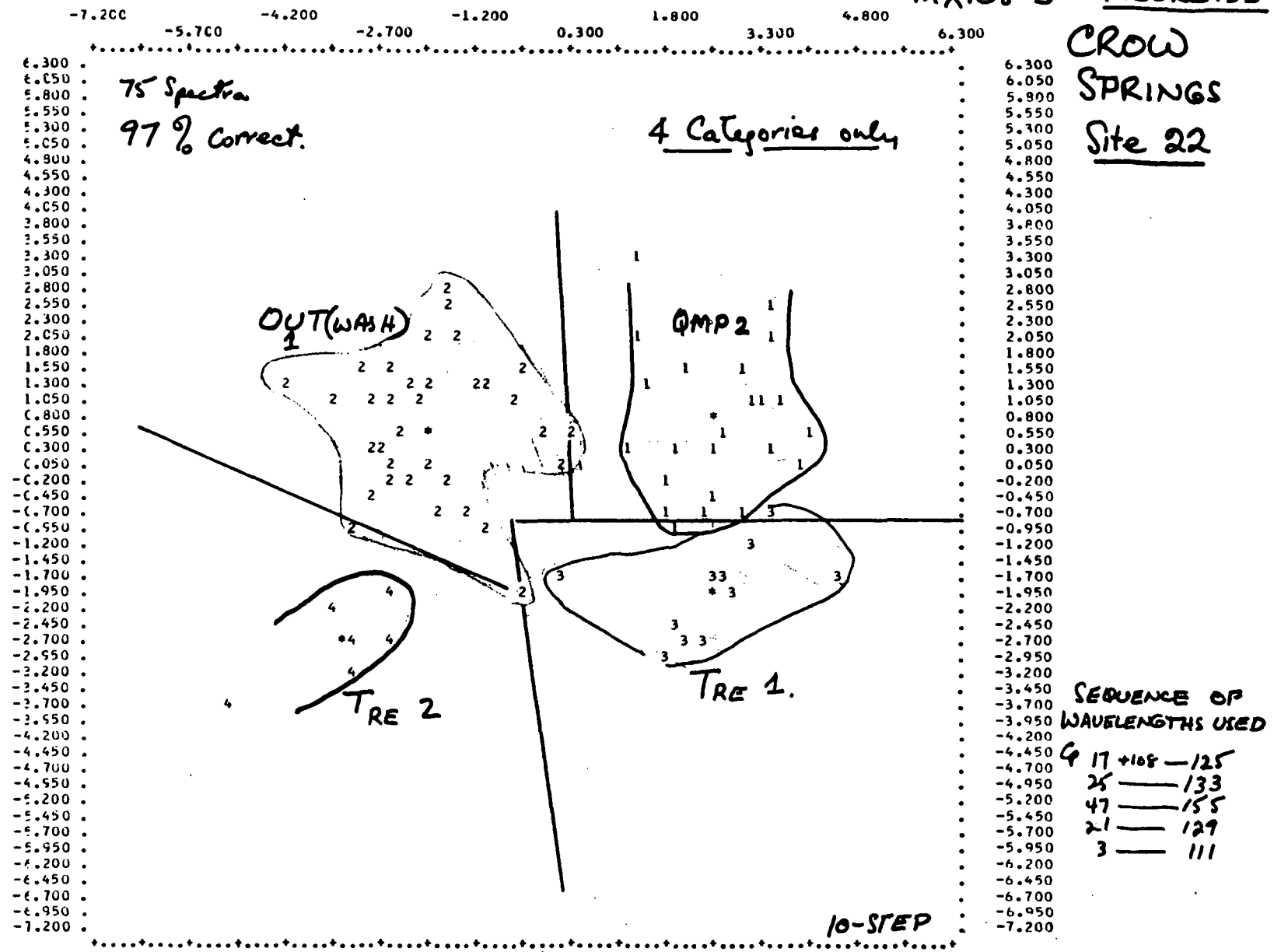

SEQUENCE OF WAVELENGTHS USED

9 17 +108 — 125
25 — 133
47 — 155
21 — 129
3 — 111

4/1/71

54

E. Color-Coding of Spectra Using I^2S-Digicol Additive Color Unit

Spectral curve data are difficult to examine visually. As a surrogate we used a colorized equivalent by using the BMDO7M program to select the 3 "best" wavelengths in the data sets. At these points the several spectral groups can be best differentiated (see results in Figs. 10-13). The wavelengths selected were those indicated (in preference) as X, Y (and Y') and Z, as a tie developed between Y-Y'. These may be seen at the bottom of Fig. 8, and in Table VI.

X	Cp #116	8.565 μm (0.1 μm band, center)
Y	121	8.965
(Y'	129	9.615)
Z	153	11.525

The emittance levels from the normalized spectra were quantized into 16-levels (as required by the color-bar generator matrix) and these levels set on the color-TV unit. Similarities and contrasts between the spectra can be readily observed. Color slides can be taken and chips cut from color prints to place on maps at those sites from which the spectra came. (See paper by Moore et al., 5th Remote Sensing Symposium).

Work is progressing on this method of visual-display of spectral data.

F. Direct Comparison of Spectral Groups with Emittance-Ratio Imagery

1. Concept of Emittance-Ratio Imagery

Optical scanners can make images of the terrain over which they are flown. These may be either in a single band or multibands, if the wavelengths are split by a dispersive element and the requisite number of detectors and recording channels are simultaneously used.

Robert Vincent (Univ. of Michigan) prepared a paper for the 7th Remote Sensing Symposium on "image-contrast ratios,"[1] using two relatively wide bands within the 8 to 13 μm "thermal band". These bands are from 8.2 to 10.9 μm and 9.4 to 12.0 μm, which overlap in bandpass. He used the analog-ratio of these 2 bands to form a third image which enhances the information content related to emittance differences of the terrain seen in these bands (see Fig. 9). Luckily his imaged data (flown by the Univ. of Michigan aircraft) contain the two lines down which the P3 flew for our MX108, Flight 1. Accordingly we can both compare our spectral and imaged data.

2. "Science" Manuscript

A manuscript of a paper on the relations between our work at Pisgah and Vincent's "imagery ratios" has been submitted to Science for possible publication. A preprint of this significant comparison between the two methods has been included as Appendix B.3 (RSL 71-5).

3. Problem Areas

In previous work (1969 , reported in Monthly Report #26, Sept.) we followed up an earlier Univ. of Michigan feasibility report on an imaging spectral scanner.[2] The Michigan Report had indicated that the narrowest (non-overlapping) bandpasses possible (with a good S/N ratio) would be 0.5 μm wide, in the region 8 to 13 μm. We "banded together our higher resolution "90-channel" data into paired-, triplets-, and quintruplet-data bands. As a test of the differentiation of rock types now possible with these wide bandpasses, we used the BMDO7M program sequentially with the 2-, 3- and 5-band data. Our classification success-rate dropped markedly after 3 points were banded together, indicating a loss of sensitivity in our newly created data.

	Success %
Paired data points (2) 0.2 μm wide	85 est.
Triplets of data points (3) 0.3 μm wide	82.5
Quintruplets of data points (5) 0.4 μm wide	65.0

1) Vincent, R.J. & Thomson, F.J. (1971). "Discrimination of Basic Silicate Rock by Recognition Maps Processed from Aerial Infrared Data." Proc. 7th Rem. Sens. Environ. Symp., pp. 247-252.

2) Lowe, D.S., Braithwaite, J. & Larrowe, V.L. (1966). "An Investigative Study of Spectrum-Matching Imaging System." Final Report Contract NAS8-21000, Huntsville, Ala., by U. of Michigan (IST) Ann Arbor, pp. 105.

Clearly these results are at variance with those of Vincent, who used to, 2.5 μm wide bands (which also overlapped by 1.5 μm). Further work is to be devoted to solving this inigma.

G. Spectral Files

Normalized emittance spectra for both flights of Mission 108 are listed in Table VII (on Flight 1 line) and Table VIII (various locations).

The actual curves, showing the plot of mean curve, plus 1 S.D. either side of the mean are enclosed (Sheets E and F) immediately following these Tables. The basic raw (millivolt) data, raw plot, S.D. plot appear in Appendix A.2.

Sheet A	Times for spectrum start, radiometer data
B	Mean curve, S.D. and (mV) listing
C	Mean curve plot $\pm$ 1 S.D. (mV)
D	S.D. plot (mV)
Sheet E	Normalized, smoothed, clipped, inverted emittance spectrum
F	Plot of same.

TABLE VII

DESCRIPTIONS OF SPECTRAL GROUPS - ON FLIGHT 1 LINE

MX108-1-PISGAH

LOC	NAME	NO. OF SPECTRA	GMT START	GMT STOP
1.	Alluvium C	25	18:49:44078	18:49:51360
2.	Alluvium AC	30	18:50:22915	18:50:31410
3.	Sand over Basalt II-C	11	19: 9:23685	19: 9:26719
4.	Alluvium A	27	18:49:58035	18:50:05923
5.	Alluvium B	30	18:50:35050	18:50:43864
6.	Sand over Basalt I-B	21	19: 8:37569	19: 8:43636
7.	Sand over Basalt I-C	9	18:50:52041	18:50:54468
8.	Pisgah Flow III	6	19: 8:27252	19: 8:28784
9.	Pisgah Flow II	4	19: 8:25750	19: 8:26647
10.	Pisgah Flow I	15	19: 8:20896	19: 8:25143
11.	Lava Flow II-A	13	18:51:04785	18:51:13887
12.	Lava Flow II-D	9	19: 8:12083	19: 8:16649
13.	Pisgah Lava III-A	19	18:51:16921	18:51:22383
14.	P-Train Lava (not included)	31	19: 7:57521	19: 8:06623
15.	Pisgah Lava III-B	17	18:51:23596	18:51:28452
16.	Pisgah Lava III-C	18	18:51:29058	18:51:34231
17.	Lava III-G	10	19: 7:48418	19: 7:55701
18.	Pisgah Lava III-D	12	18:51:34837	18:51:38161
19.	Lava III-H	8	19: 7:40241	19: 7:46309
20.	Pisgah Lava II-F	21	18:51:47263	18:51:53332
21.	Lava III-J	16	19: 7:31746	19: 7:39317
22.	Alluvium D	21	18:51:58186	18:52:04254
23.	Lava I-K	16	19: 7:15652	19: 7:20506
24.	Lava II-C	10	19: 7:08371	19: 7:14439
25.	Lava Flow II-B	10	18:52:12461	18:52:16998
26.	Pisgah Lava I-E	21	18:52:19136	18:52:25204
27.	Dry Lake Sediments B	23	19: 6:44098	19: 6:50774
28.	Dry Lake Sediments A	53	18:57:38314	18:57:54090
29.	Dry Lake Sediments C	25	19: 6:34390	19: 6:41671
30.	Alluvium F	42	19: 6:14078	19: 6:26501
31.	Alluvium E	27	18:52:59793	18:53:07681

TABLE VIII

DESCRIPTION OF SPECTRAL GROUPS - VARIOUS LOCATIONS

MX108-1-PISGAH

NAME	NO. of SPECTRA	GMT START	GMT STOP
Pisgah Lava III (A-D)	53	18:51:21169	18:51:36948
P-Train III (G+H+J)	34	19: 7:57521	19: 8:06623
P Lava III (A+B+C+D)	34	18:51:17239	18:51:38161
P Lava II (A+D)	22	18:51:04785	19: 8:16649
P Lava II (B+C)	20	18:52:12461	19: 7:14439
Pisgah Cinders III	9	18:50:58427	18:51:00855
Dry Lake Seds (A+B+C)	101	18:57:38314	19: 6:41671
Alluvium (Younger) (A+AC+C)	82	18:49:58035	18:49:51360
MX108-1-SUNSHINE			
Sunshine Lava A	22	18:57:11905	18:57:18290
Sunshine Lava B	25	18:57:04017	18:57:11297
Sunshine Cinders C	17	18:56:54626	18:56:59480
Sinshine Cinders D	20	18:56:47633	18:56:53412
MX108-3-CROW SPRINGS			
Q. M. P. 1	23	17:13:58084	17:14:05359
Q. M. P. 2	23	17:22:44634	17:22:51303
PEBL I	27	17:13:07466	17:13:15347
(Basaltic Pebbles on Playa)			
PEBL II	27	17:21:56429	17:22:04311
OUT I (Outwash)	35	17:13:35960	17:13:46267
TVA I	64	17:13:16252	17:13:35354
(Tertiary Volcanic Ash Soils)			
TVA II	63	17:22:04917	17:22:23712
TVA II (C8)	3 (low)	17:22:52814	17:22:53420
(Lavender Volcanics)			
TRE I (B9)	11	17:14:10517	17:14:13847
TRE II (C3A)	6 (low)	17:22:28870	17:22:30381

RECORDED FROM 15 16 42339 TO 15 17 813.
THESE SPECTRA HAVE BEEN RATIOED, NORMALIZED AND INVERTED.
COUNTERS RANGE FROM 8.0 TO 12.2 MICRONS.

PRE FLIGHT ROCK A

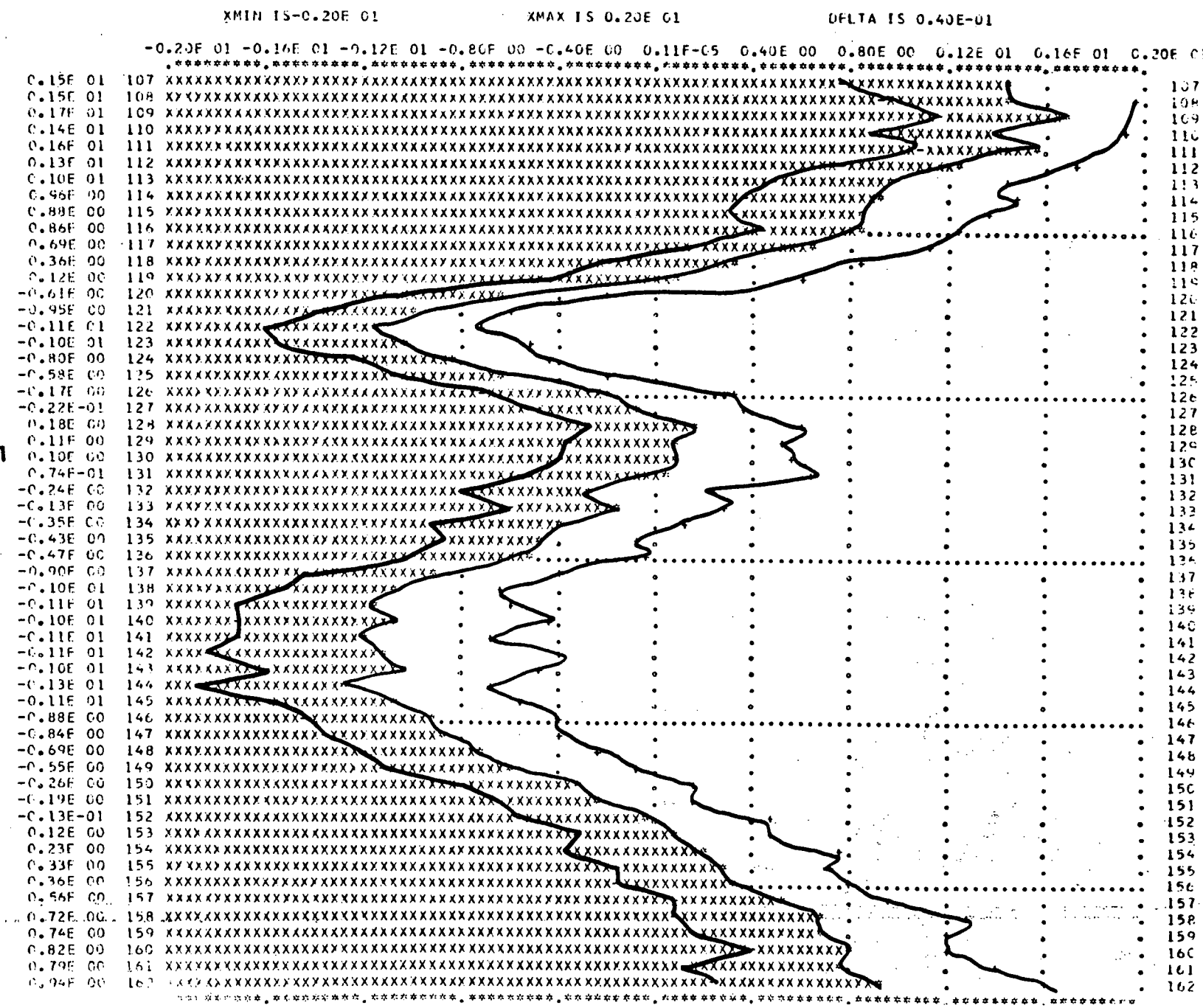

60

PRE FLIGHT ROCK B

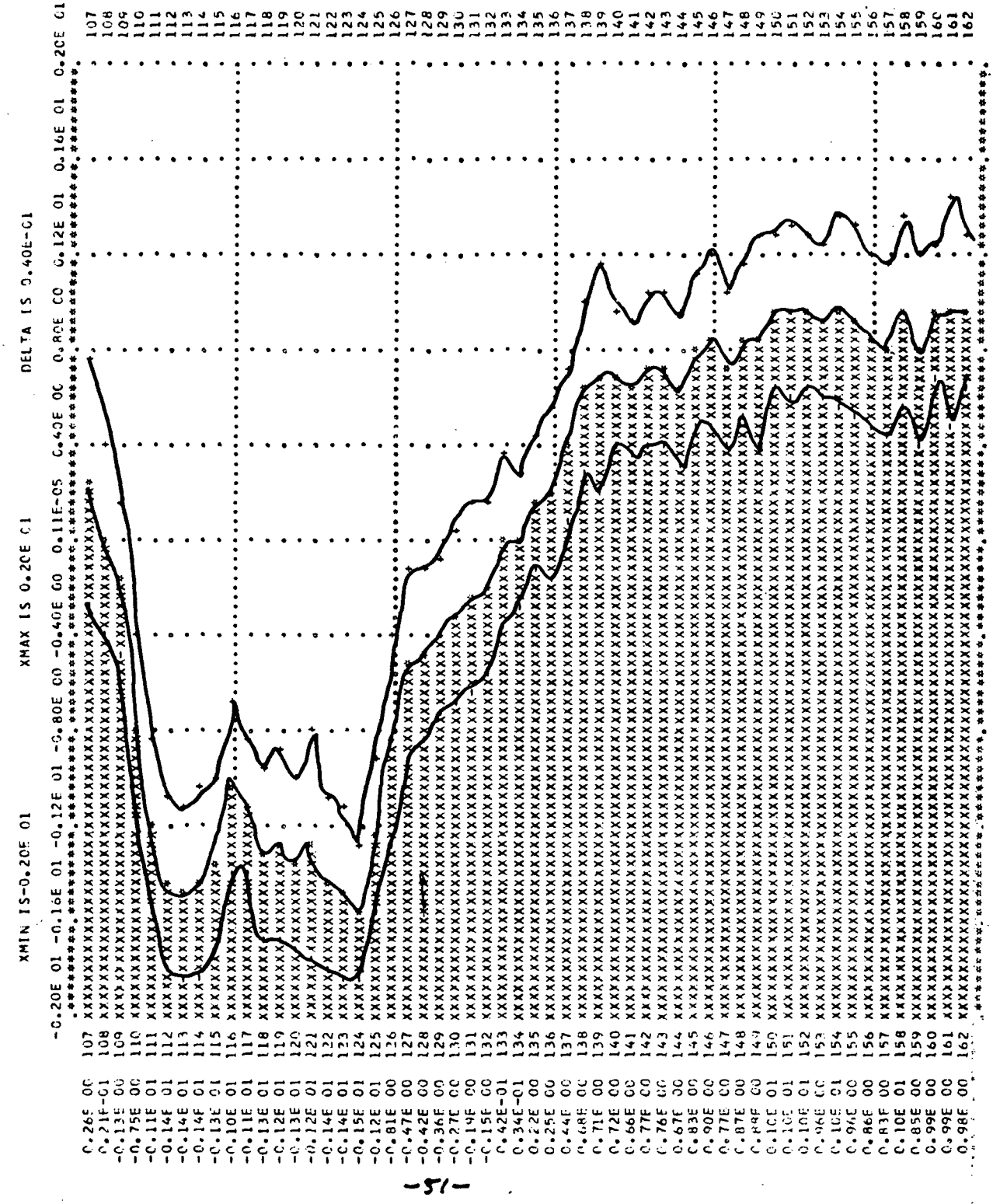

THESE SPECTRA HAVE BEEN **RATIOED, NORMALIZED AND INVERTED**
COUNTERS RANGE FROM 8.0 TO 12.2 MICRONS.

UP RAMP SPECTRUM GROUP CALLED -- MX108-1 ALLUVIUM GROUP C 6C011101 02000000

NUMBER OF SPECTRA IN GROUP: 25
RECORDED FROM 18 49 44C78 TO 18 49 51360.
THESE SPECTRA HAVE BEEN RATIOED, SMOOTHED, NORMALIZED, AND INVERTED.

(1)

ALLUVIAL C.

XMIN IS-0.20E 01 XMAX IS 0.20E 01 DELTA IS 0.40E-01

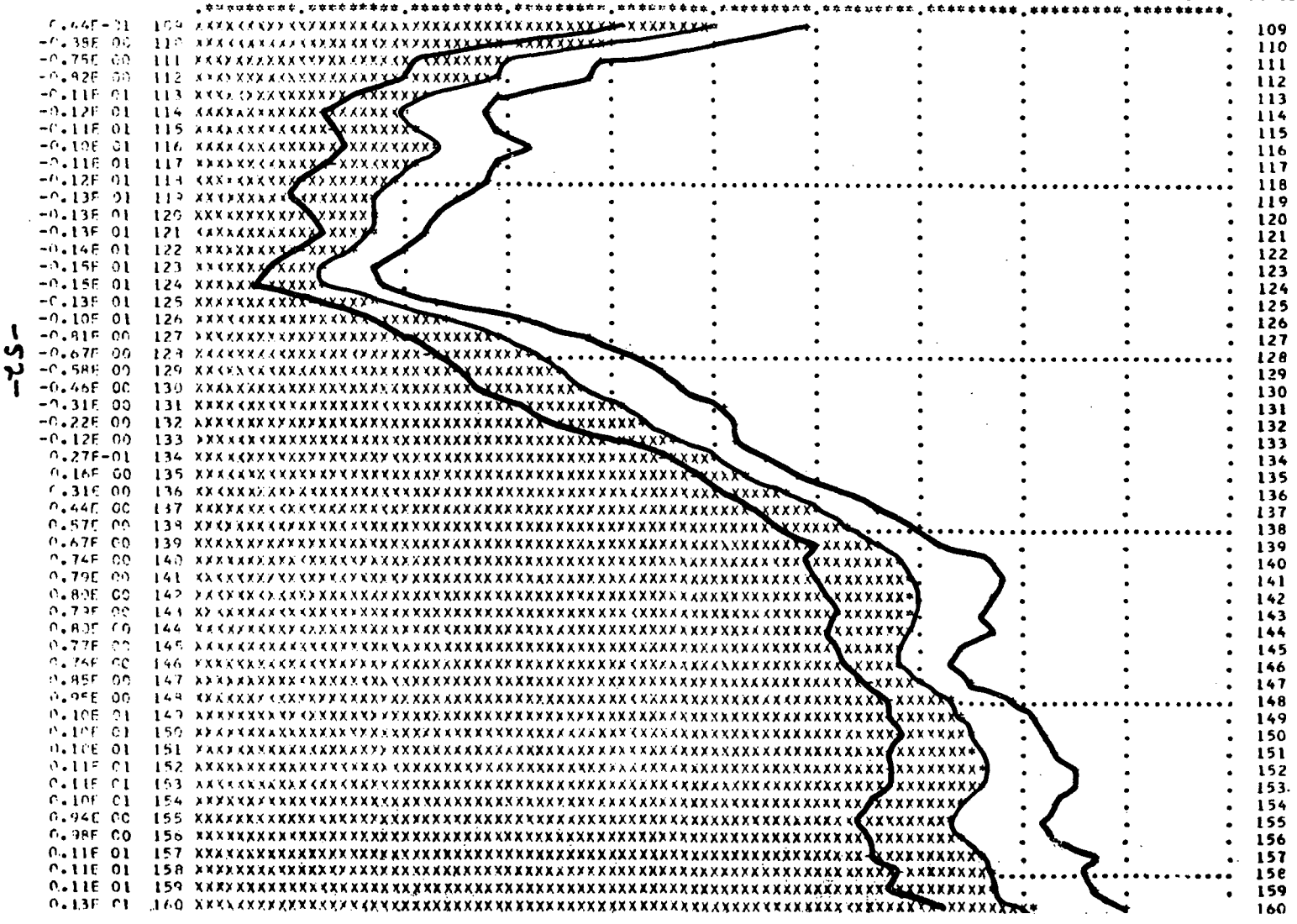

UP RAMP SPECTRUM GROUP CALLED -- 4X109-1 ALLUVIUM GROUP AC 6C011101 02000000
NUMBER OF SPECTRA IN GROUP: 30
RECORDED FROM 13 50 22915 TO 13 50 31410.
THESE SPECTRA HAVE BEEN RATIOED, SMOOTHED, NORMALIZED, AND INVERTED.

(2)

ALLUVIAL AC

XMIN IS -0.20E 01 XMAX IS 0.20E 01 DELTA IS 0.40E-01

-0.20E 01 -0.16E 01 -0.12E 01 -0.80E 00 -0.40E 00 0.11E-05 0.40E 00 0.80E 00 0.12E 01 0.16E 01 0.20E 01

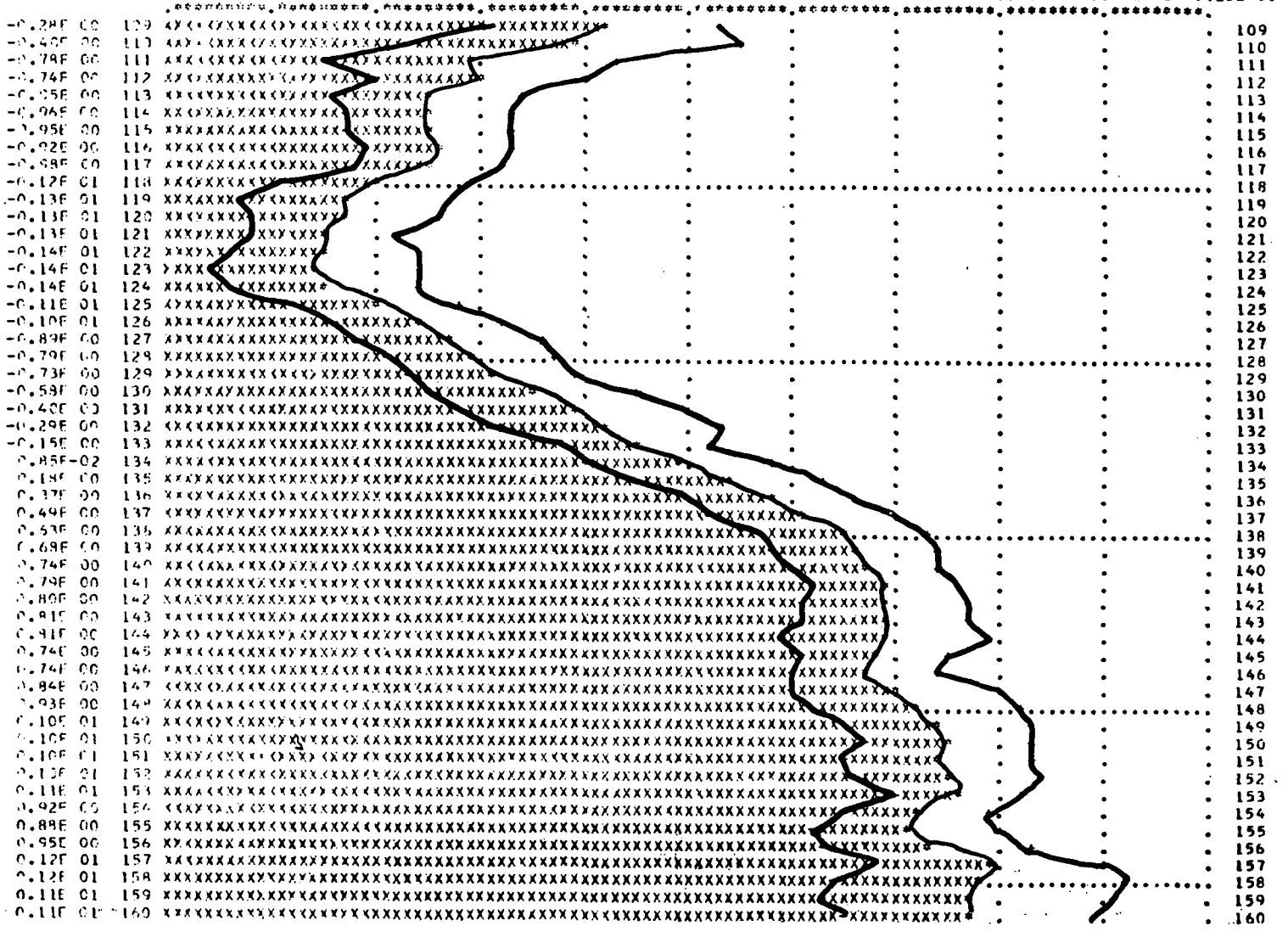

③

UP RAMP SPECTRUM GROUP CALLED -- MX108-1 SAND OVER BASALT II-C 6C011102 02000000 SUN 05/09/71 (12:02)
NUMBER OF SPECTRA IN GROUP: 11
RECORDED FROM 19 9 23685 TO 19 9 26719.
THESE SPECTRA HAVE BEEN RATIOED, SMOOTHED, AND NORMALIZED.

XMIN IS -0.20E 01 XMAX IS 0.20E 01 DELTA IS 0.40E-01

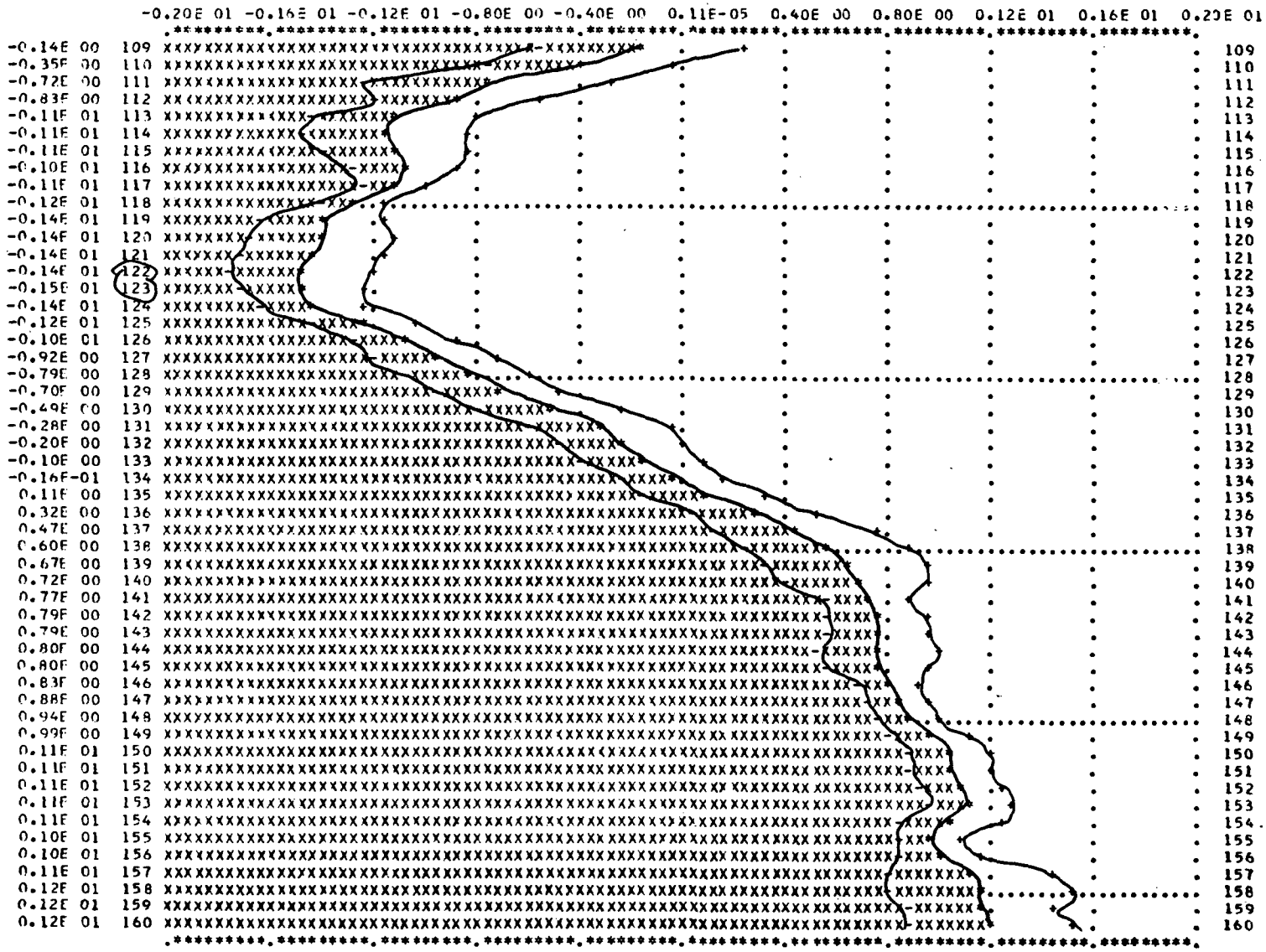

=Y. allowing

SAND OVER BASALT II-C

-54-

64

ALLUVIAL A.

4

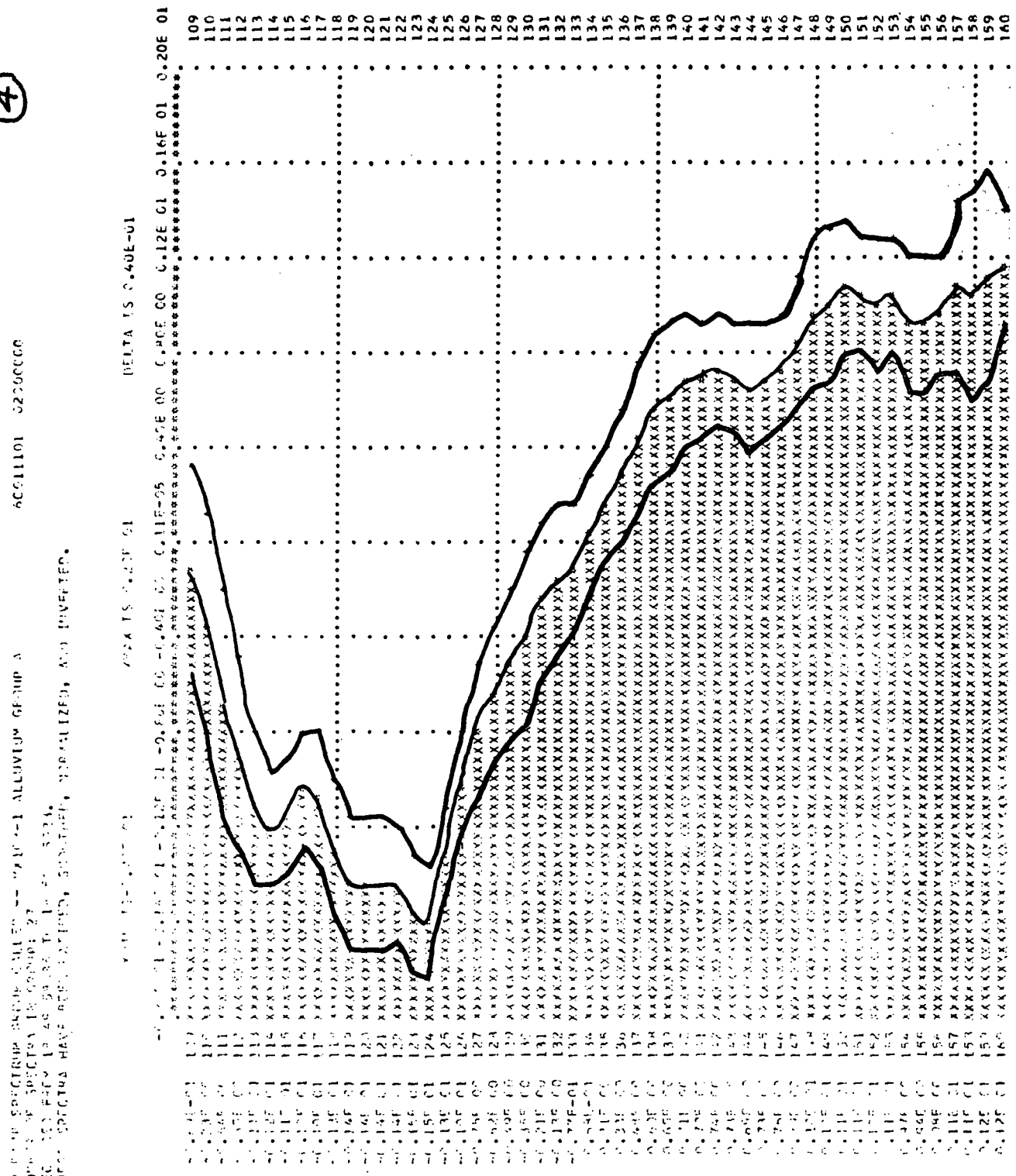

-55-

(5)

UP RAMP SPECTRUM GROUP CALLED -- MX108-1 ALLUVIUM GROUP 6 6C011101 02000000
NUMBER OF SPECTRA IN GROUP: 30
RECORDED FROM 18 50 31050 TO 18 50 43864.
THESE SPECTRA HAVE BEEN RATIOED, SMOOTHED, NORMALIZED, AND INVERTED.

XMIN IS -0.20E 01 XMAX IS 0.20E 01 DELTA IS 0.40E-01

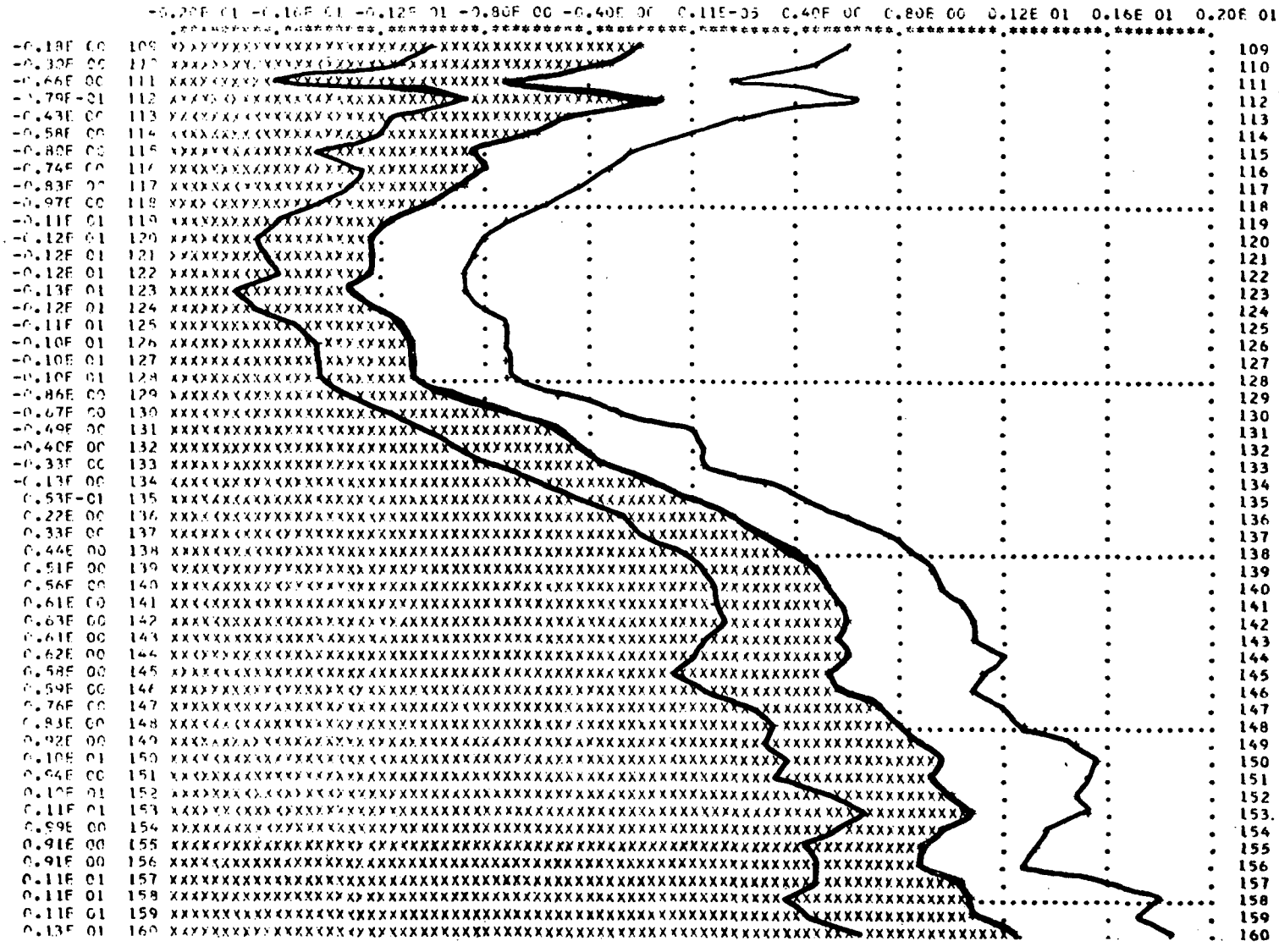

ALLUVIAL B.

-25-

66

SAND OVER BASALT IB

SAND OVER BASALT I-A.

SAND OVER BASALT (170)

(7)

-58-

UP RAMP SPECTRUM GROUP CALLED -- MX108-1 PISGAH FLOW III 60011102 02000000
NUMBER OF SPECTRA IN GROUP: 6
RECORDED FROM 19 8 27252 TO 19 8 28784.
THESE SPECTRA HAVE BEEN RATIOED, SMOOTHED, NORMALIZED, AND INVERTED.

Reproduced from best available copy.

(8)

XMIN IS -0.20E 01 XMAX IS 0.20E 01 DELTA IS 0.40E-01

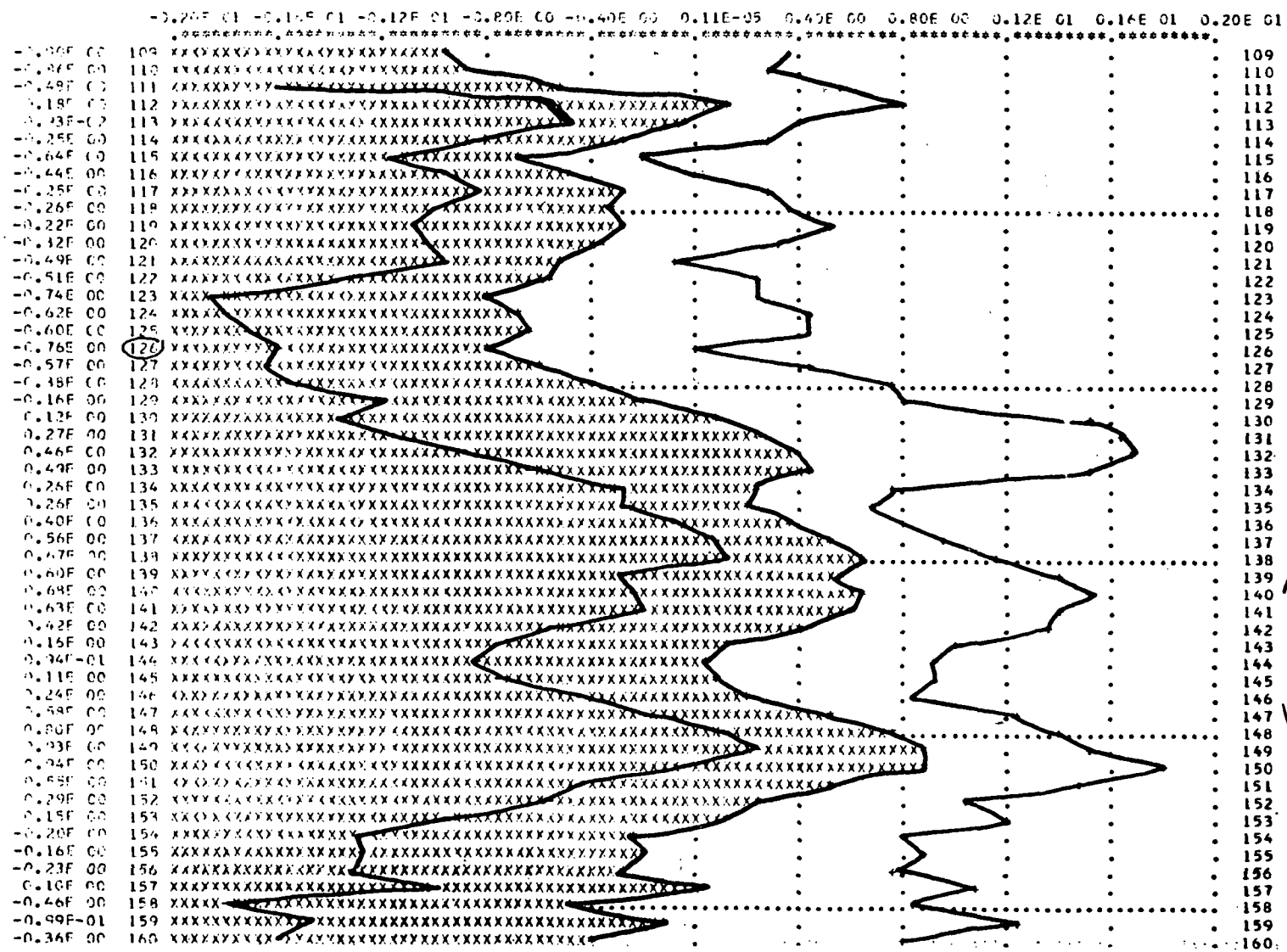

P FLOW III

N=6 (not used)

P FLOW III (1702)

-59-

69

(9)

UP LAMP SPECTRUM GROUP CALLED -- MX108-1 PISGAH FLOW II 6C011102 02000000
NUMBER OF SPECTRA IN GROUP: 4
RECORDED FROM 19 8 25750 TO 19 8 26647.
THESE SPECTRA HAVE BEEN RATIOED, SMOOTHED, NORMALIZED, AND INVERTED.

XMIN IS -0.20E 01 XMAX IS 0.20E 01 DELTA IS 0.40E-01

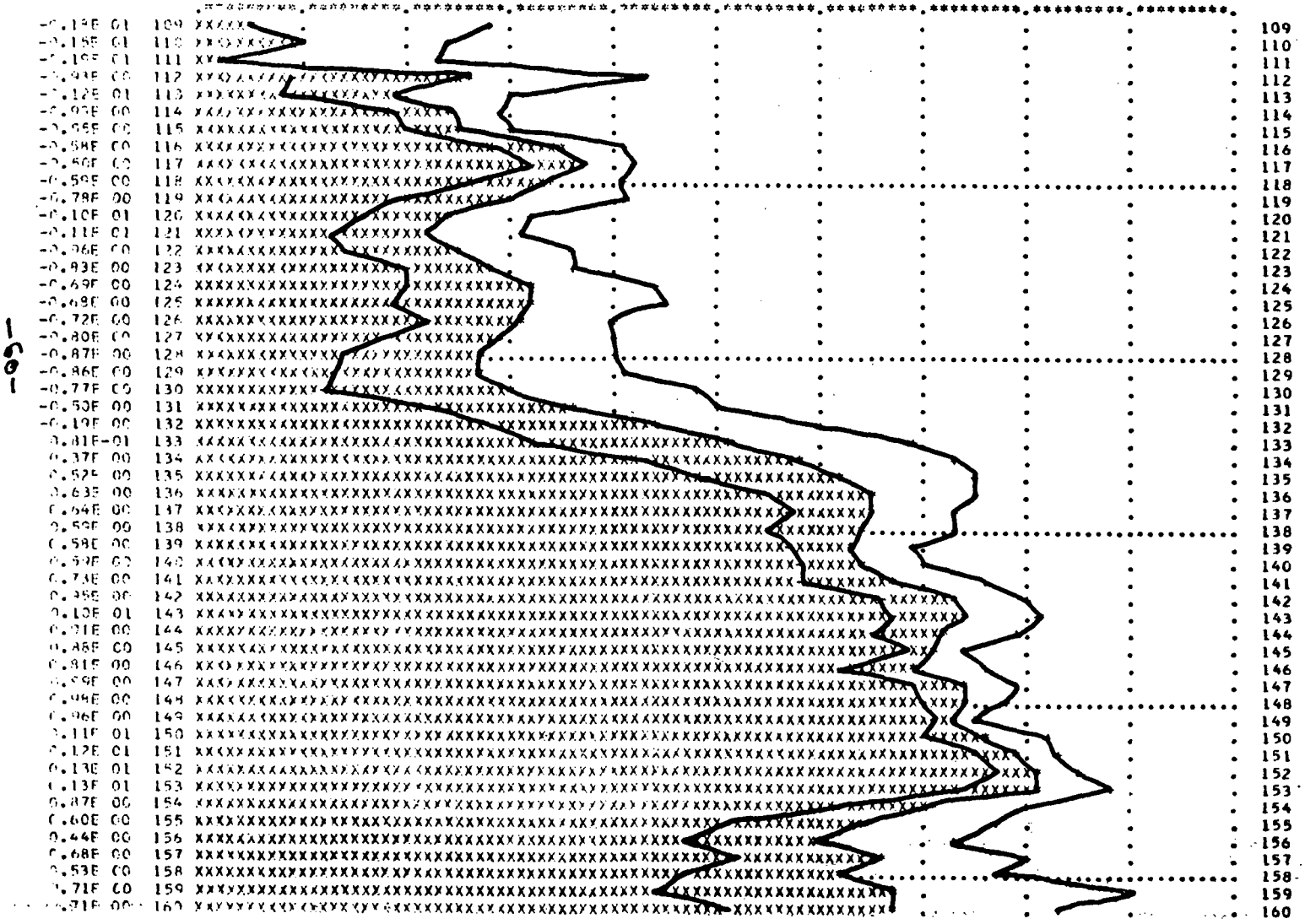

P FLOW II N=4 (not used) P FLOW II (rad)

70

(10)

P FLOW I

P FLOW
I (1202)

-61-

(11)

UP RAMP SPECTRUM GROUP CALLED -- MX108-1 LAVA FLOW II-A 6C011101 02000000 FRI 05/07/71 (15:10)
NUMBER OF SPECTRA IN GROUP: 13
RECORDED FROM 18 51 4785 TO 18 51 13887.
THESE SPECTRA HAVE BEEN RATIOED, SMOOTHED, AND NORMALIZED.

XMIN IS-0.20E 01 XMAX IS 0.20E 01 DELTA IS 0.40E-01

-0.20E 01 -0.16E 01 -0.12E 01 -0.80E 00 -0.40E 00 0.11E-05 0.40E 00 0.80E 00 0.12E 01 0.16E 01 0.20E 01

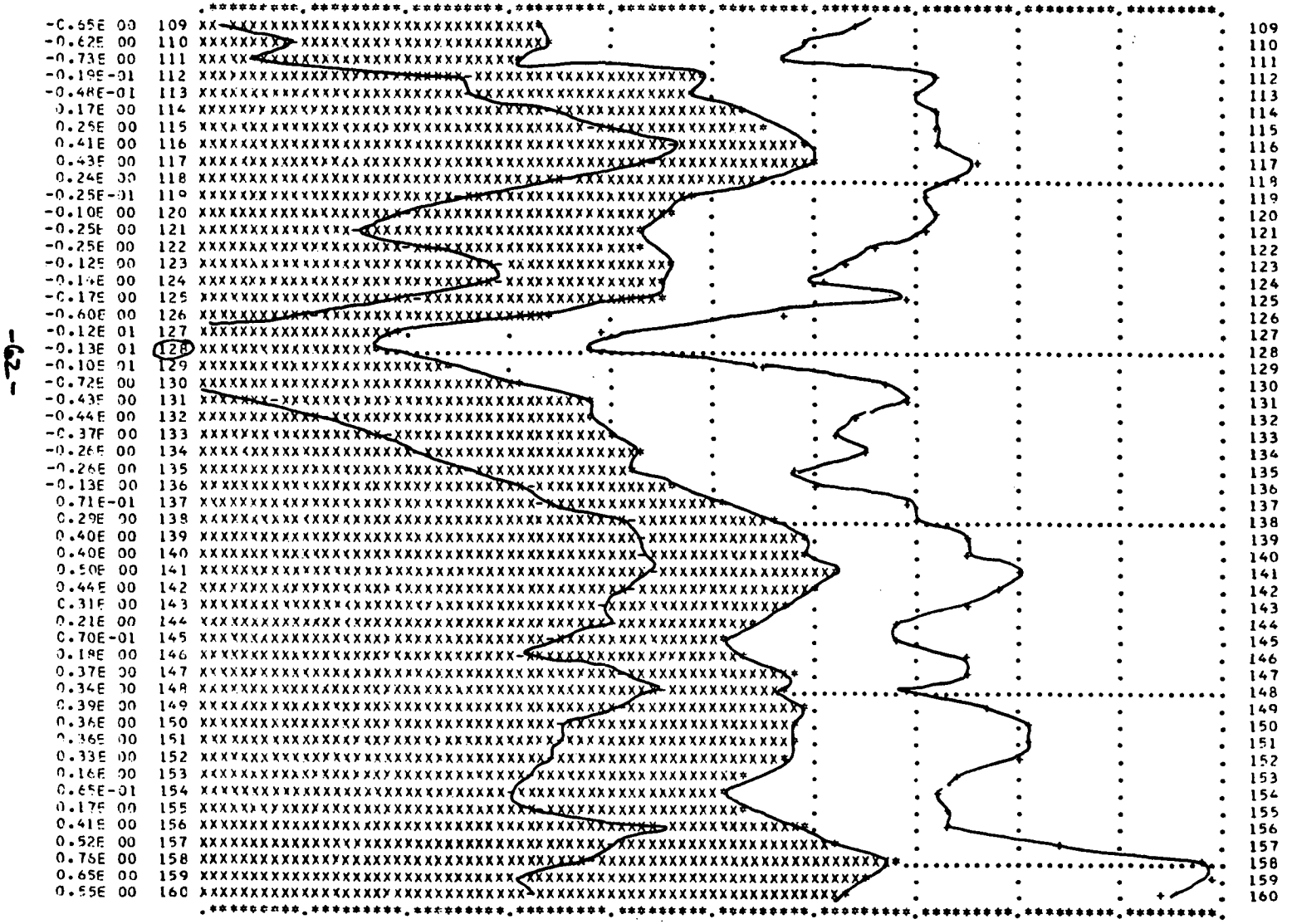

LAVA FLOW II-A.

UP RAMP SPECTRUM GROUP CALLED -- MX108-1 LAVA FLOW II-D 6C011102 02000000 FRI 05/07/71 (15:10)

NUMBER OF SPECTRA IN GROUP: 9

RECORDED FROM 19 8 12083 TO 19 8 16649.

THESE SPECTRA HAVE BEEN RATIOED, SMOOTHED, AND NORMALIZED.

XMIN IS-0.20E 01 XMAX IS 0.20E 01 DELTA IS 0.40E-01

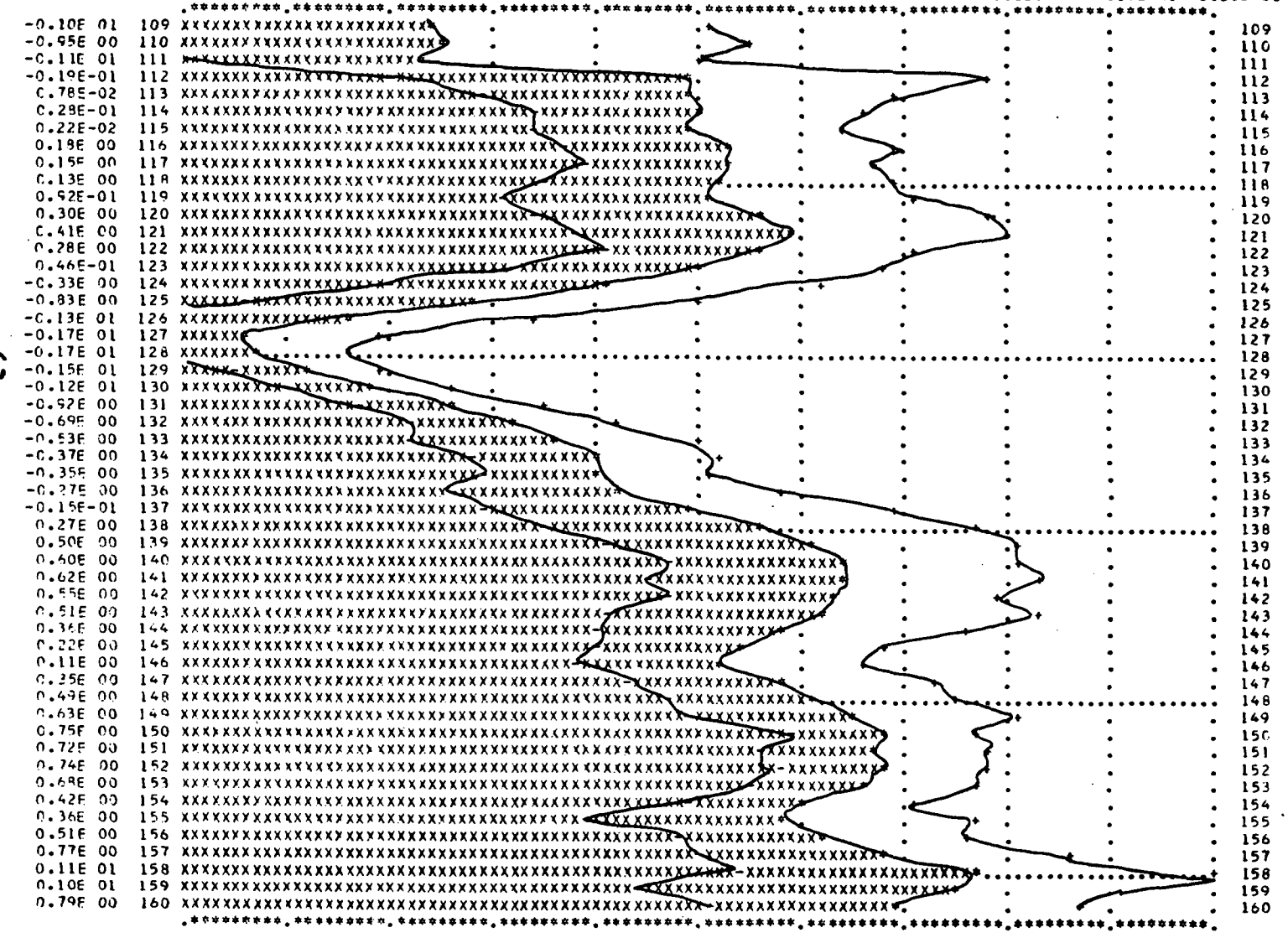

(12)

LAVA FLOW II-D

2

73

P LAVA III A

P LAVA
III - A

(13)

Reproduced from best available copy.

P LAVA III-B

(15)

-65-

P-LAVA III C

P LAVA
III - C

(16)

-66-

UP RAMP SPECTRUM GROUP CALLED -- MX108-1 LAVA III-G 6C011102 02000000 SUN 05/09/71 (12:02)

NUMBER OF SPECTRA IN GROUP: 10

RECORDED FROM 19 7 48418 TO 19 7 55701.

THESE SPECTRA HAVE BEEN RATIOED, SMOOTHED, AND NORMALIZED.

XMIN IS-0.20E 01 XMAX IS 0.20E 01 DELTA IS 0.40E-01

-0.20E 01 -0.16E 01 -0.12E 01 -0.80E 00 -0.40E 00 0.11E-05 0.40E 00 0.80E 00 0.12E 01 0.16E 01 0.20E 01

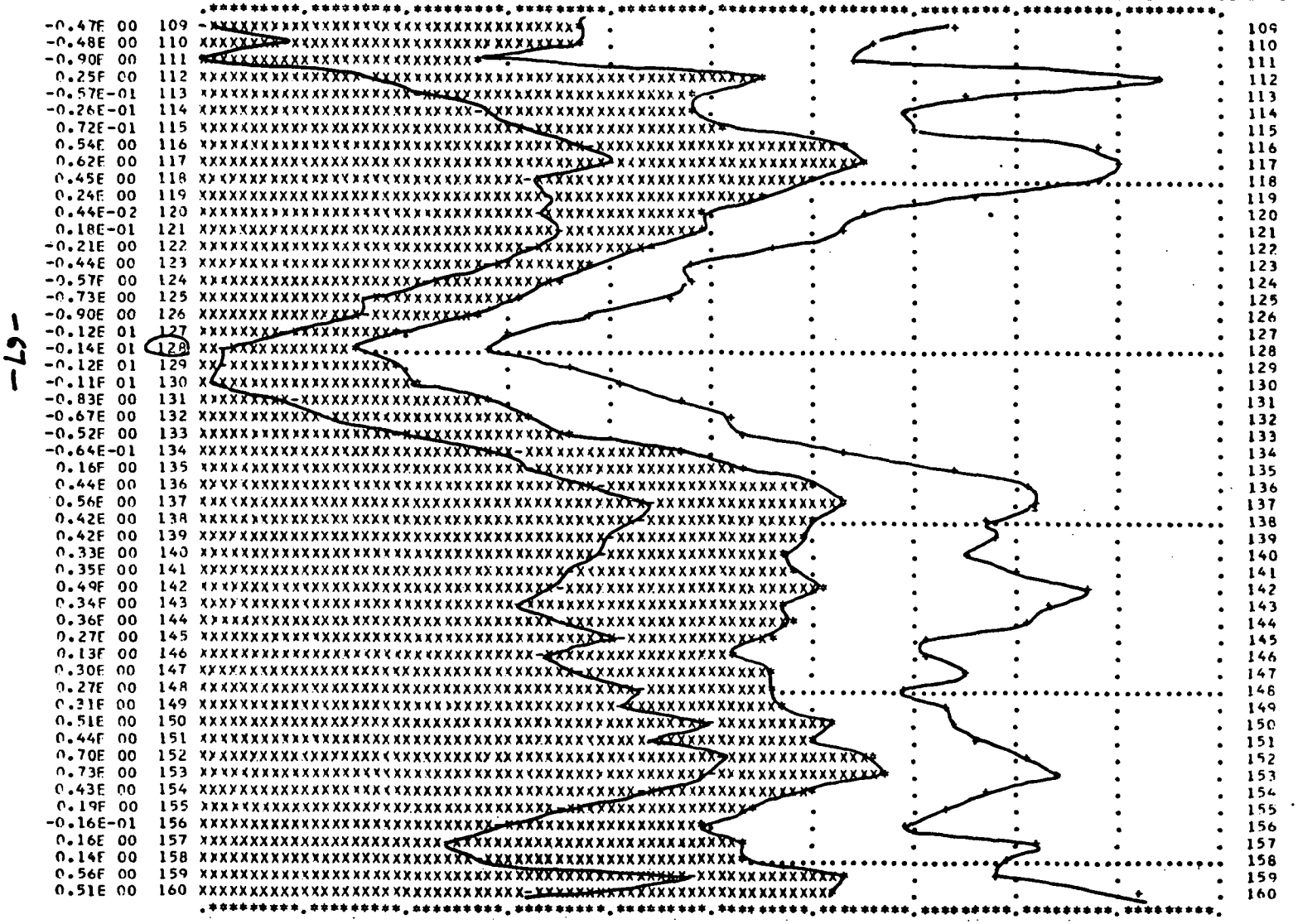

-0.47E 00 109
-0.48E 00 110
-0.90E 00 111
0.25E 00 112
-0.57E-01 113
-0.26E-01 114
0.72E-01 115
0.54E 00 116
0.62E 00 117
0.45E 00 118
0.24E 00 119
0.44E-02 120
0.18E-01 121
-0.21E 00 122
-0.44E 00 123
-0.57E 00 124
-0.73E 00 125
-0.90E 00 126
-0.12E 01 127
-0.14E 01 128
-0.12E 01 129
-0.11E 01 130
-0.83E 00 131
-0.67E 00 132
-0.52E 00 133
-0.64E-01 134
0.16E 00 135
0.44E 00 136
0.56E 00 137
0.42E 00 138
0.42E 00 139
0.33E 00 140
0.35E 00 141
0.49E 00 142
0.34E 00 143
0.36E 00 144
0.27E 00 145
0.13E 00 146
0.30E 00 147
0.27E 00 148
0.31E 00 149
0.51E 00 150
0.44E 00 151
0.70E 00 152
0.73E 00 153
0.43E 00 154
0.19E 00 155
-0.16E-01 156
0.16E 00 157
0.14E 00 158
0.56E 00 159
0.51E 00 160

-67-

UP RAMP SPECTRUM GROUP CALLED -- VXIC4-1 PISGAH LAVA (GROUP 01). 6C011101 02000C00

NUMBER OF SPECTRA IN GROUP: 12

RECORDED FROM 18 51 34837 TO 18 51 38161.

THESE SPECTRA HAVE BEEN FATIJED, SMOOTHED, NORMALIZED, AND INVERTED.

(18)

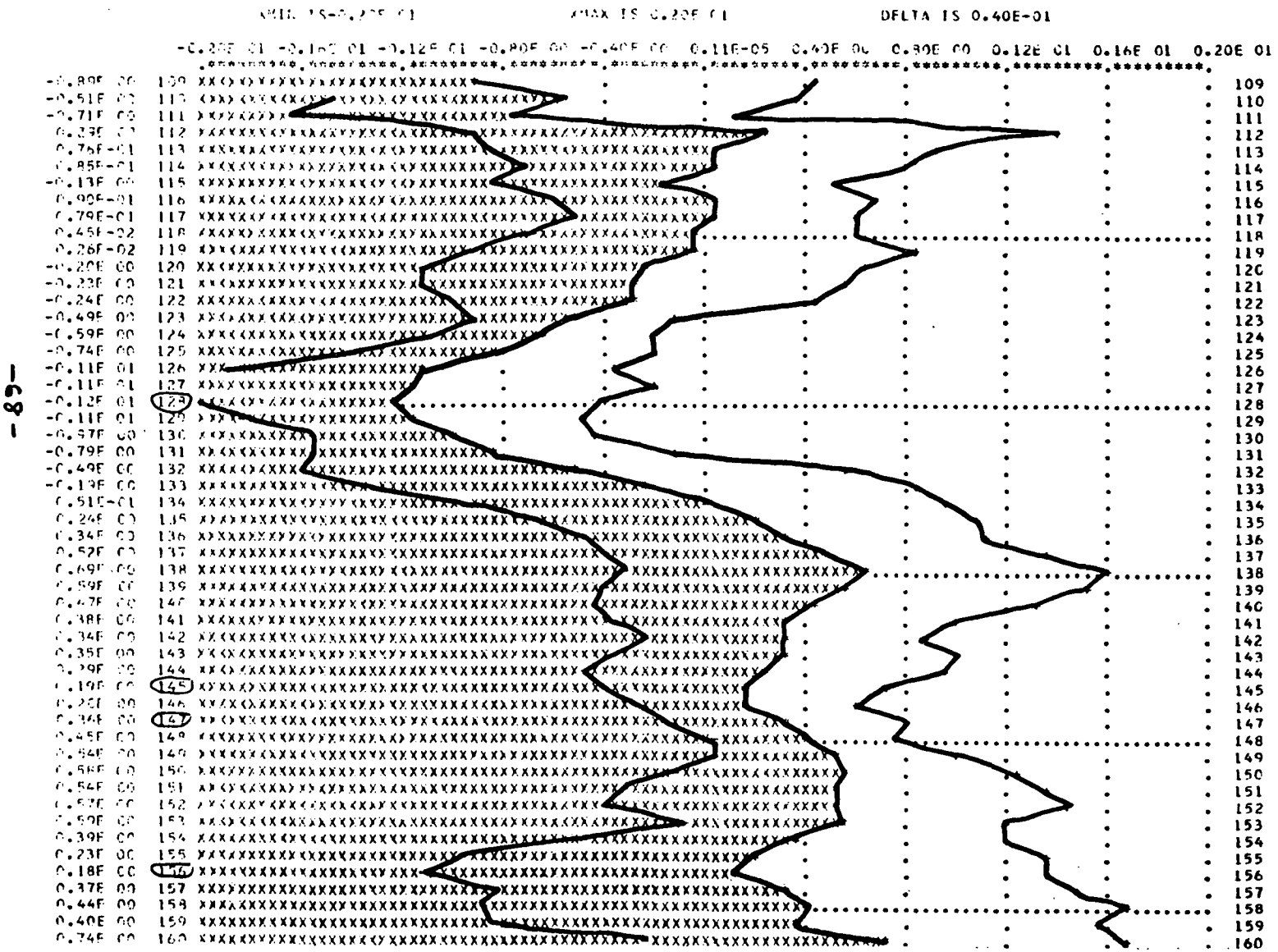

-89-

84

PLATE III-D

UP RAMP SPECTRUM GROUP CALLED -- MX108-1 LAVA III-H oC011102 02000000 SUN 05/09/71 (12:02)

NUMBER OF SPECTRA IN GROUP: 8

RECORDED FROM 19 7 46241 TO 19 7 46309.

THESE SPECTRA HAVE BEEN RATIOED, SMOOTHED, AND NORMALIZED.

TYPE 3

(19)

XMIN IS-0.20E 01 XMAX IS 0.20E 01 DELTA IS 0.40E-01

-0.20E 01 -0.16E 01 -0.12E 01 -0.80E 00 -0.40E 00 0.11E-05 0.40E 00 0.80E 00 0.12E 01 0.16E 01 0.20E 01

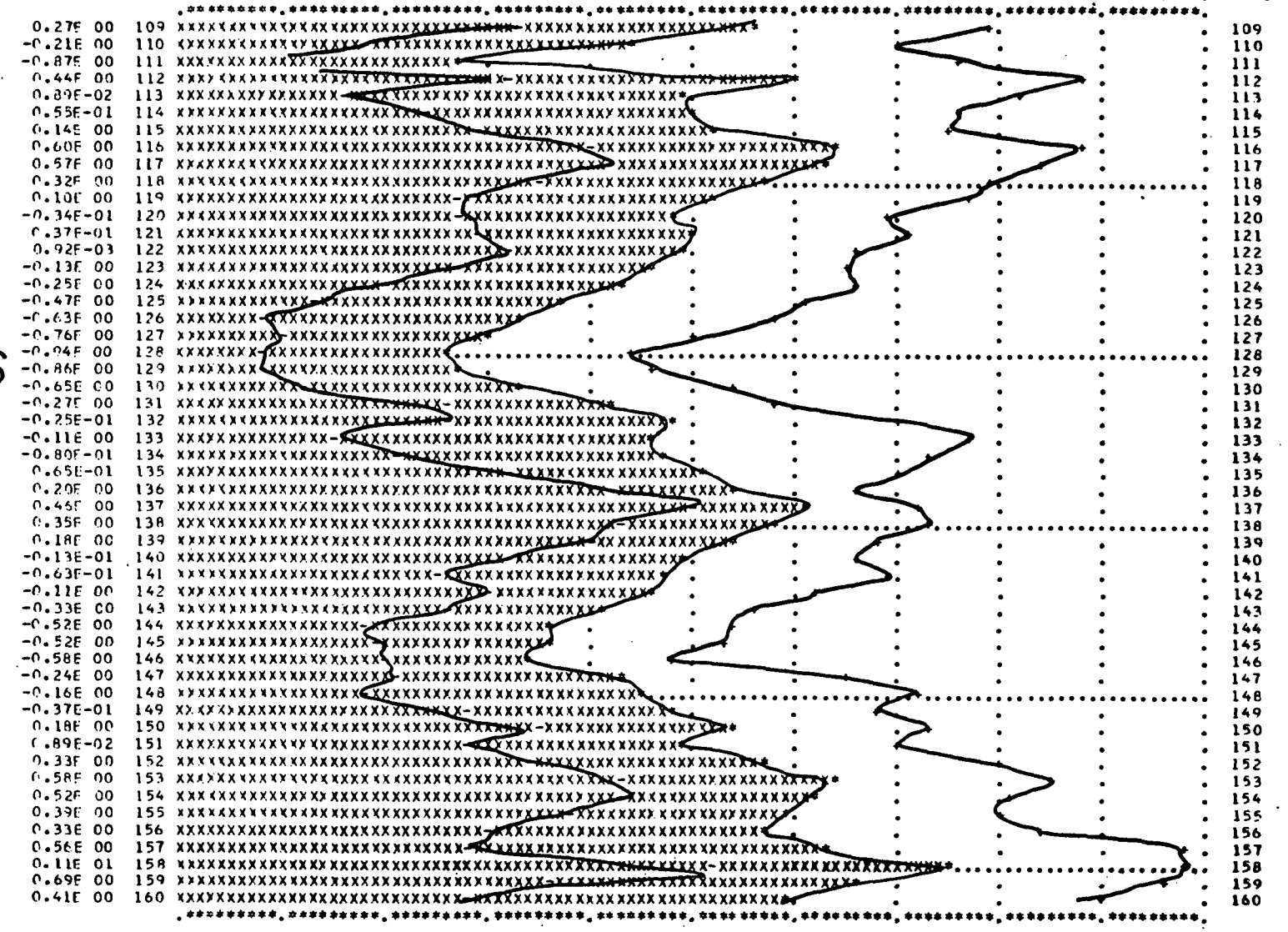

III-H Type 3

62

DELTA IS 0.40E-01
0.40E 00 0.80E 00 0.12E 01 0.16E 01 0.20E 01

UP RAMP SPECTRUM GROUP CALLED -- MX10R-1 LAVA III-J (21) 6C011102 02000000 SUN 05/09/71 (12:02) (21)
NUMBER OF SPECTRA IN GROUP: 16
RECORDED FROM 19 7 31746 TO 19 7 39317.
THESE SPECTRA HAVE BEEN RATIOED, SMOOTHED, AND NORMALIZED.

XMIN IS-0.20E 01 XMAX IS 0.20E 01 DELTA IS 0.40E-01

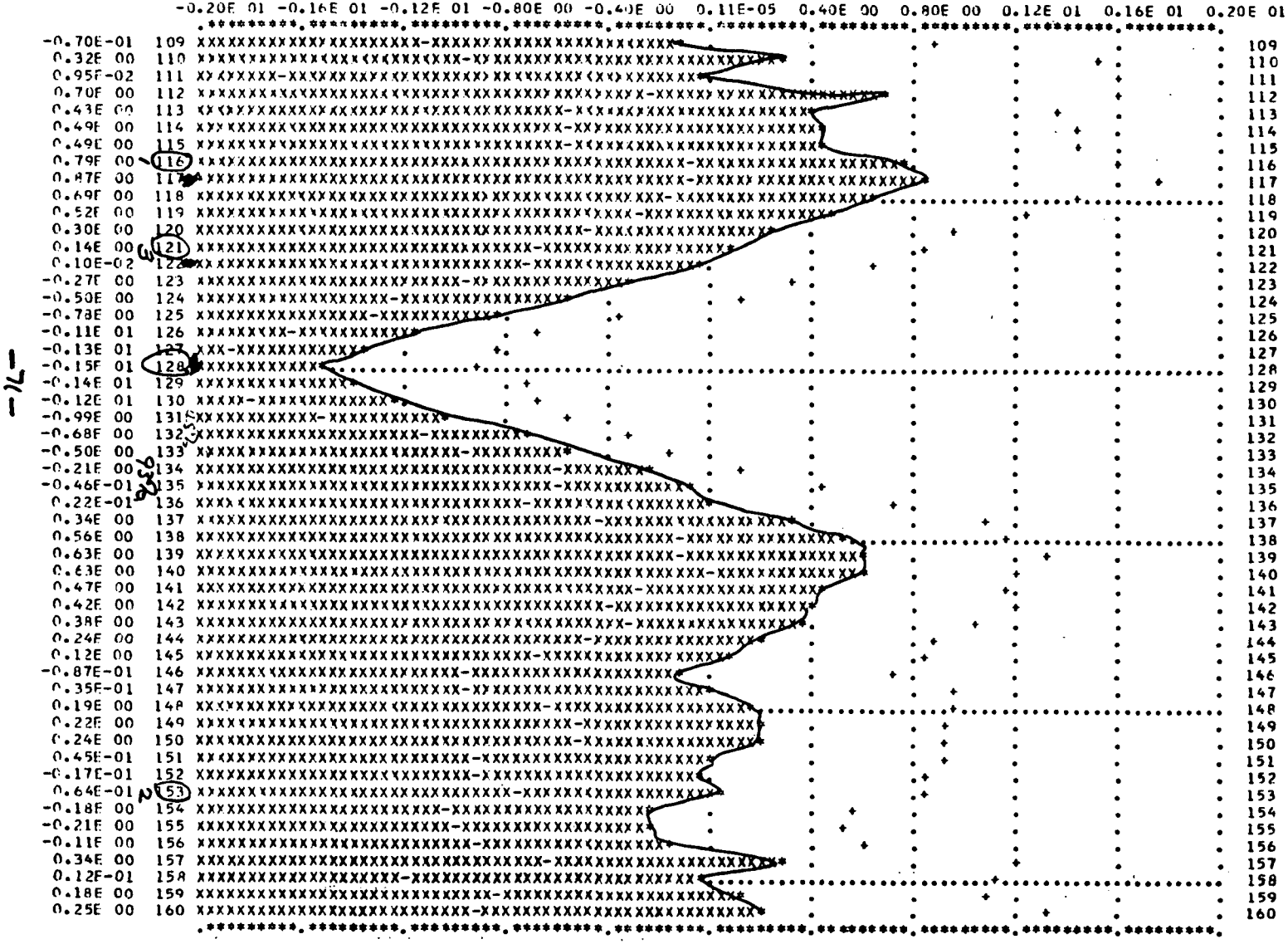

(22)

UP BAND SPECTRUM GROUP CALLED -- MYICA-1 ALLUVIUM GROUP 0 6C011101 02000000
NUMBER OF SPECTRA IN GROUP: 21
RECORDED FROM 18 51 58196 TO 18 52 4254.
THESE SPECTRA HAVE BEEN RATIOED, SMOOTHED, NORMALIZED, AND INVERTED.

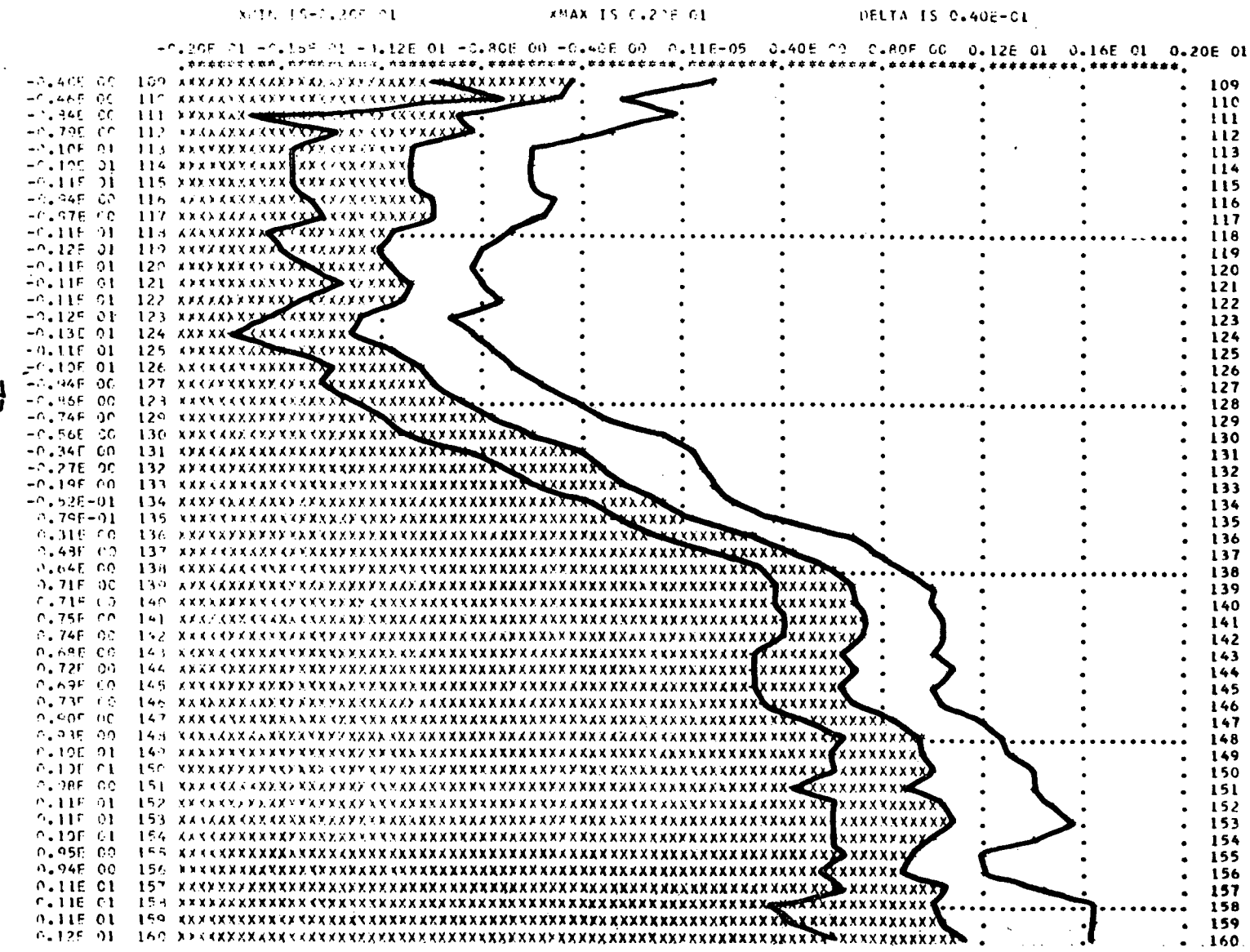

-72-

28

UP RAMP SPECTRUM GROUP CALLED -- MX108-1 LAVA I-K 6CC11102 02000000 SUN 05/09/71 (12:02) (23)
NUMBER OF SPECTRA IN GROUP: 16
RECORDED FROM 19 7 15652 TO 19 7 20506.
THESE SPECTRA HAVE BEEN RATIOED, SMOOTHED, AND NORMALIZED.

XMIN IS-0.20E 01 XMAX IS 0.20E 01 DELTA IS 0.40E-01

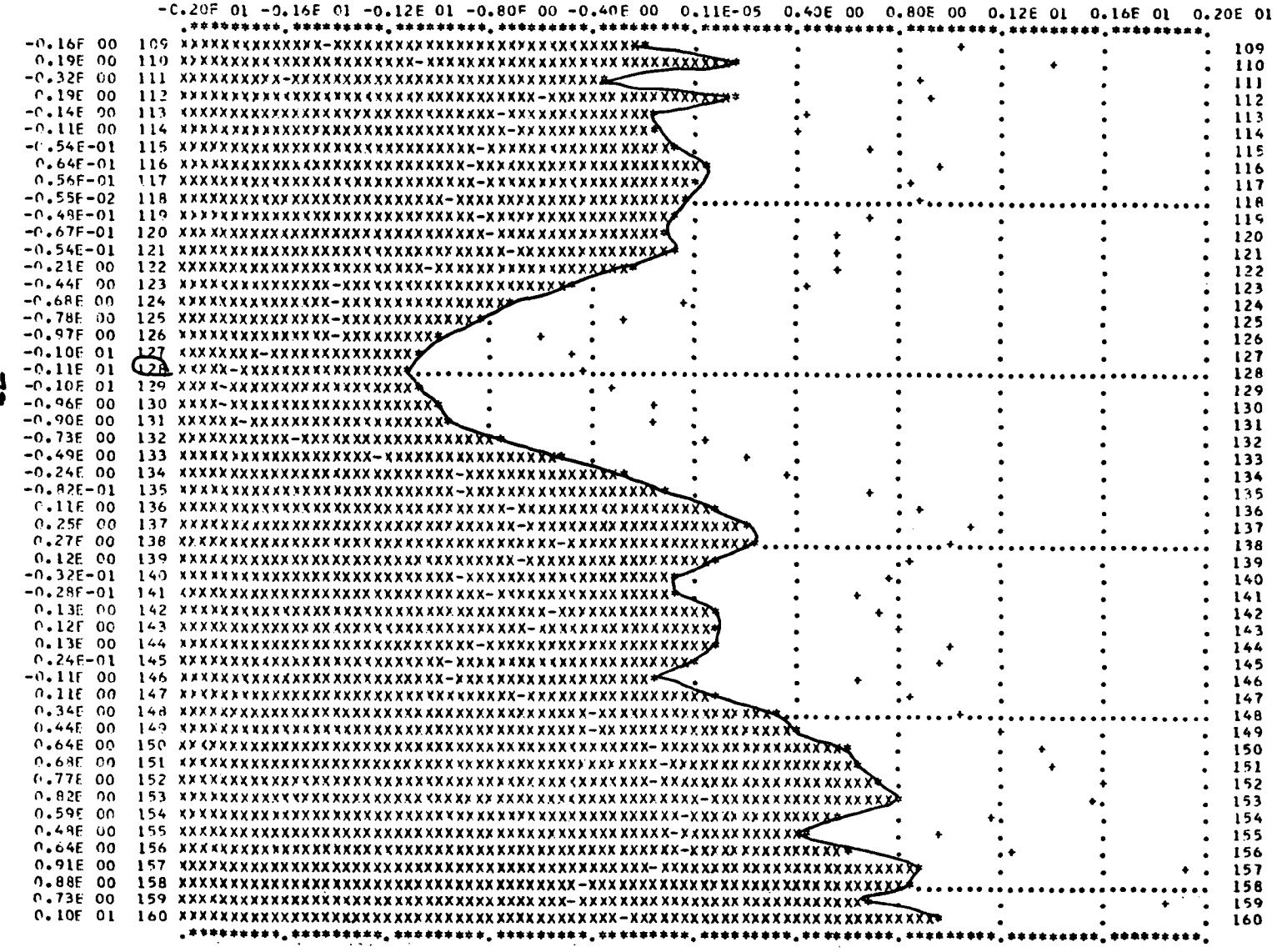

-73-

83

(24)

UP RAMP SPECTRUM GROUP CALLED -- MX109-1 LAVA FLOW II-C 6C011102 02000C00 FRI 05/07/71 (15:10)
NUMBER OF SPECTRA IN GROUP: 10
RECORDED FROM 19 7 8371 TO 19 7 14439.
THESE SPECTRA HAVE BEEN RATIOED, SMOOTHED, AND NORMALIZED.

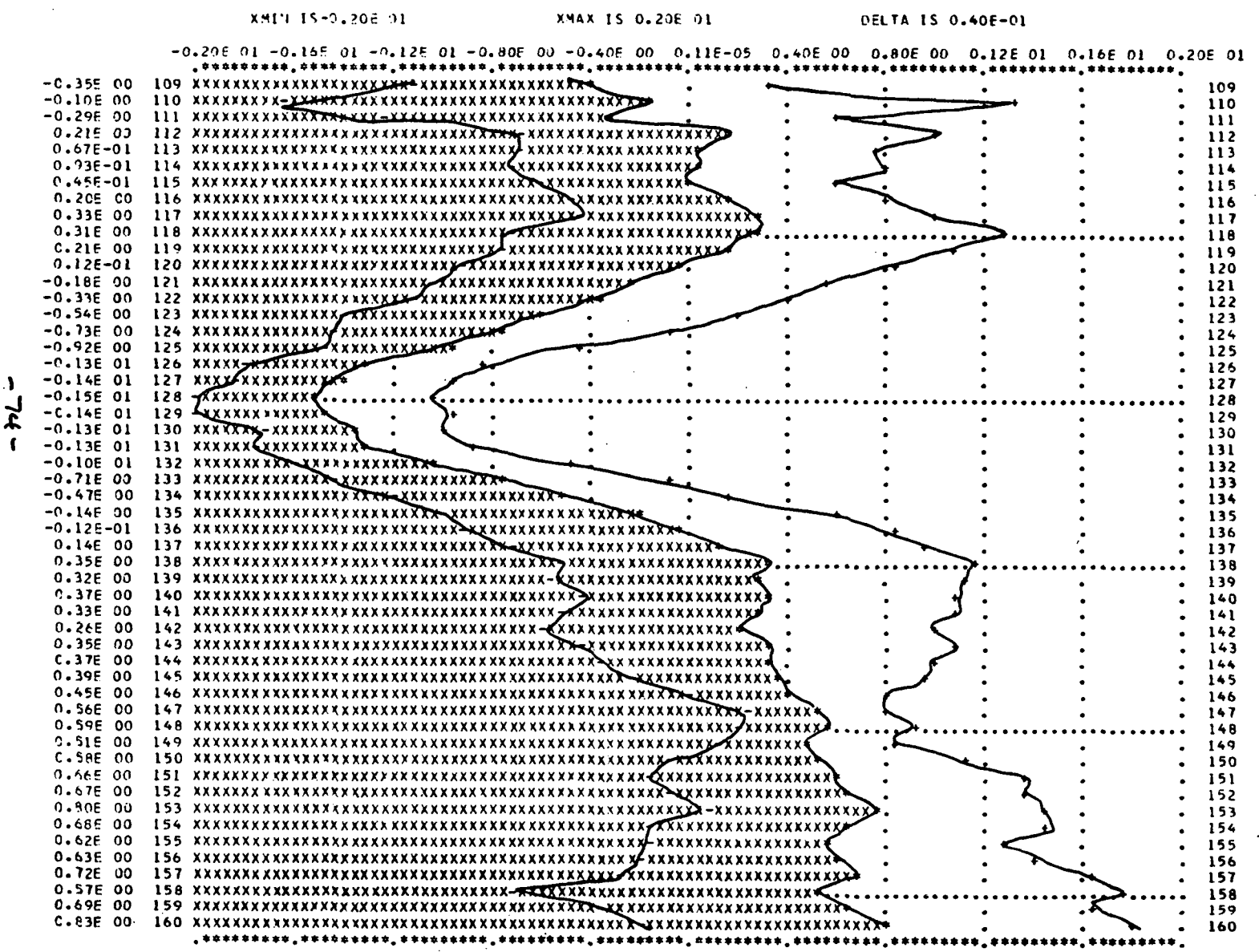

-74-

84

UP RAMP SPECTRUM GROUP CALLED -- MX108-1 LAVA FLOW II-B 6C011101 02000000 FRI 05/07/71 (15:10)

NUMBER OF SPECTRA IN GROUP: 10

RECORDED FROM 18 52 12461 TO 18 52 16998.

THESE SPECTRA HAVE BEEN RATICED, SMOOTHED, AND NORMALIZED.

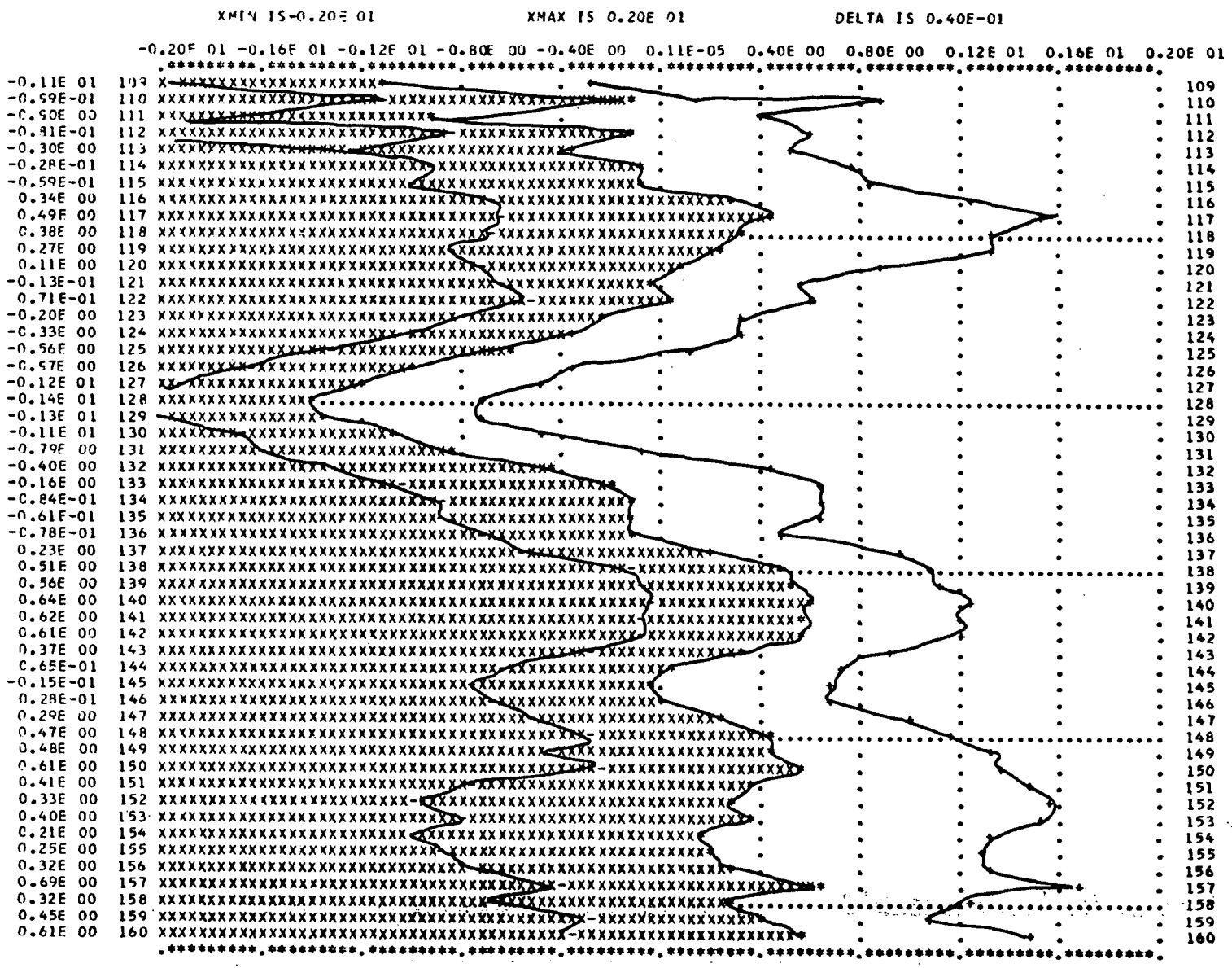

P LAVA
I E

UP RAMP SPECTRUM GROUP CALLED -- [illegible] DRY LAKE SEDIMENTS B 60311102 02000000

NUMBER OF SPECTRA IN GROUP: 24

RECORDED FROM 13 [illegible] TO 14 [illegible].

THESE SPECTRA HAVE BEEN RATIOED, SMOOTHED, NORMALIZED, AND INVERTED.

(27)

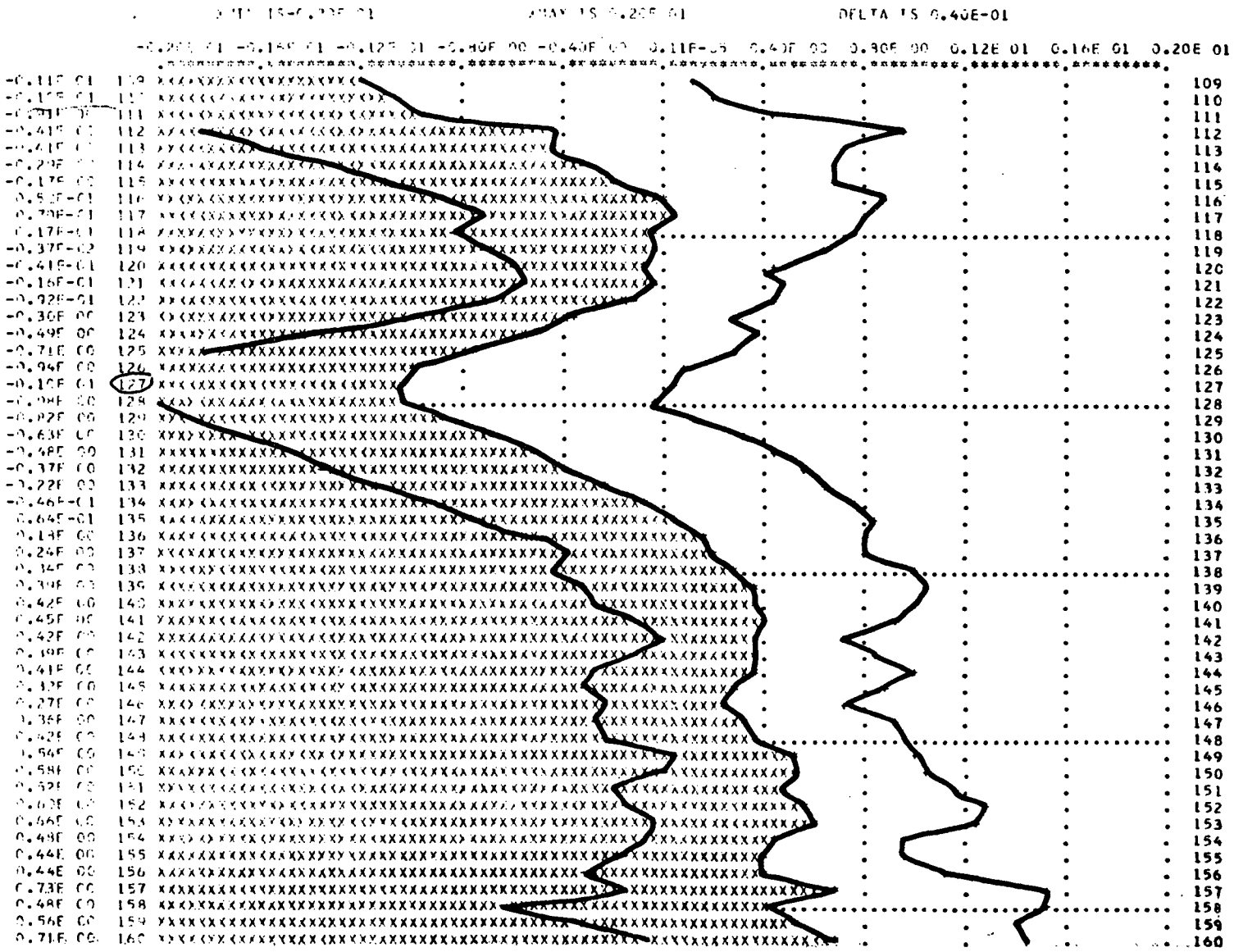

-77-

87

UP RAMP SPECTRUM GROUP CALLED -- MXI 3-1 DRY LAKE SEDIMENTS A 5C011201 02000000
NUMBER OF SPECTRA IN GROUP: 53
RECORDED FROM 13 57 [illegible] TO 13 57 [illegible].
THESE SPECTRA HAVE BEEN RATIOED, SMOOTHED, NORMALIZED, AND INVERTED.

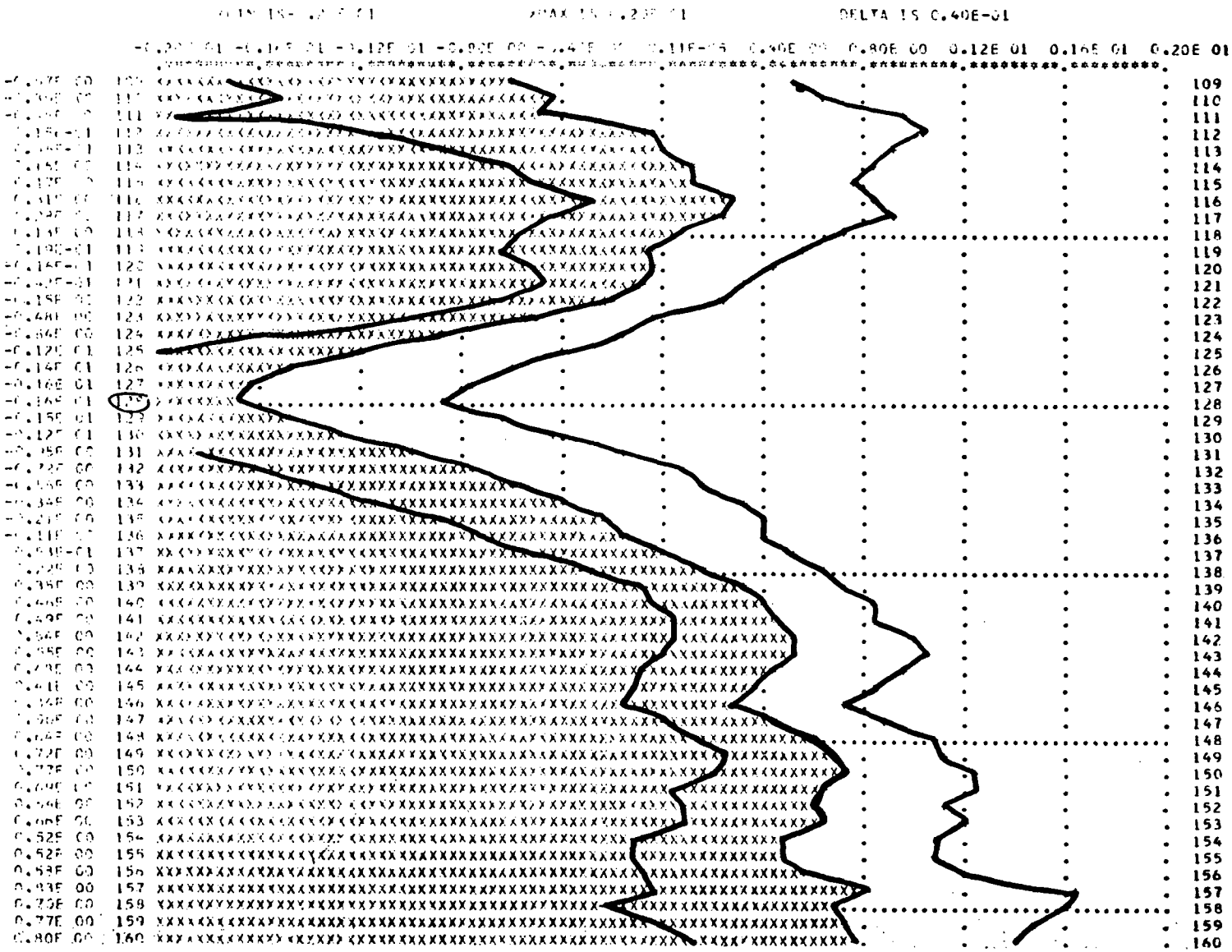

88

(29)

UP DAMP SPECTRUM GROUP CALLED -- MX108-1 DRY LAKE SEDIMENTS C 6C011102 02000000
NUMBER OF SPECTRA IN GROUP: 25
RECORDED FROM 19 6 34392 TO 19 6 41671.
THESE SPECTRA HAVE BEEN RATIOED, SMOOTHED, NORMALIZED, AND INVERTED.

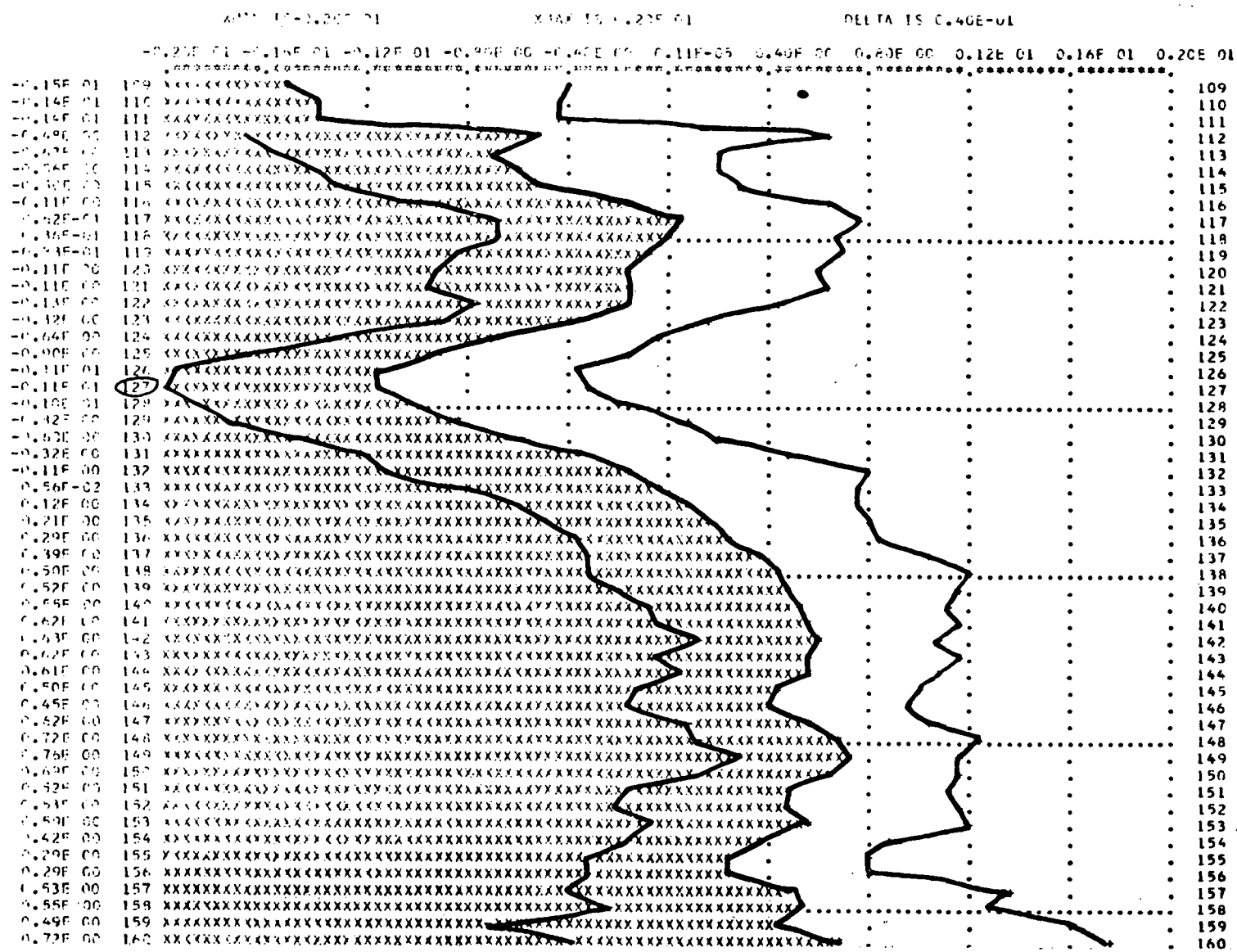

-79-

89

(30)

UP RAMP SPECTRUM GROUP CALLED -- MX118-1 ALLUVIUM GROUP F 6C011102 02000000
NUMBER OF SPECTRA IN GROUP: 42
RECORDED FROM 19 6 14078 TO 19 6 26501.
THESE SPECTRA HAVE BEEN RATIOED, SMOOTHED, NORMALIZED, AND INVERTED.

XMIN IS -0.20E 01 XMAX IS 0.20E 01 DELTA IS 0.40E-01

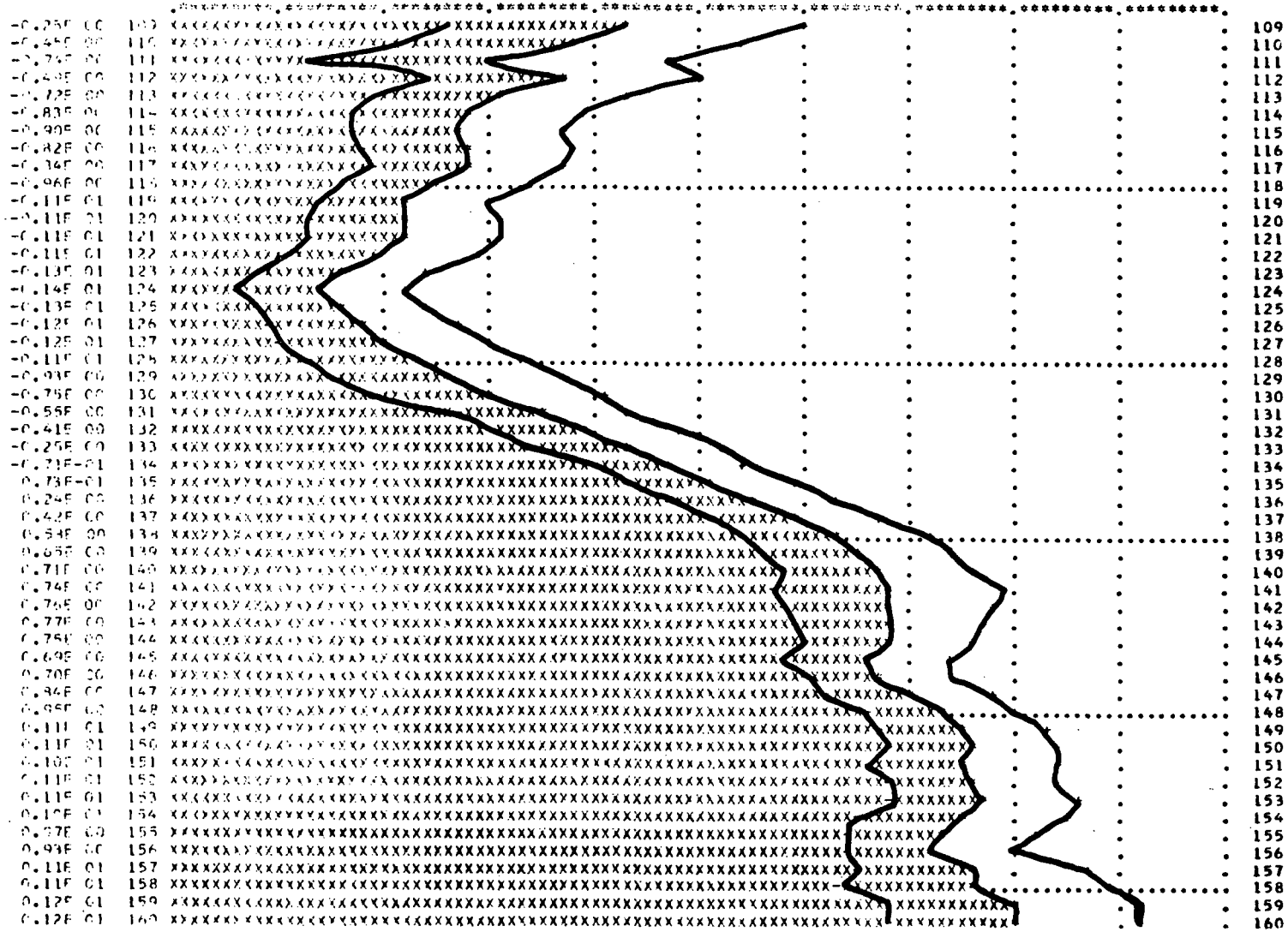

90

(31)

UP RAMP SPECTRUM GROUP CALLED -- [illegible]-1 ALLUVIUM GROUP E 5C011101 02000000
NUMBER OF SPECTRA IN GROUP: 27
RECORDED FROM 18 52 [illegible] TO 18 53 7681.
THESE SPECTRA HAVE BEEN RATIOED, SMOOTHED, NORMALIZED, AND INVERTED.

XMIN IS -0.20E 01 XMAX IS 0.20E 01 DELTA IS 0.40E-01

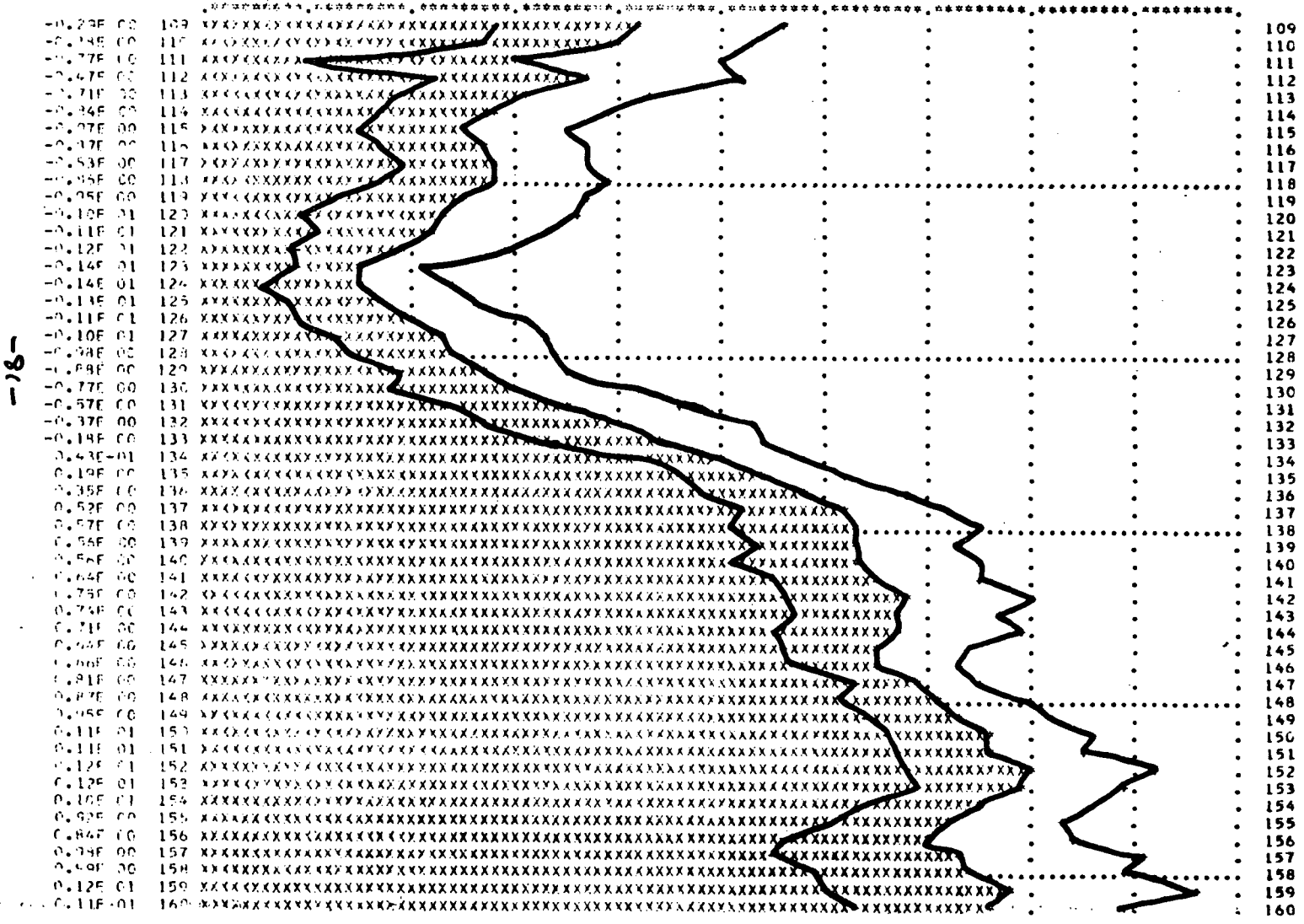

91

P TRAIN LAVA III

PLANA III (A-D) (13+15+16+18) Type 2.

PLANA
(A-D) III

P LAVA IV 6+H+J
(17+19+21)

-84-

P LAVA III A+B+C+D
N = 34.
≡ III(A-D)(13+15+16+18)

P LAVA II (A+D)

(11+12)

-86-

P LAVA II(B+C) (25+24)

-87-

Pisgah Cinder III N=9. no site #

-88-

DRY LAKE SEDS A+B+C.

(28+27+29 Silts)

-89-

Alluvial A+AC+C

(Site 4+2+1)

Sunshine Lava A.

-91

Semehnie Lava B

Sunshine Cinders C.

Sunshine Cinder D.

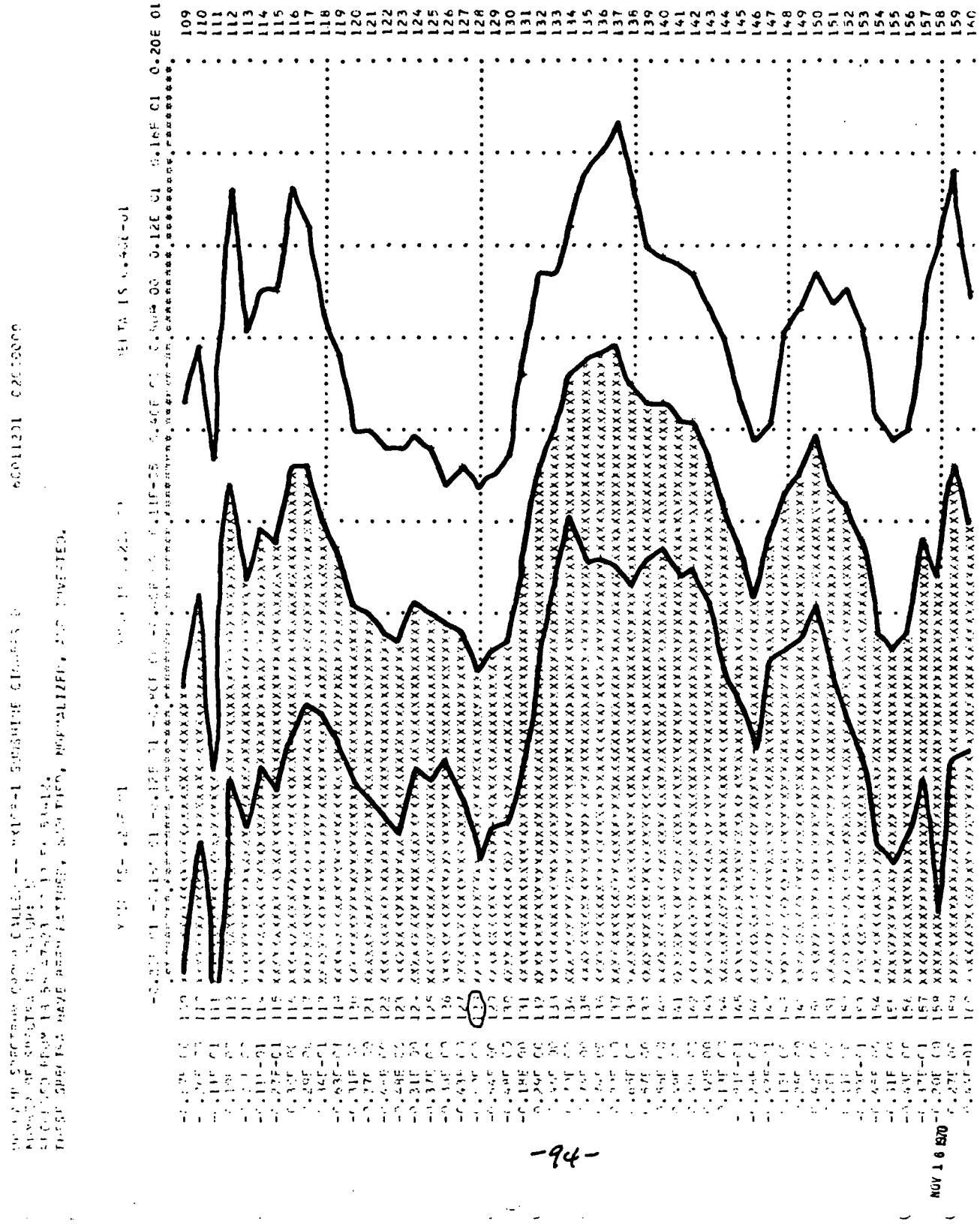

MX108-3- (1)

UP RAMP SPECTRUM GROUP CALLED -- MX103-3 GMP I 60033502 16000000 TRK 047/1471 (15330)
NUMBER OF SPECTRA IN GROUP: 23
RECORDED FROM 17 13 56084 TO 17 14 5359.
THE SPECTRA HAVE BEEN RATIOED, SMOOTHED, AND NORMALIZED.

XMIN IS -0.20E 01 XMAX IS 0.20E 01 DELTA IS 0.40E-01

-0.20E 01 -0.16E 01 -0.12E 01 -0.80E 00 -0.40E 00 0.11E-05 0.40E 00 0.80E 00 0.12E 01 0.16E 01 0.20E 01

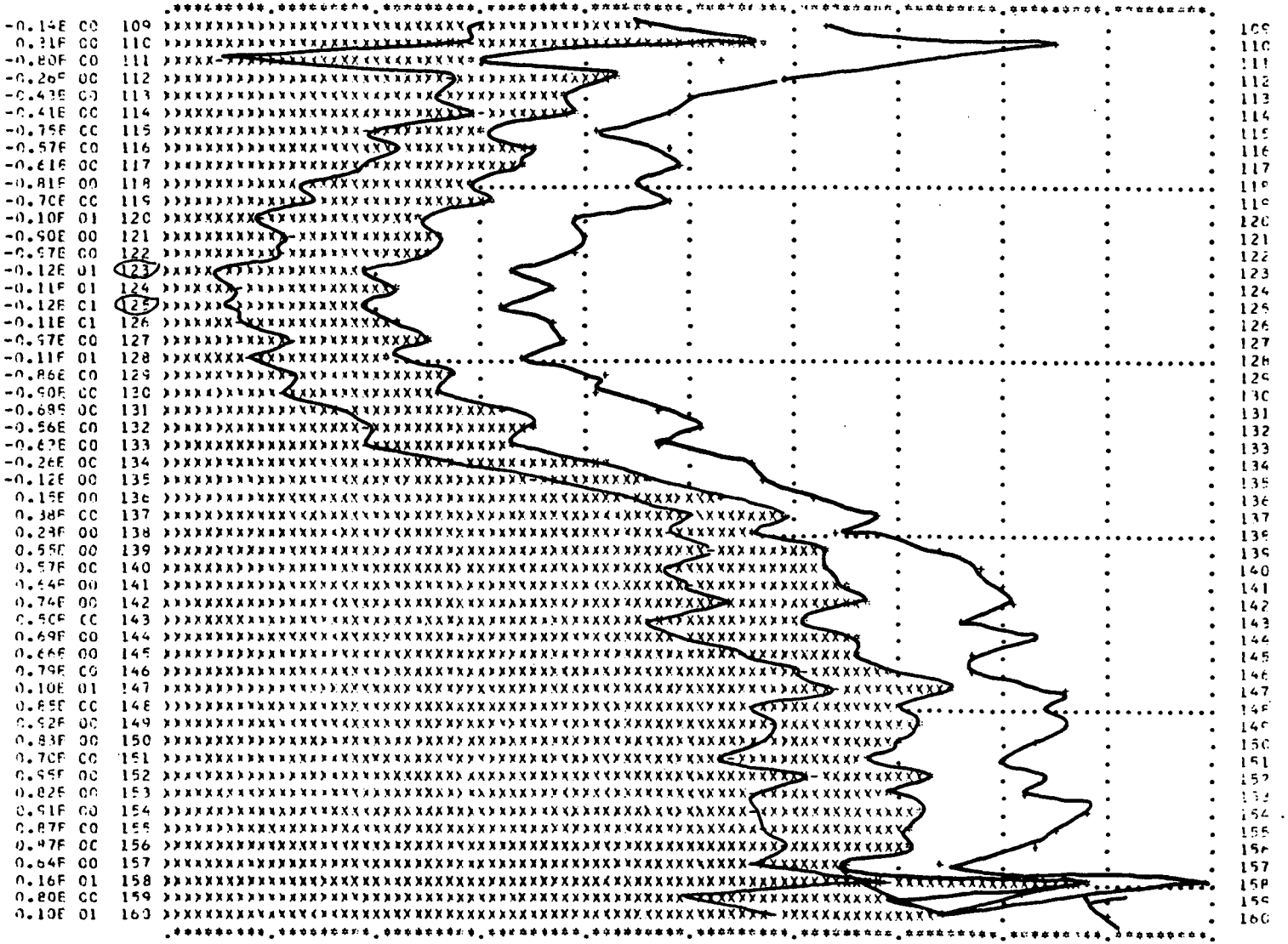

QMP I

N=23

-95-

105

②

MX108-3 -

OMP II

N=23

Basaltic Pebbles on Playa

PEB I

N = 27

MX10P-3-

(3)

-97-

MX108-3- ④

UP RAMP SPECTRUM GROUP CALLED -- MX108-3 PEBBLES II 6C030903 16000000 THR 04/01/71 (15:30)
NUMBER OF SPECTRA IN GROUP: 27
RECORDED FROM 17 21 56429 TO 17 22 4311.
THE SPECTRA HAVE BEEN RATIOED, SMOOTHED, AND NORMALIZED.

XMIN IS-0.20E 01 XMAX IS 0.20E 01 DELTA IS 0.40E-01

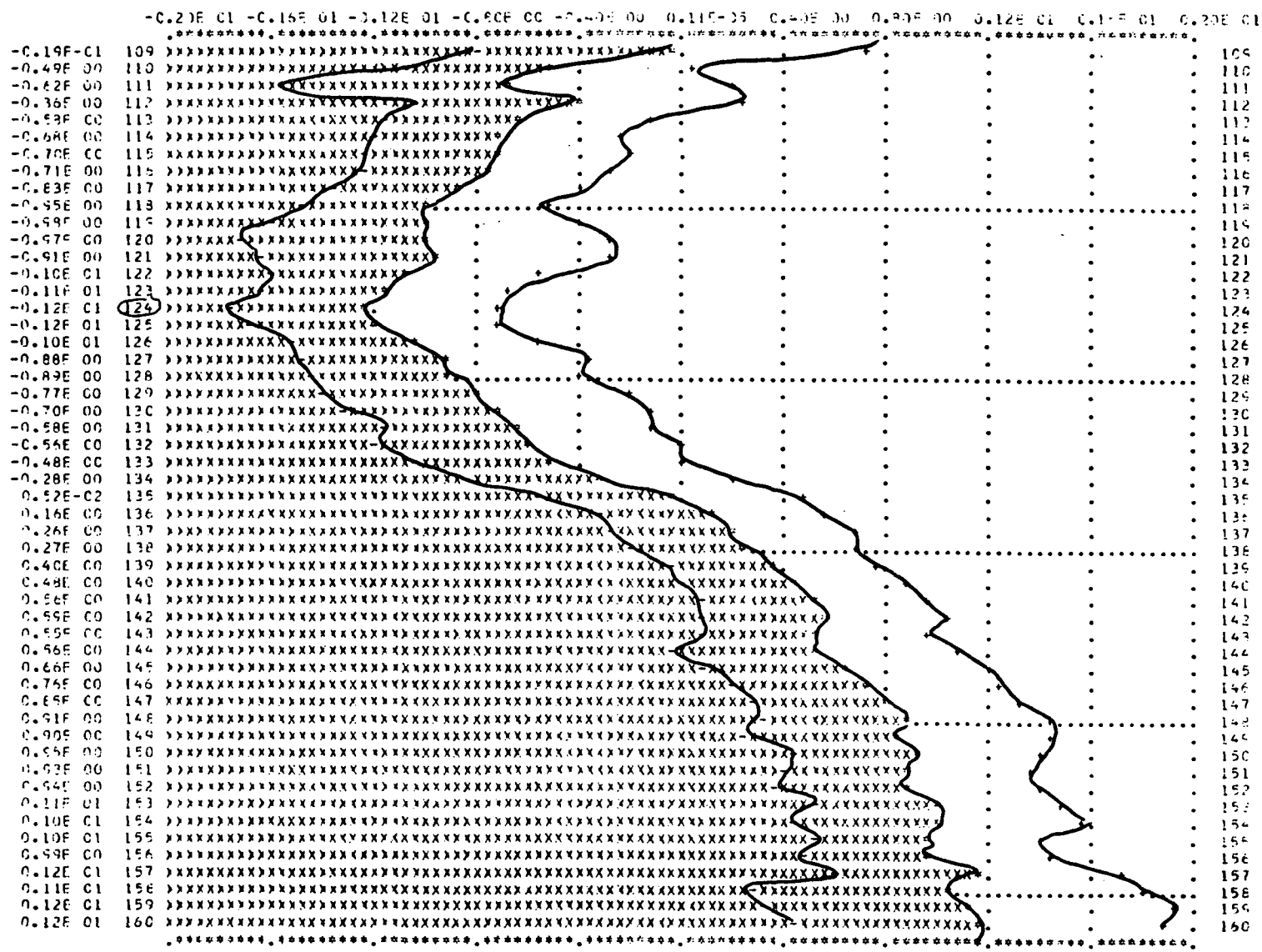

Barattie Pebbles on Playa
PEB II
N=27

108

MX108-3- (5)

UP RAMP SPECTRUM GROUP CALLED -- MX109-3 OUT I 60030502 16000000 THR 04/01/71 (15:30)
NUMBER OF SPECTRA IN GROUP: 35
RECORDED FROM 17 13 35560 TO 17 13 46267.
THE SPECTRA HAVE BEEN RATICED, SMOOTHED, AND NORMALIZED.

XMIN IS-0.20E 01 XMAX IS 0.20E 01 DELTA IS 0.40E-01

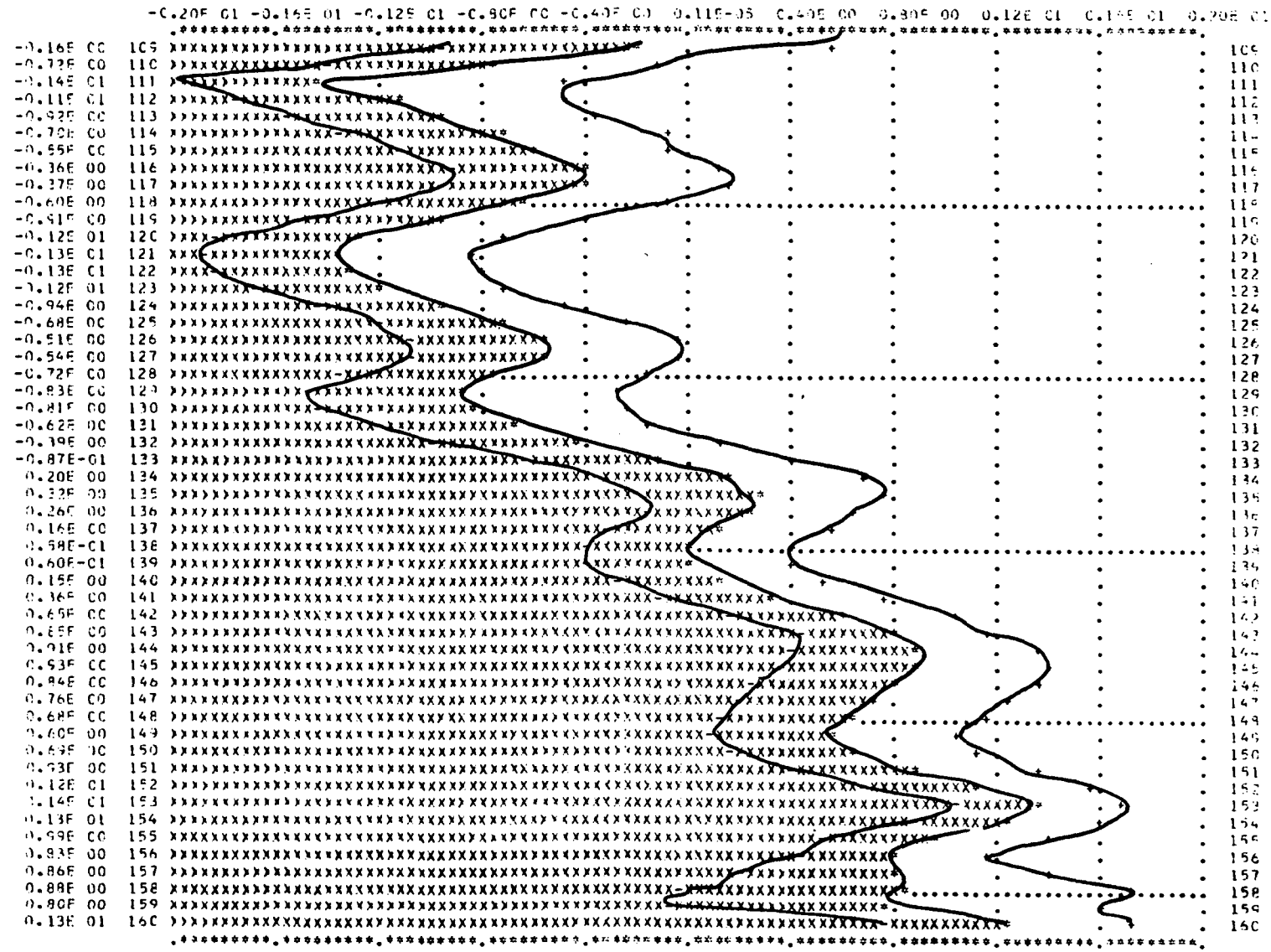

OUT I N = 35 MX 108-3

-99-

Tertiary Volcanic Ash Soils

TVA I N = 64

MX108 -3 - (6)

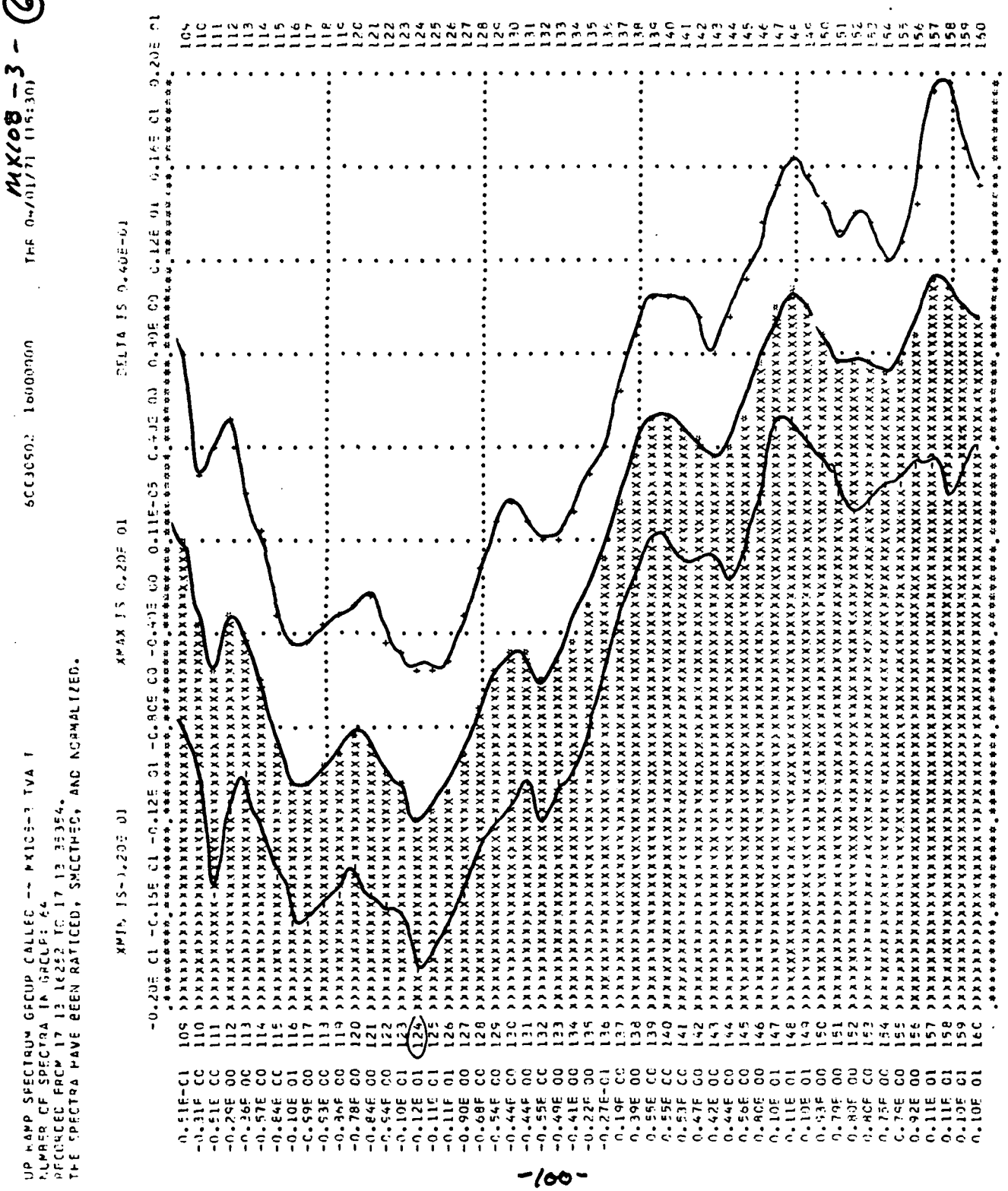

Tertiary Volcanic Ash soils

TVA II N = 63

MX108-3- (7)

UP RAMP SPECTRUM GROUP CALLED -- MXIC8-3 TVA II
NUMBER OF SPECTRA IN GROUP: 63
RECORDED FROM 17 22 4517 TO 17 22 23712.
THE SPECTRA HAVE BEEN RATICED, SMOOTHED, AND NORMALIZED.

Lavender Volcs C8

TAV II

N = 3.

MX108-3-(8)

-102-

112

MX108-3-(9)

LP RAMP SPECTRUM GROUP CALLED -- MX109-3 TRE I
NUMBER OF SPECTRA IN GROUP: 11
RECORDED FROM 17 14 10517 TO 17 14 11947.
THE SPECTRA HAVE BEEN RATIOED, SMOOTHED, AND NORMALIZED.

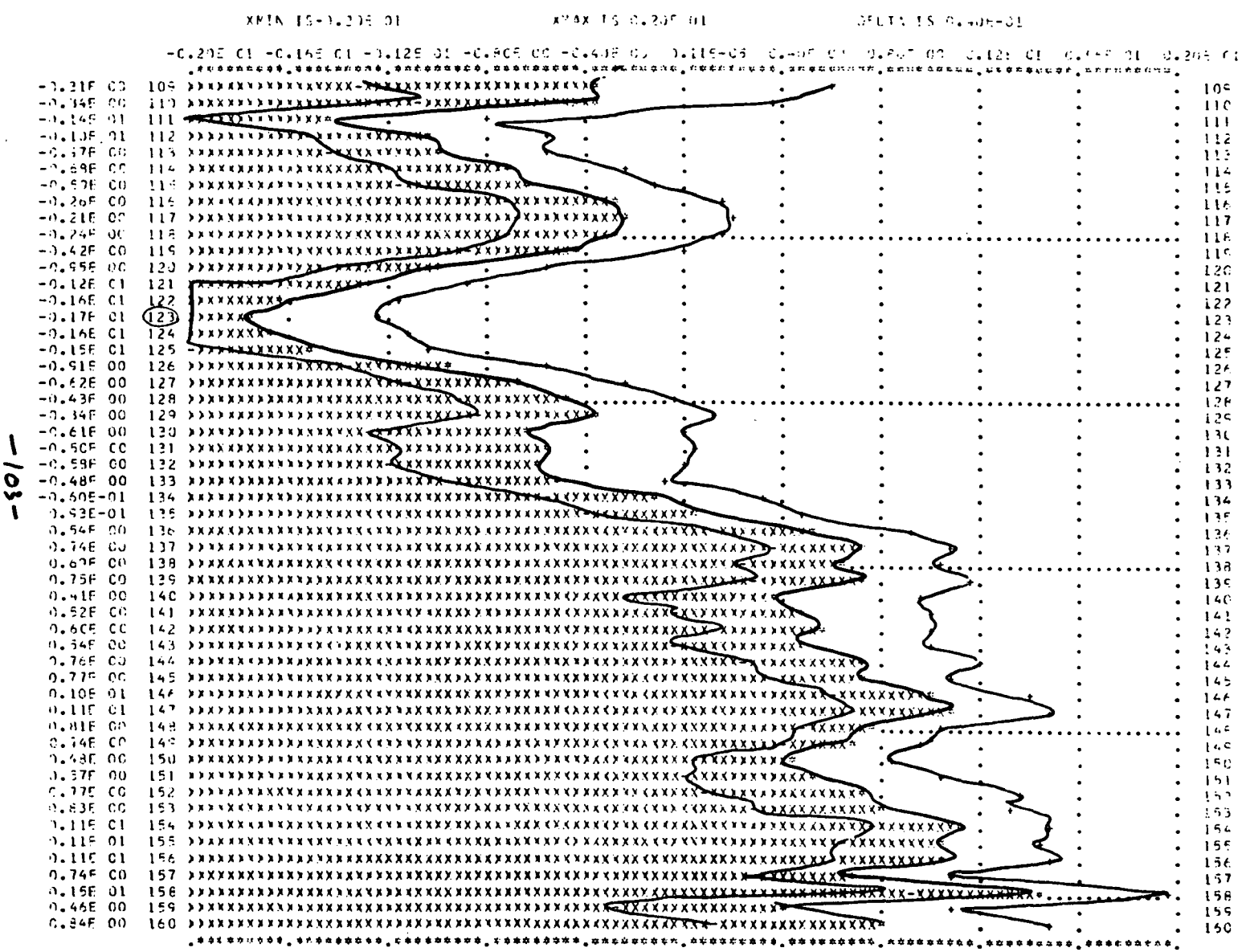

TRE I (89) N= 11

TRE 11 (C3A)

N=6

MX108-3- (10)

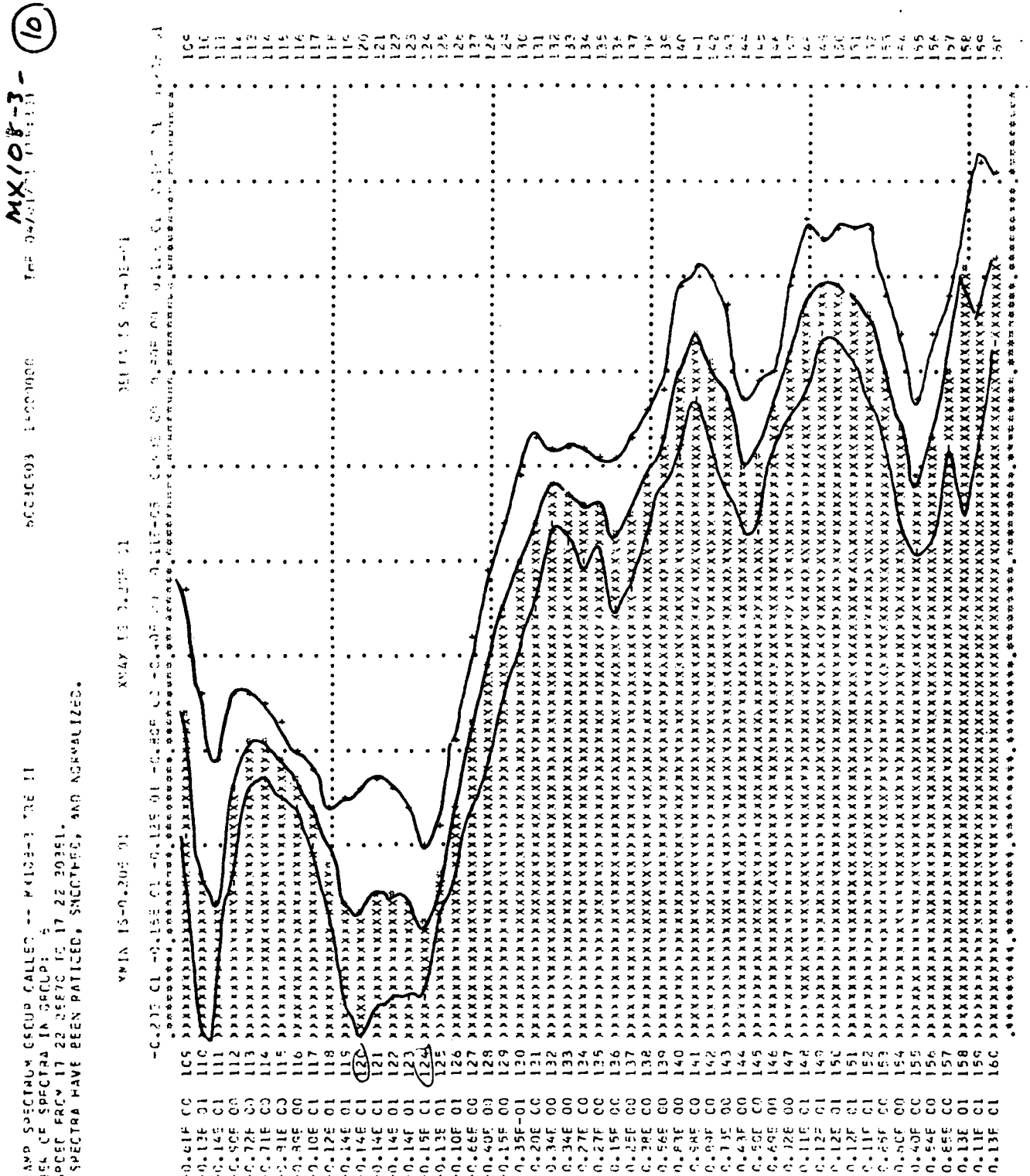

V. DELIVERABLE ITEMS

The contract calls for four (4) items to be delivered. In sequence these are as follows.

A. (4.1) Report on Feasibility Study. This is comprised of three items, (1) Section IV of this report, representing a summary of the MX108 Mission, (2) a paper published in IEEE, which details the calibration steps and shows flight methodologies and results for operational use (See Appendix B2, herein) and (3) a manuscript (prepared for Science magazine) which further details the flight results and shows the integration of those data with the emittance-ratio imagery of Pisgah Crater site (See Appendix B3, herein).

B. (4.2) Technical Report on MSC Aircraft Mission. The report on NASA/MSC Mission 108 is (a) contained in Section IV of this report and (b) in the Science manuscript (See Appendix B3).

C. (4.3) Library Spectra of Geological Materials. These are reduced spectra and have been supplied to MSC, under separate cover, both in output-printer listings and in tape-recorded form. Punched card deck equivalents have also been prepared but are being left at Stanford in the RSL laboratories because of their bulk.

D. (4.4) Final Summary Report. This document represents part (C) of three parts of the Final Report. The two others are

Part A - Software (Computer Programming) RSL 71-2.
"1970/71 Stanford Spectral Data Management Programs"
by A. A. Marshall.

Part B - Digital Data Acquisition System - RSL 71-3 by Lee Lu.

Together, these three reports make up the Final Summary Report.

APPENDIX A1
CALIBRATION
STEPS

Computed Spectral Data Groups -- Mission 108

Page #	Subject
BB 1	Radiance (N) values for T = 328, 323, 318, 313°K.
BB 2	(Same, for T = 308, 303, 298°K).
BB 3	Plots of Calc. Radiance Difference (DIFFRAD) Envelopes, for an internal BB reference in the spectrometer at 333°K (60°C) viewing a target, variously at 328, 323, 318, 313, 308, 303, 298°K.
	**Note -- 1) The higher the target temperature, the lower the DIFFRAD. 2) The difference between 2 BB's has a similar shape to a single BB.
BB 4-9	Calc. Difference plots for BB targets of 323, 318, 313, 308, 303, 298°K.
AIRPTH 10A	Airpath (atmospheric transmission spectra) between the aircraft and Palmdale Lake -- airborne spectra.
10B	(Same, for Shallow Lake).
TRAN 11	Calculated Radiance Difference ("TRUE"), or DIFFRAD for "40° EXT BB" target, pre-flight.
TRAN 12	Observed DIFFRAD for same target.
TRAN 13	"INSTRAN" (Instrument Transfer Function), or 1/optical transfer function, or 1/A.t(λ).
TRAN 14	OPTICAL TRANSFER FUNCTION (A.t(λ)). (Pre-flight data).
TRAN 15	Observed "Post-flight 40°C BB".
TRAN 16	Post-flight "INSTRAN."
TRAN 17	Post-flight Optical Transfer Function.
BB 18 A,B	Pre-flight 40°BB (raw), list and plot.
19 A,B	Post-flight 40°BB (raw), list and plot.
BB 20 A,B	Preflight Ambient BB (raw), list and plot.
BB 21 A,B	Postflight

RKA 22 A,B	Pre-flight Rock A (raw), list and plot.
RKA 23 A,B	Post-flight Rock A (raw), list and plot.
RKB 24 A,B	Pre-flight Rock B (raw), list and plot.
RKB 25 A,B	Post-flight Rock B (raw), list and plot.
LKBB 26 A,B	Palmdale Lake (airborne, raw) list and plot.
LKBB 27 A,B	Shallow Lake (airborne, raw) list and plot.
POLY 28	Measured Transmission of ARSS POLY (LMSC data).
POLY 29	Calc. POLY seen with a BB target of "40°C EXT BB."
POLY 30	Airborne POLY II, (raw), plot.

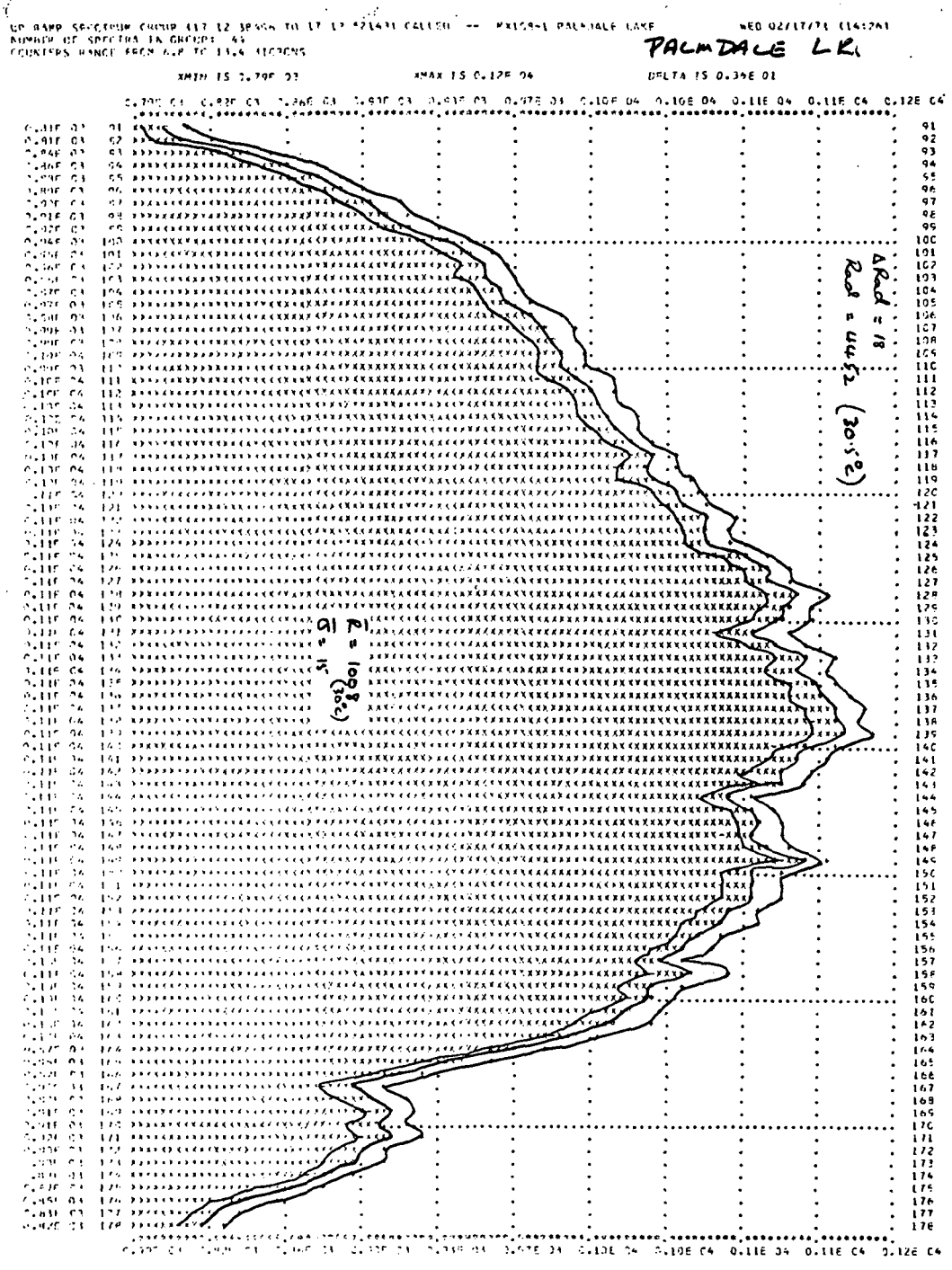

Reproduced from best available copy.

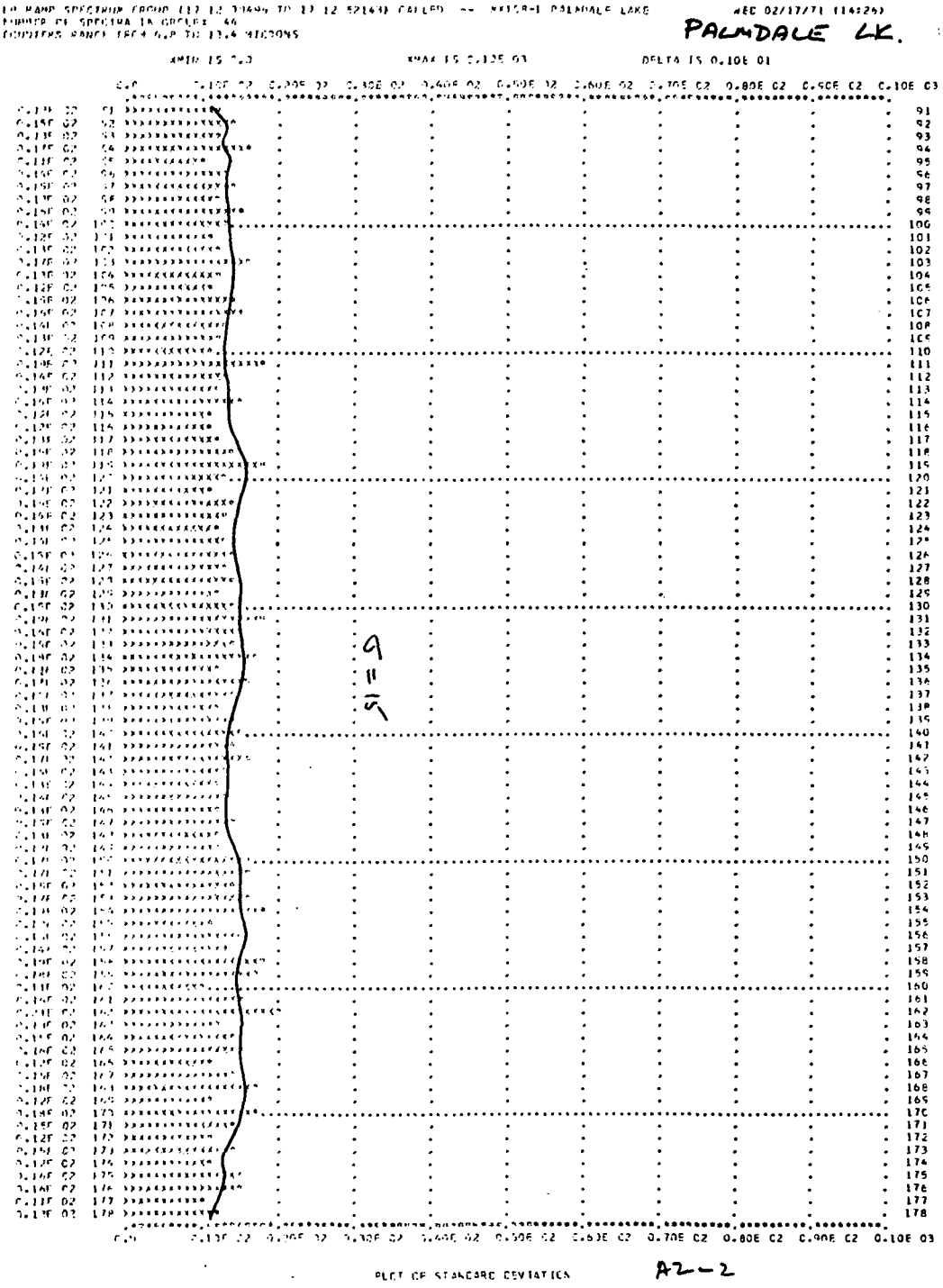
PALMDALE LK.
PLOT OF STANDARD DEVIATION
A2-2

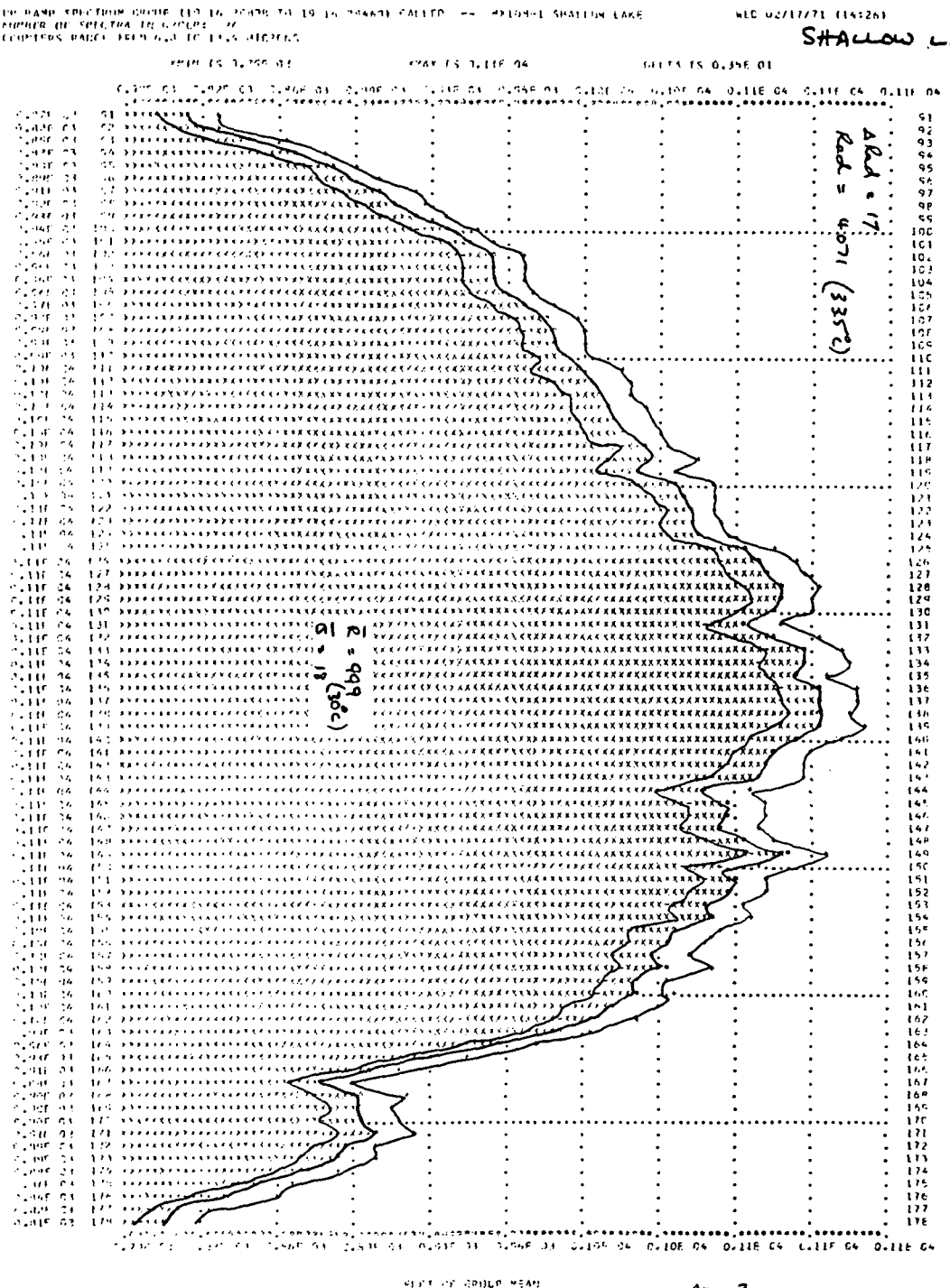

A2-3

LP RAMP SPECTRUM GROUP (IC 16 2[illegible] TO 19 16 284691 CALLED -- MX108-1 SHALLOW LAKE WED 02/17/71 (14:26)
NUMBER OF SPECTRA IN GROUP: 26
COUNTERS RANGE FROM 6.3 TO 13.4 MICRONS

SHALLOW LK

XMIN IS 0.0 XMAX IS 0.10E 03 DELTA IS 0.10E 01

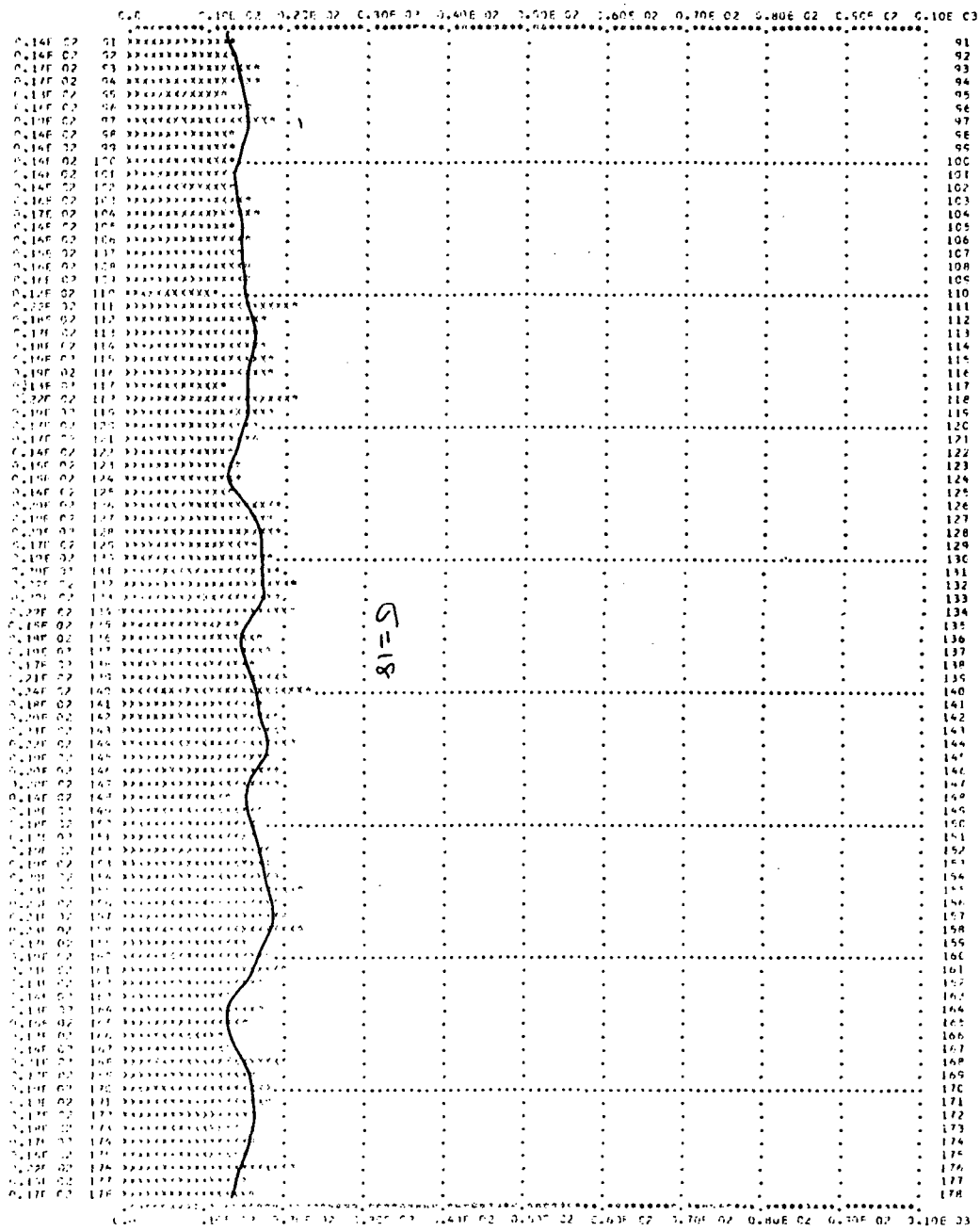

PLOT OF STANDARD DEVIATION

A2-4

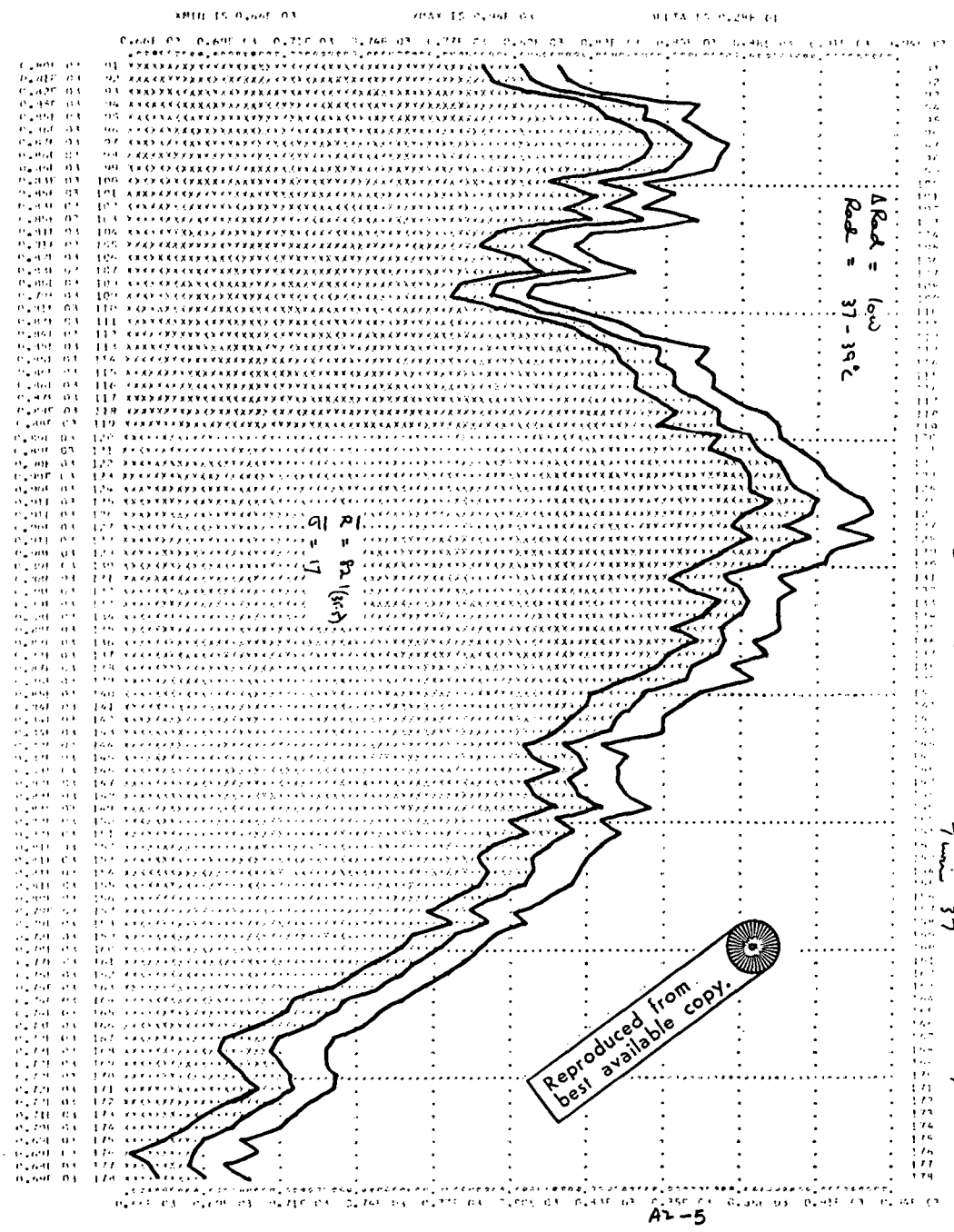
PISGAH ALLUVIAL C
ΔT
X̄: 820 N = 25
σ̄ = 17.5
ΔT̄ 37.5 - 38.2°C
Tmax 39
Tmin 37
Tspec 35.5
ΔRad = low
Rad = 37 - 39°C
R̄ = 82 (35.5)
σ̄ = 17
Reproduced from best available copy.
A2-5

LP RAMP SPECTRUM GROUP (18 49 44C00 TO 19 49 51' 01 CALLED -- [illegible] ALLUVIAL-C

NUMBER OF SPECTRA IN GROUP: 25

COUNTERS RANGE FROM 6.8 TO 13.4 MICRONS

XMIN IS 0.0 XMAX IS 0.10E 03 DELTA IS 0.10E 01

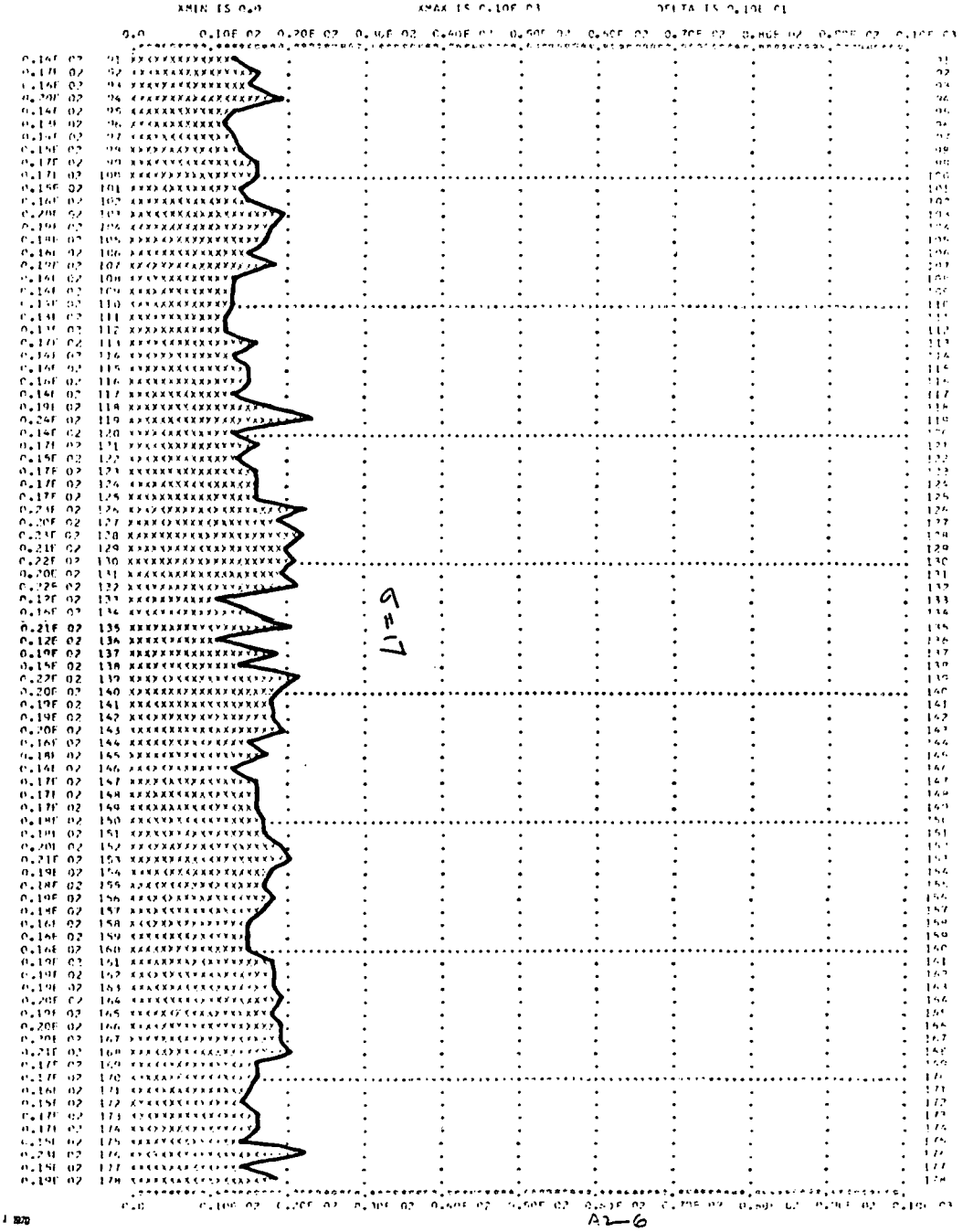

SEP 1 1 1970

A2-6

PLOT OF STANDARD DEVIATION

UP RAMP SPECTRUM GROUP (18 50 22831 TO 18 50 31583) CALLED -- 9X108 ALLUVIAL-AC 1701

(2)

NUMBER OF SPECTRA IN GROUP: 30

COUNTERS RANGE FROM 6.8 TO 13.4 MICRONS

XMIN IS 0.64E 03 XMAX IS 0.89E 03 DELTA IS 0.25E 01

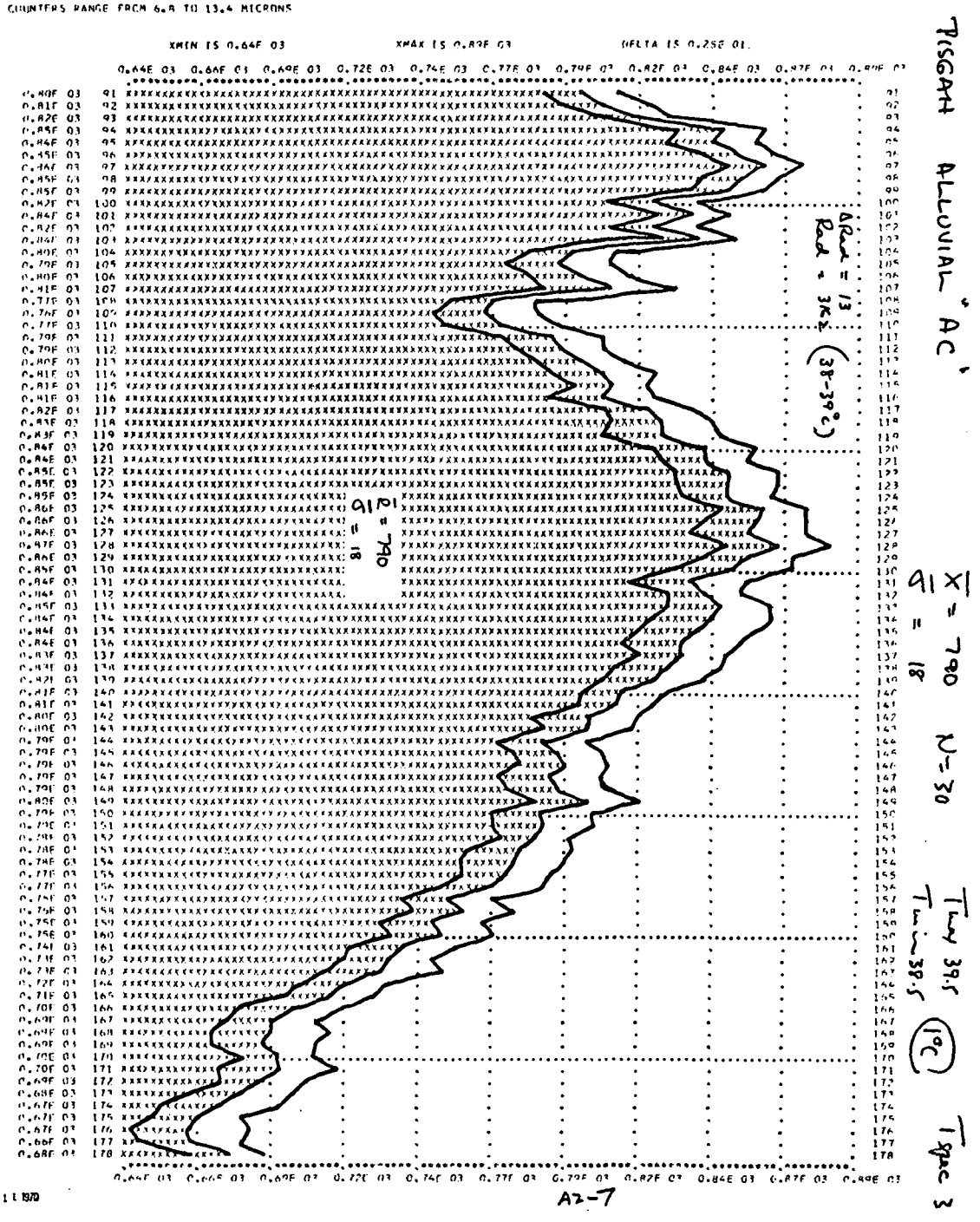

PISGAH ALLUVIAL "AC"

7-

A2-7

SEP 1 1 1970

UP RAMP SPECTRUM GROUP (18 SC 22833 TO 18 SC 31583) CALLED -- MXIOB ALLUVIAL-AC

(2)

NUMBER OF SPECTRA IN GROUP: 30

COUNTERS RANGE FROM 6.8 TO 13.4 MICRONS

XMIN IS 0.0 XMAX IS 0.10E 03 DELTA IS 0.10E 01

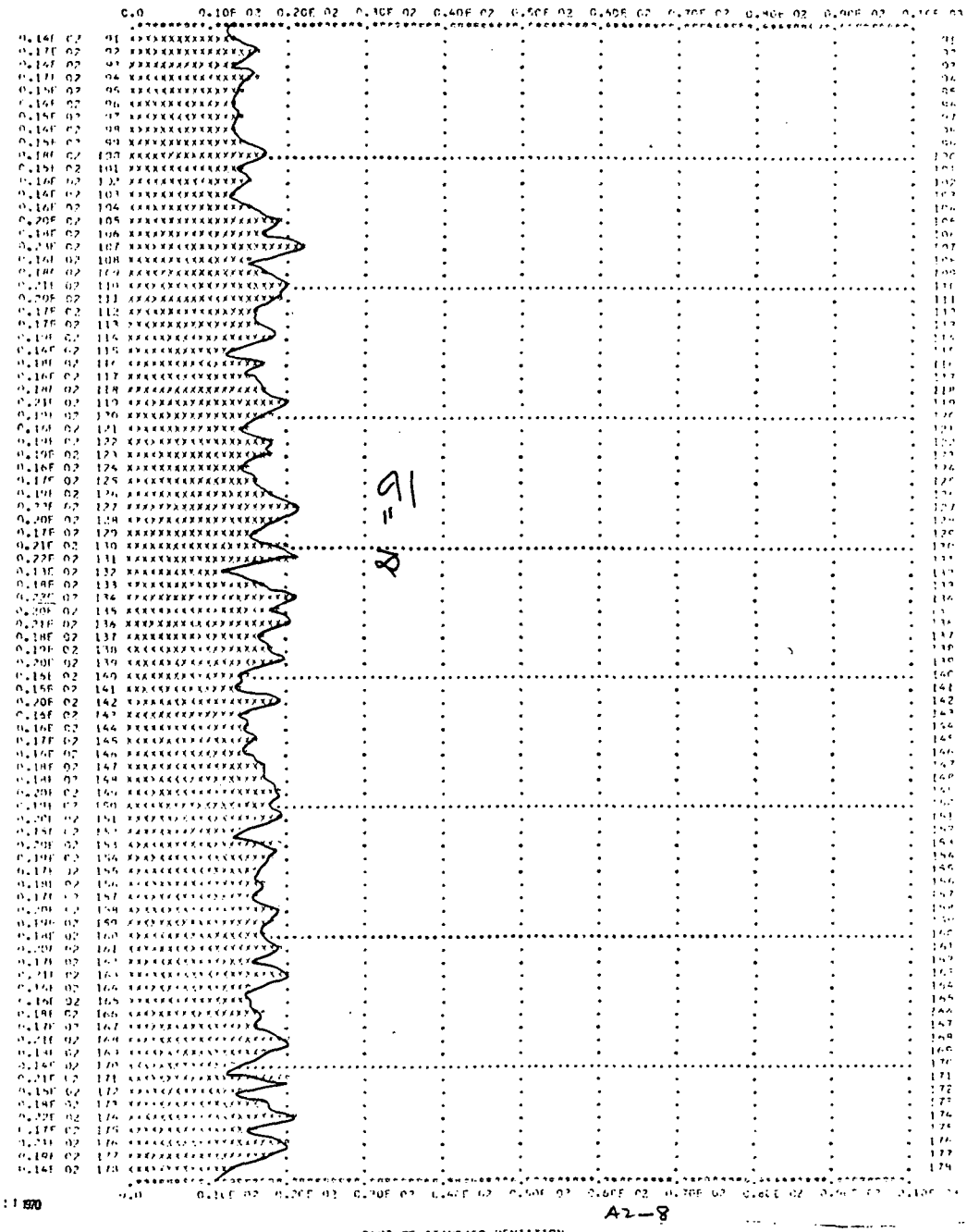

SEP 1 1970

A2-8

PLOT OF STANDARD DEVIATION

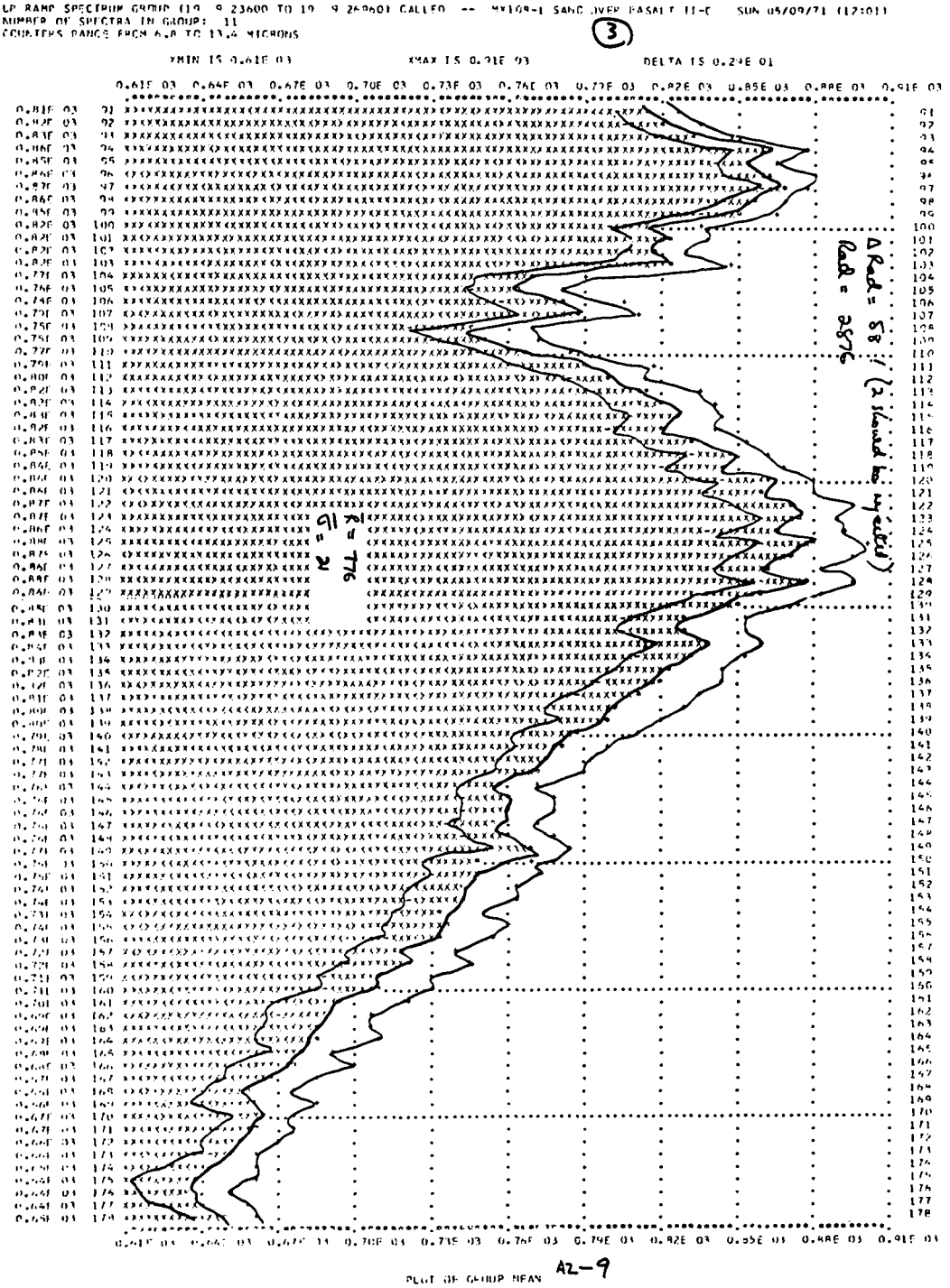

Sand over Basalt II-C

(3)

AZ-9

AZ-9

UP RAMP SPECTRUM GROUP 119 @ 23600 TO 19 @ 24960 CALLED -- MX104-1 SAND OVER BASALT 11-C SUN 05/09/71 (12:01)
NUMBER OF SPECTRA IN GROUP: 11
COUNTERS RANGE FROM 6.8 TO 11.4 MICRONS

(3)

XMIN IS 0.0 XMAX IS 0.10E 03 DELTA IS 0.10E 01

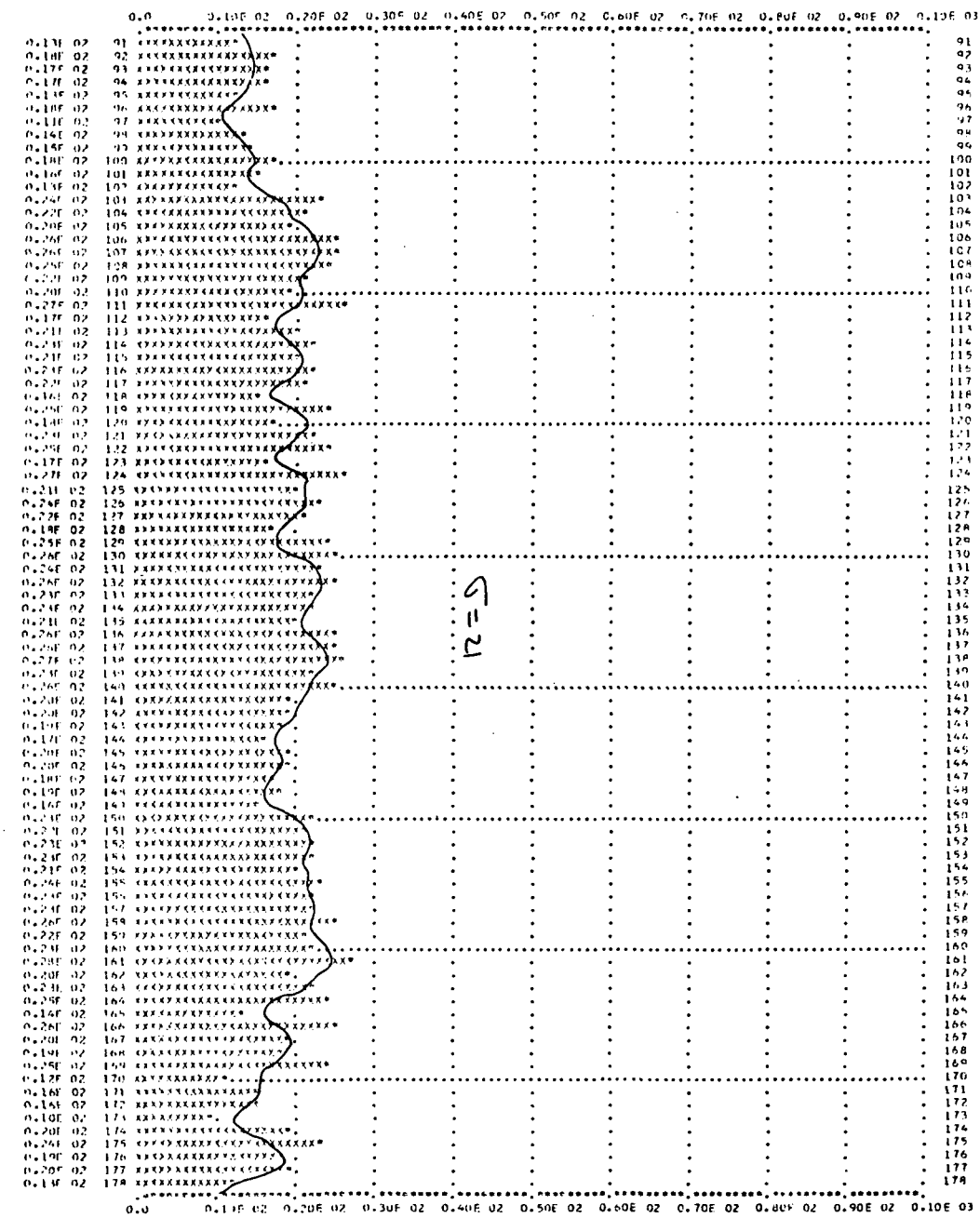

PLOT OF STANDARD DEVIATION

A2-10

UP RAMP SPECTRUM GROUP (18 49 57933 TO 18 50 61581 CALLED -- MK108 ALLUVIAL-A

(4) 1701

NUMBER OF SPECTRA IN GROUP: 27

COUNTERS RANGE FROM 6.8 TO 13.4 MICRONS

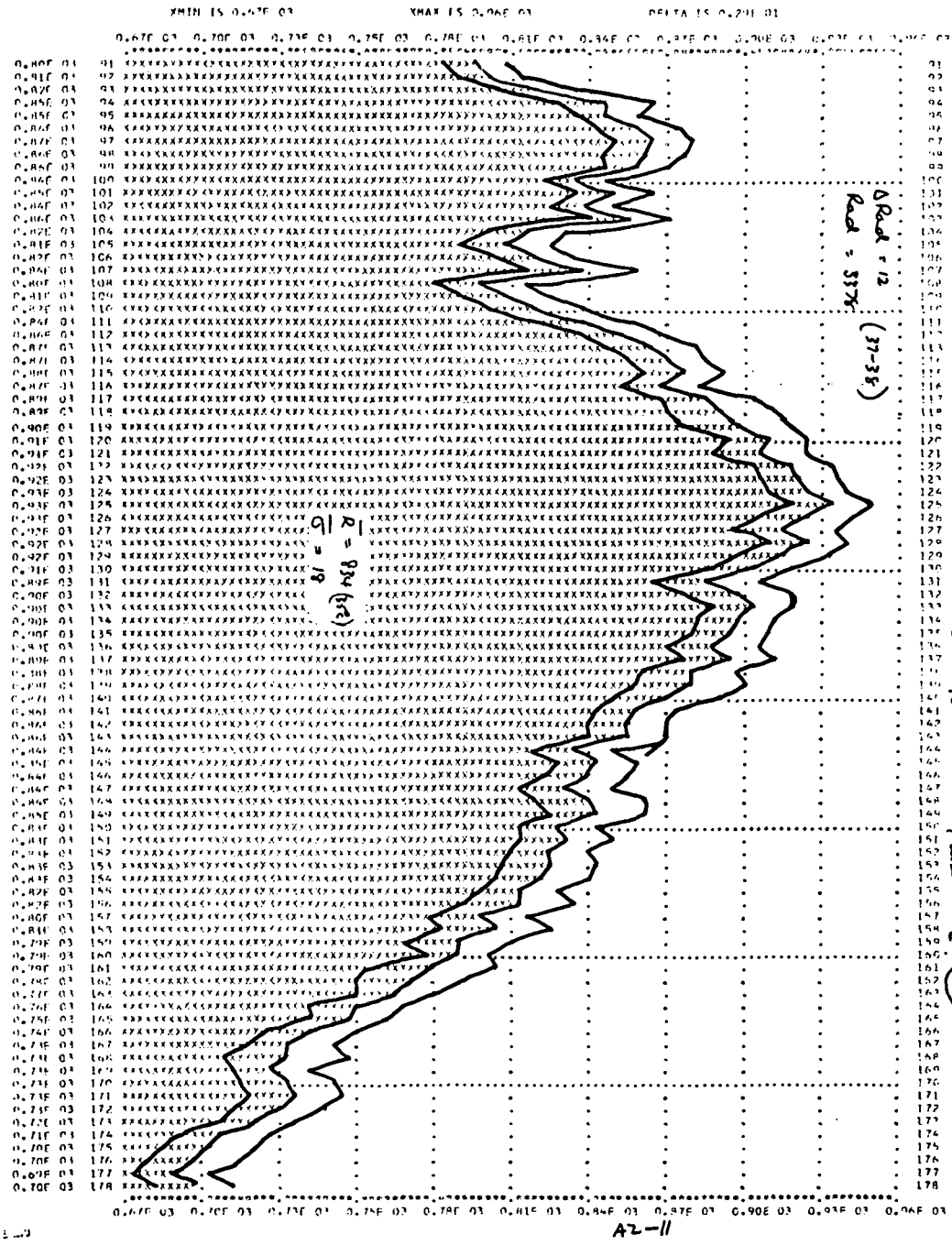

11-

LP RAMP SPECTRUM GROUP (18 49 57933 TO 18 50 6158) CALLED -- MX16S ALLUVIAL-A

(4)

NUMBER OF SPECTRA IN GROUP: 27

COUNTERS RANGE FROM 6.8 TO 13.4 MICRONS

XMIN IS 0.0 XMAX IS 0.10E 03 DELTA IS 0.10E 01

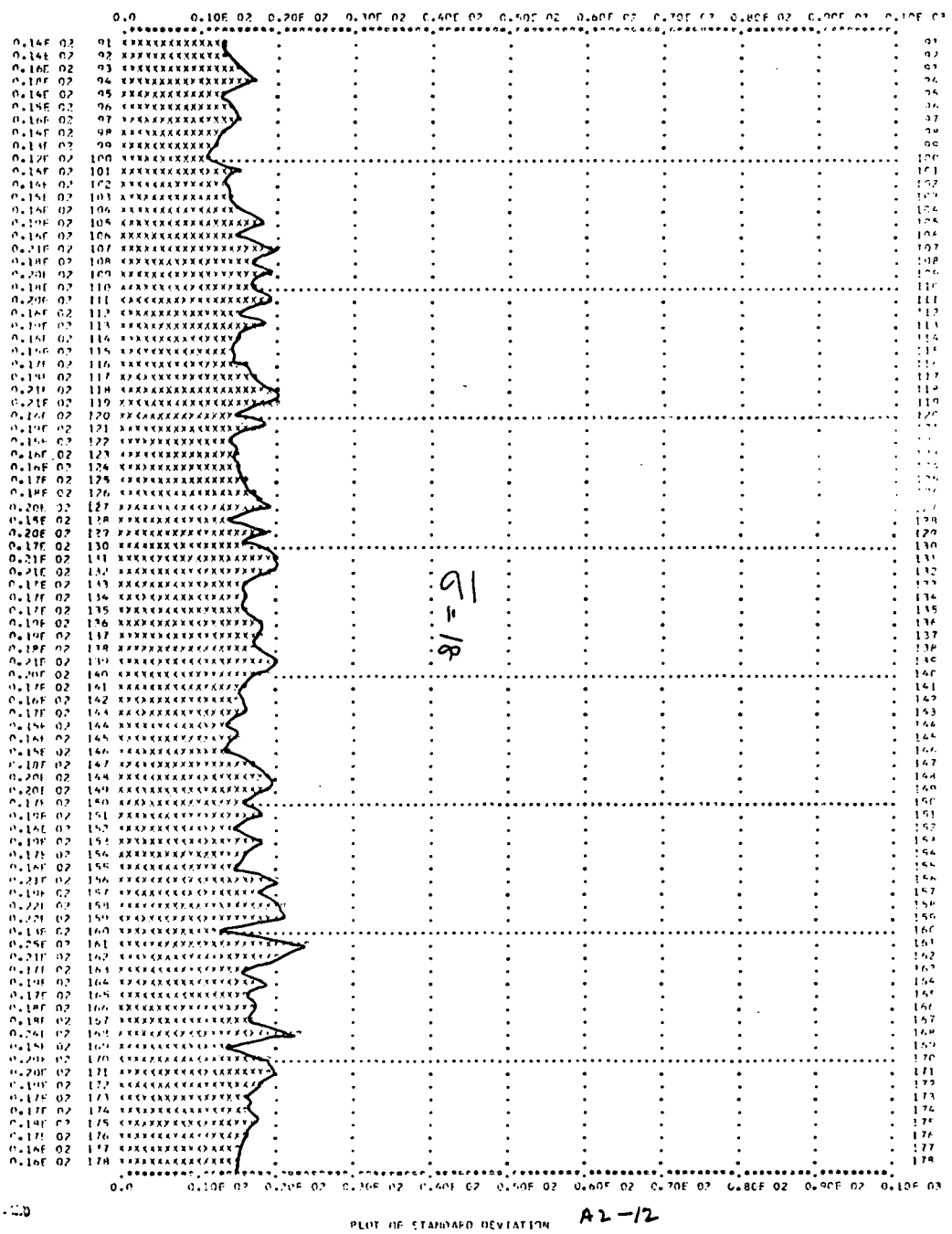

PLOT OF STANDARD DEVIATION

A2-12

GP RAMP SPECTRUM GROUP (18 50 34994 TO 18 50 46090) CALLED -- MXICA ALLUVIAL-B 1701

(5)

NUMBER OF SPECTRA IN GROUP: 30

COUNTERS RANGE FROM 6.8 TO 13.4 MICRONS

XMIN IS 0.61E 03 XMAX IS 0.88E 03 DELTA IS 0.26E 01

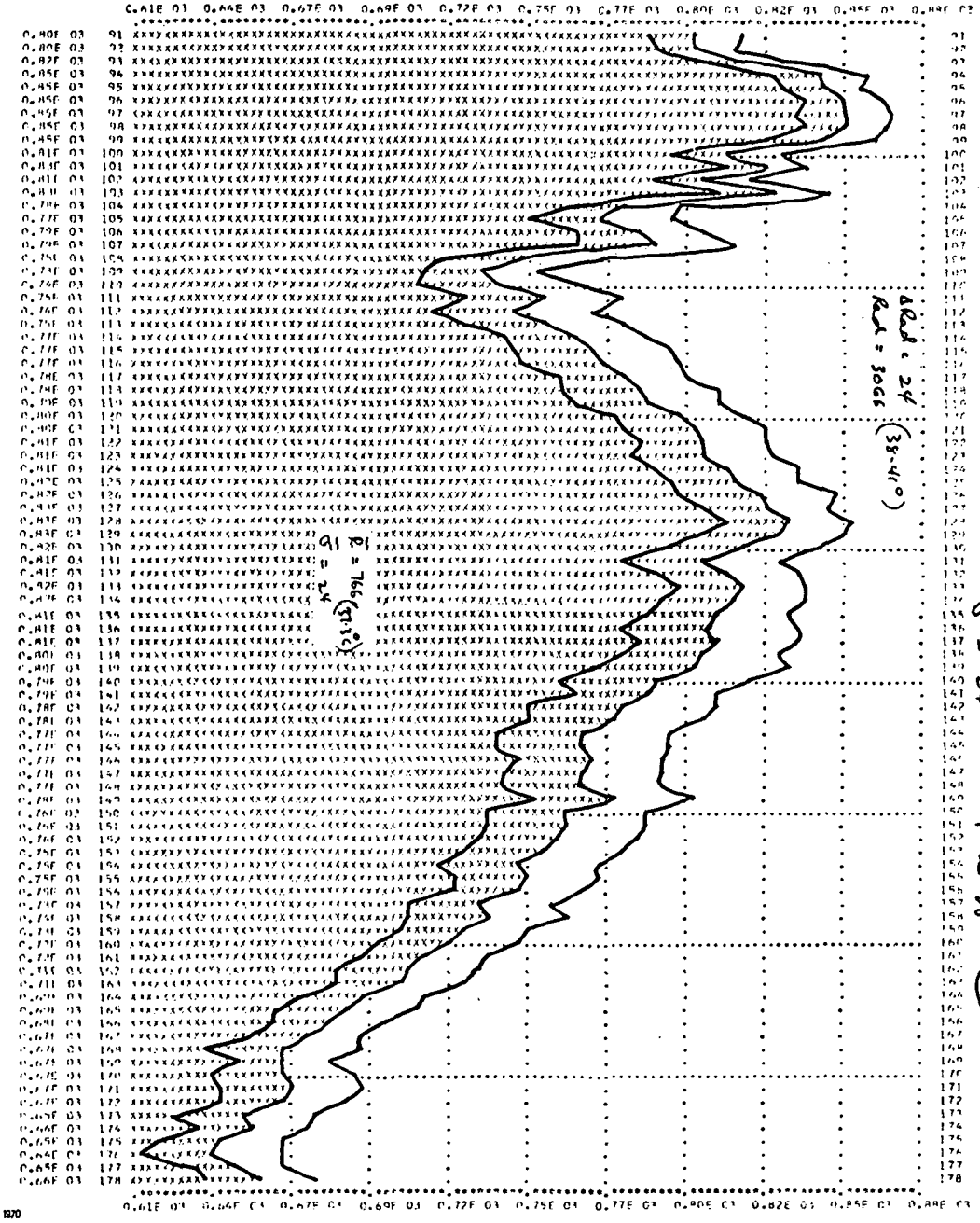

PISGAH ALLUVIAL - B

N=30

$\bar{X}$ = 766

$\bar{\sigma}$ = 24

Tmax 41

Tmin 38

(3°C)

Tspec 37.3°C

SEP 1 1 1970

A2-13

B-

UP RAMP SPECTRUM GROUP (IR 50 14588 TO IR 50 44090) CALLED -- [illegible] ALLUVIAL-8

5

NUMBER OF SPECTRA IN GROUP: 30

COUNTERS RANGE FROM 6.8 TO 13.4 MICRONS

XMIN IS 0.0 XMAX IS 0.10E 03 DELTA IS 0.10E 01

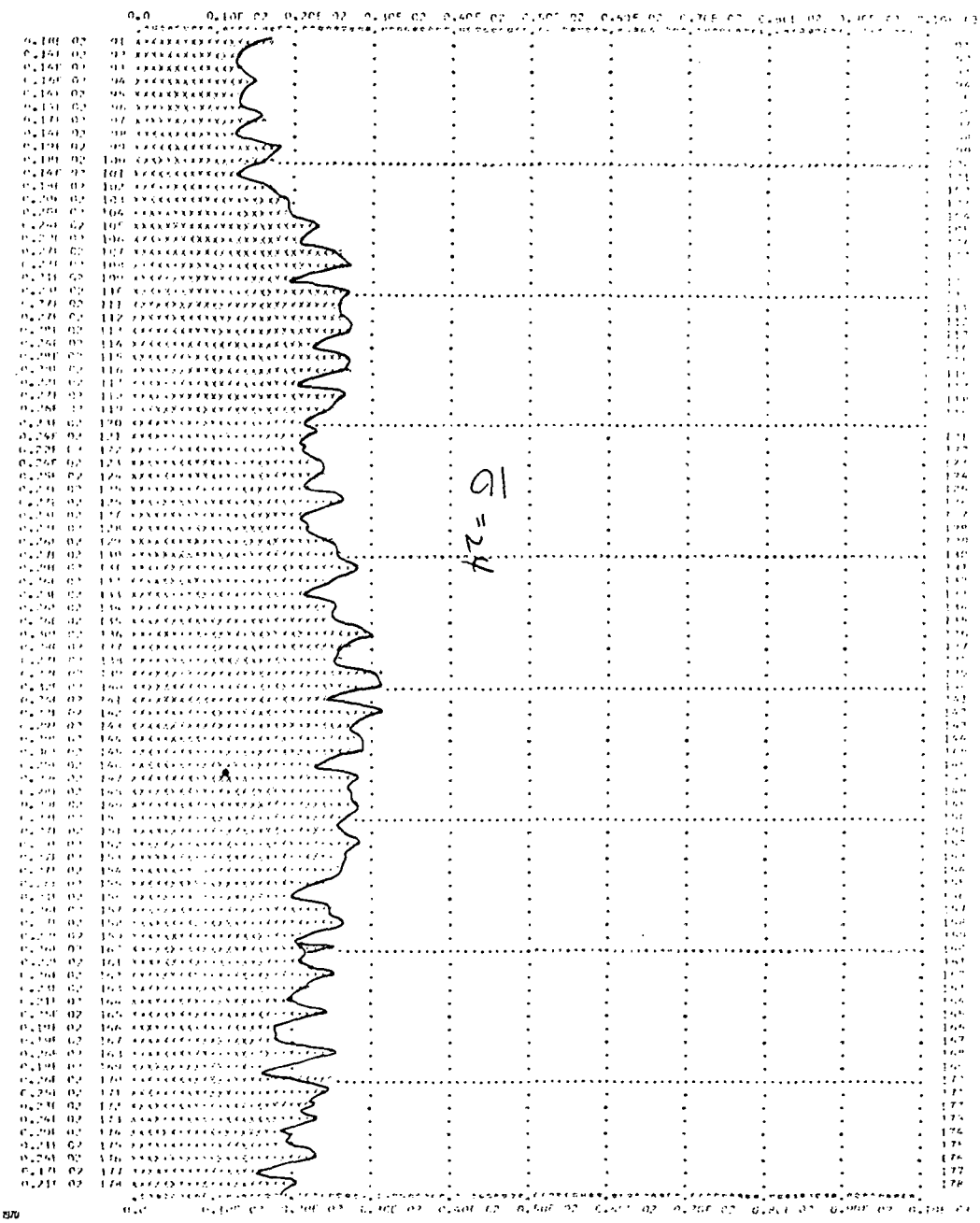

SEP 1 1 1970

PLOT OF STANDARD DEVIATION

A2-14

RAMP SPECTRUM GROUP (19 B 37500 TO 19 - 438771 CALLED -- MXIOR SAND-BASALT

(6) 1702

NUMBER OF SPECTRA IN GROUP: 21

COUNTERS RANGE FROM 6.8 TO 13.4 MICRONS

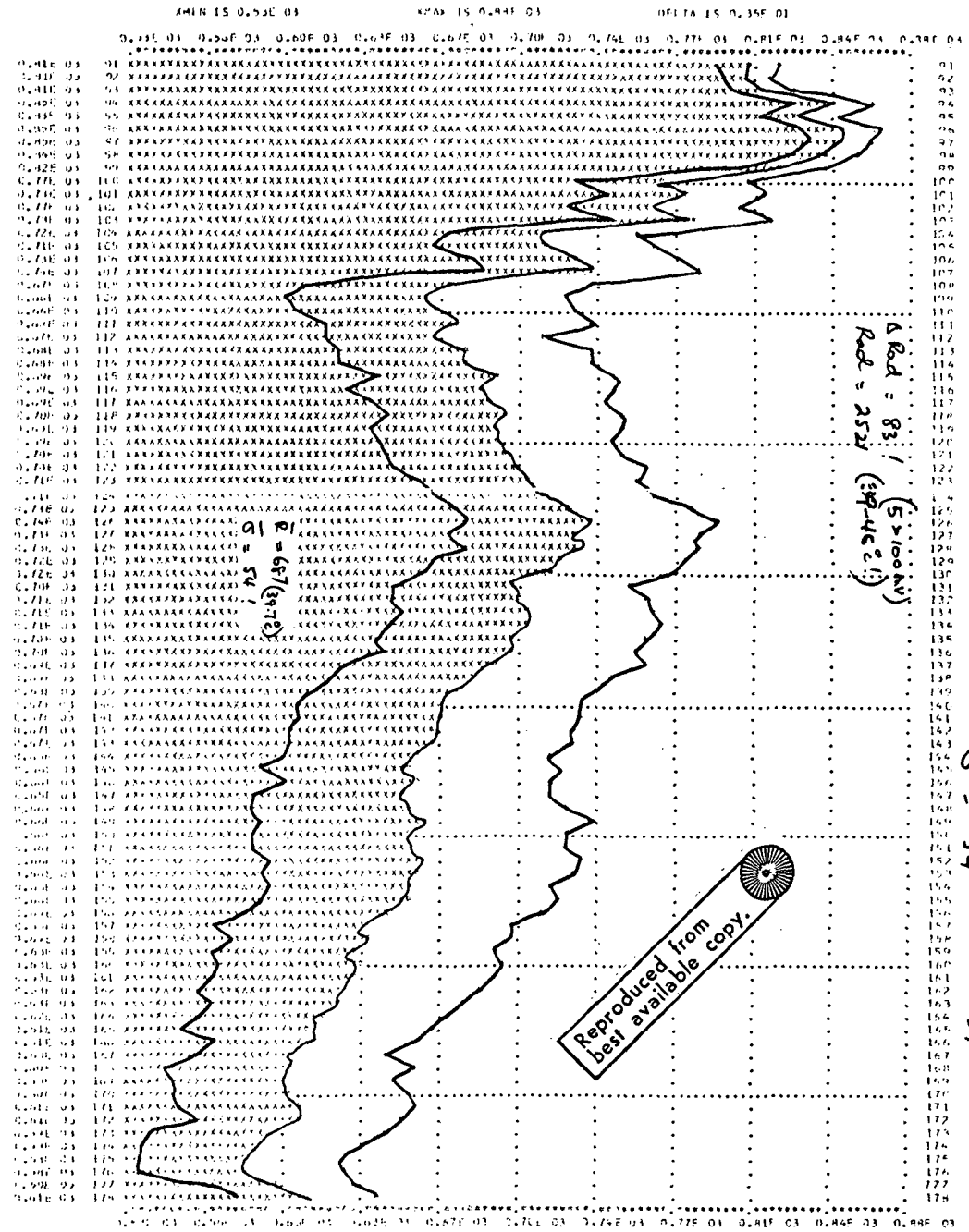

Reproduced from best available copy.

BLOWN SAND OVER BASALT
Nr. PISGAH CRATER

N = 21

X̄ = 687

σ = 54

Tmax 46.5°C

Tmin 39 (7°)

Tspec 39.7

A2-15

SEP 11 1970

OP RAMP SPECTRUM GROUP (19 8 37500 TO 19 8 438771 CALLED -- 4X10M SAND-BASALT (6)

NUMBER OF SPECTRA IN GROUP: 21

COUNTERS RANGE FROM 6.8 TO 13.4 MICRONS

XMIN IS 0.0 XMAX IS 0.10E 03 DELTA IS 0.10E 01

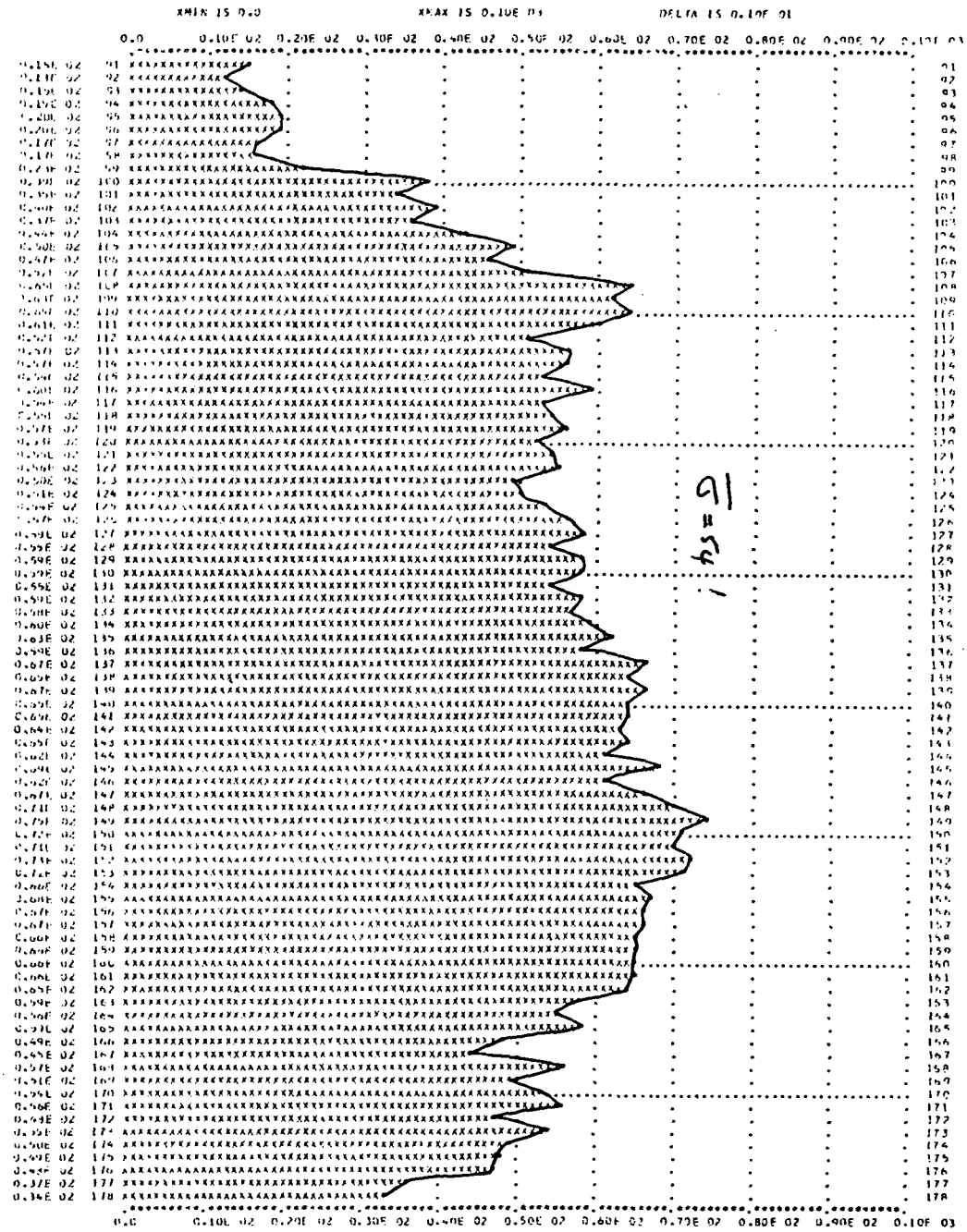

SEP 1 1 1970

PLOT OF STANDARD DEVIATION

A2-16

UP RAMP SPECTRUM GROUP (18 50 51826 TO 18 50 54710) CALLED -- MX108 SAND OVER BASALT

(7) 1701

NUMBER OF SPECTRA IN GROUP: 9

COUNTERS RANGE FROM 6.8 TO 13.4 MICRONS

XMIN IS 0.60E 03 XMAX IS 0.88E 03 DELTA IS 0.27E 01

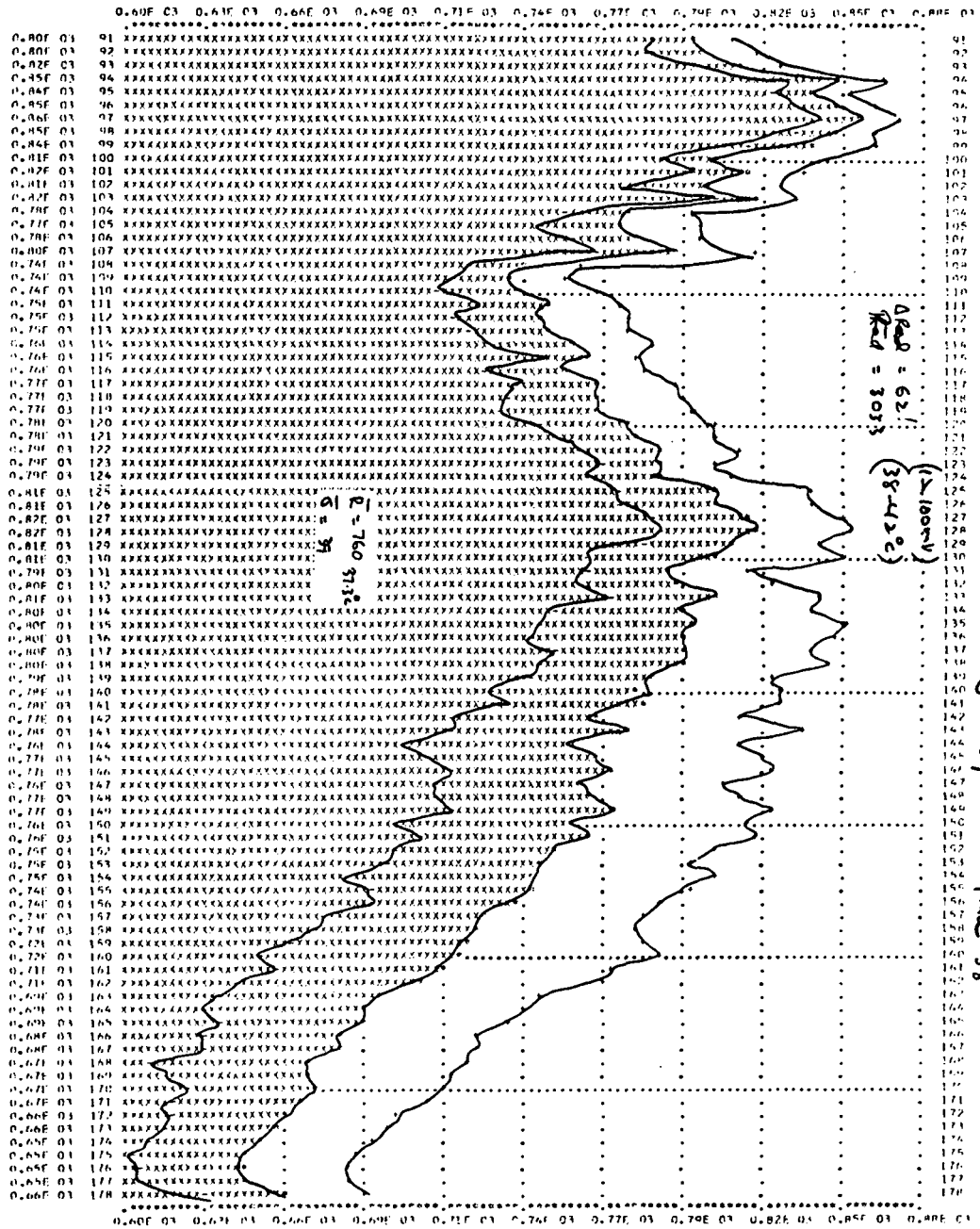

DISGAN SAND OVER BASALT A

N = 9

$\bar{X}$ = 760

$\bar{\sigma}$ = 39

T_{max} 42°C

T_{min} 38

(4°C)

T_{space} 37.3'

SEP 1 1 1970

A2-17

UP RAMP SPECTRUM GROUP (18 50 51820 TO 18 50 54710) CALLED -- "XXIGR SAND OVER BASALT"

(7)

NUMBER OF SPECTRA IN GROUP: 9

COUNTERS RANGE FROM 6.8 TO 13.4 MICRONS

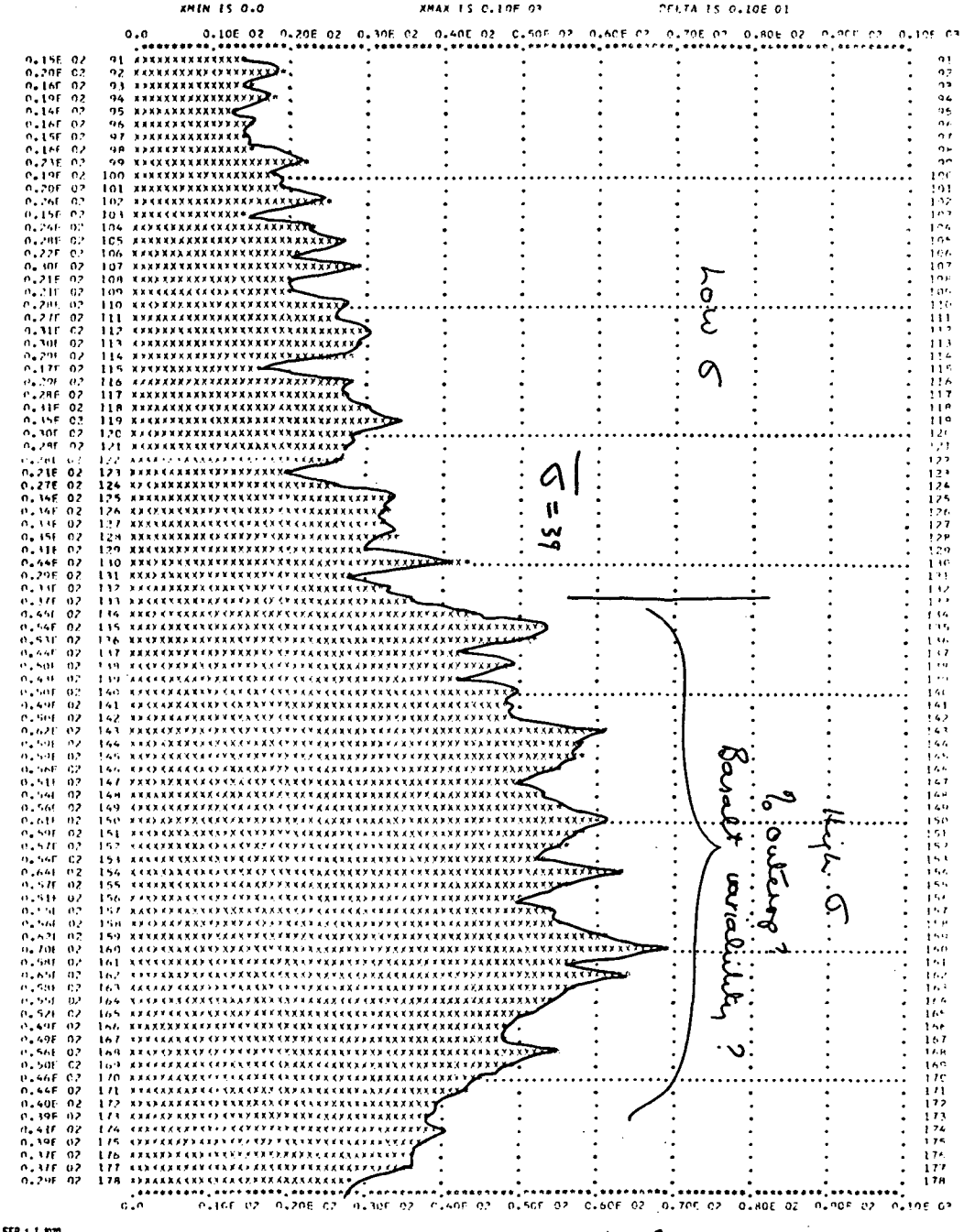

SEP 1 1 1970

PLOT OF STANDARD DEVIATION A2-18

RAMP SPECTRUM GROUP 119 8 20887 TO 19 8 29011 CALIB -- PISGAH FLOW III

1702 (8)

111 -(A) (8)

NUMBER OF SPECTRA IN GROUP: (6)

COUNTERS RANGE FROM 6.8 TO 13.4 MICRONS

XMIN IS 0.41E 03 XMAX IS 0.88E 03 DELTA IS 0.49E 01

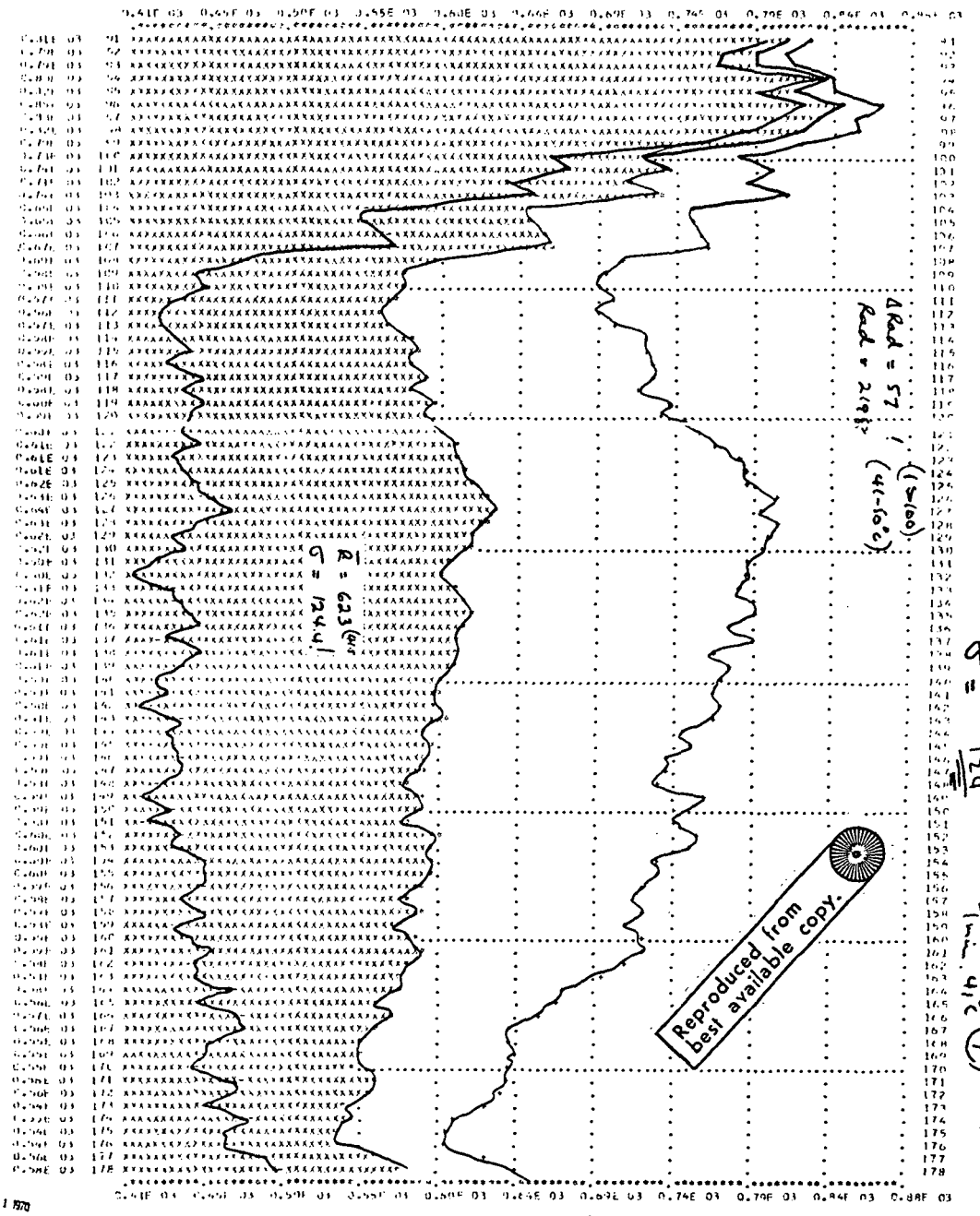

PISGAH FLOW Phase III

N = 6

X̄ = 621

σ = 124

Tmax 50°C

Tmin 41°C (9°) Tspec 41.5

Reproduced from best available copy.

SEP 11 1970

A2 -19

UP RAMP SPECTRUM GROUP (19 8 26887 TO 19 8 29011) CALLED -- MX108 PISGAH FLOW III

NUMBER OF SPECTRA IN GROUP: 6

COUNTERS RANGE FROM 6.8 TO 13.4 MICRONS

XMIN IS 0.0 XMAX IS 0.10E 03 DELTA IS 0.10E 01

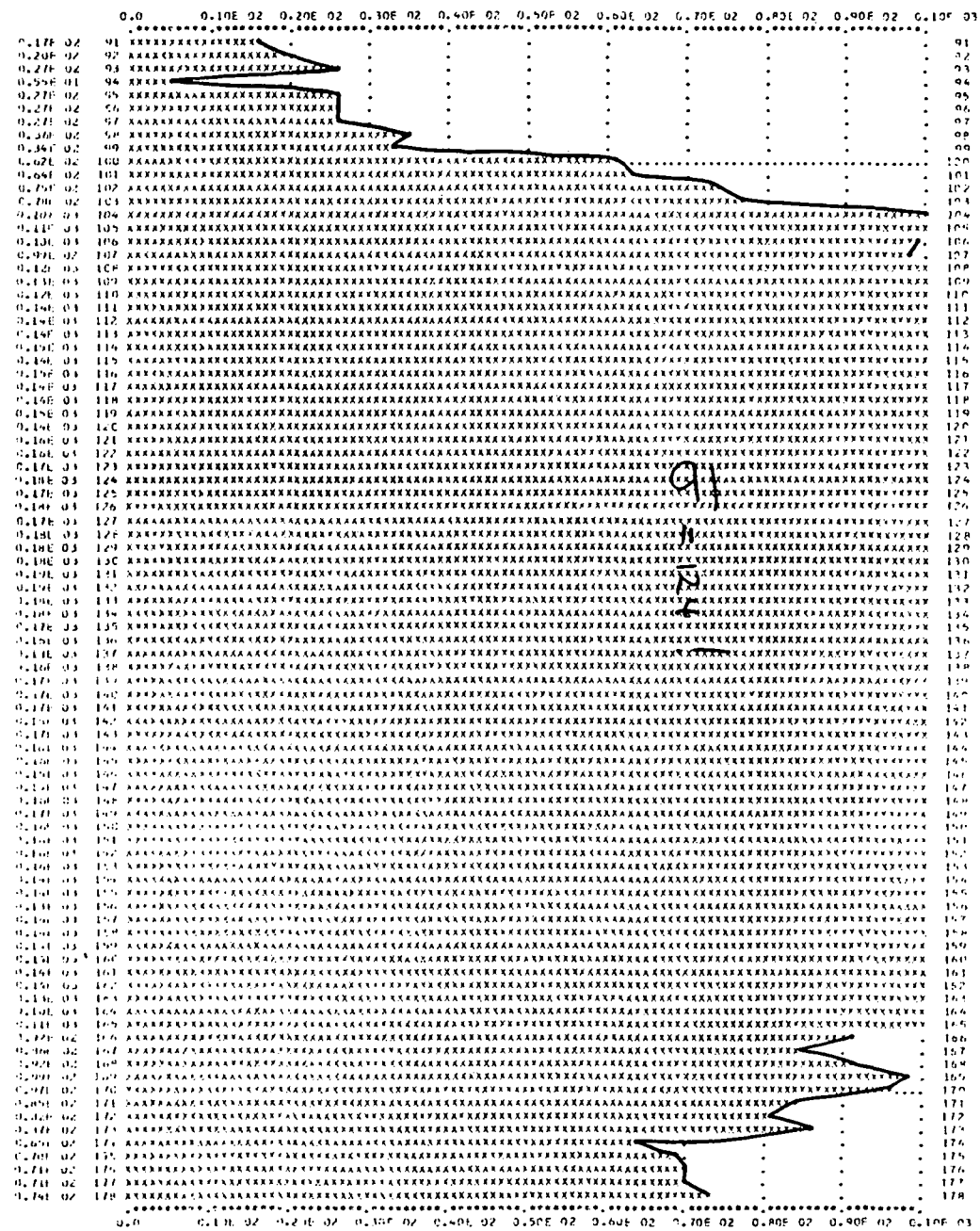

SEP 11 1970

PLOT OF STANDARD DEVIATION

A2-20

II-(A)

PISGAH FLOW PHASE II

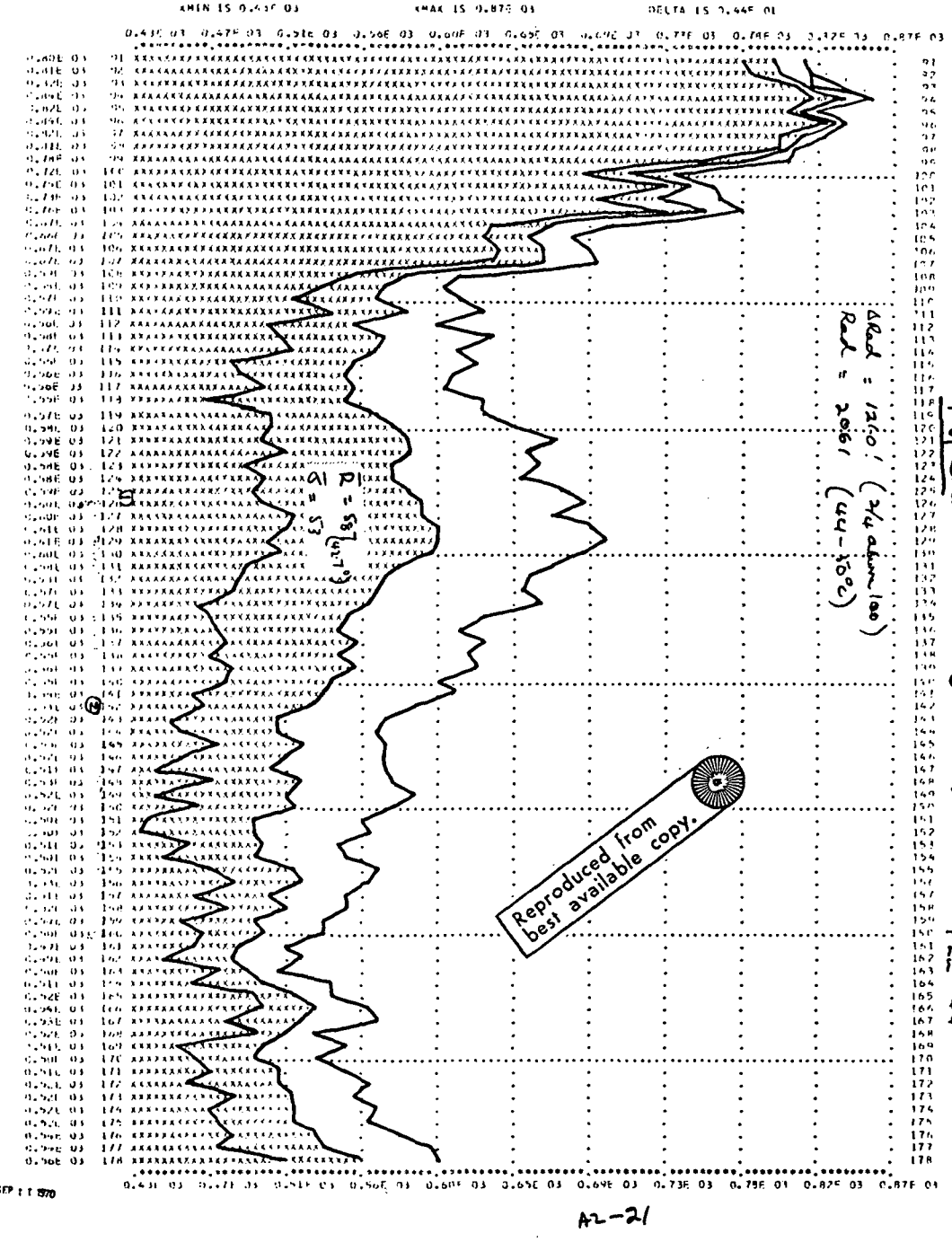

HP RAMP SPECTRUM GROUP (19 8 25370 TO 19 8 26887) CALLED 94139 PISSAN FLOW II

NUMBER OF SPECTRA IN GROUP: 4

COUNTERS RANGE FROM 0.0 TO 13.4 MICRONS

XMIN IS 0.0 XMAX IS 0.10E 03 DELTA IS 0.10E 01

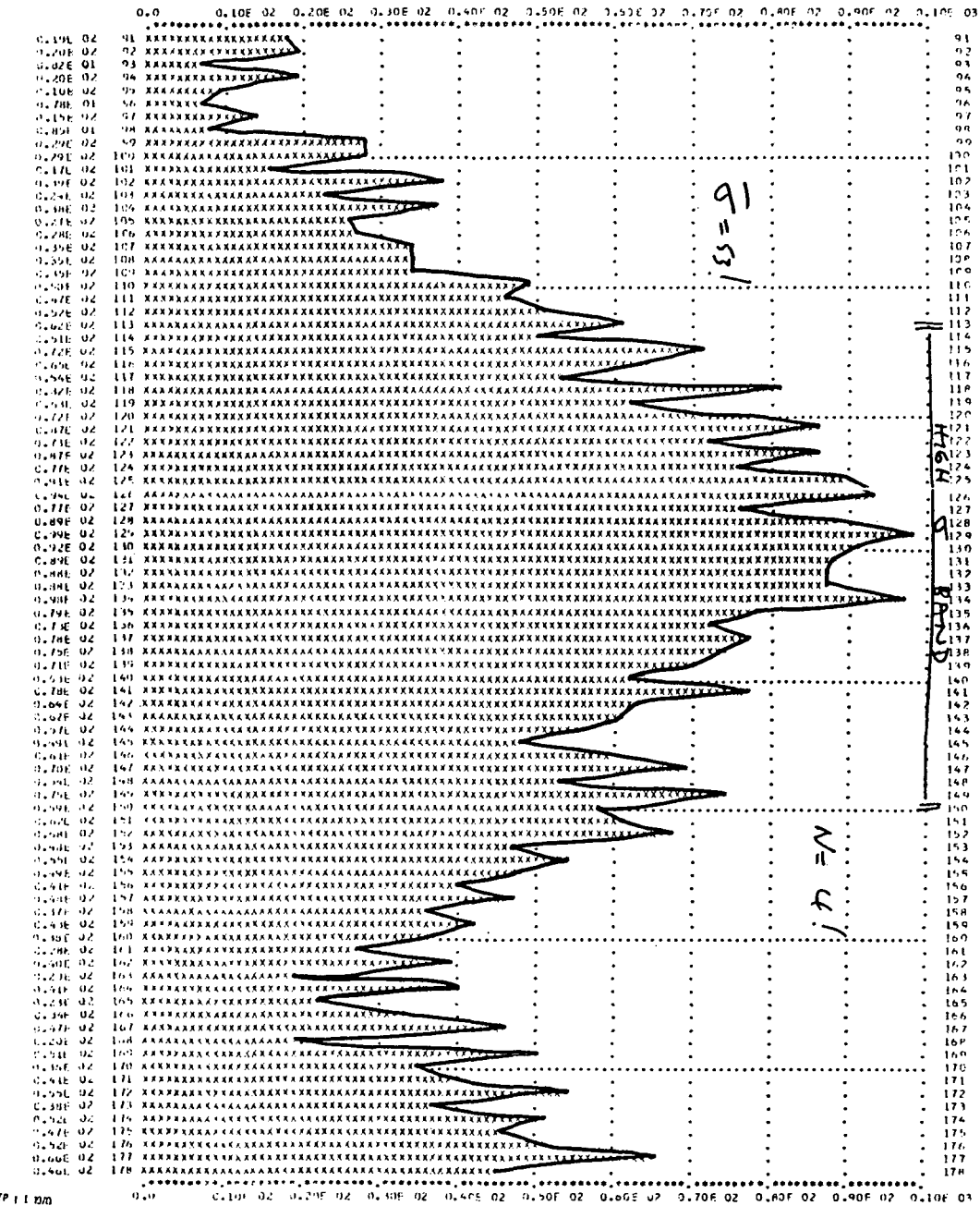

PLOT OF STANDARD DEVIATION A2-22

UP RAMP SPECTRUM GROUP (19 A 20819 TO 19 A 25370) CALLED -- MX108 PISGAH FLOW I (10)

NUMBER OF SPECTRA IN GROUP: 15

COUNTERS RANGE FROM 6.8 TO 13.4 MICRONS

1702 B/S 425-436

I-(A)

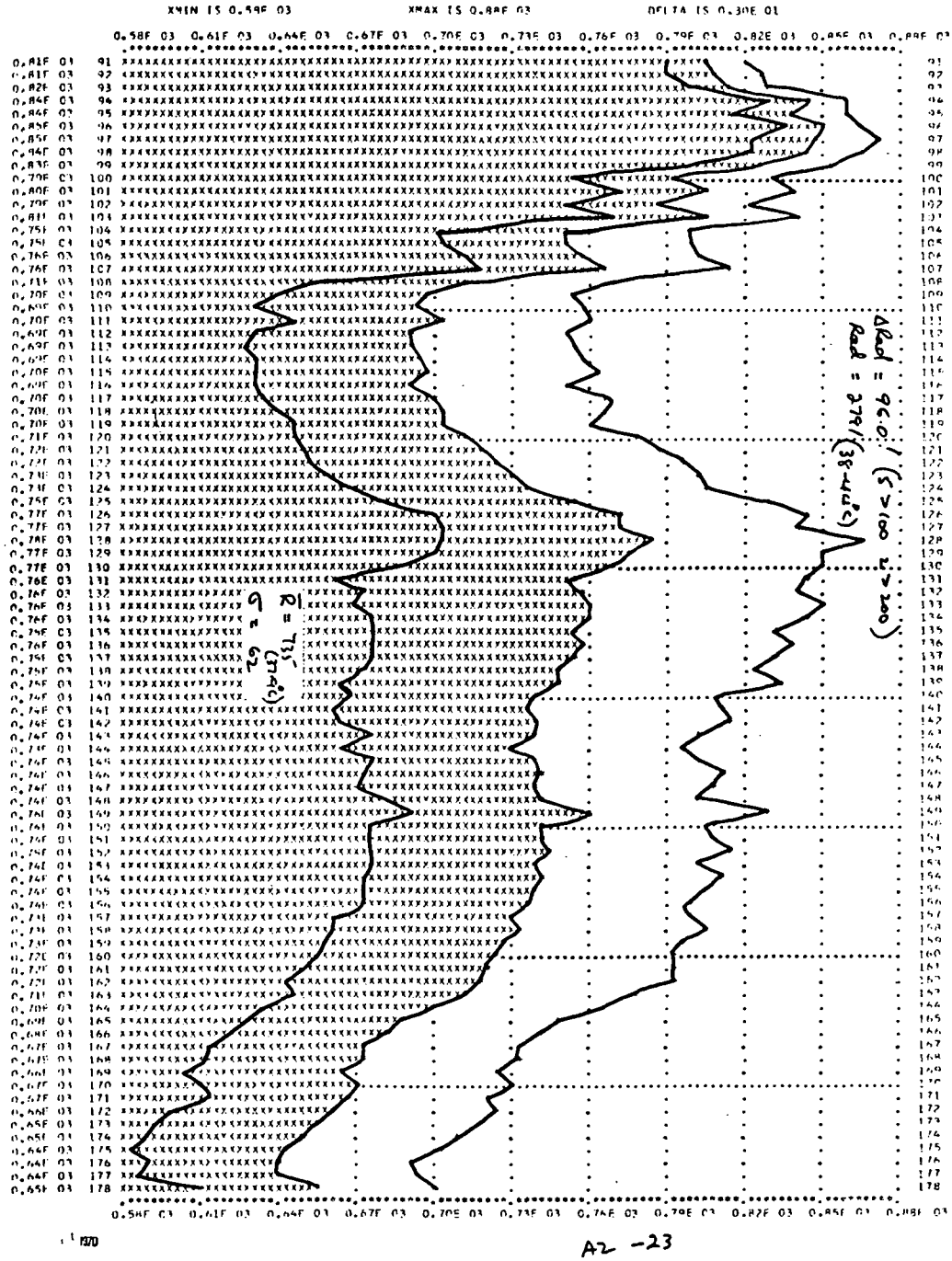

PISGAH FLOW - I

N = 15

$\bar{X}$ = 735

σ = 62

T_{max} 44°

T_{min} 38° (60)

T_{grnd} 37.9°

UP RAMP SPECTRUM GROUP (19 8 20819 TO 19 8 25370) CALLED -- MXTCR RISGAR FLOW I

(10)

NUMBER OF SPECTRA IN GROUP: 15

COUNTERS RANGE FROM 6.8 TO 13.4 MICRONS

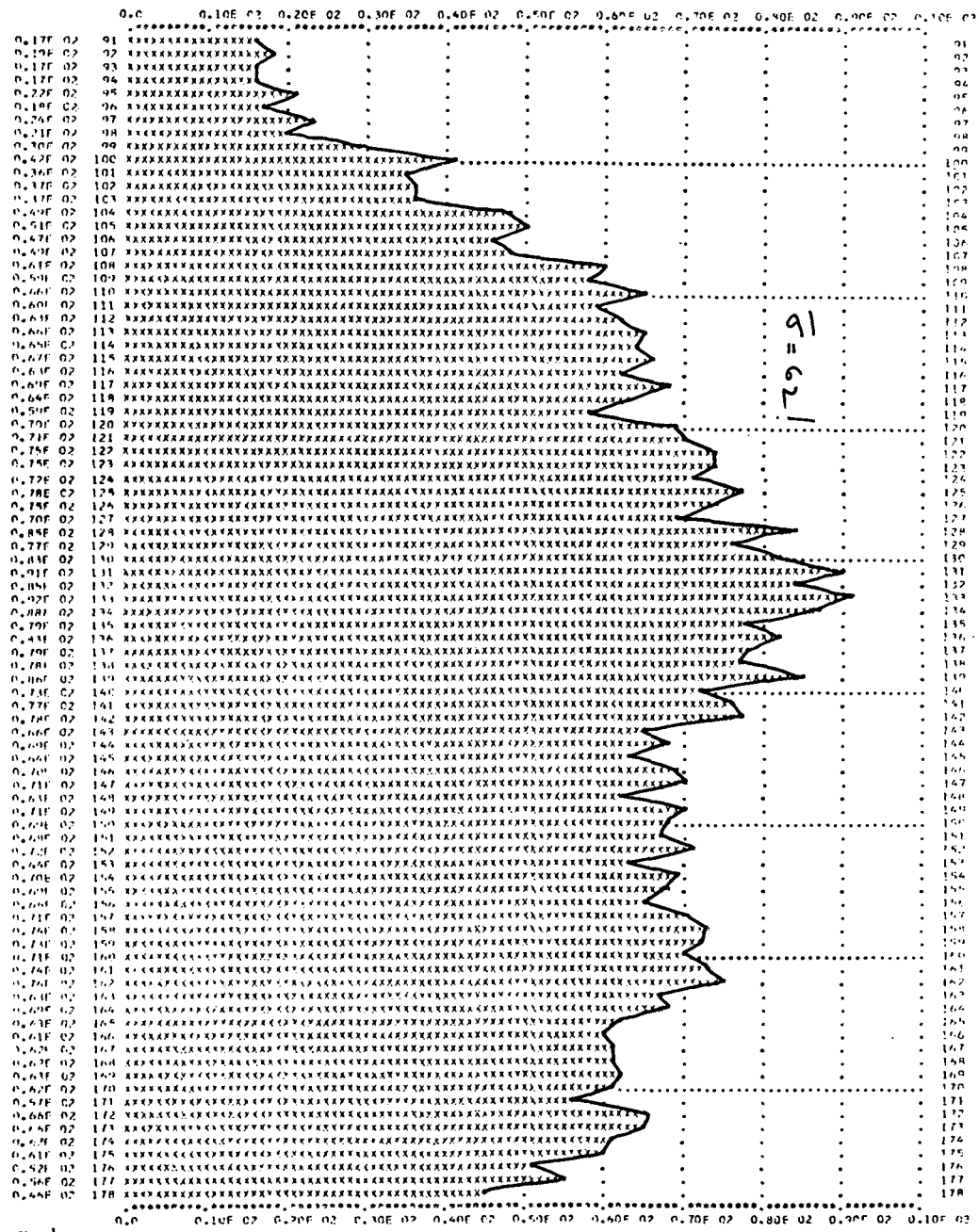

SEP 1 1 1970

PLOT OF STANDARD DEVIATION

A2-24

UP RAMP SPECTRUM GROUP 118 51 4100 TO 18 51 141001 CALLED -- MX108-1 LAVA FLOW II-A (11) FRI 05/07/71 (14:45)
NUMBER OF SPECTRA IN GROUP: 11
COUNTERS RANGE FROM 4.8 TO 13.4 MICRONS

XMIN IS 0.58E 03 XMAX IS 0.93E 03 DELTA IS 0.35E 01

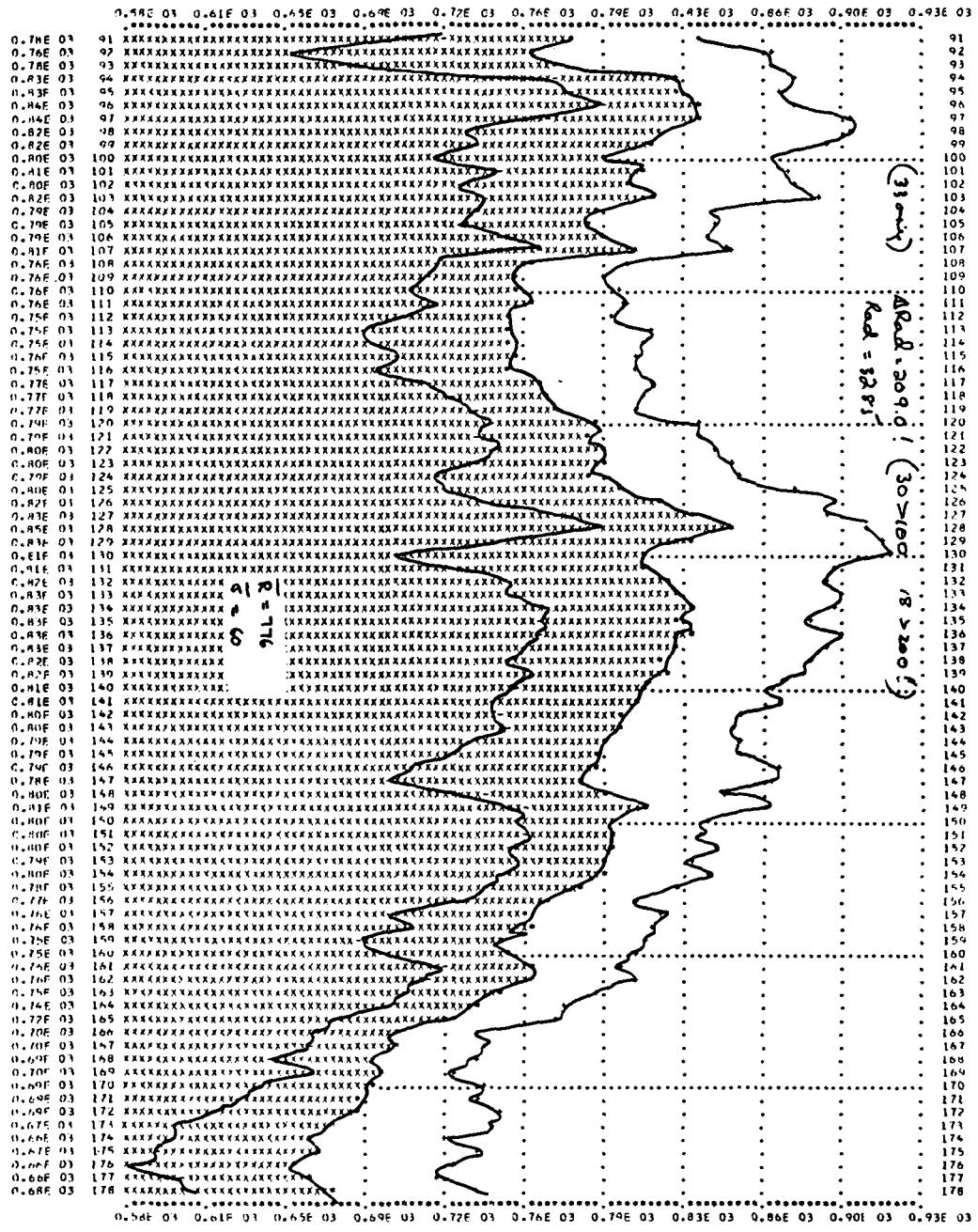

A2-25

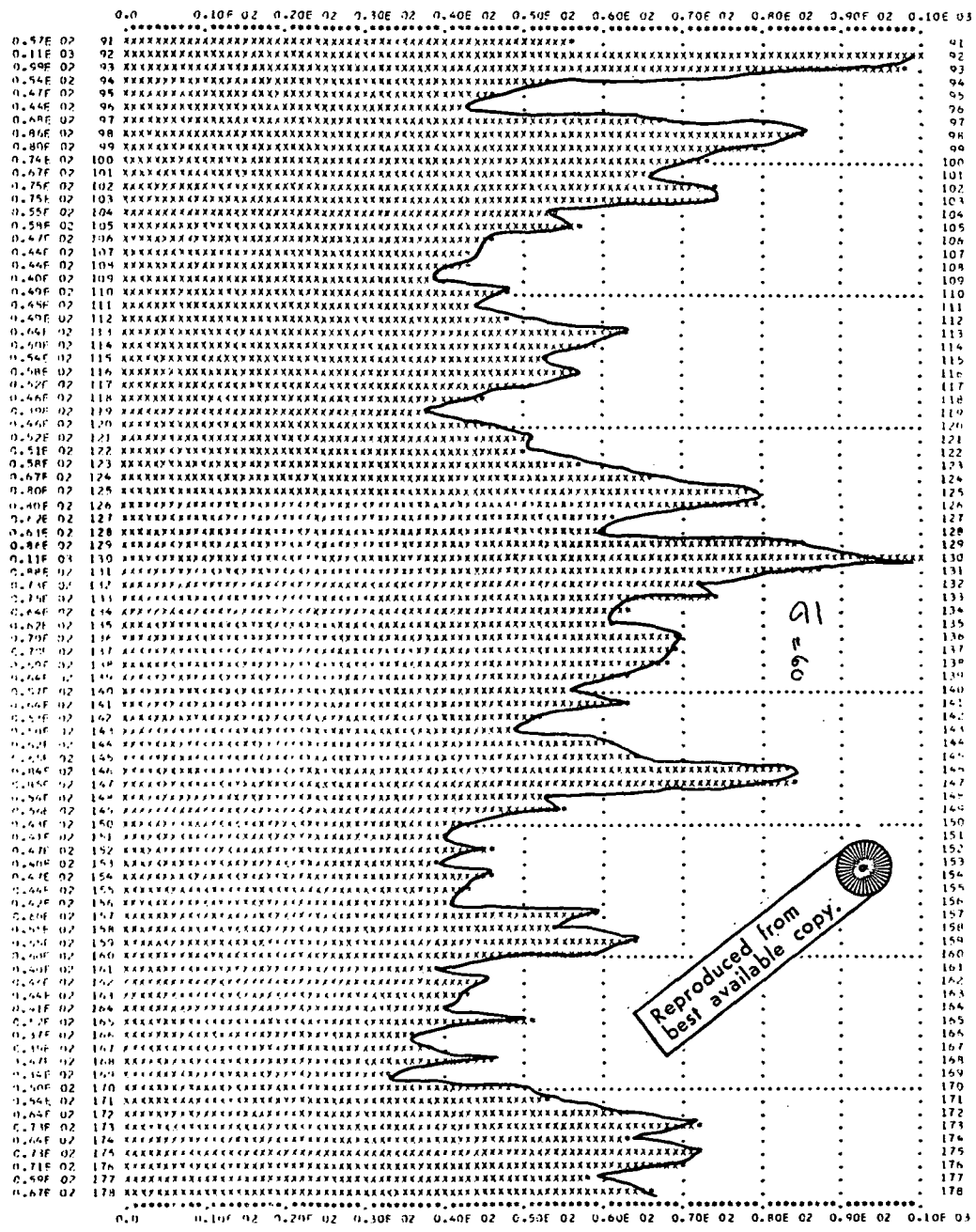

PLOT OF STANDARD DEVIATION A2-26

UP RAMP SPECTRUM GROUP (19 8 11410 TO 19 8 19900) CALLED -- MX108-1 LAVA FLOW II-D FRI 05/07/71 (14:45)
NUMBER OF SPECTRA IN GROUP: 9
COUNTERS RANGE FROM 6.8 TO 13.4 MICRONS

(12)

XMIN IS 0.56E 03 XMAX IS 0.87E 03 DELTA IS 0.32E 01

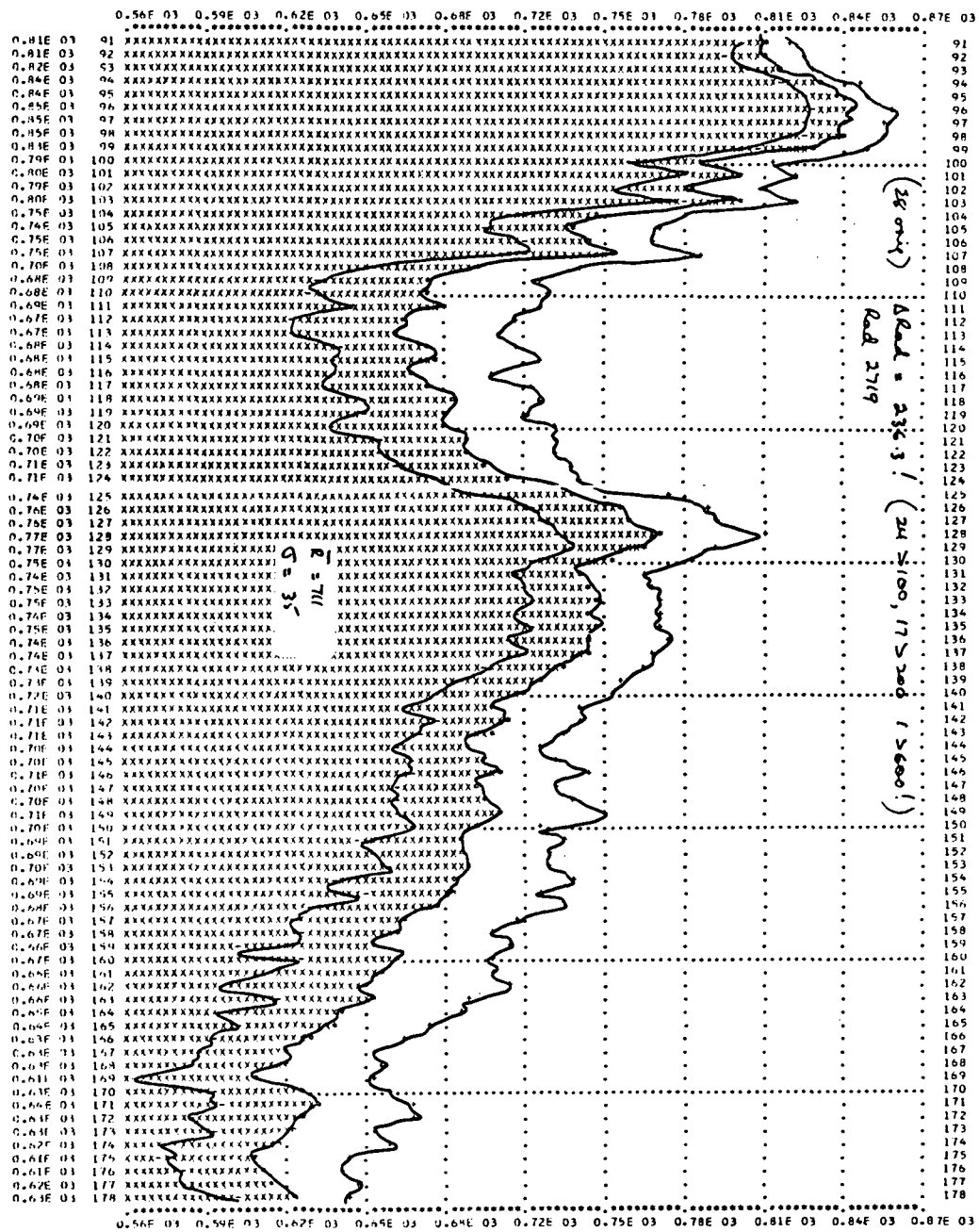

PLOT OF GROUP MEAN

A2-27

UP RAMP SPECTRUM GROUP 119 @ 11410 TO 19 8 19900) CALLED -- MX108-1 LAVA FLOW 11-0 FRI 05/07/71 (14:45)
NUMBER OF SPECTRA IN GROUP: 9
COUNTERS RANGE FROM 6.8 TO 13.4 MICRONS

(12)

XMIN IS 0.0 XMAX IS 0.10E 03 DELTA IS 0.10E 01

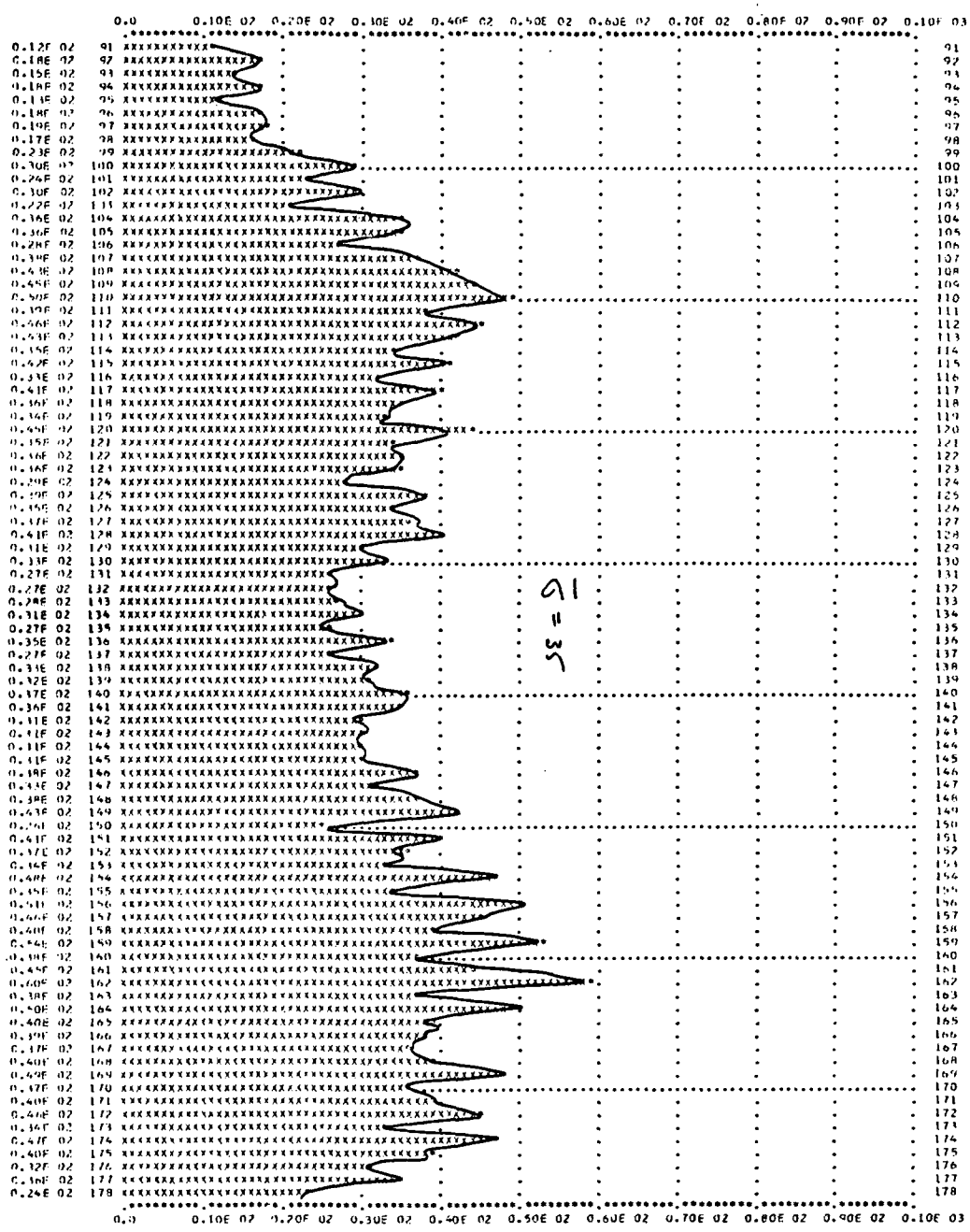

PLOT OF STANDARD DEVIATION AL-28

UP RAMP SPECTRUM GROUP (18 51 16854 TO 18 51 22621) CALLED -- MX108 P-LAVA (SUBGROUP A)

NUMBER OF SPECTRA IN GROUP: 19 (13) 1701

COUNTERS RANGE FROM 6.9 TO 13.4 MICRONS

(13) MX108-1 PISGAH P-LAVA "A"

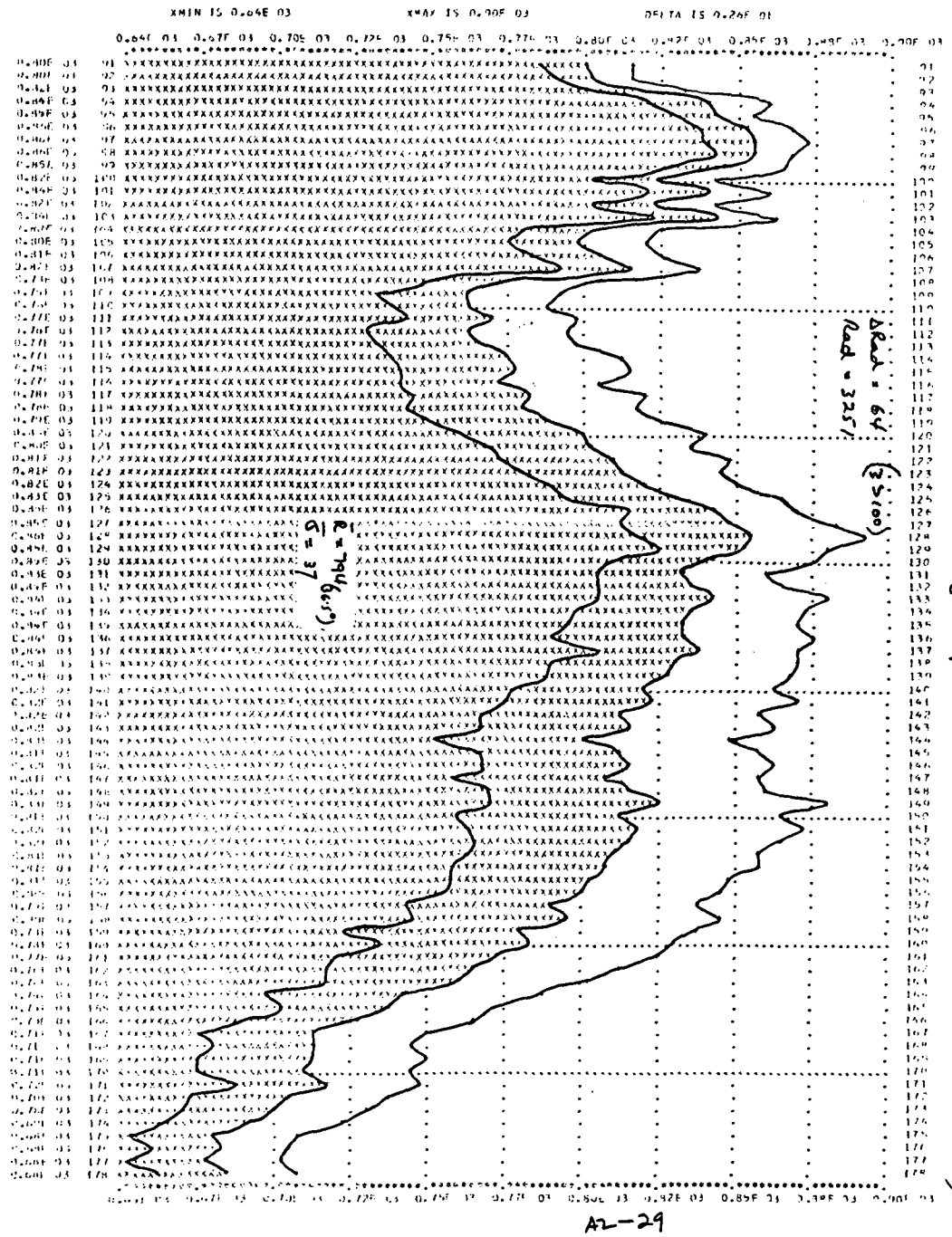

X̄ = 794 N = 19
σ̄ = 37

A2-29

SEP 8 1970

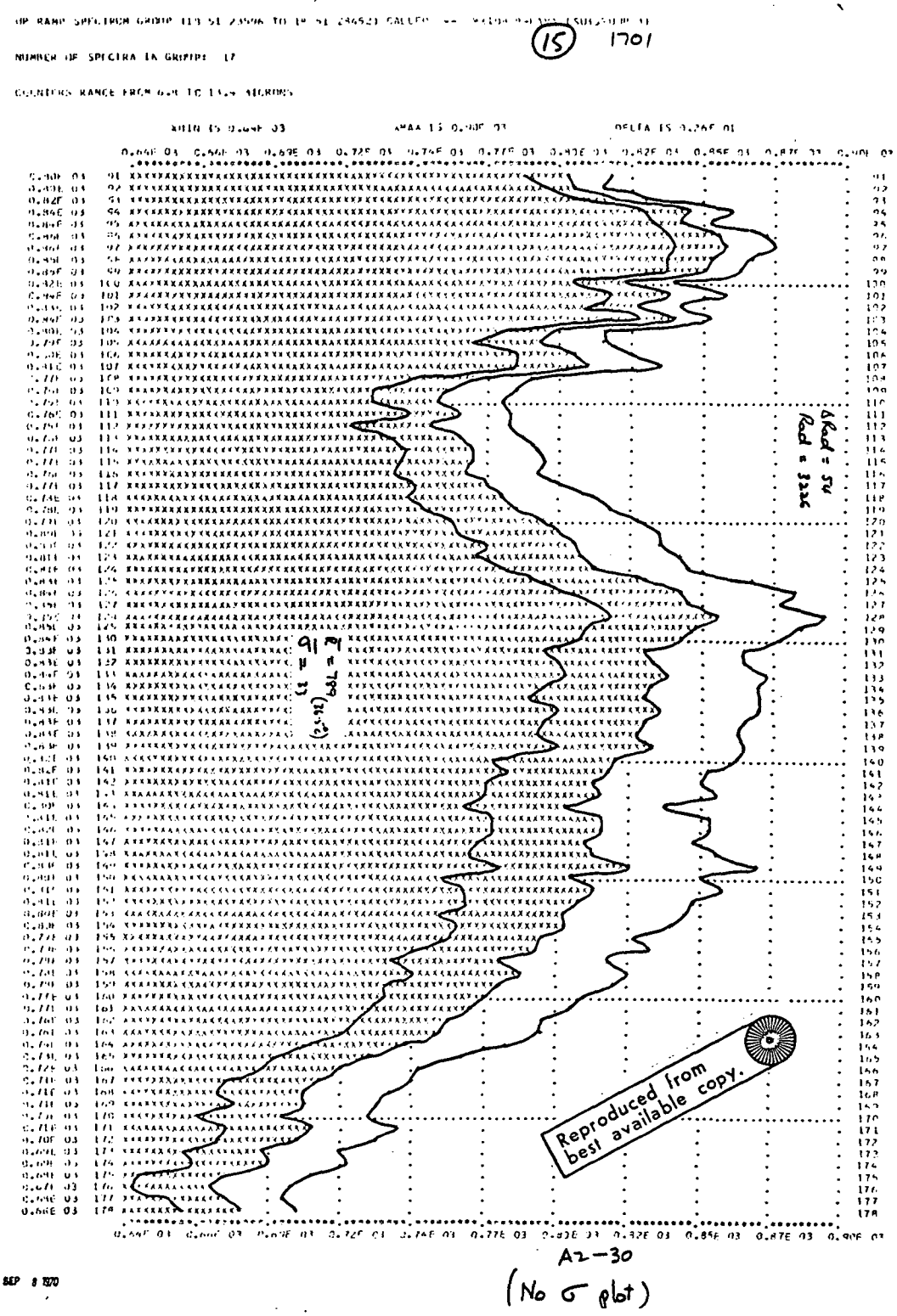

MX108-1 PISGAH PLAQA "B"

C(A)

G. RAMP SPECTRUM GROUP (18 51 28769 TO 18 51 34231) CALLED -- MX108 P-LAVA (SUBGROUP C)

NUMBER OF SPECTRA IN GROUP: 18

COUNTERS RANGE FROM 6.8 TO 13.4 MICRONS

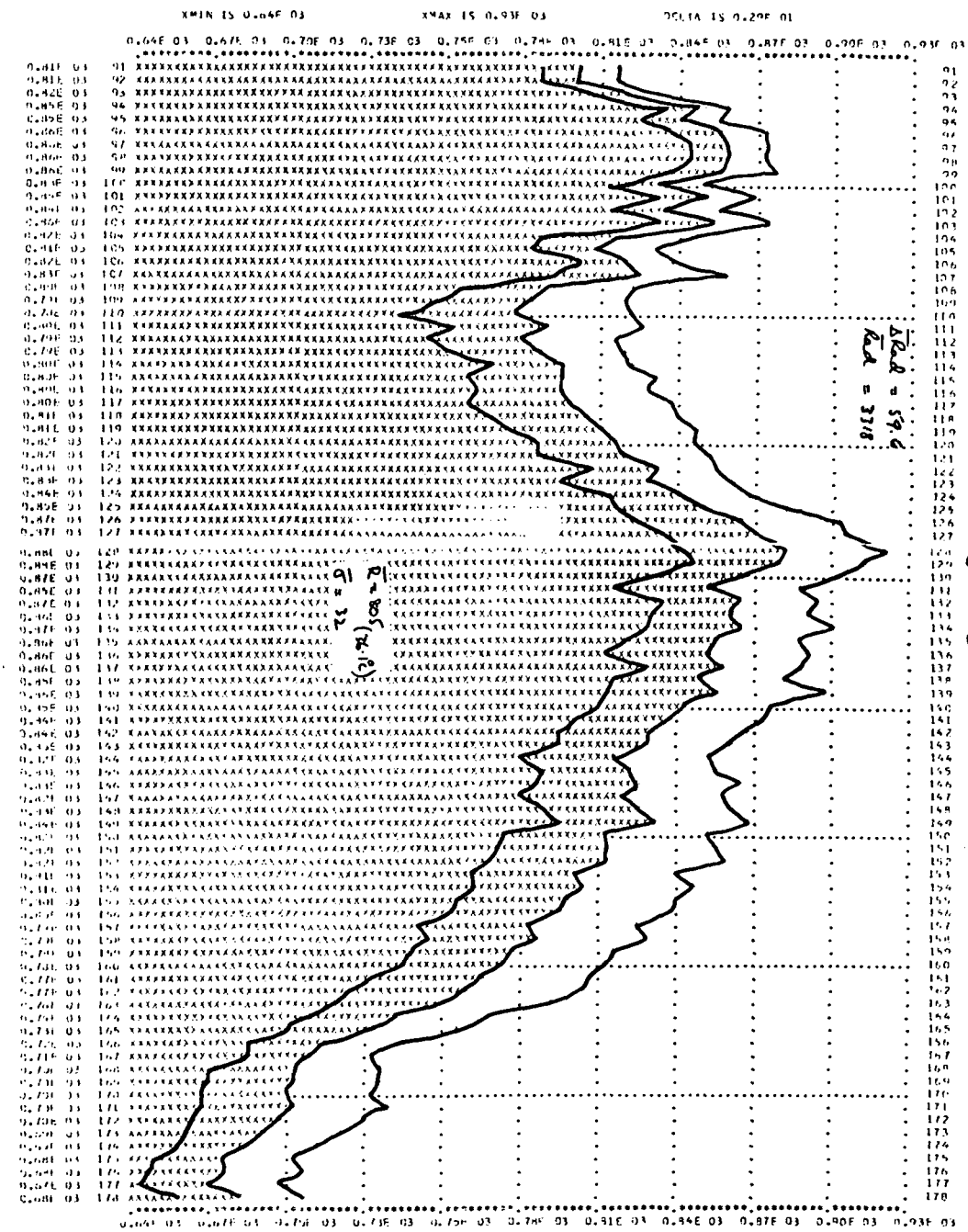

MX108-1 PISGAH P-LAVA "C"

$\bar{x}$ = 805

σ = 32

N = 18

(Tspec = 35.1°C)

A2-31

(No σ plot)

SEP 1970

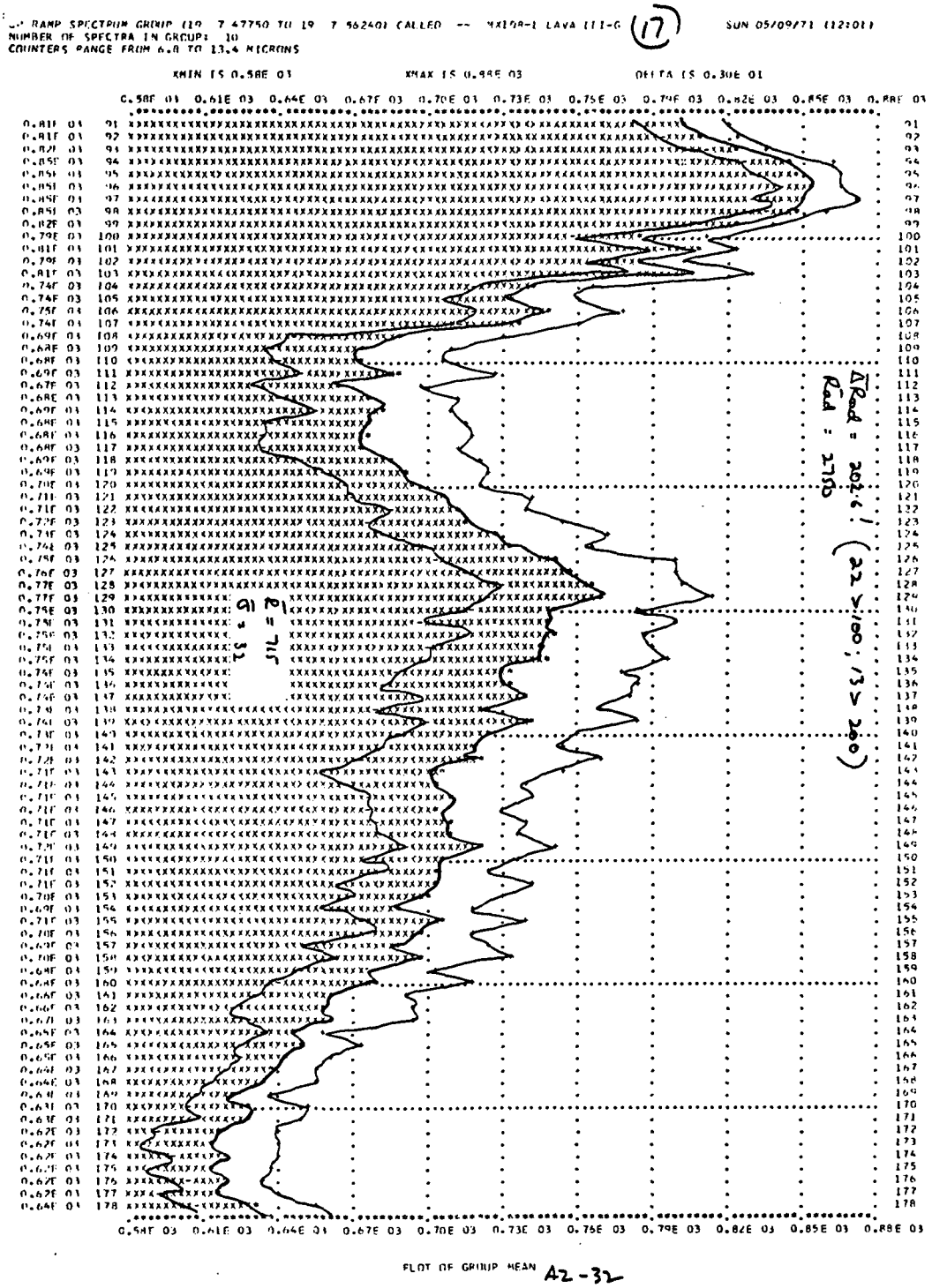

LAVA II G.

A2-32

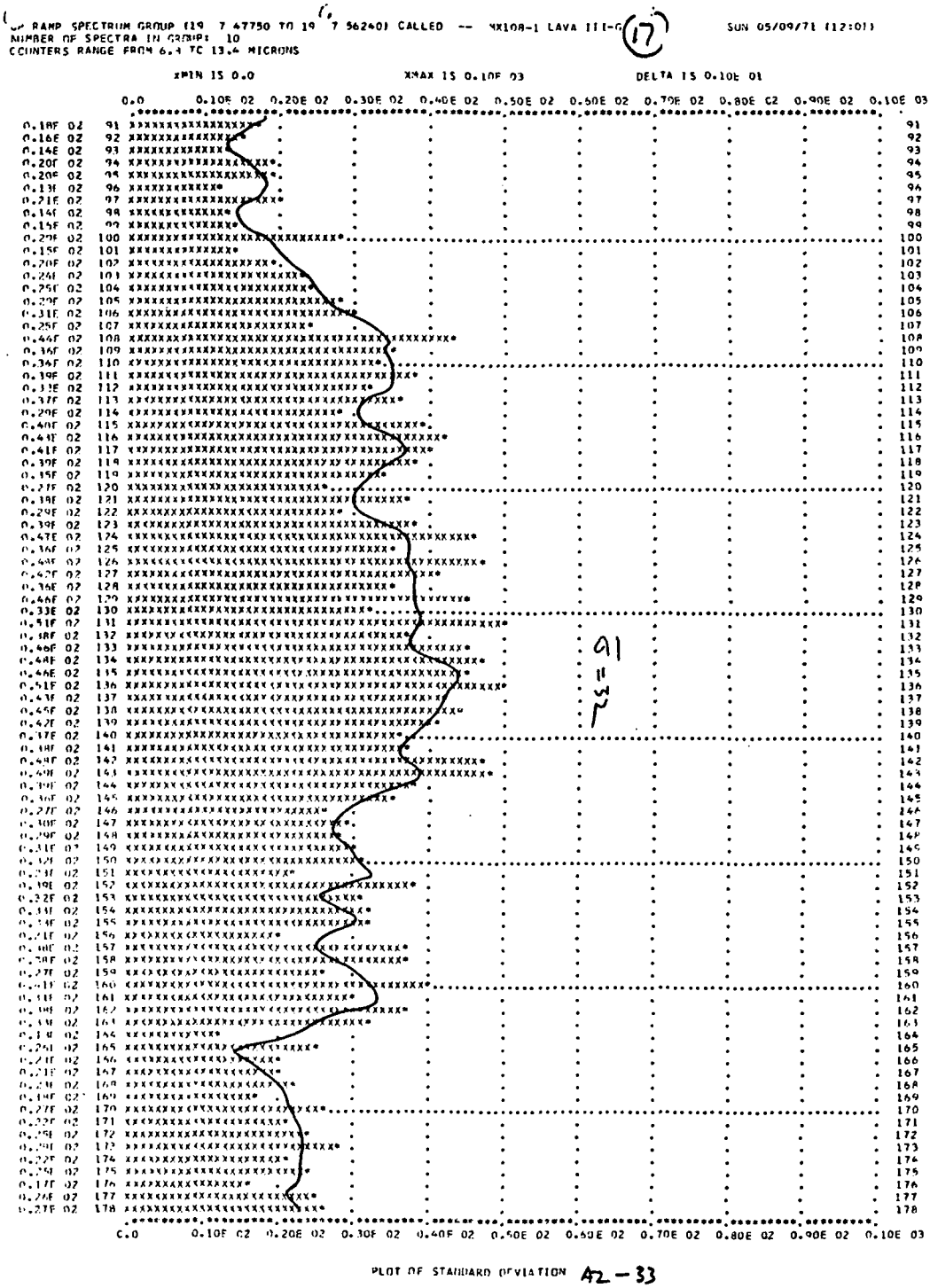

PLOT OF STANDARD DEVIATION 42 – 33

UP RAMP SPECTRUM GROUP (LB 51 34837 TO LB 51 38457) CALLED -- MX108 P-LAVA (SUBGROUP D)

(18) 1701

D(A)

NUMBER OF SPECTRA IN GROUP: 12

COUNTERS RANGE FROM 6.8 TO 13.4 MICRONS

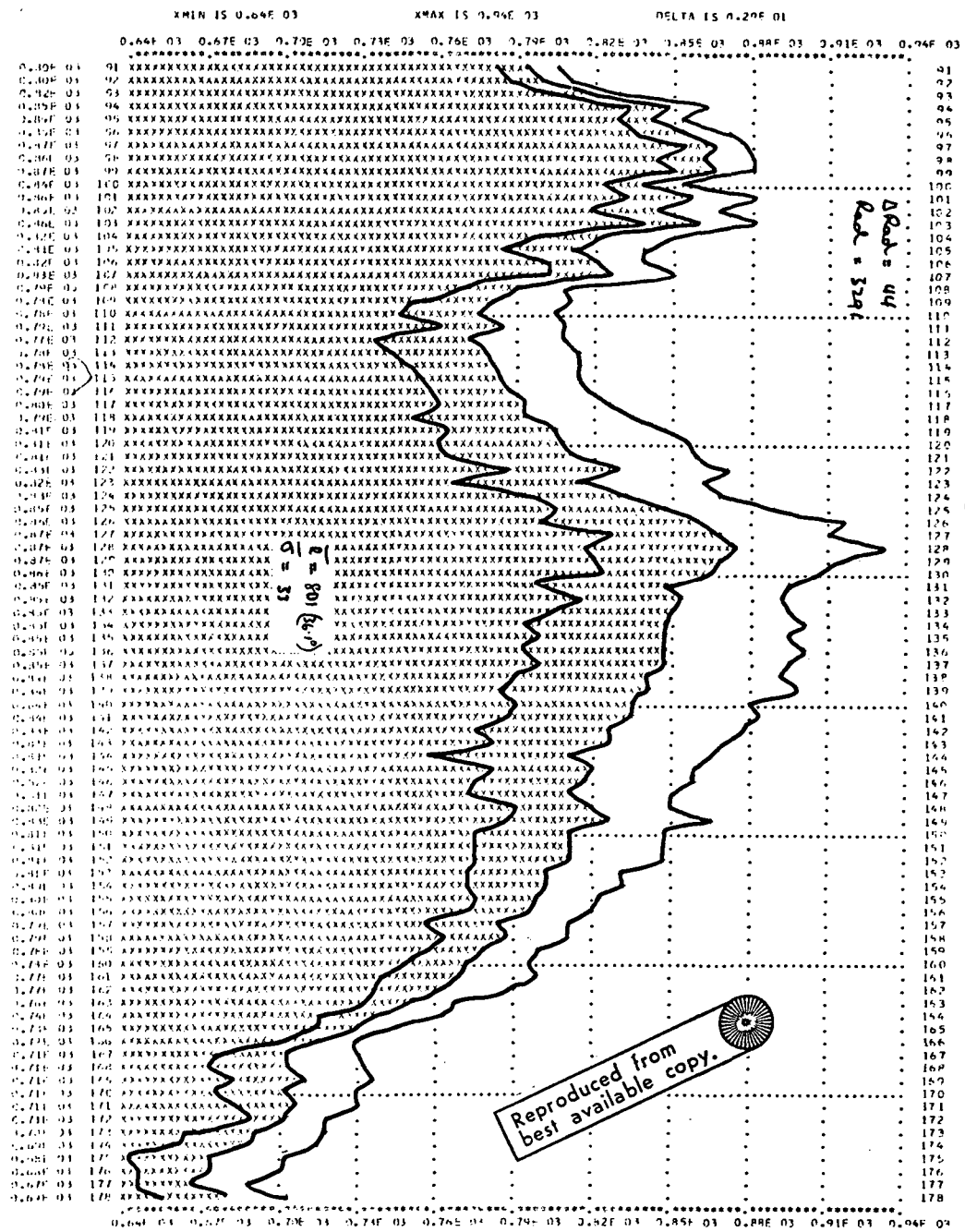

MX108-1 PISGAH P-LAVA D

(Tspace 36.1°C)

A2-34

(No S.D. plot)

SEP 8 1970

Reproduced from best available copy.

UP RAMP SPECTRUM GROUP (17 7 40160 TO 19 7 47440) CALLED -- MX109-1 LAVA III-H (19) SUN 05/09/71 (12:01)
NUMBER OF SPECTRA IN GROUP: 8
COUNTERS RANGE FROM 6.8 TO 13.4 MICRONS

XMIN IS 0.63E 03 XMAX IS 0.89E 03 DELTA IS 0.27E 01

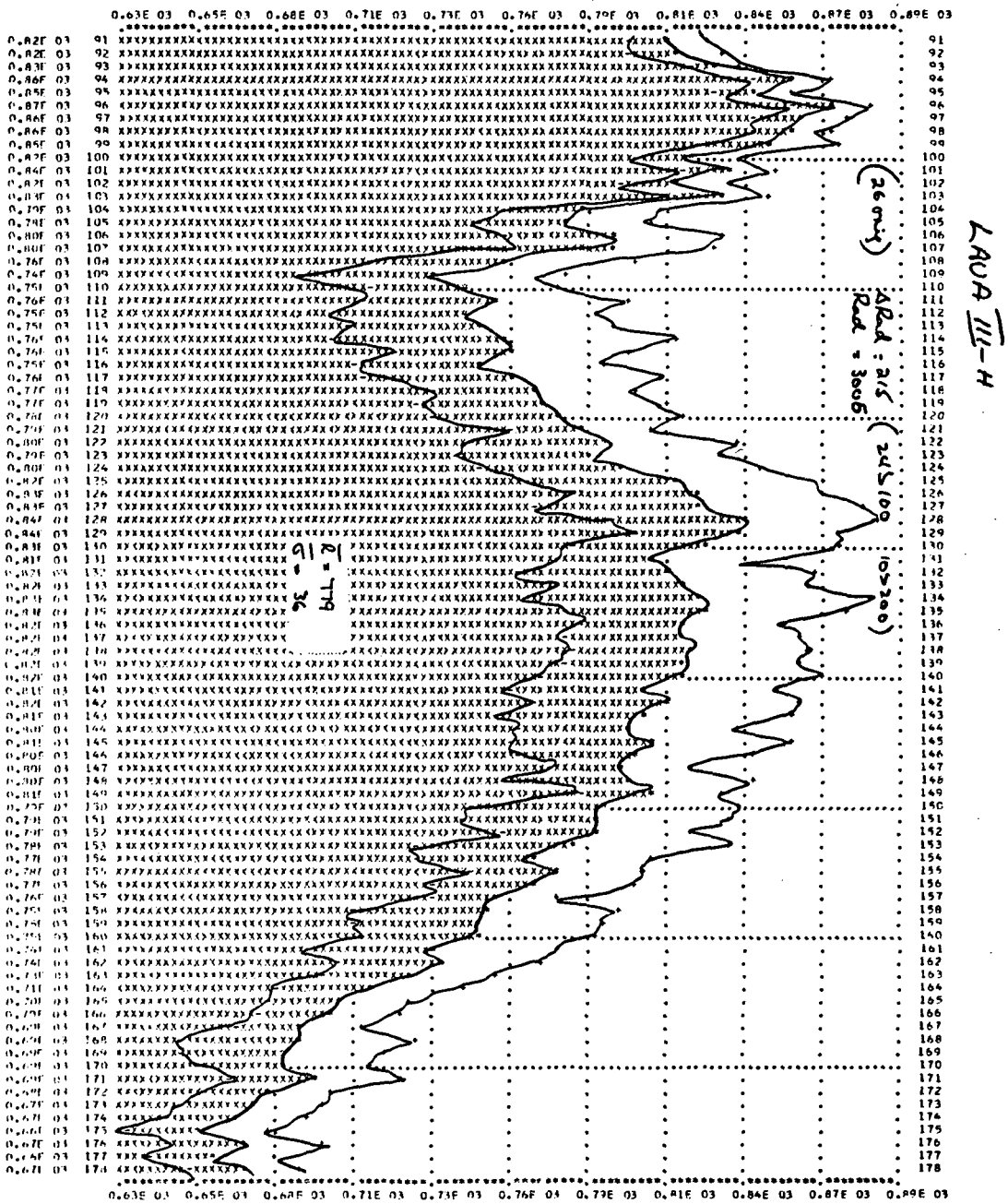

PLOT OF GROUP MEAN A2-35

RAMP SPECTRUM GROUP (17 7 40160 TO 19 7 474401 CALLED -- 4X10R-1 LAVA III-H (19) SUN 05/09/71 (12:01)
NUMBER OF SPECTRA IN GROUPS 8
COUNTERS RANGE FROM 6.9 TO 13.4 MICRONS

XMIN IS 0.0 XMAX IS 0.10E 01 DELTA IS 0.10E 01

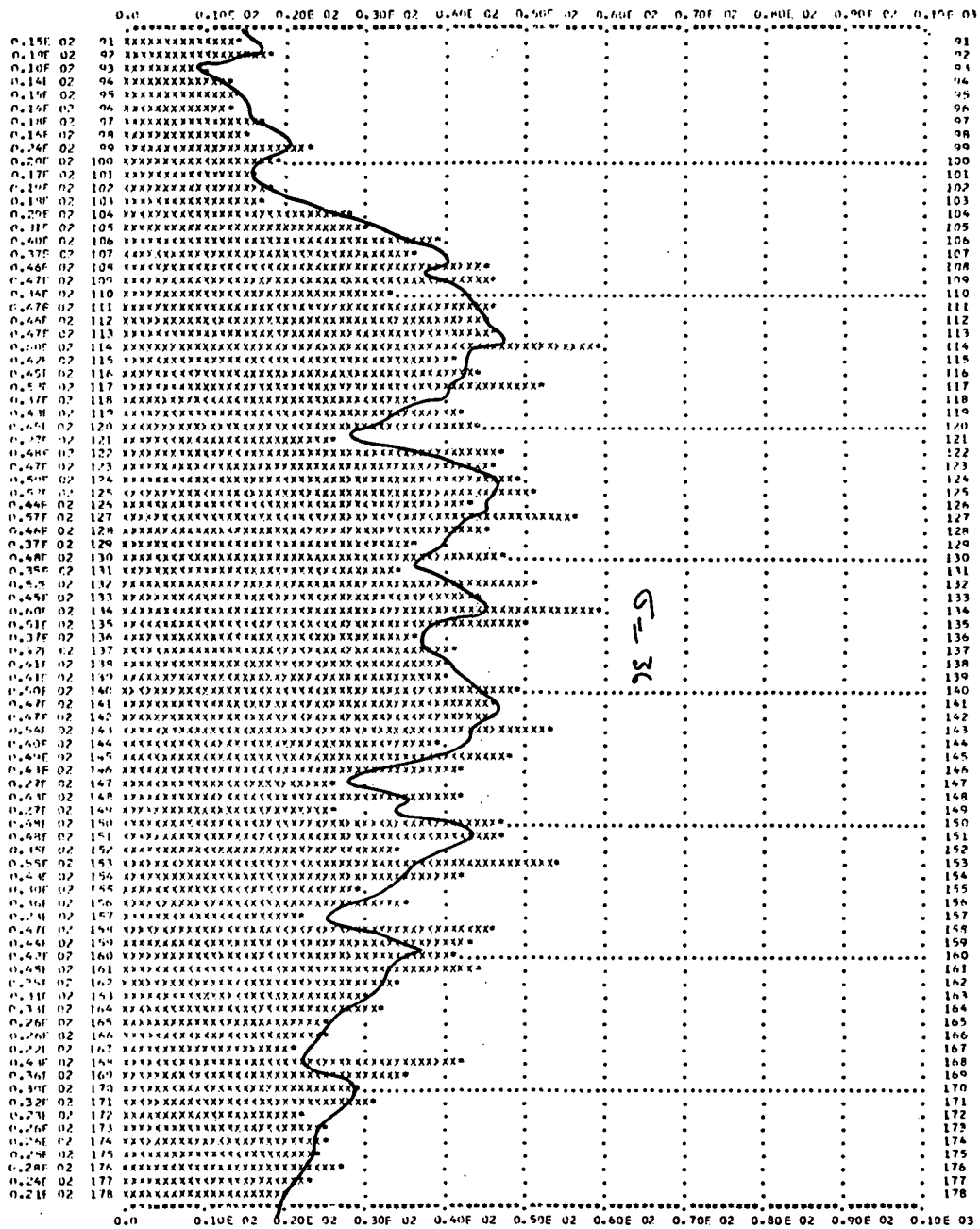

PLOT OF STANDARD DEVIATION A2-36

UP RAMP SPECTRUM GROUP (18 51 47199 TO 18 51 53568) CALLED -- MX108 PISGAH P-LAVA II (F) (20) F(A)

1701

NUMBER OF SPECTRA IN GROUP: 21

COUNTERS RANGE FROM 6.8 TO 13.4 MICRONS

XMIN IS 0.66E 03 XMAX IS 0.92E 03 DELTA IS 0.26E 01

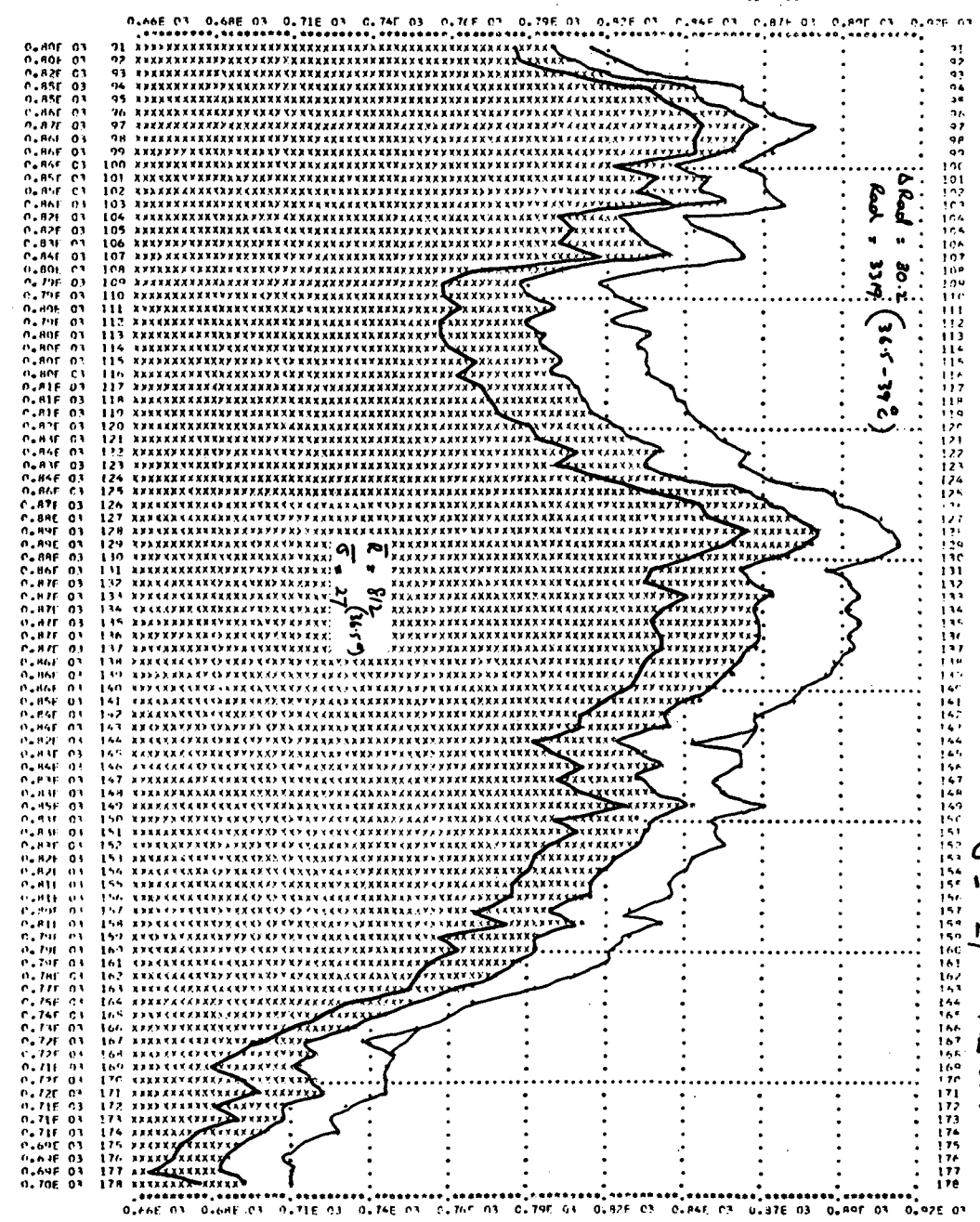

PISGAH P-LAVA Phase II (F)

N = 21 X̄ = 812 Tmax 39 (3) Tspec 36.5

σ̄ = 27 Tmin 36.5

SEP 11 1970

A2-37

LP RAMP SPECTRUM GROUP (18 51 47199 TO 18 51 535681 CALLED -- MX108 PISGAH P-LAVA IT (F)

(20)

NUMBER OF SPECTRA IN GROUP: 21

COUNTERS RANGE FROM 6.8 TO 13.4 MICRONS

XMIN IS 0.0 XMAX IS 0.10E 03 DELTA IS 0.10E 01

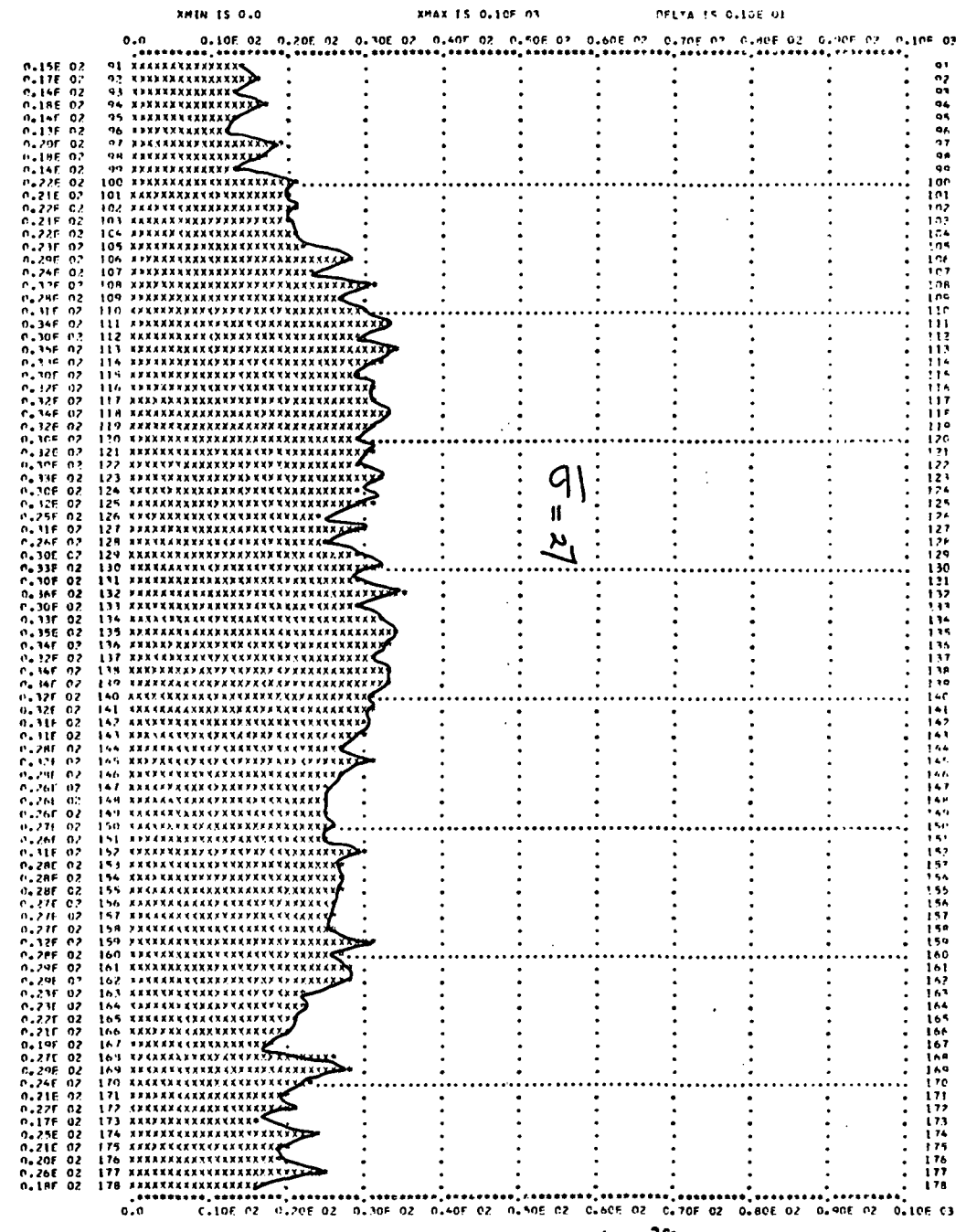

PLOT OF STANDARD DEVIATION

A2-38

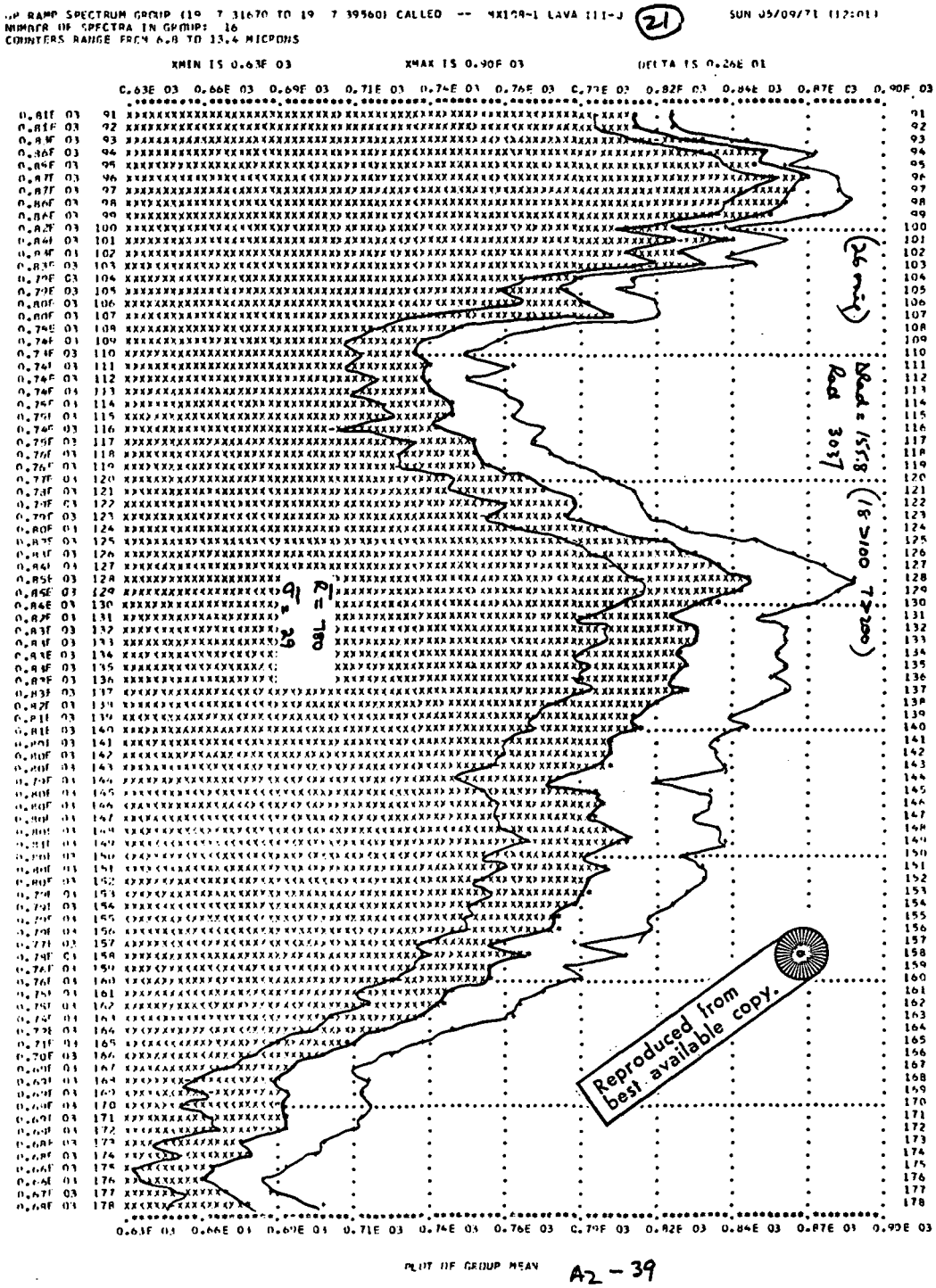

LAVA III J

A2 - 39

UP RAMP SPECTRUM GROUP 119 T 31670 TO 19 7 39560 CALLED -- HX108-1 LAVA 111-J (21) SUN 05/09/71 (12:01)
NUMBER OF SPECTRA IN GROUP: 16
COUNTERS RANGE FROM 6.8 TO 13.4 MICRONS

XMIN IS 0.0 XMAX IS 0.10E 03 DELTA IS 0.10E 01

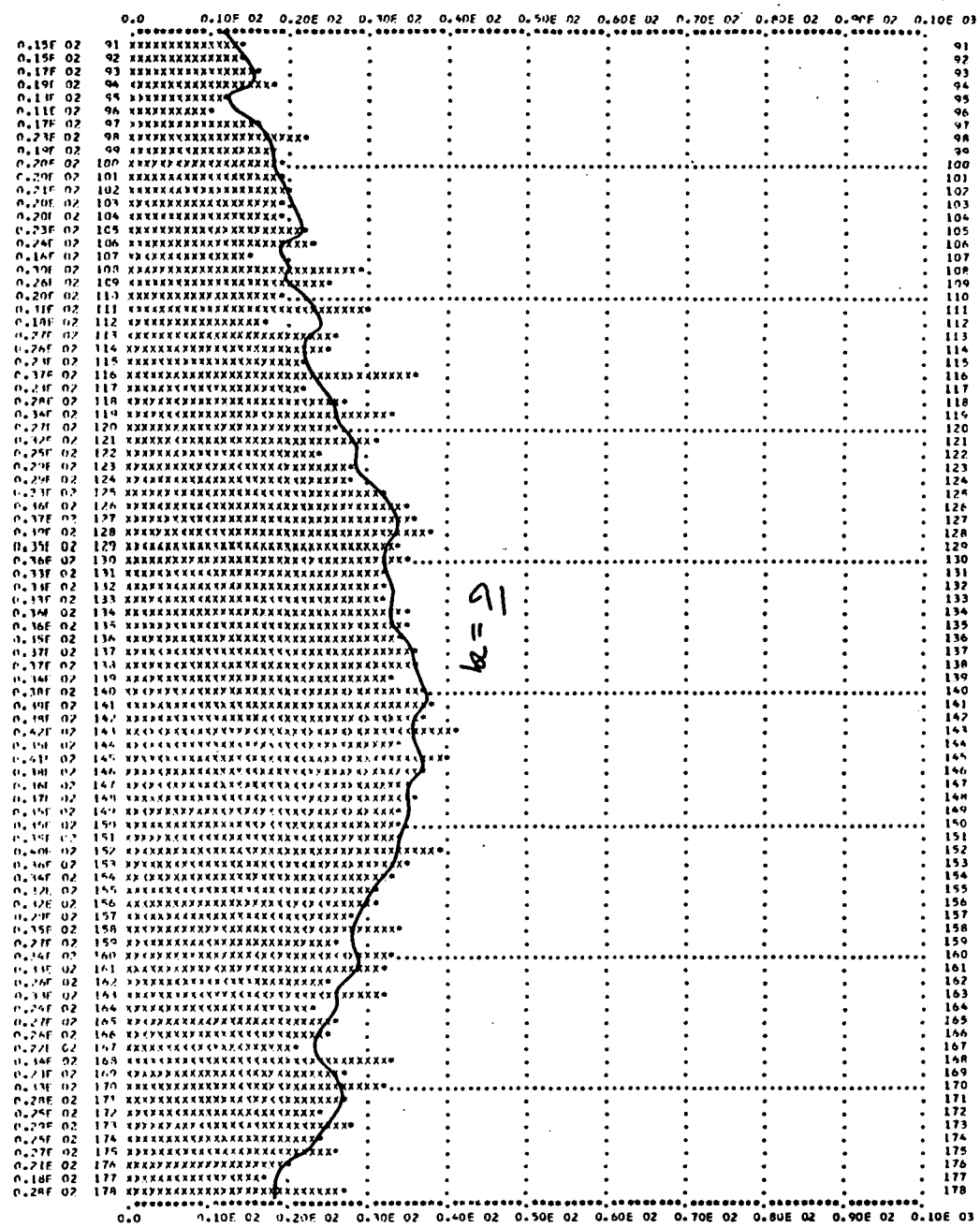

PLOT OF STANDARD DEVIATION A2-40

UP RAMP SPECTRUM GROUP (18 51 58125 TO 18 52 4493) CALLED -- MXIC4 ALLUVIAL-D

(22) 1701 D(A)

NUMBER OF SPECTRA IN GROUP: 21

COUNTERS RANGE FROM 6.8 TO 13.4 MICRONS

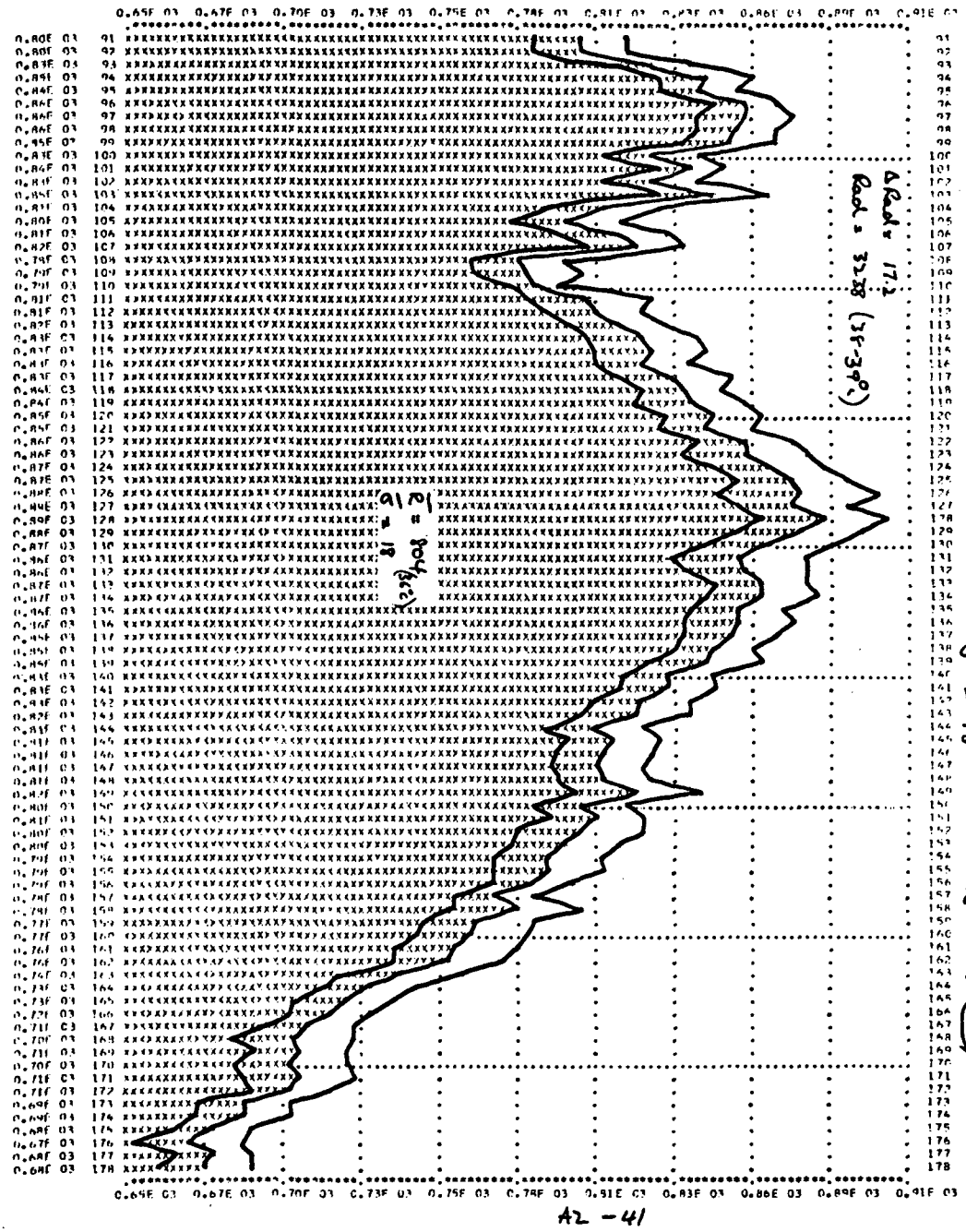

PISGAH ALLUVIAL D

N = 21

$\overline{X}$ = 804

$\overline{\sigma}$ = 18

$\overline{T}_{max}$ = 39

$\overline{T}_{min}$ = 38 (1°C)

$\overline{T}_{spec}$ 36°C

ΔRad = 17.2

Rad = 32.38 (38-39°C)

$\overline{\sigma}$ = 804 (36°C)

$\overline{\sigma}$ = 18

A2 - 41

SEP 1 1 1970

UP RAMP SPECTRUM GROUP (18 51 5R125 TO 18 52 44931 CALLED -- MX10R ALUMINAL-D

(22)

NUMBER OF SPECTRA IN GROUP: 21

COUNTERS RANGE FROM 6.8 TO 13.4 MICRONS

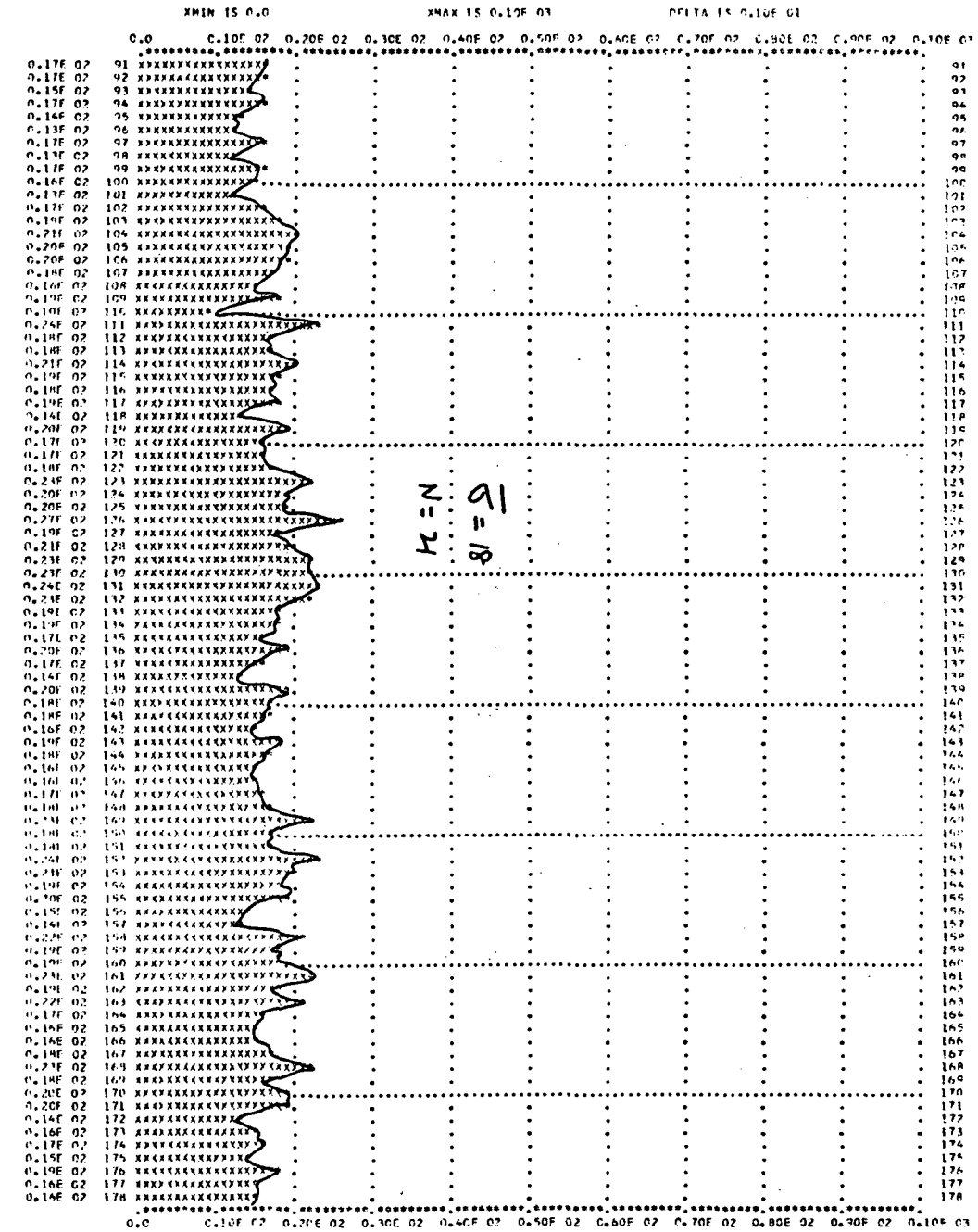

SEP 1 1 1970

PLOT OF STANDARD DEVIATION A2-42

HP RAMP SPECTRUM GROUP (19 7.15580 TO 19 7.20740) CALLED -- MX104-1 LAVA 1-K (23) SUN 05/09/71 (12:01)
NUMBER OF SPECTRA IN GROUP: 16
COUNTERS RANGE FROM 0.8 TO 13.4 MICRONS

XMIN IS 0.64E 03 XMAX IS 0.90E 03 DELTA IS 0.27E 01

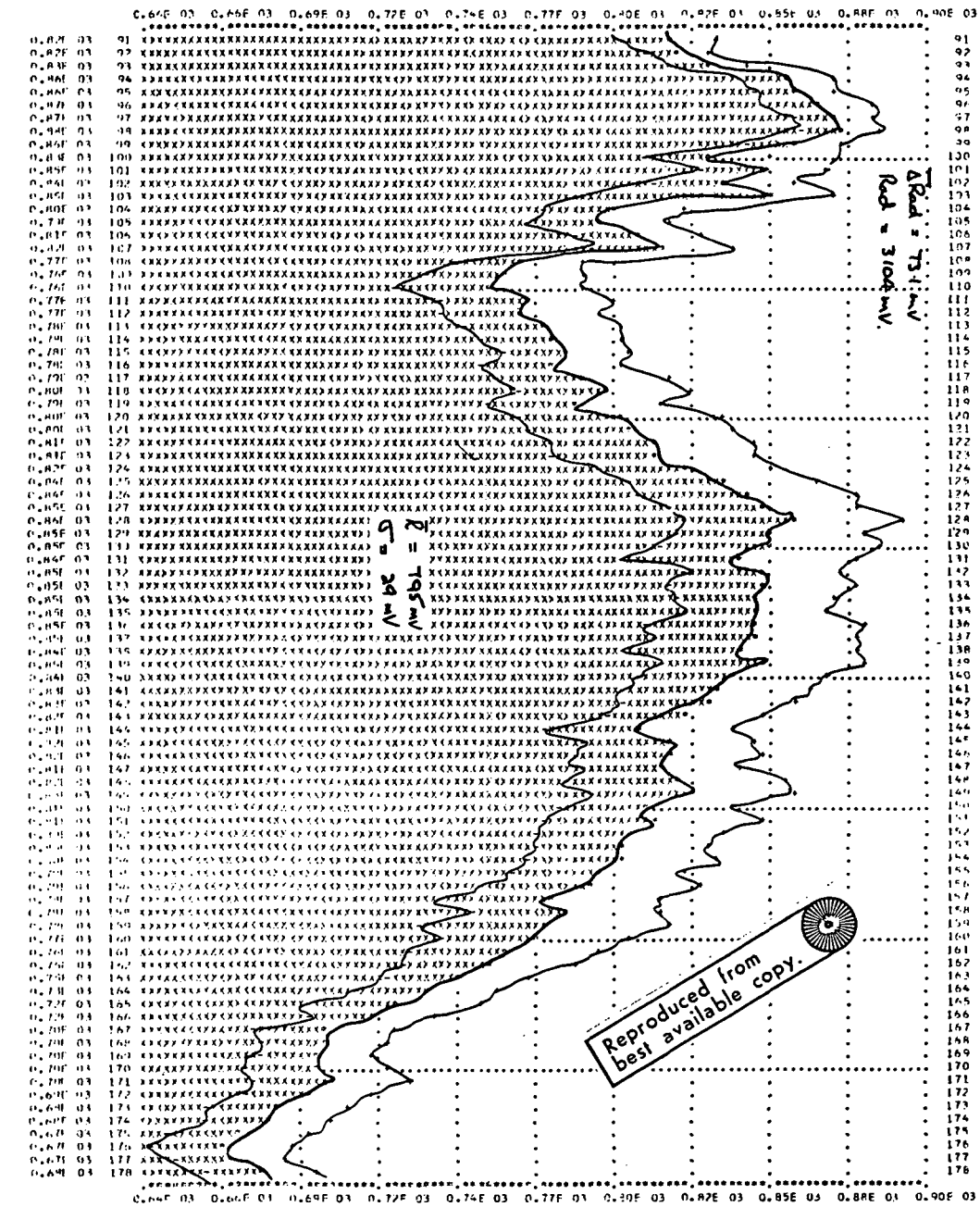

Reproduced from best available copy.

PLOT OF GROUP MEAN A2-43

UP RAMP SPECTRUM GROUP (19 7 15580 TO 19 7 207401 CALLED -- MX108-1 LAVA I-K (23) SUN 05/09/71 (12:01)
NUMBER OF SPECTRA IN GROUP: 16
COUNTERS RANGE FROM 0.8 TO 13.4 MICRONS

XMIN IS 0.0 XMAX IS 0.10E 03 DELTA IS 0.10E 01

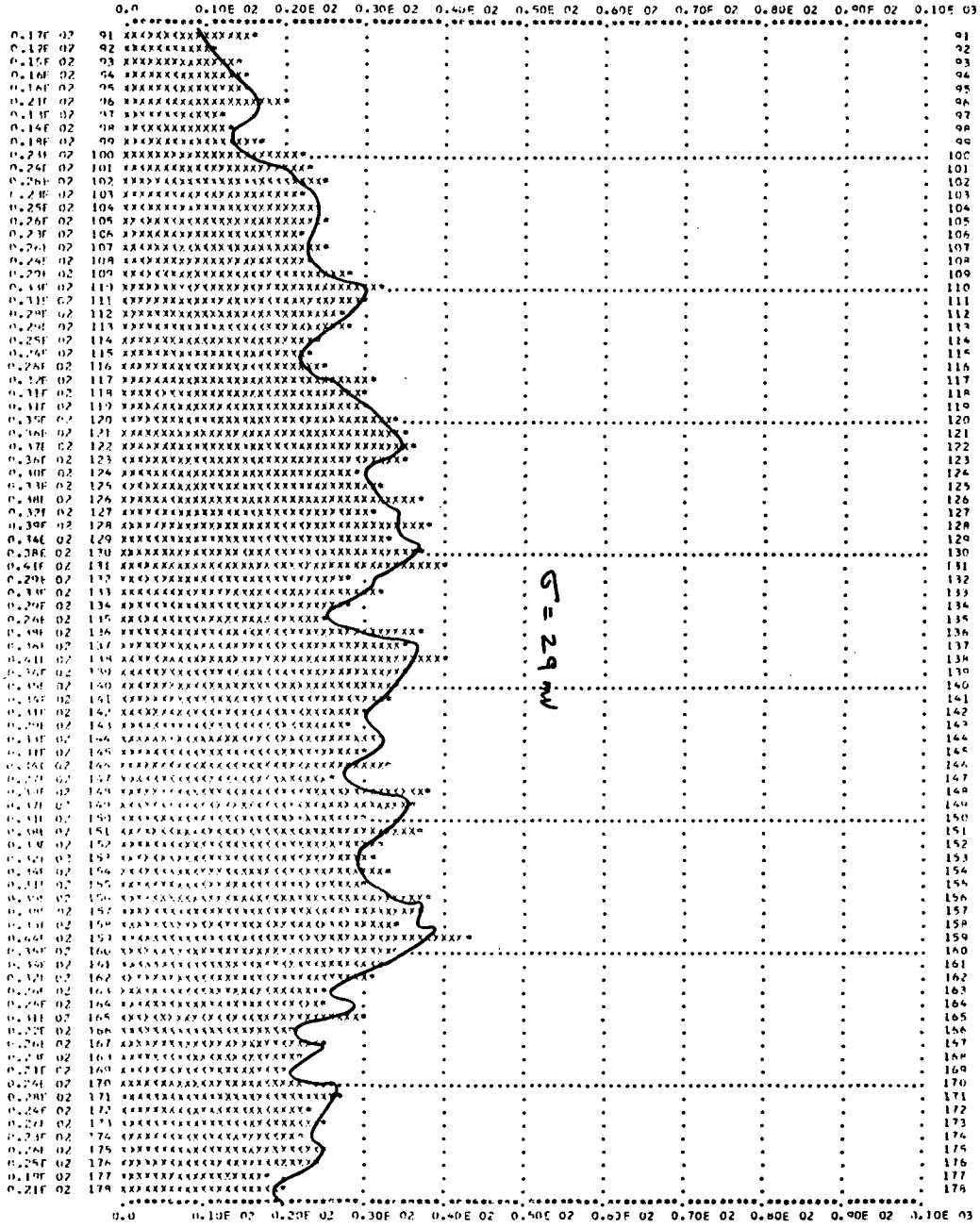

PLOT OF STANDARD DEVIATION A2-44

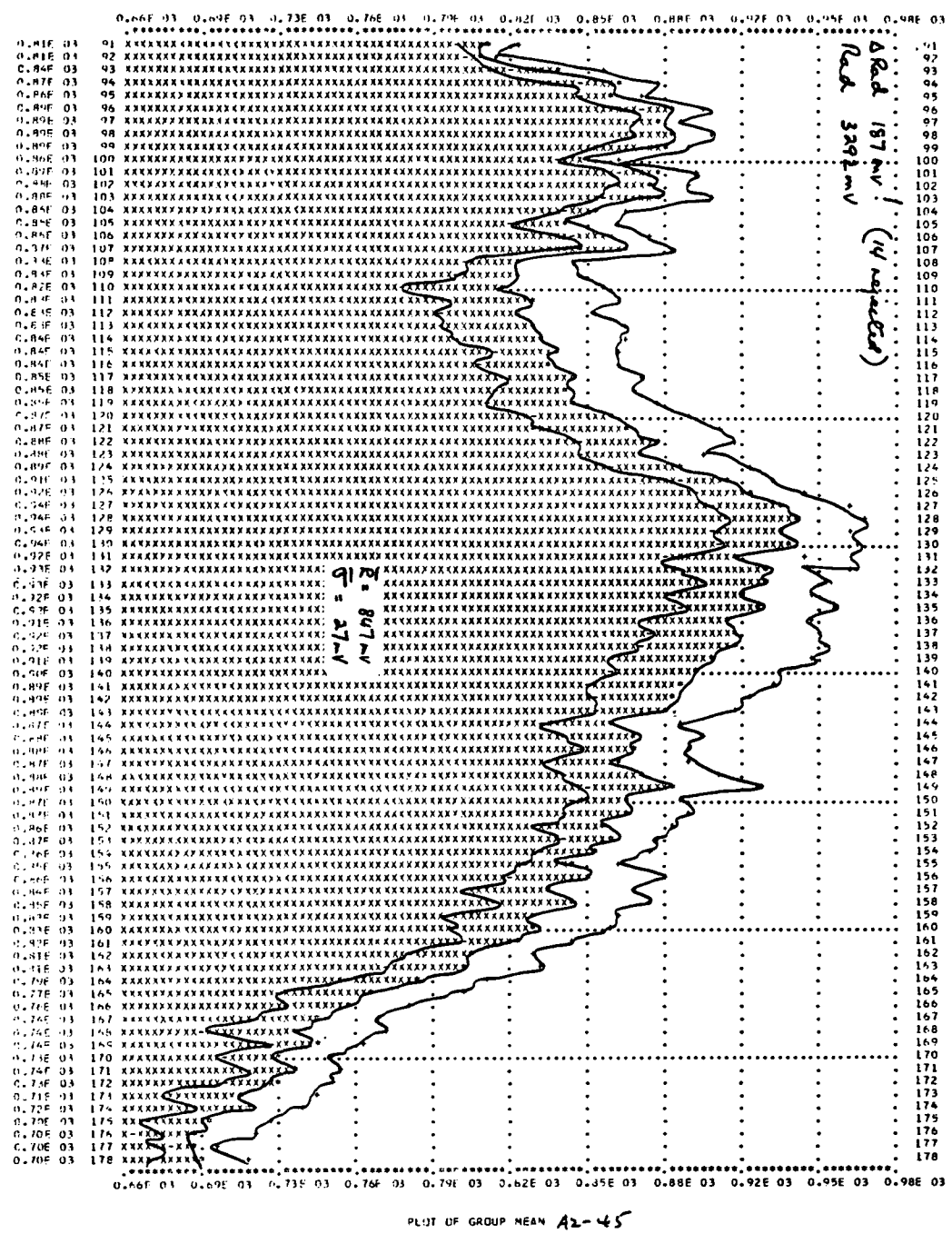
NUMBER OF SPECTRA IN GROUP: 13
COUNTERS RANGE FROM 0.8 TO 13.4 MICRONS
XMIN IS 0.66E 03
XMAX IS 0.98E 03
DELTA IS 0.32E 01
0.66E 03 0.69E 03 0.73E 03 0.76E 03 0.79E 03 0.82E 03 0.85E 03 0.88E 03 0.92E 03 0.95E 03 0.98E 03
ΔRad 187 mV (4 spectra)
Rad 329 mV
91 R. 847 mV
27 mV
PLOT OF GROUP MEAN A2-45

RAMP SPECTRUM GROUP (19 7 8009 TO 19 7 15280) CALLED -- MKIOR-1 LAVA FLOW II-C (24) FRI 05/07/71 (14:45)
NUMBER OF SPECTRA IN GROUP: 10
COUNTERS RANGE FROM 6.8 TO 13.4 MICRONS

XMIN IS 0.0 XMAX IS 0.10E 03 DELTA IS 0.10E 01

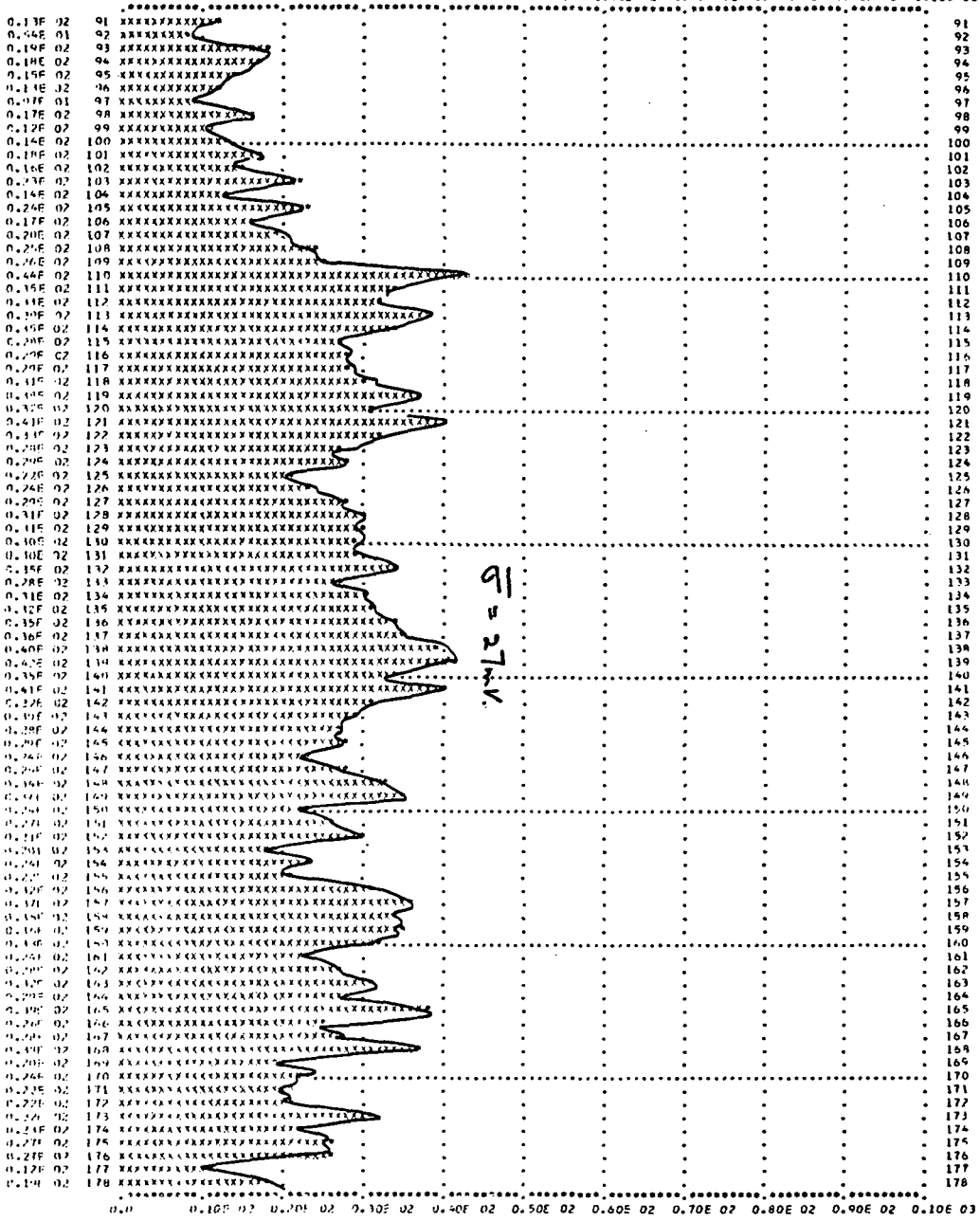

PLOT OF STANDARD DEVIATION A2-46

UP RAMP SPECTRUM GROUP (18 52 12000) TO 18 52 17000) CALLED -- MX108-1 LAVA FLOW II-8 FRI 05/07/71 (14:45)
NUMBER OF SPECTRA IN GROUP: 10
COUNTERS RANGE FROM 6.8 TO 13.4 MICRONS

(25)

XMIN IS 0.62E 03 XMAX IS 0.92E 03 DELTA IS 0.30E 01

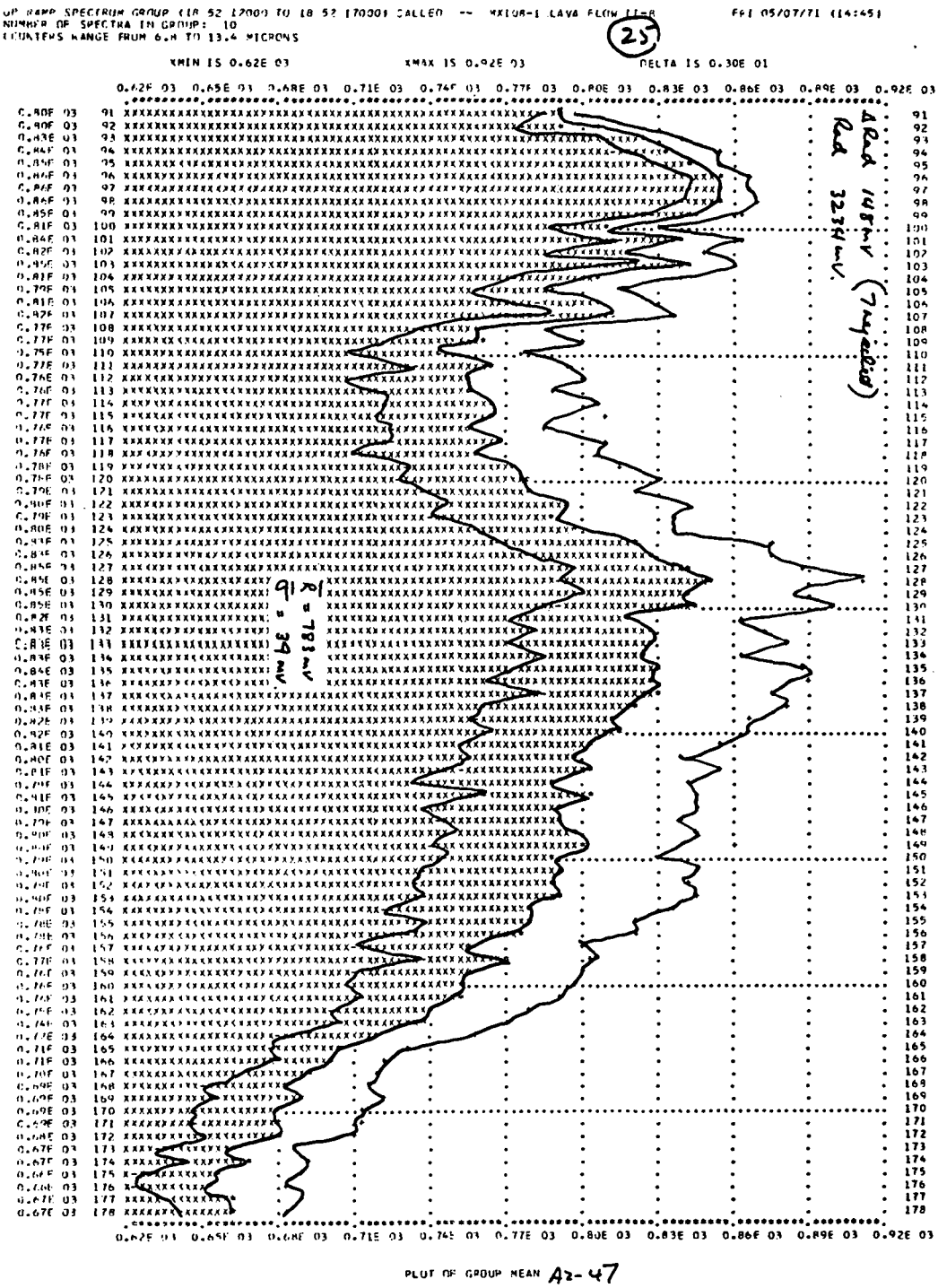

PLOT OF GROUP MEAN A2-47

UP RAMP SPECTRUM GROUP (18 52 12000 TO 18 52 17000) CALLED -- MX108-1 LAVA FLOW 11-8 FRI 05/07/71 (14:45)
NUMBER OF SPECTRA IN GROUP: 10
POINTERS RANGE FROM 6.8 TO 13.4 MICRONS

(25)

XMIN IS 0.0 XMAX IS 0.10E 03 DELTA IS 0.10E 01

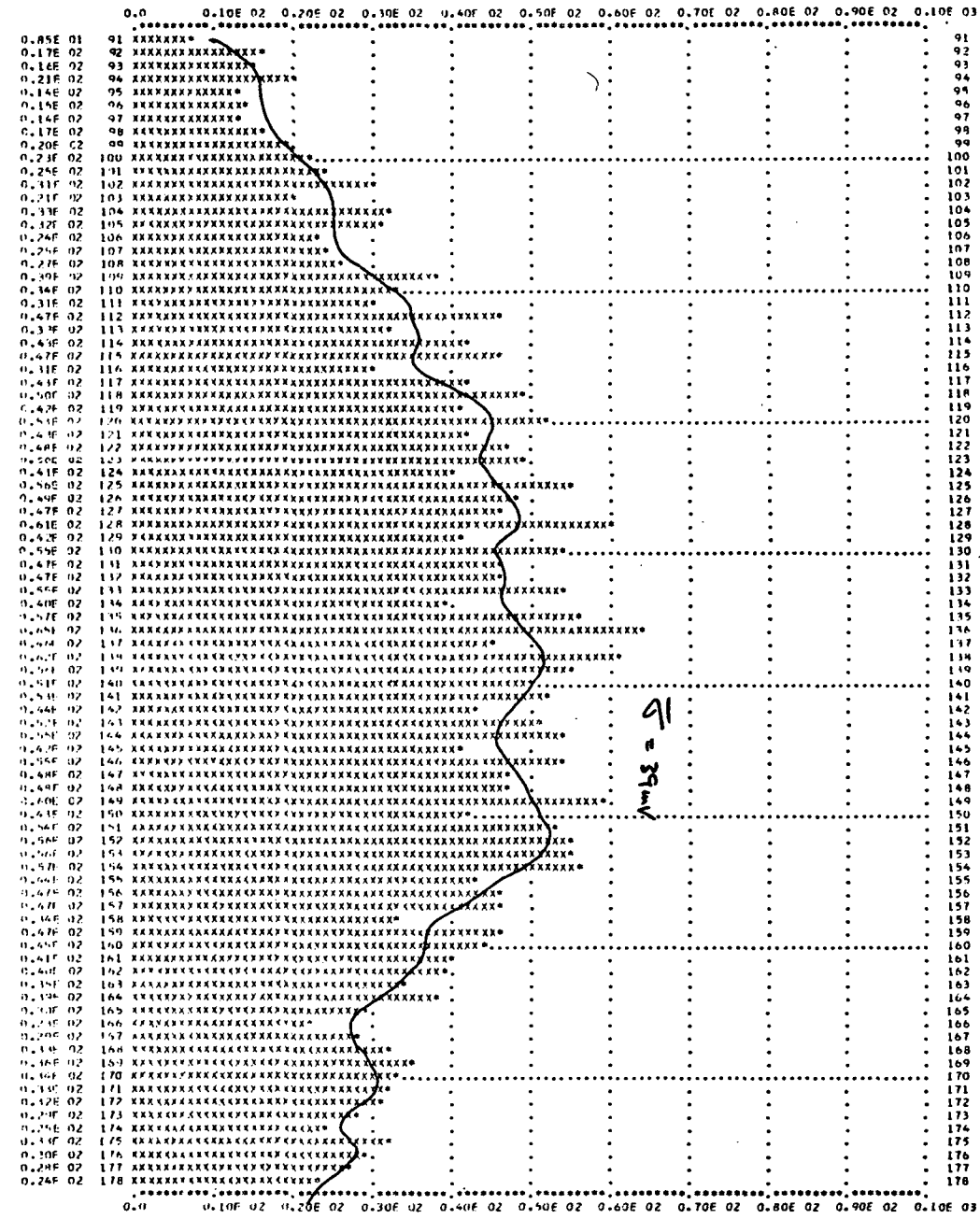

PLOT OF STANDARD DEVIATION A2-48

UP RAMP SPECTRUM GROUP (18 52 19059 TO 18 52 25430) CALLED -- MX108 PISGAH P-LAVA II (E)

1701 (26)

E (A)

NUMBER OF SPECTRA IN GROUP: 21

COUNTERS RANGE FROM 6.8 TO 13.4 MICRONS

XMIN IS 0.64E 03 XMAX IS 0.88E 03 DELTA IS 0.25E 01

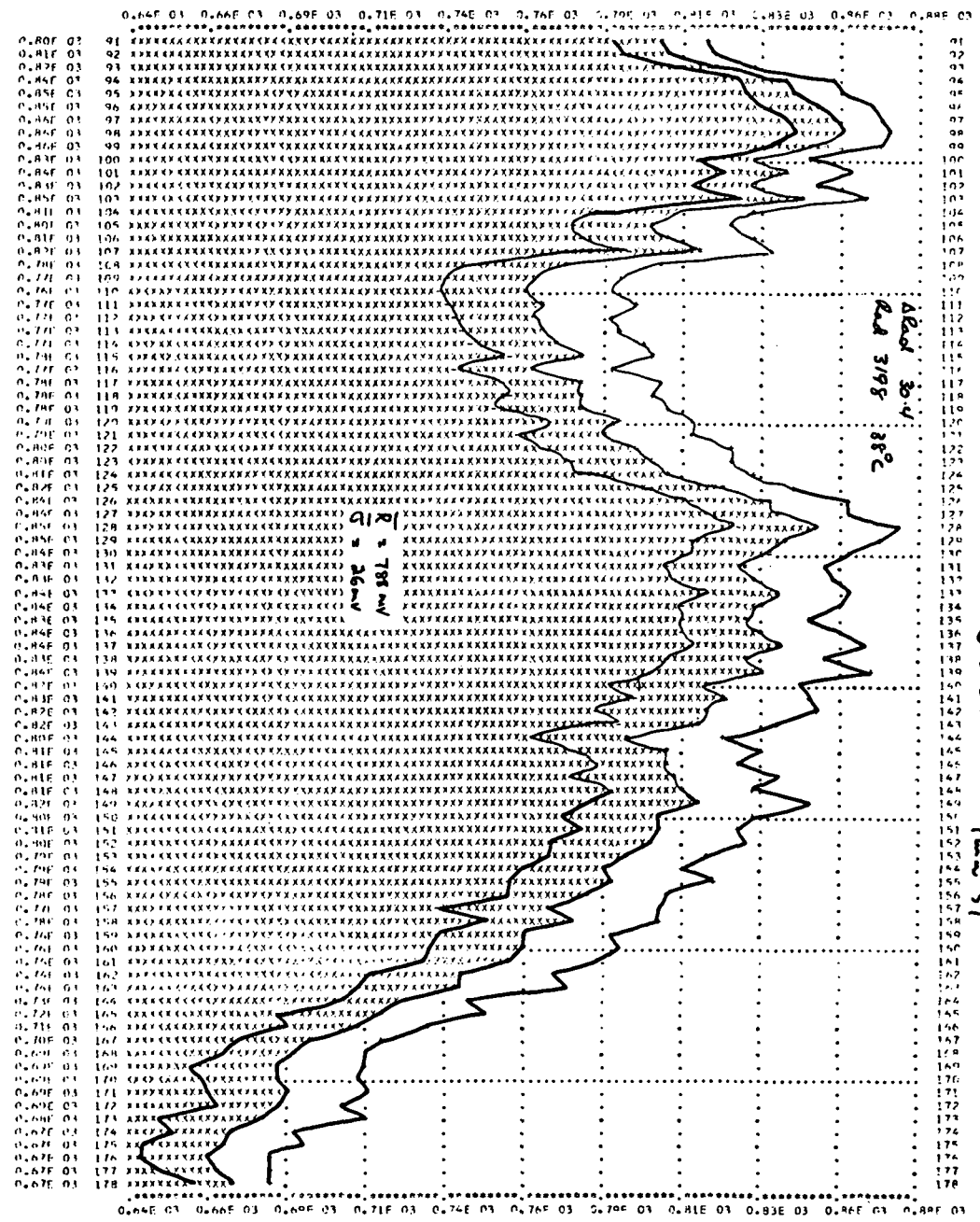

PISGAH P-LAVA II (E)

N = 21

$\bar{X}$ = 788

σ = 26

Tmax 40°

Tmin 37° (3°)

Tspec 36.7°C

A2- 49

SEP 1 1970

UP RAMP SPECTRUM GROUP (18 52 19059 TO 18 52 25430) CALLED -- MX169 PISGAH P-LAVA II (E)

(26)

NUMBER OF SPECTRA IN GROUP: 21

COUNTERS RANGE FROM 6.8 TO 13.4 MICRONS

XMIN IS 0.0 XMAX IS 0.10E 03 DELTA IS 0.10E 01

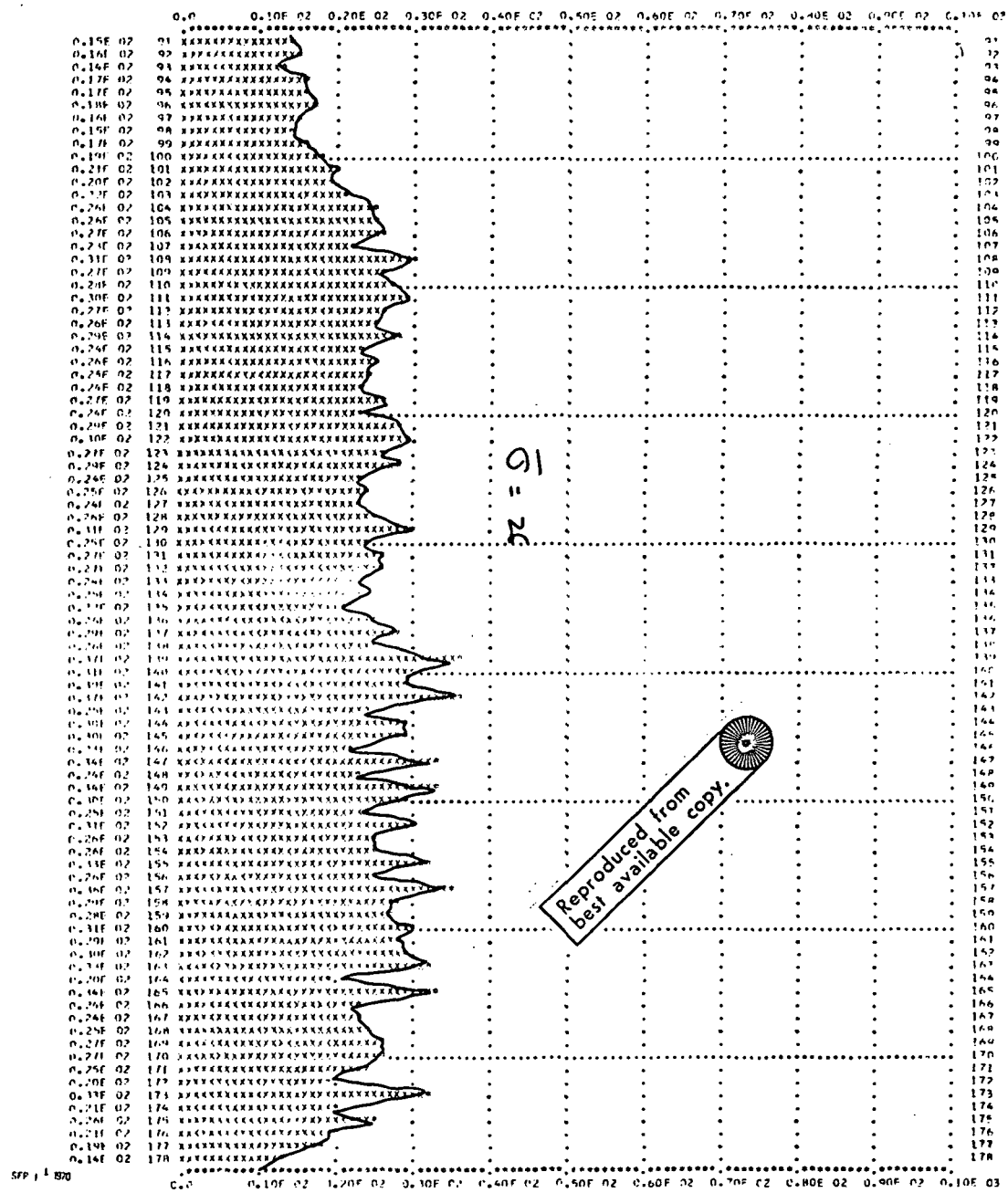

Reproduced from best available copy.

SEP 1 1970

PLOT OF STANDARD DEVIATION A2-50

UP RAMP SPECTRUM GROUP (19 6 44034 TO 19 6 51018) CALLED -- MX108 DRY LAKE SEDS B (27) B(A)

NUMBER OF SPECTRA IN GROUP: 23 1702 B/S 111-133

COUNTERS RANGE FROM 6.8 TO 13.4 MICRONS

XMIN IS 0.67E 03 XMAX IS 0.97E 03 DELTA IS 0.30E 01

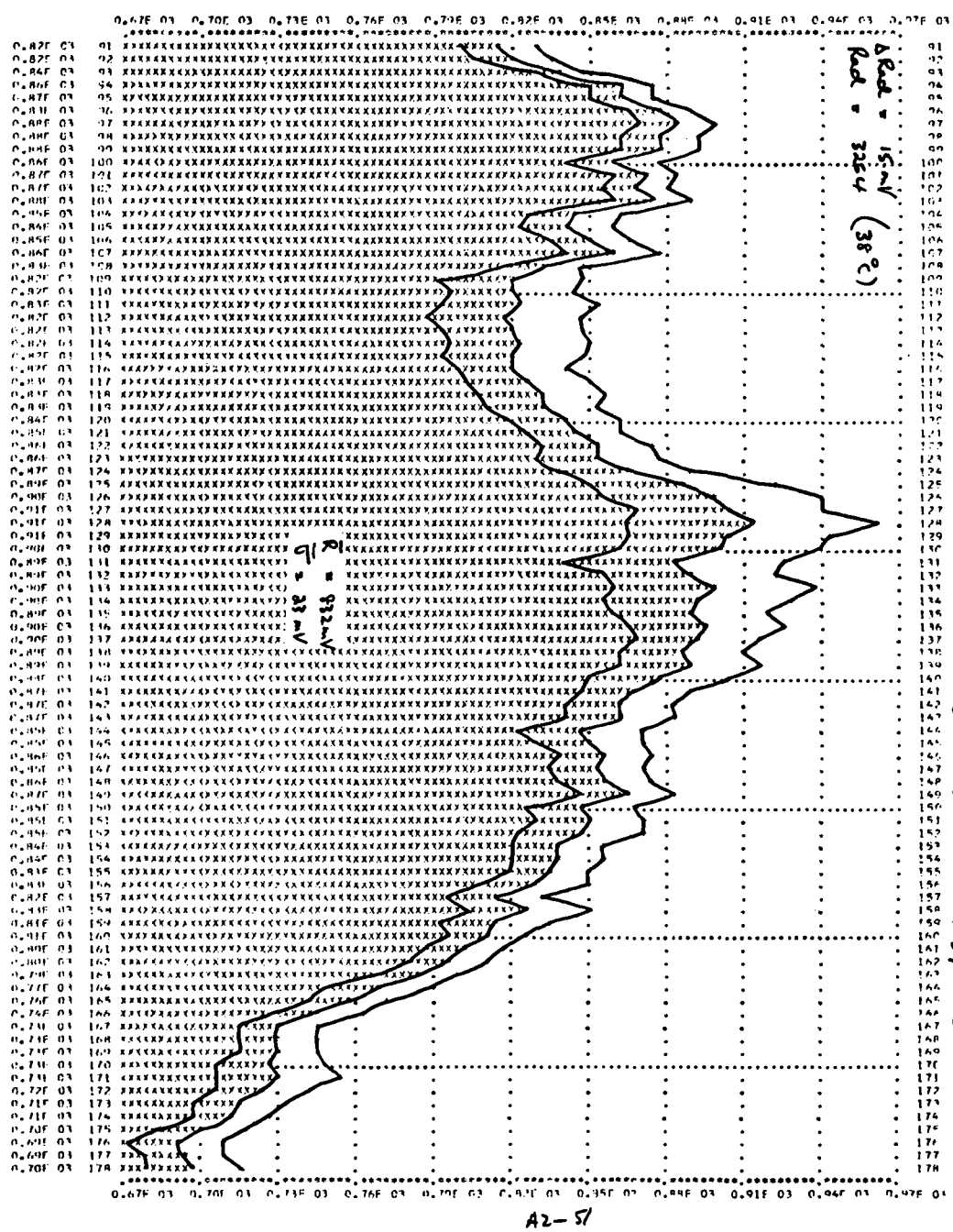

PISGAH DRY LAKE SEDS "B"

N = 23 X̄ = 832 σ̄ = 23

Tmax 39 Tmin 37 (2°C)

Tspac 35.2°C

A2-51

UP RAMP SPECTRUM GROUP (19 A 44034 TO 19 A 51018) CALLED -- MIXOR DRY LAKE SPEC (27)

NUMBER OF SPECTRA IN GROUP: 23

COUNTERS RANGE FROM 4.8 TO 13.4 MICRONS

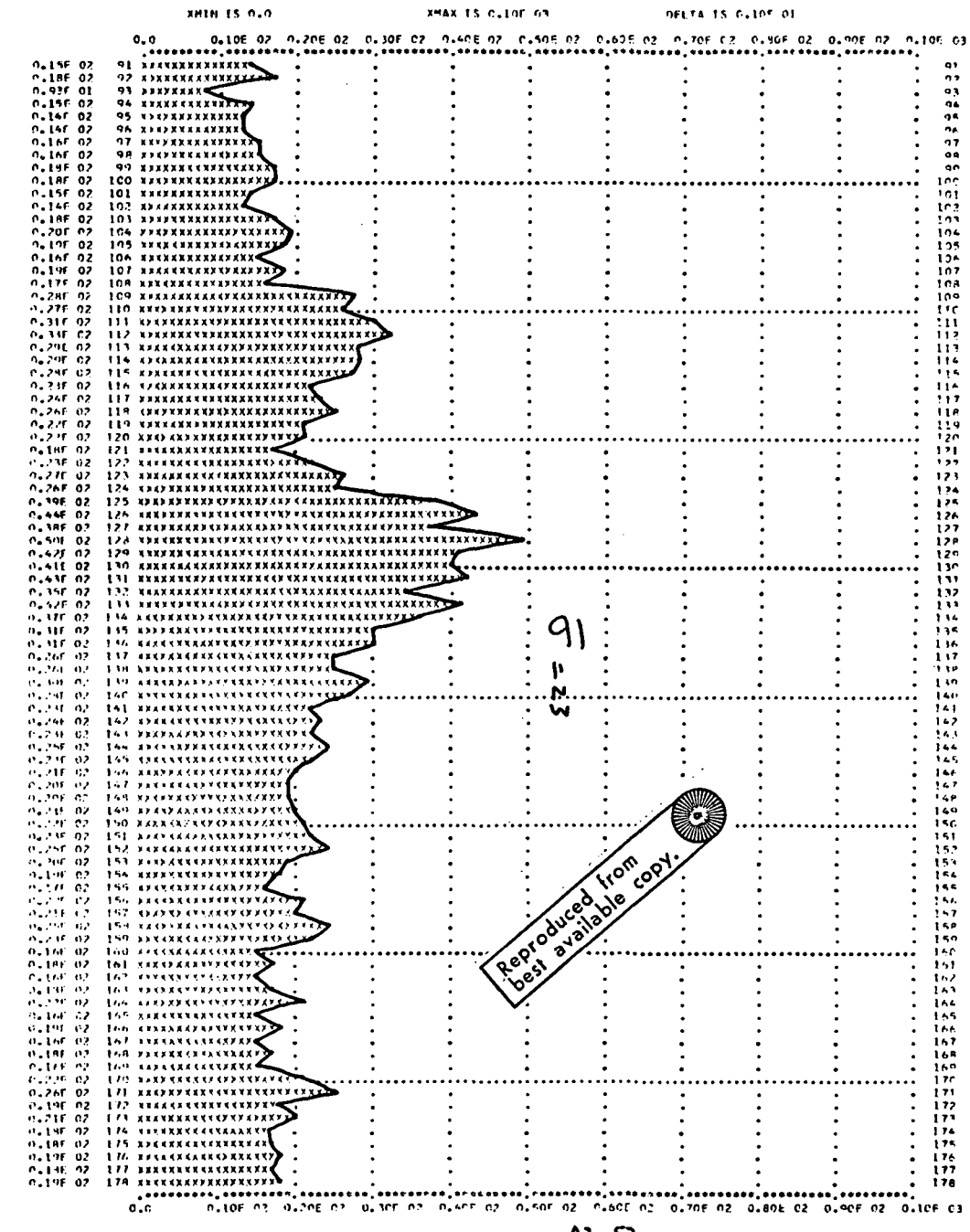

SEP 11 80

PLOT OF STANDARD DEVIATION

A2-52

UP RAMP SPECTRUM GROUP (18 57 38137 TO 18 57 54271) CALLED -- MX108 DRYLKSEDS A 1801 B/S 193-246 A(A)

(28)

NUMBER OF SPECTRA IN GROUP: 53

COUNTERS RANGE FROM 6.8 TO 13.4 MICRONS

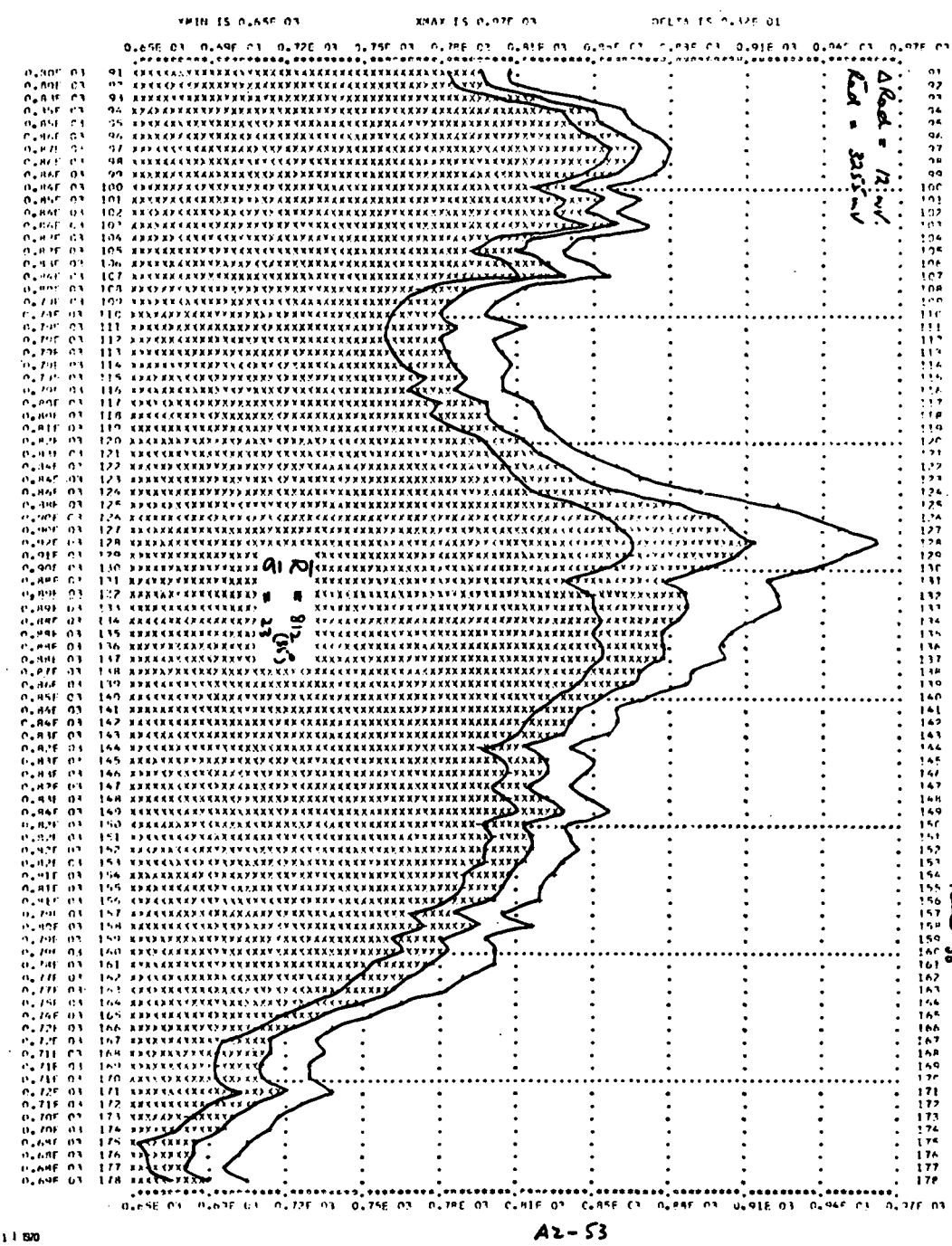

MX108-1 DRY CAKE SEDS "A"

$\bar{X}$ = 812 T_{ϕ} = 315 N = 53

σ = 22

Tmax 39°C

Tmin 37

Tave 38

(19)

T spec

SEP 1 1 1970

A2-53

UP RAMP SPECTRUM GROUP (18 57 38131 TO 18 57 54271) CALLED -- MX164 DRYLASERS A

(28)

NUMBER OF SPECTRA IN GROUP: 53

COUNTERS RANGE FROM 6.8 TO 13.4 MICRONS

XMIN IS 0.0 XMAX IS 0.10E 03 DELTA IS 0.10E 01

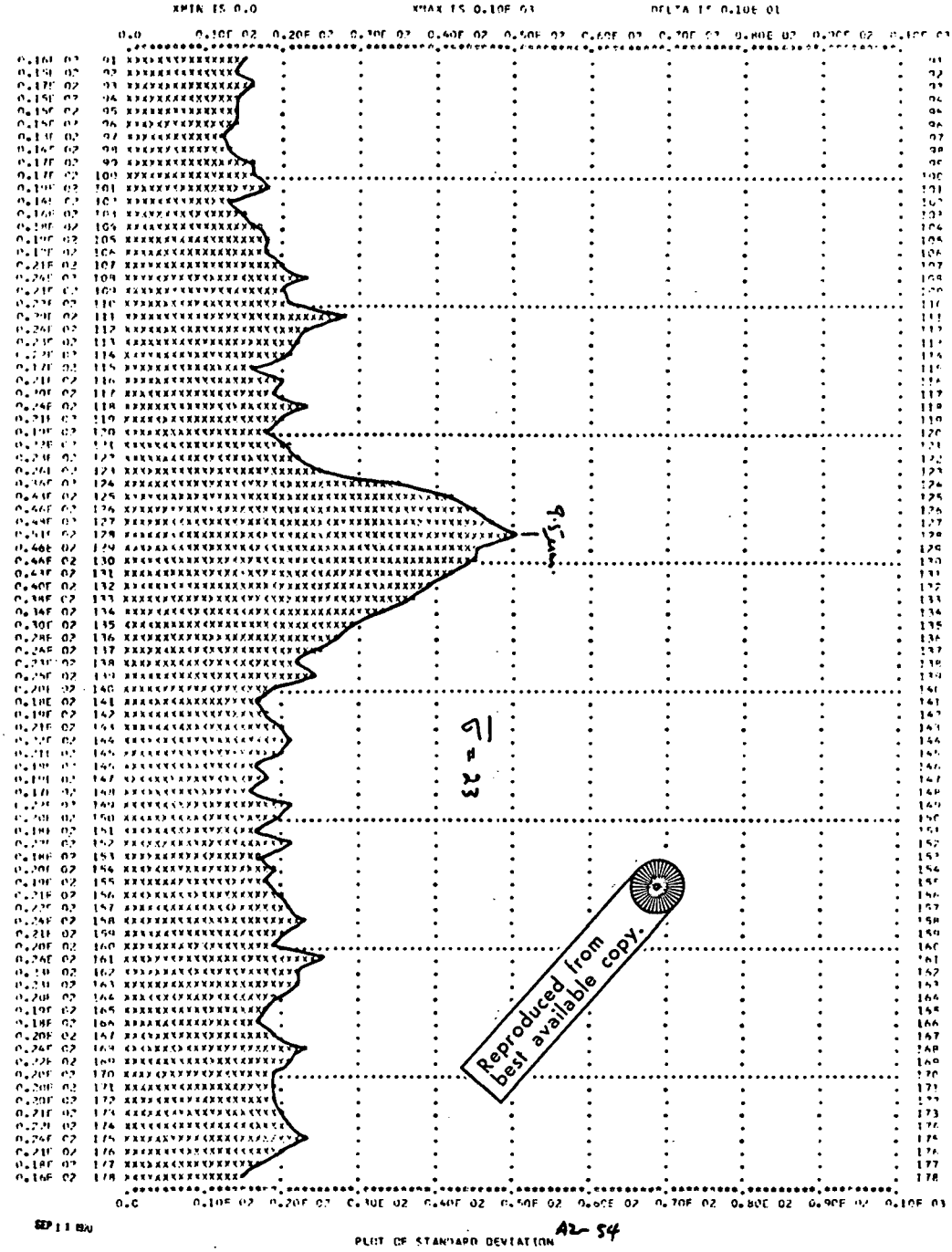

SEP 11 80

PLOT OF STANDARD DEVIATION

A2-54

Reproduced from best available copy.

UP RAMP SPECTRUM GROUP (19 6 34328 TO 19 6 41914) CALLED -- MX108 DRY LAKE SEDS C (29) C(A)

1702 B/S 78-104

NUMBER OF SPECTRA IN GROUP: 25

COUNTERS RANGE FROM 6.8 TO 13.4 MICRONS

XMIN IS 0.65E 03 XMAX IS 0.92E 03 DELTA IS 0.26E 01

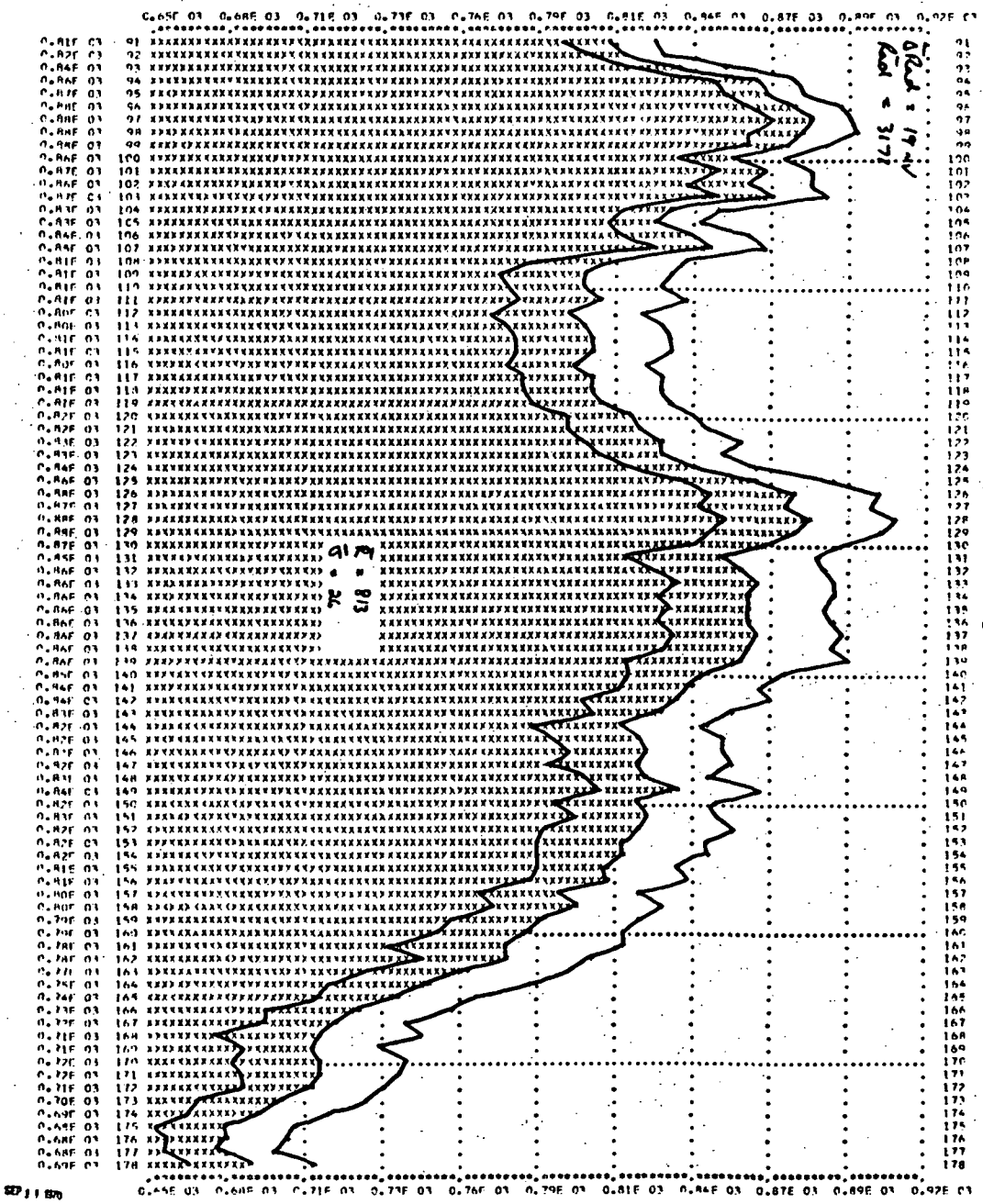

DRY LAKE SEDS 'C'

N = 25

$\bar{X}$ = 812

$\bar{\sigma}$ = 26

$\bar{\sigma}_{Rad}$ = 19 μV

$\bar{R}_{Rad}$ = 3171

$\bar{R}$ = 813

$\bar{\sigma}$ = 26

7 page

A2-55

UP RAMP SPECTRUM GROUP (19 6 14328 TO 19 6 419141 CALLED -- MX109 DRY LAKE SEDS (29)

NUMBER OF SPECTRA IN GROUP: 25

CHANNELS RANGE FROM 4.9 TO 13.4 MICRONS

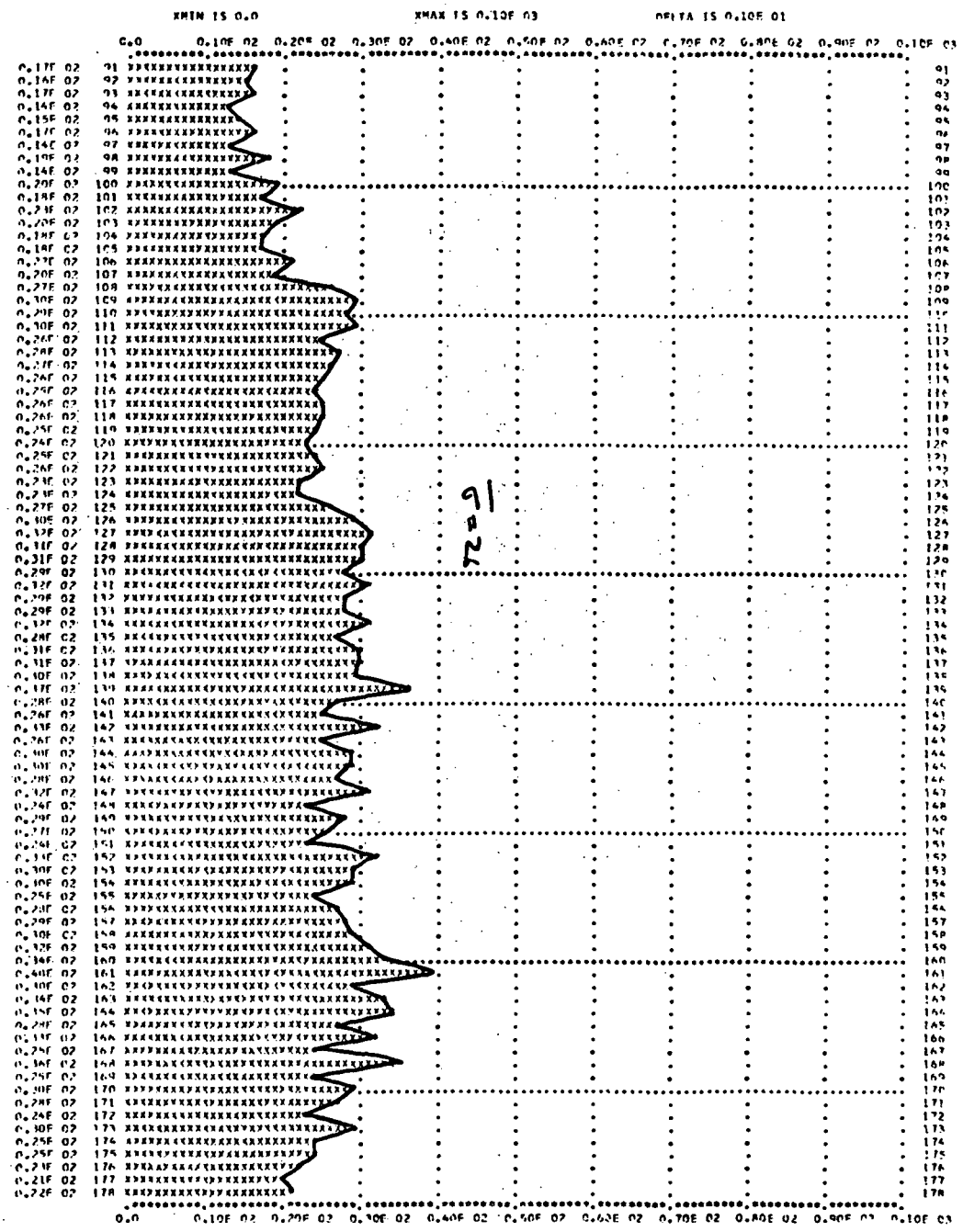

SEP 1 1 80

PLOT OF STANDARD DEVIATION A2.56

UP RAMP SPECTRUM GROUP (19 6 14002 TO 19 6 26742) CALLED -- MX108 ALLUVIUM F

(30) 1702

F(A)

NUMBER OF SPECTRA IN GROUP: 42

COUNTERS RANGE FROM 6.8 TO 13.4 MICRONS

XMIN IS 0.61E 03 XMAX IS 0.89E 03 DELTA IS 0.28E 01

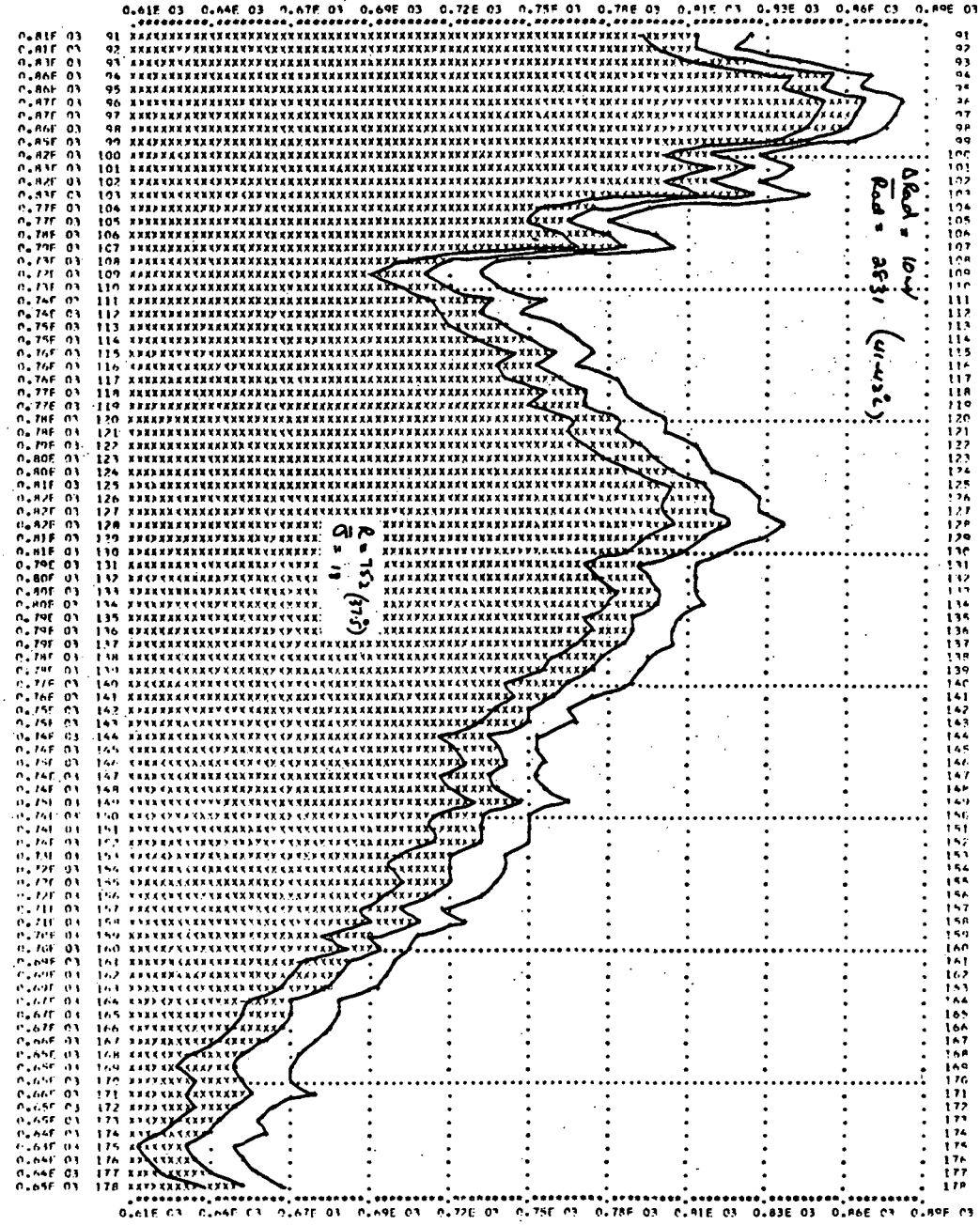

PISGAH ALLUVIUM F

N = 42

$\bar{X}$ = 752

$\bar{\sigma}$ = 18

T_{max} = 42

T_{min} = 41

(41°C)

T_{spec} 37.5°C

A2-57

SEP 11 1970

UP RAMP SPECTRUM GROUP 119 A 14002 TO 19 A 267421 CALLED -- MX109 ALLUVIUM F

(30)

NUMBER OF SPECTRA IN GROUP= 42

COUNTERS RANGE FROM 4.4 TO 13.4 MICRONS

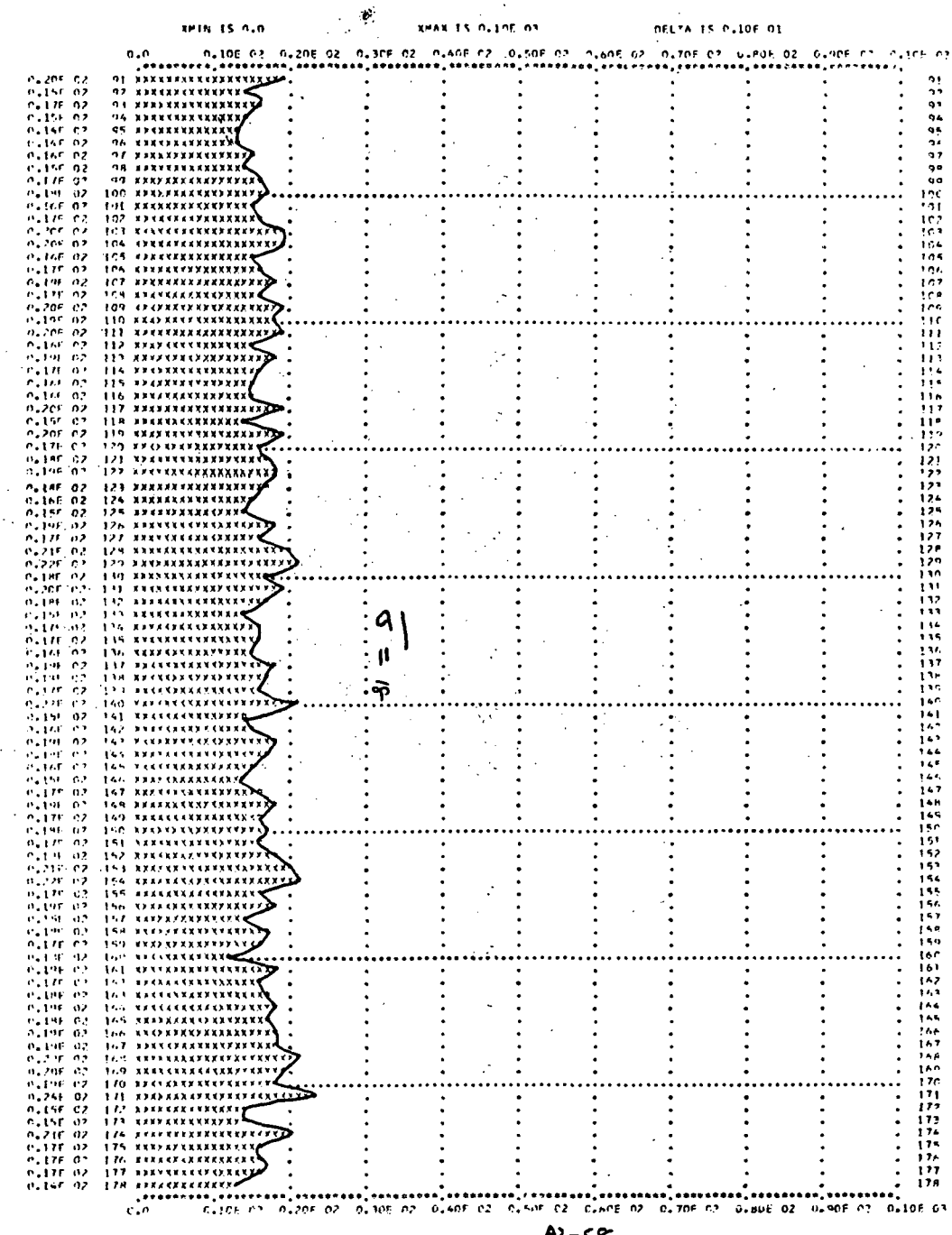

PLOT OF STANDARD DEVIATION

A2-58

SEP 11 1970

UP RAMP SPECTRUM GROUP (18 52 59593 TO 18 53 7897) CALLED -- MX108 ALLUVIAL-E

(31) 1701 E(A)

NUMBER OF SPECTRA IN GROUP: 27

COUNTERS RANGE FROM 6.8 TO 13.4 MICRONS

XMIN IS 0.61E 03 XMAX IS 0.88E 03 DELTA IS 0.27E 03

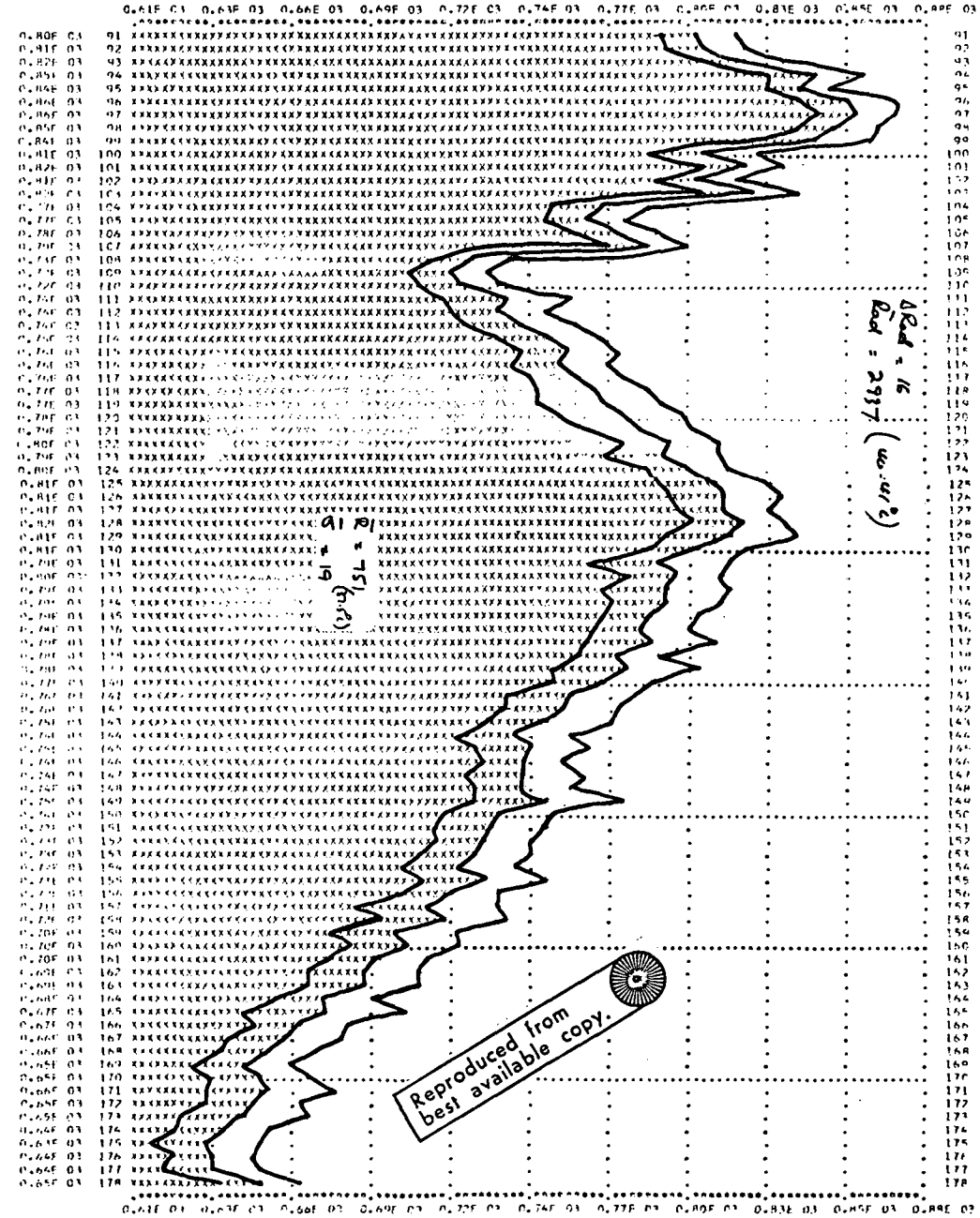

MX108-1 PISGAH ALLUVIAL "E"

$\bar{X}$ = 751
σ = 19

N=27

Tmax 41
Tmin 40

ΔT 1°C

Tspace 37.5°C

A2 -59

UP RAMP SPECTRUM GROUP (18 52 59593 TO 18 53 7897) CALLED -- MX108 ALLUVIAL-E

(31)

E(A)

NUMBER OF SPECTRA IN GROUP: 27

COUNTERS RANGE FROM 6.8 TO 13.4 MICRONS

XMIN IS 0.0 XMAX IS 0.10E 03 DELTA IS 0.10E 01

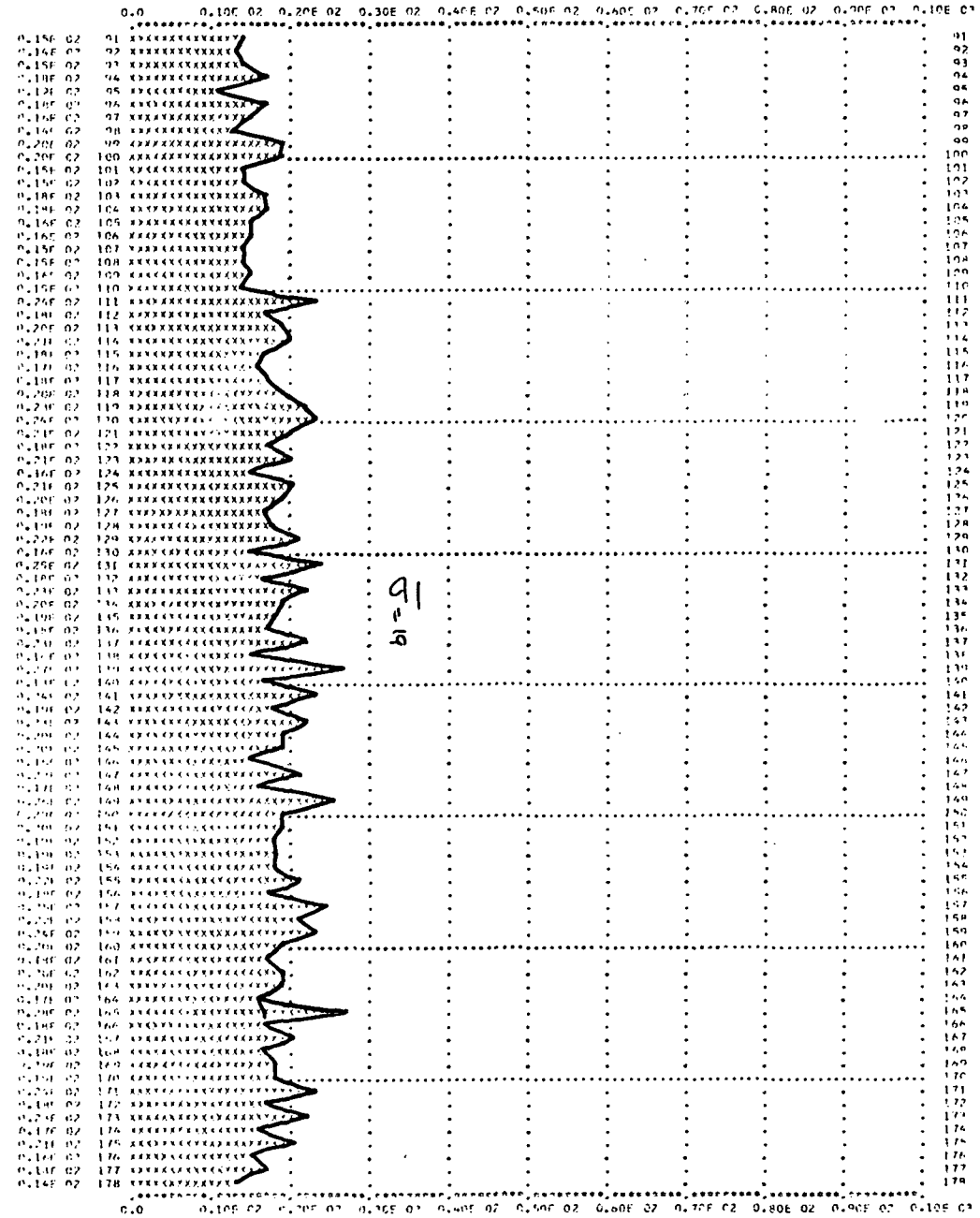

A2-60

PLOT OF STANDARD DEVIATION

1 (9)

A

OP RAMP SPECTRUM GROUP (18 51 20957 TO 18 51 37206) CALLED -- MX108 P-LAVA 1701

A-D 13+15+16+18

NUMBER OF SPECTRA IN GROUP: 53

CHANTERS RANGE FROM 6.8 TO 13.4 MICRONS

XMIN IS 0.64E 03 XMAX IS 0.92E 03 DELTA IS 0.28E 01

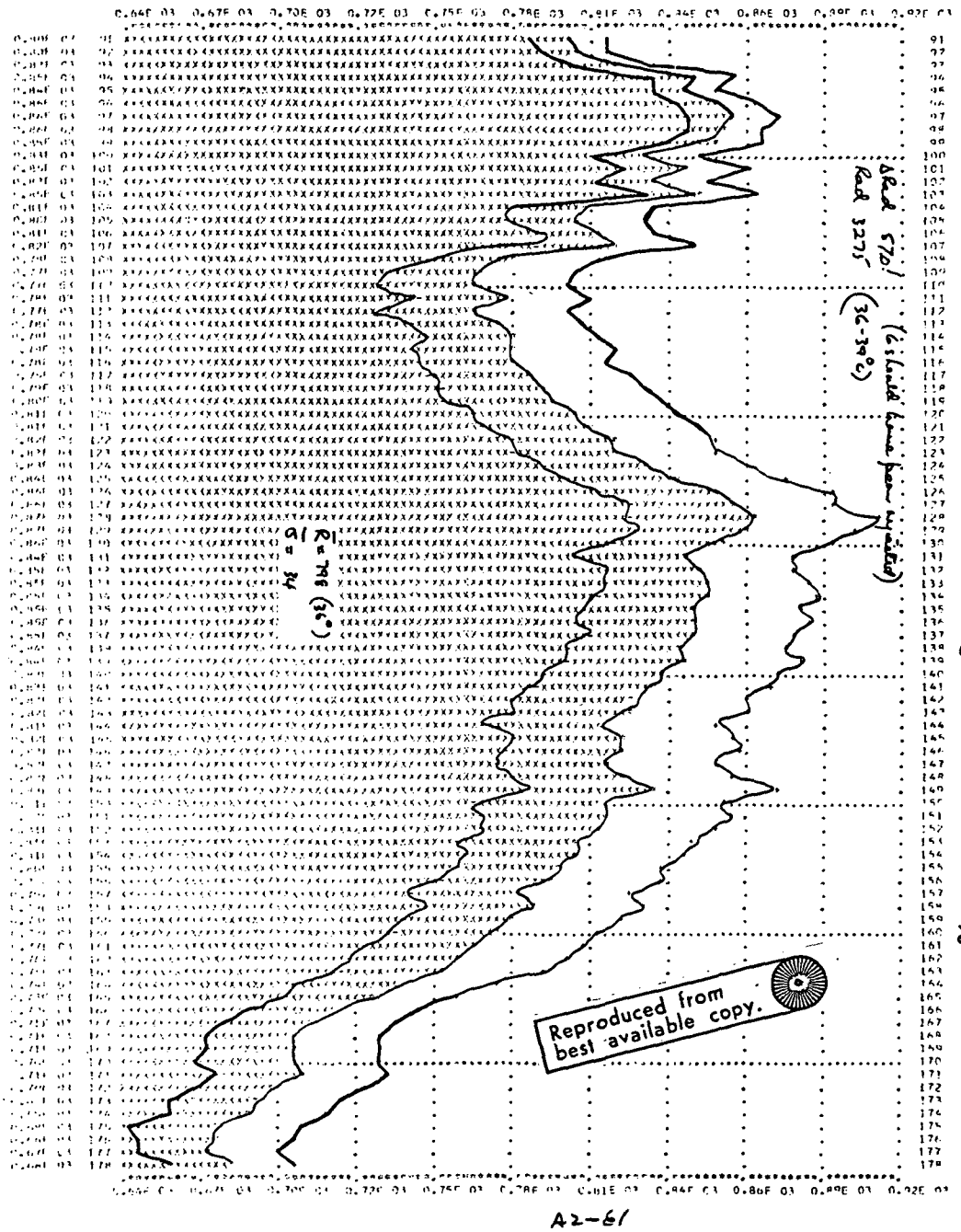

Reproduced from best available copy.

PISGAH. P-LAVA

N = 53

$\bar{X}$ = 798 Tmax = 39

$\bar{\sigma}$ = 34 Tmin = 36 (3)

Tspec 36.1

A2-61

SEP 1 0 1970

UP RAMP SPECTRUM GROUP (18 51 20957 TO 14 51 17206) CALLED -- MINOR P-LWS

NUMBER OF SPECTRA IN GROUP: 53

(13 + 15 + 16 + 18)

COUNTERS RANGE FROM 0.0 TO 13.4 MICROS

XMIN IS 0.0 XMAX IS 0.50E 02 DELTA IS 0.50E 00

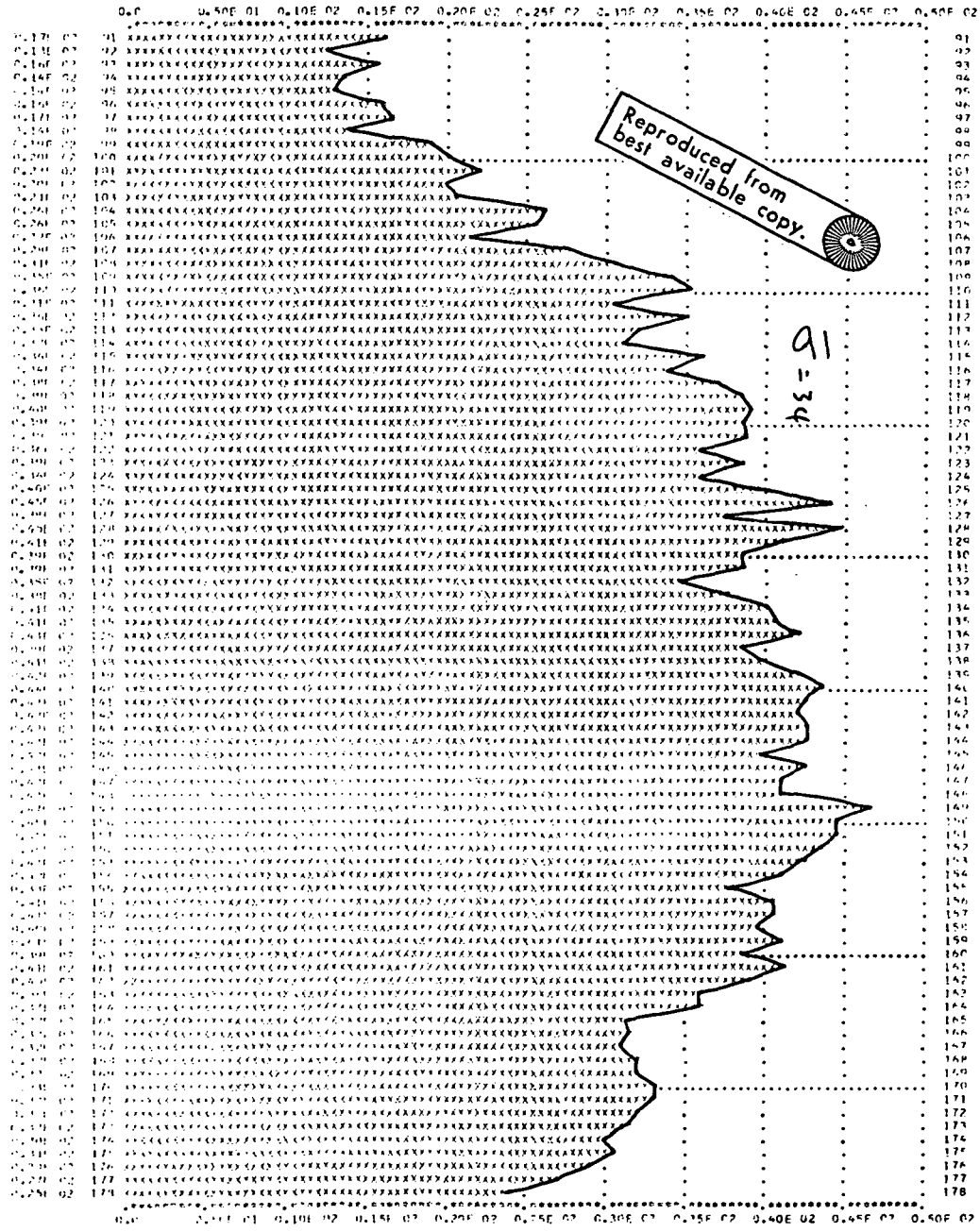

PLOT OF STANDARD DEVIATION A2-62

SEP 3 0 1980

TRAIN (A)

GP RAMP SPECTRUM GROUP (19) F 57256 TO 19 B 56311 CALLED -- MAJOR STRAIN LAVA 1702

NUMBER OF SPECTRA IN GROUP: 31 (17+19+21) B/S 355-380

COUNTERS RANGE FROM 4.0 TO 13.4 MICRONS

XMIN IS 0.46E 03 XMAX IS 0.80E 03 DELTA IS 0.32E 01

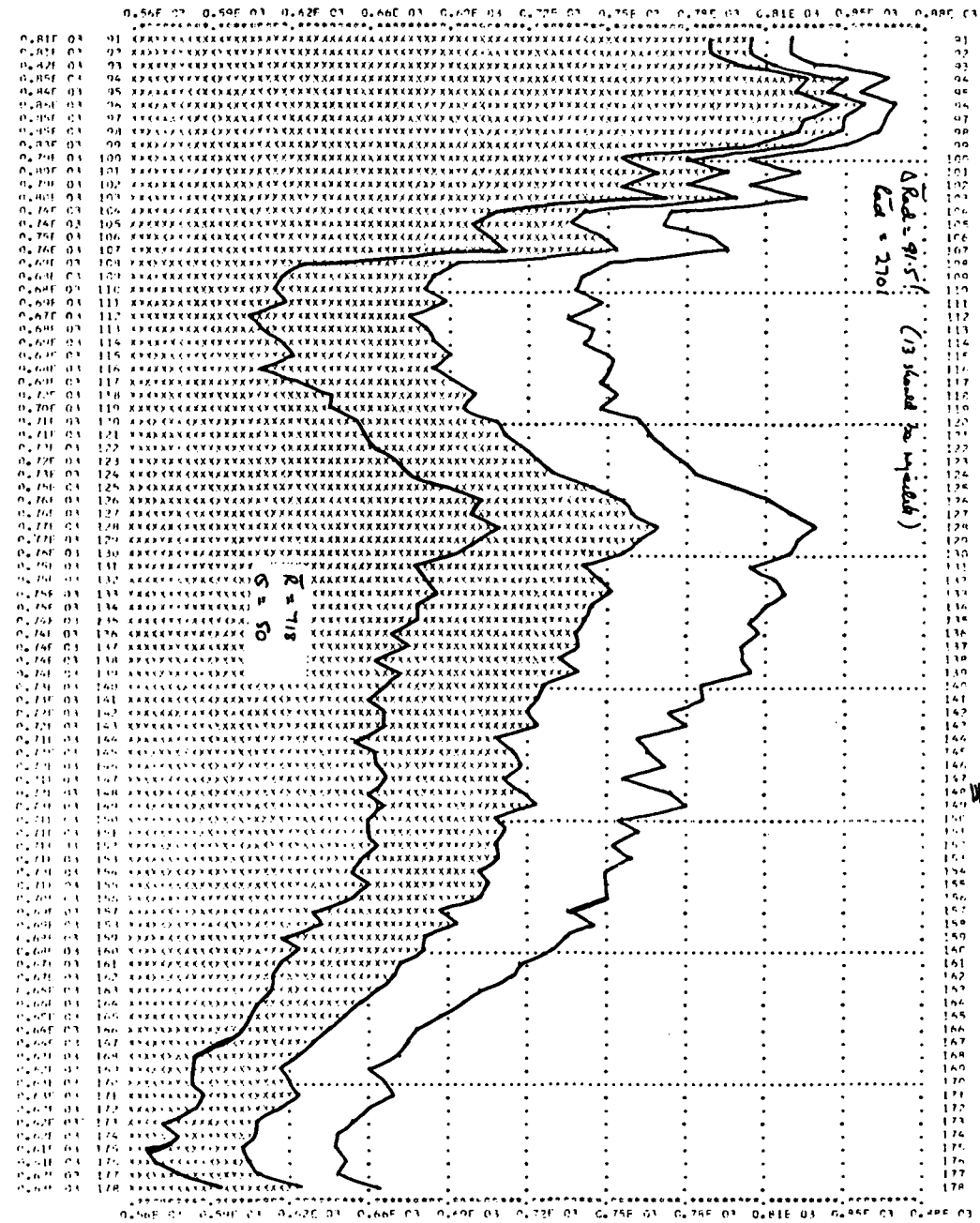

P(TRAIN) LAVA 1702

$\frac{\bar{X}}{\sigma} = \frac{718}{50}$ N = 31 V. HIGH

A2-C3

LP RAMP SPECTRUM GROUP (19 7 57256 TO 19 8 6631) CALLED -- MX108 BIRAIN LAVA

(17+19+21)

NUMBER OF SPECTRA IN GROUP: 31

COUNTERS RANGE FROM 6.8 TO 13.4 MICRONS

XMIN IS 0.0 XMAX IS 0.10E 03 DELTA IS 0.10E 01

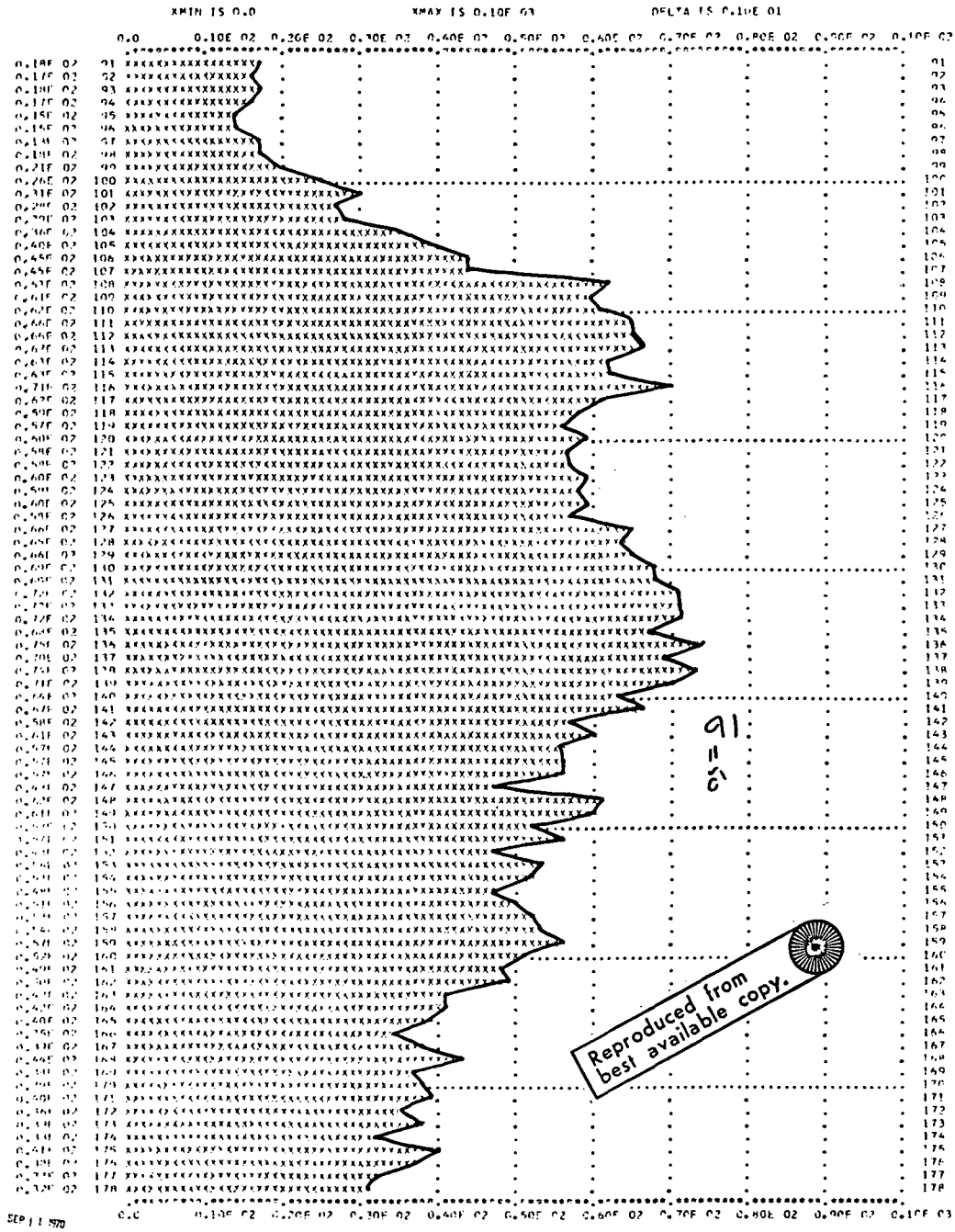

Reproduced from best available copy.

SEP 1 1 1970

PLOT OF STANDARD DEVIATION A2-64

UP RAMP SPECTRUM GROUP (18 51 0107Y TO 18 51 0350Z) CALLED -- MXIGH PISGAH BASALT FLOW III 1701 Bs/t III (A)

NUMBER OF SPECTRA IN GROUP: 7 (−) 1701 B/S 176-181 (between 7 all) N=7

COUNTERS RANGE FROM 6.8 TO 13.4 MICRONS

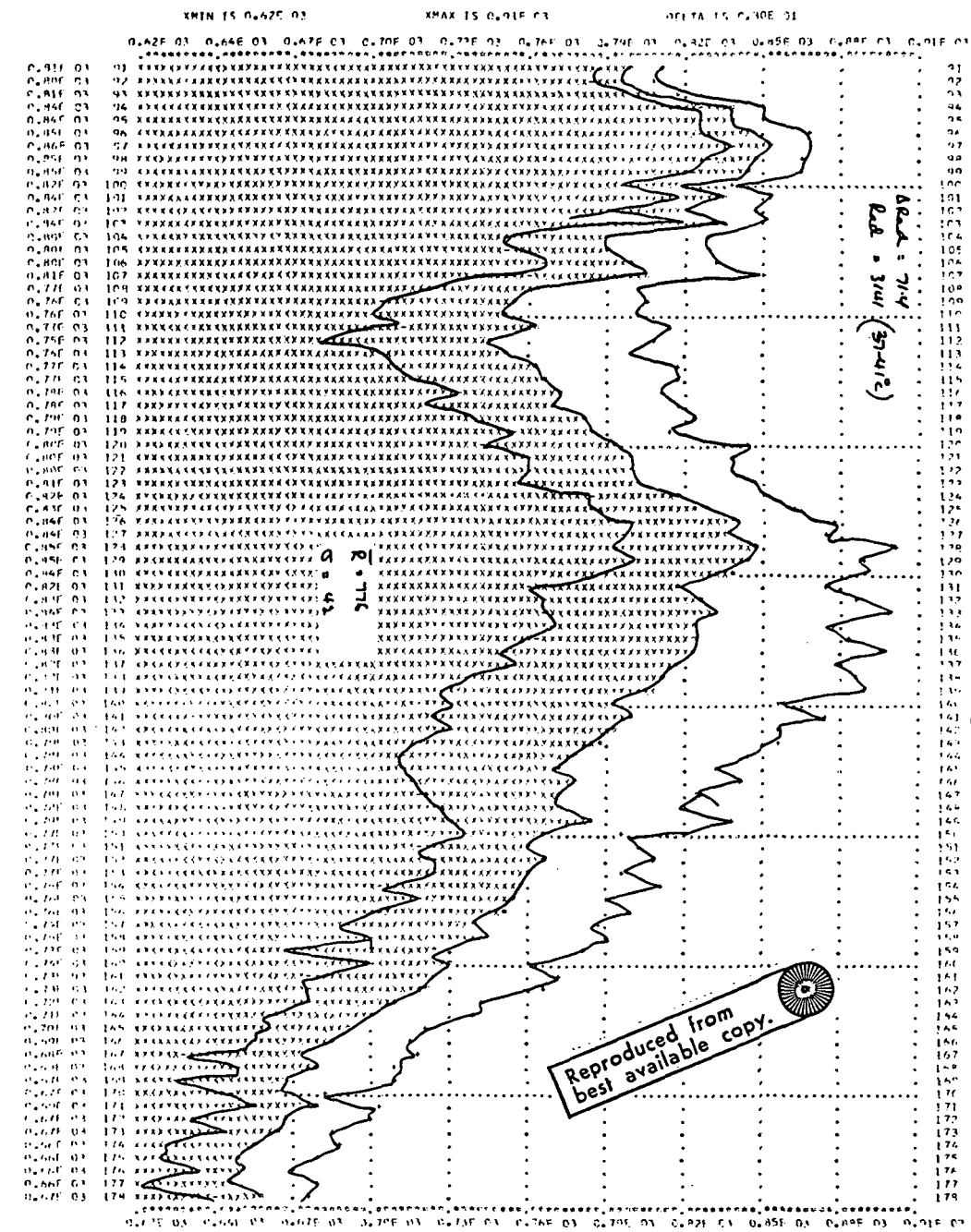

PISGAH BASALT-PHASE III

N = 7

$\bar{X}$ = 764

σ = 42

Tmax 41°C

Tmin 37 (A)

Reproduced from best available copy.

SEP 11 1970

A2-65

UP RAMP SPECTRUM GROUP (18 51 1070 TO 18 51 35C8) CALLED -- MX108 PISGAH BASALT FLOW III

NUMBER OF SPECTRA IN GROUP: 7 N=7 (-) between 7 & 11

COUNTERS RANGE FROM 6.8 TO 13.4 MICRONS

XMIN IS 0.0 XMAX IS 0.10E 03 DELTA IS 0.10E 01

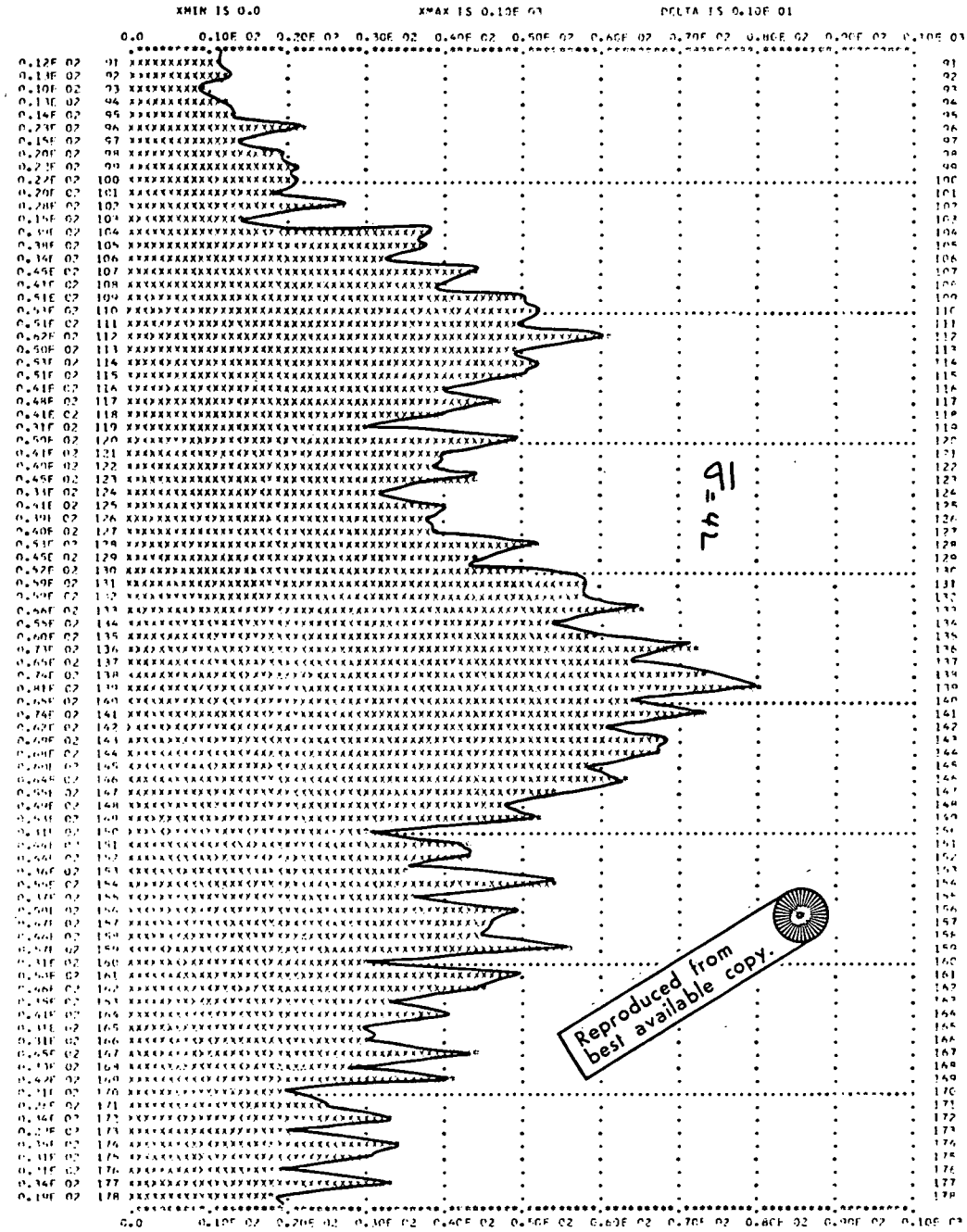

Reproduced from best available copy.

PLOT OF STANDARD DEVIATION 42-66

UP RAMP SPECTRUM GROUP (18 50 54710 TO 18 50 56229) CALLED -- MX1GR PISGAH CINDERS I

CIN $I_{(A)}$

NUMBER OF SPECTRA IN GROUP: 6

COUNTERS RANGE FROM 6.8 TO 13.4 MICRONS

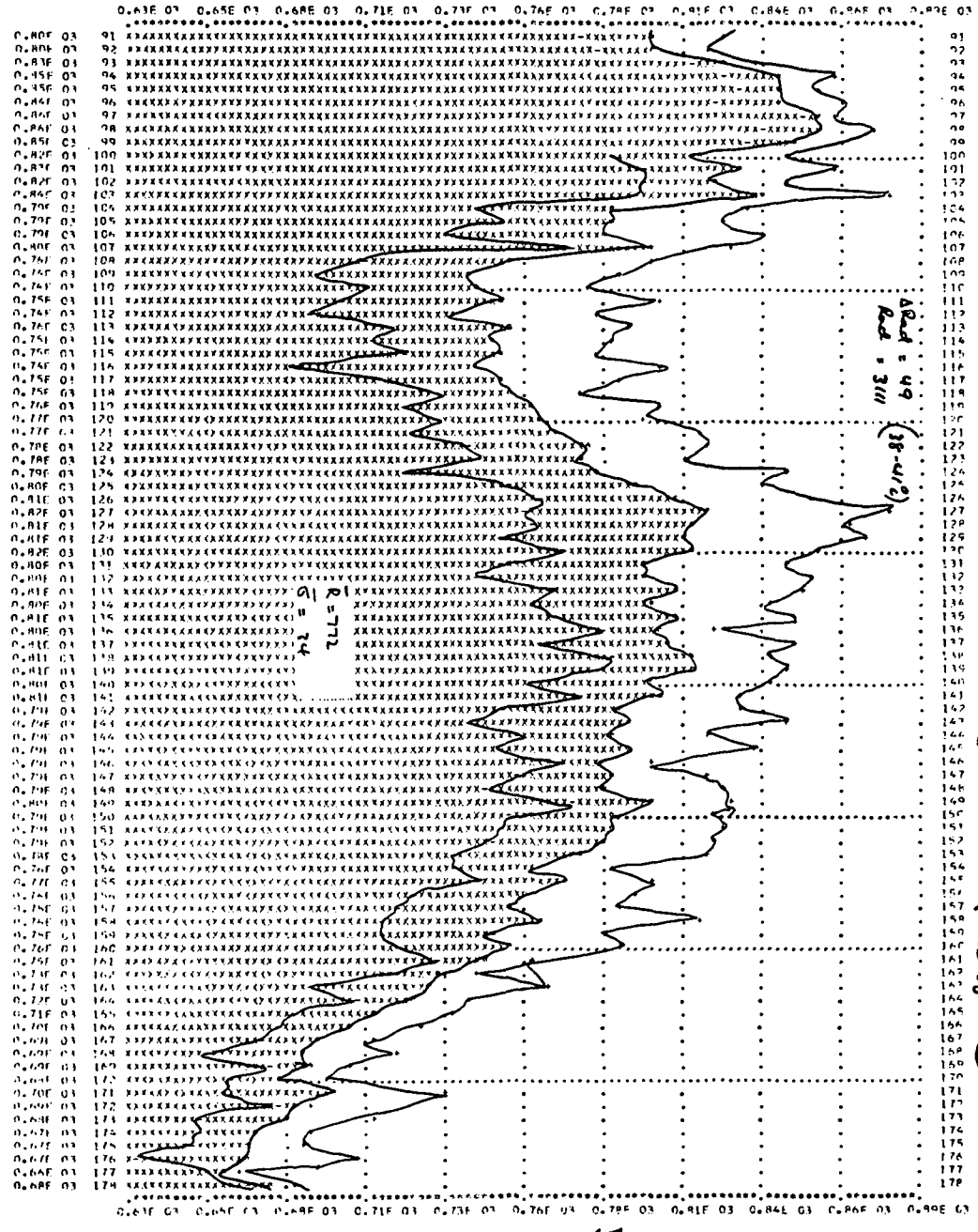

PISGAH CINDERS PHASE I

N = 4

$\bar{X}$ = 772

$\bar{\sigma}$ = 34

$\bar{T}_{max}$ 41

$\bar{T}_{min}$ 38

$\bar{T}_{spec}$ 37°

SEP 1 1 1970

A2-67

UP RAMP SPECTRUM GROUP (18 50 54710 TO 18 50 56729) CALLED -- 3X108 PISGAH CINDERS I

NUMBER OF SPECTRA IN GROUP: 4

COUNTERS RANGE FROM 6.8 TO 13.4 MICRONS

XMIN IS 0.0 XMAX IS 0.10E 03 DELTA IS 0.10E 01

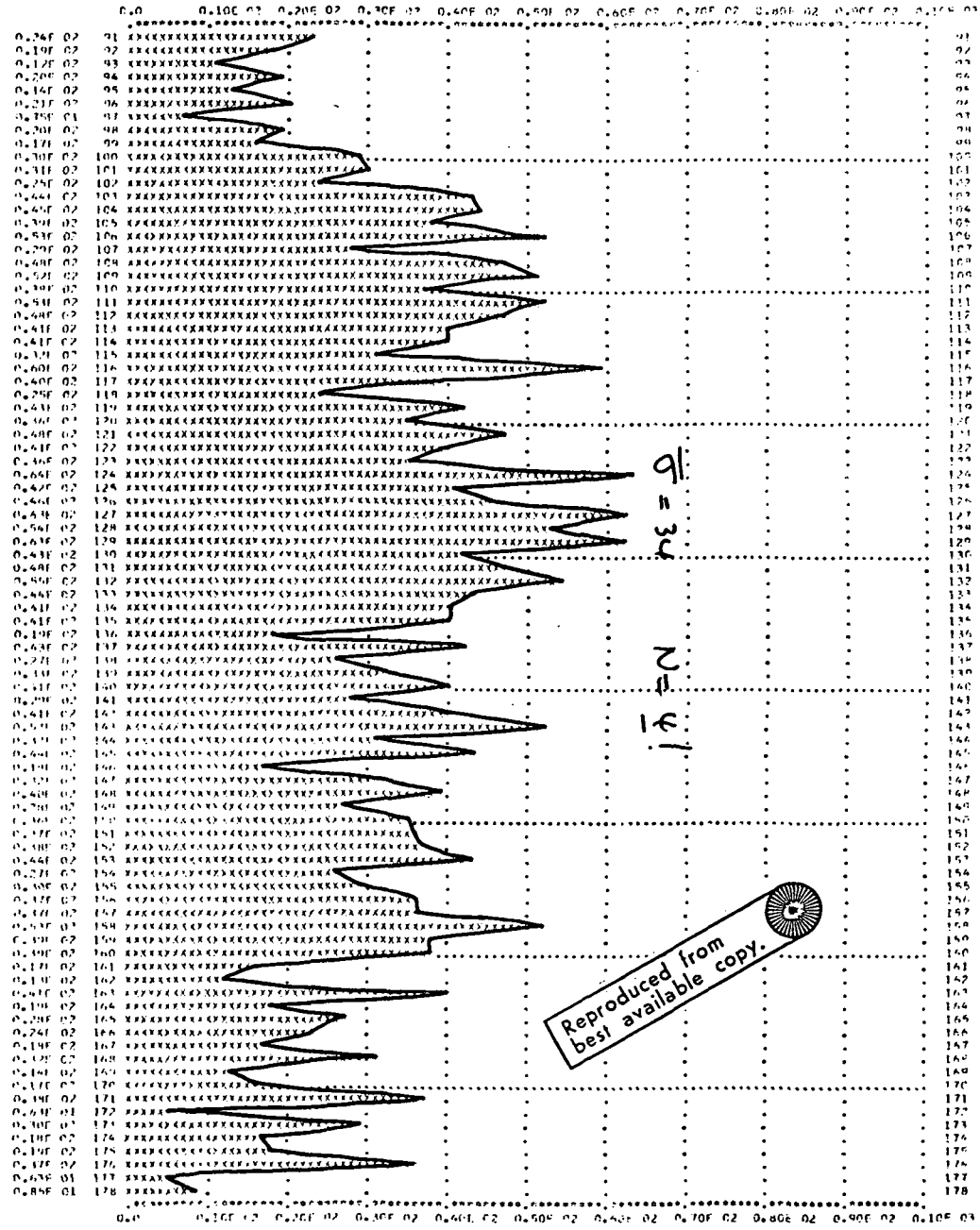

Reproduced from best available copy.

PLOT OF STANDARD DEVIATION A2-68

SEP 11 1970

UP RAMP SPECTRUM GROUP (18 50 56229 TO 18 50 59049) CALLED -- MX108 PISGAH CINDERS II 1701 CIN II(A)

NUMBER OF SPECTRA IN GROUP: 5

COUNTERS RANGE FROM 6.8 TO 13.4 MICRONS

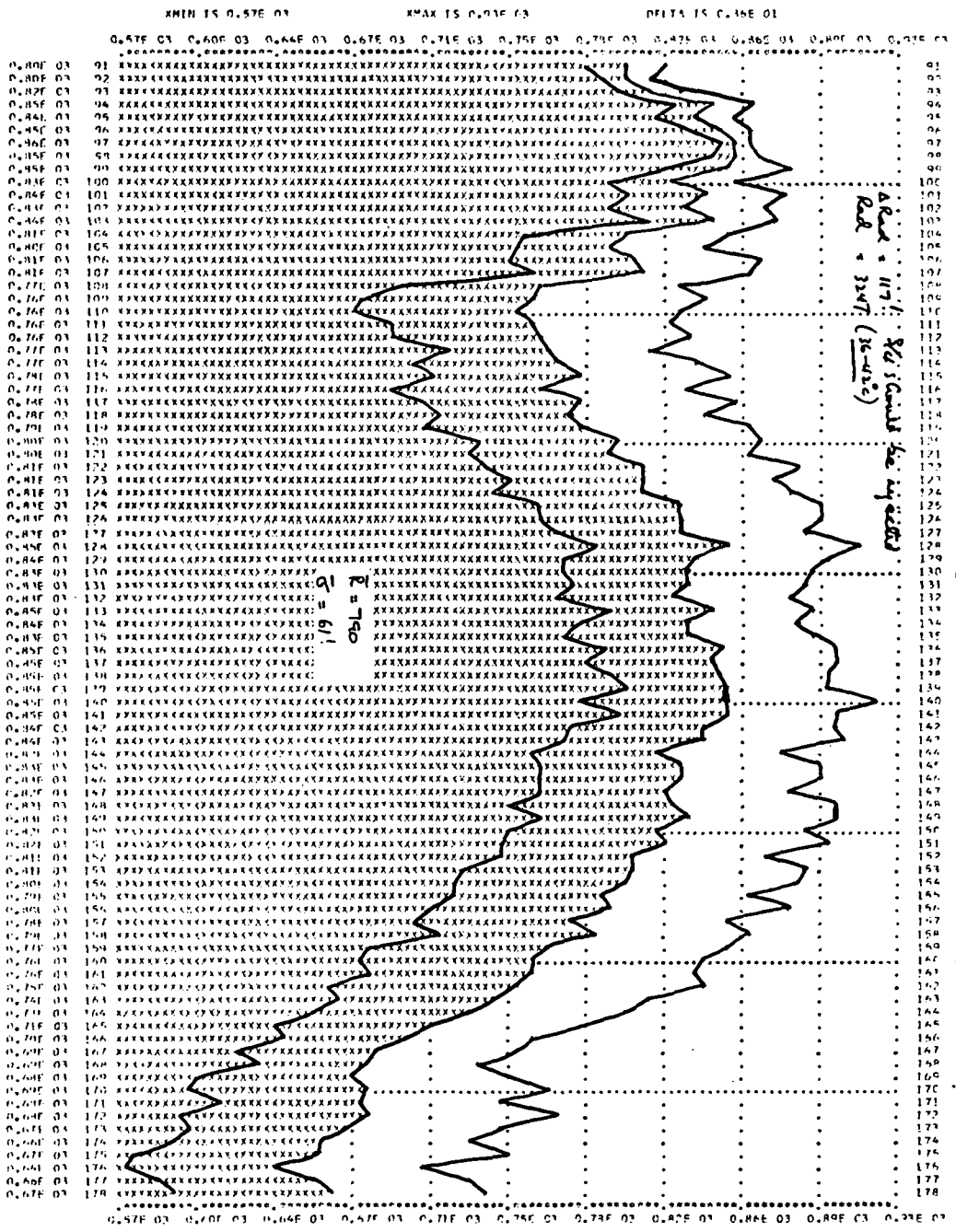

PISGAH CINDERS-II PHASE

N = 5

$\bar{x}$ = 790

$\bar{\sigma}$ = 61

ΔRad = 117.1 8/4 should be injected

Rad = 3247 (36-42°C)

$\bar{R}$ = 790

$\bar{\sigma}$ = 61.1

Tmax 42°C

Tmin 36.5 (6°)

$\bar{T}$ = 1° Tspec 36.5°C

A2-69

Reproduced from best available copy.

UP RAMP SPECTRUM GROUP (18 90 56229 TO 18 90 58049) CALLED -- MXIGR PISGAH CINDERS II

NUMBER OF SPECTRA IN GROUP: 5

COUNTERS RANGE FROM 4.8 TO 13.4 MICRONS

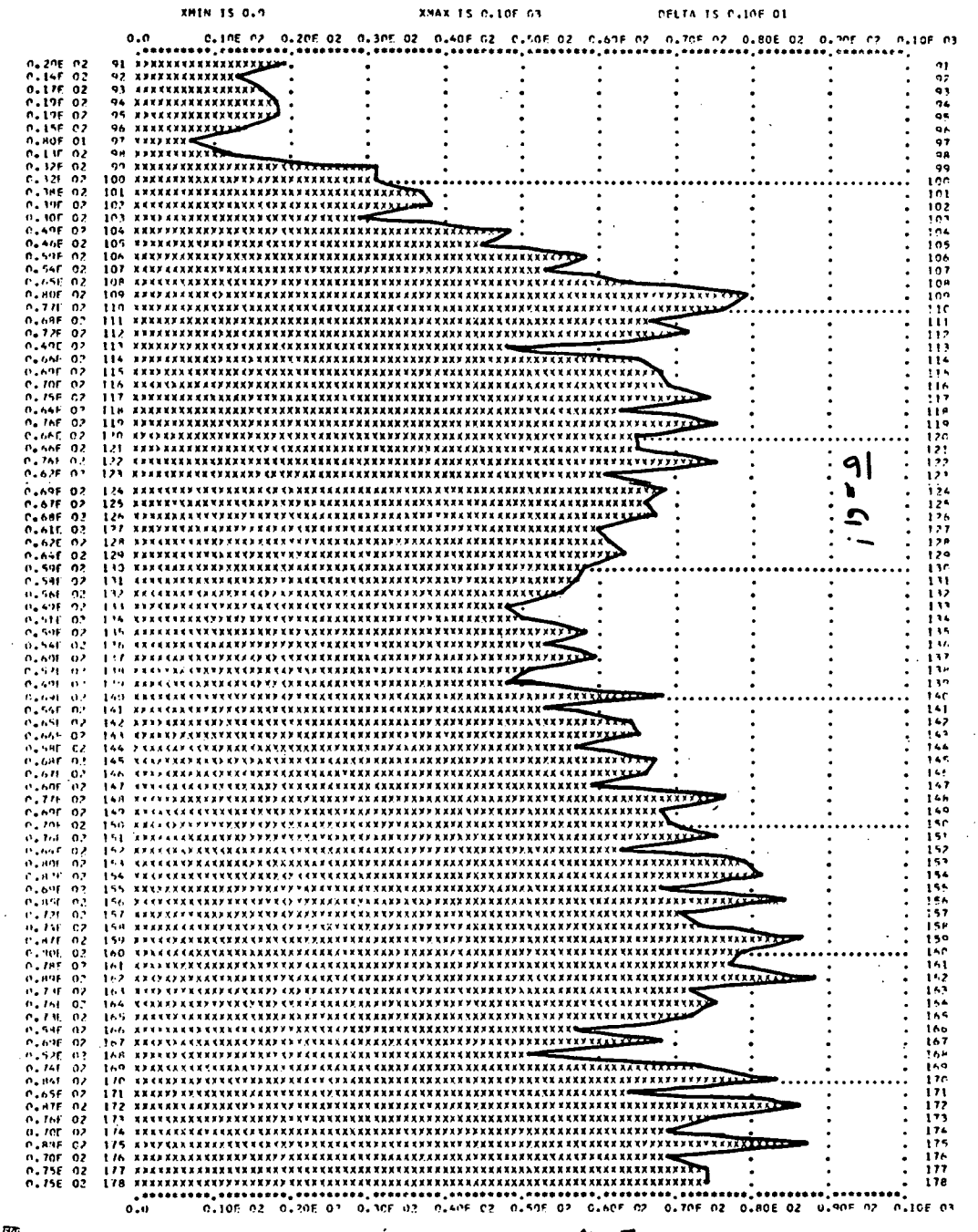

SEP 1 1 1970

PLOT OF STANDARD DEVIATION A2-70

PISGAH CINDERS III-PHASE N = 9 $\bar{X}$ = 736 $\bar{\sigma}$ = 73! Tmax 43.5 Tmin 35 (8°)

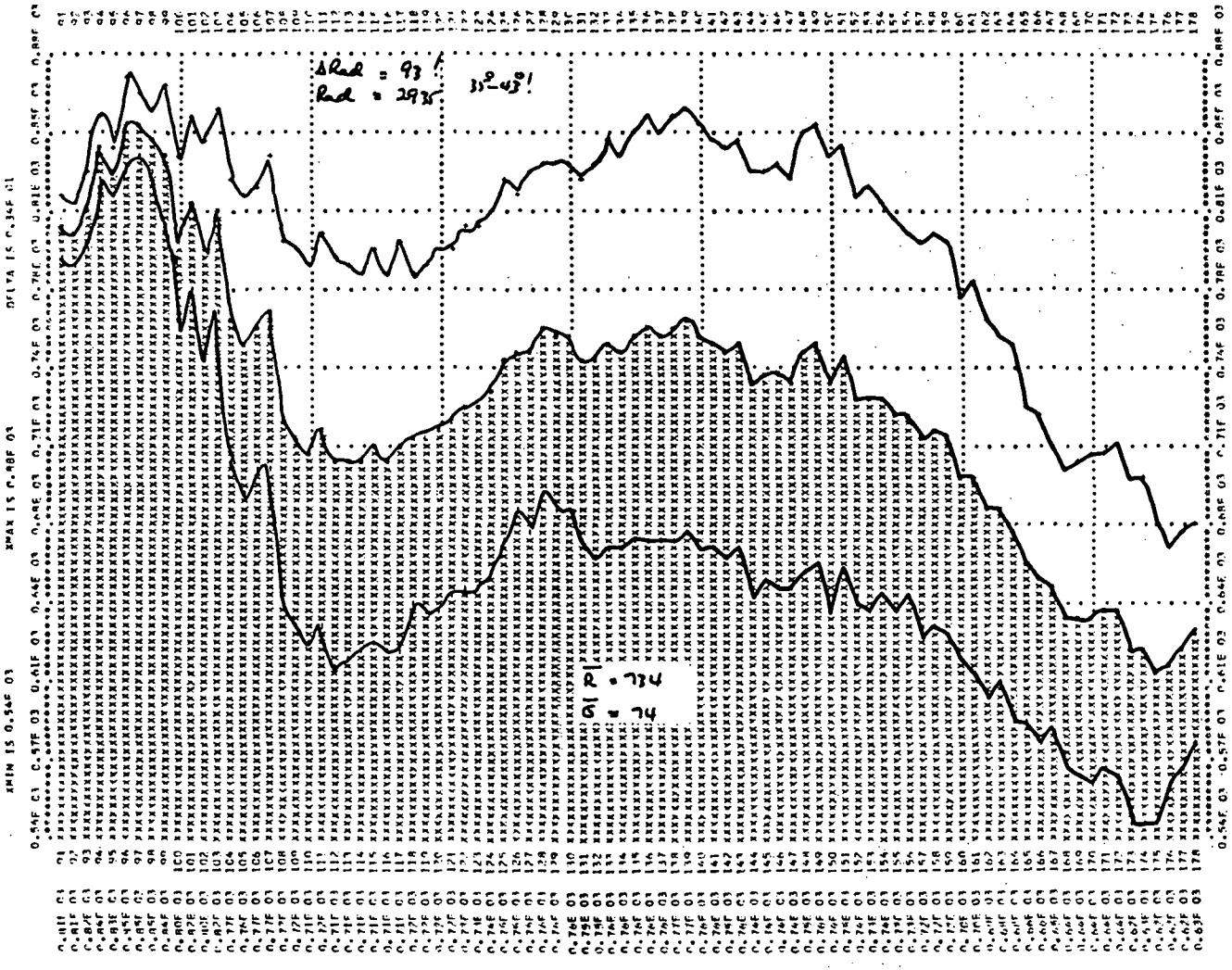

UP RAMP SPECTRUM GROUP (IR 50 58049 TO IR 51 10791 CALLED — MXICA PISGAH CINDERS III 1701 CIN III(A)

NUMBER OF SPECTRA IN GROUP: 9

COUNTERS RANGE FROM 6.8 TO 13.4 MICRONS

XMIN IS 0.54E 03 XMAX IS 0.88E 03 DELTA IS 0.34E 01

A2-71

188

LP RAMP SPECTRUM GROUP (18 50 58049 TO 18 51 10791 CALLED — 9X10A PISGAH CINDERS III

NUMBER OF SPECTRA IN GROUP: 9

CHANNELS RANGE FROM 6.8 TO 13.4 MICRONS

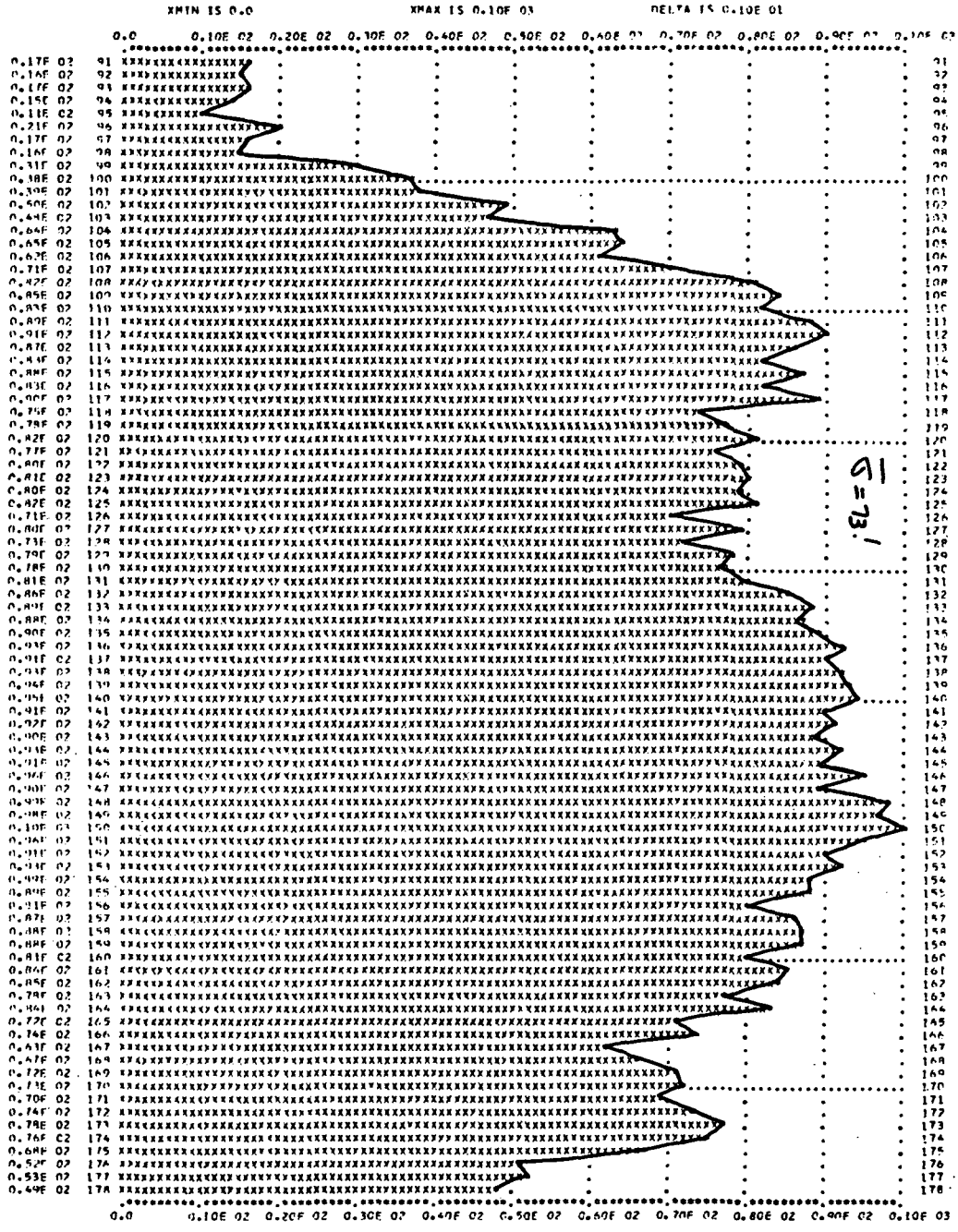

PLOT OF STANDARD DEVIATION A2-72

UP RAMP SPECTRUM GROUP 118 57 11562 TO 18 57 185161 CALLED -- MAXIGA SUNSHINE LAVA A

SLA (A)

(-)

NUMBER OF SPECTRA IN GROUP: 22

COUNTERS RANGE FROM 6.0 TO 13.4 MICRONS

XMIN IS 0.57E 03 XMAX IS 0.87E 03 DELTA IS 0.30E 01

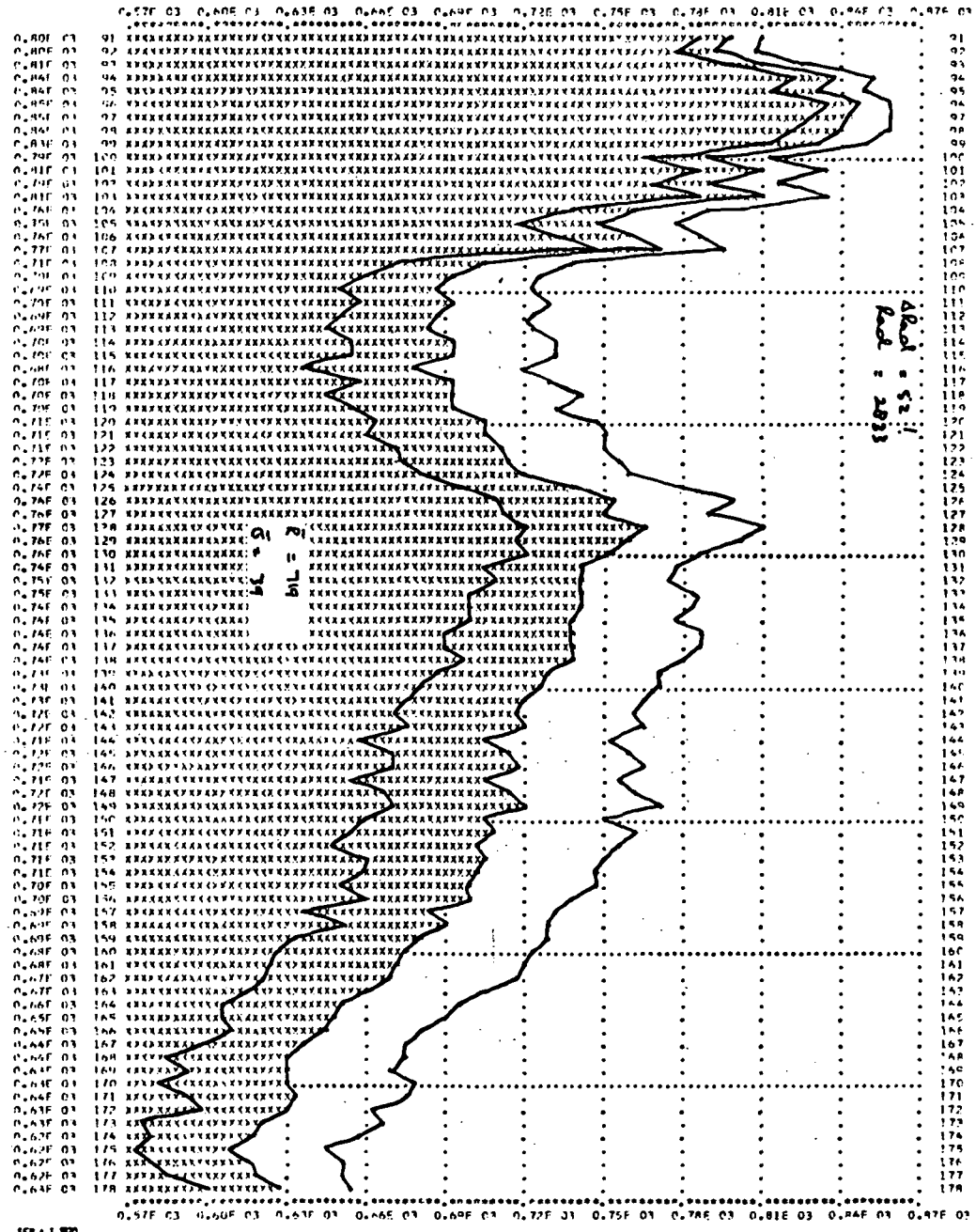

SUNSHINE LAVA A

N=22 $\bar{X}$ = 719 $\bar{\sigma}$ = 38

SEP 1 1970

A2-73

UP RAMP SPECTRUM GROUP (19 57 11542 TO 19 57 18516) CALLED -- *HIGH SUNSHINE LAVA A (-)

NUMBER OF SPECTRA IN GROUP: 22

COUNTERS RANGE FROM 6.8 TO 13.4 MICRONS

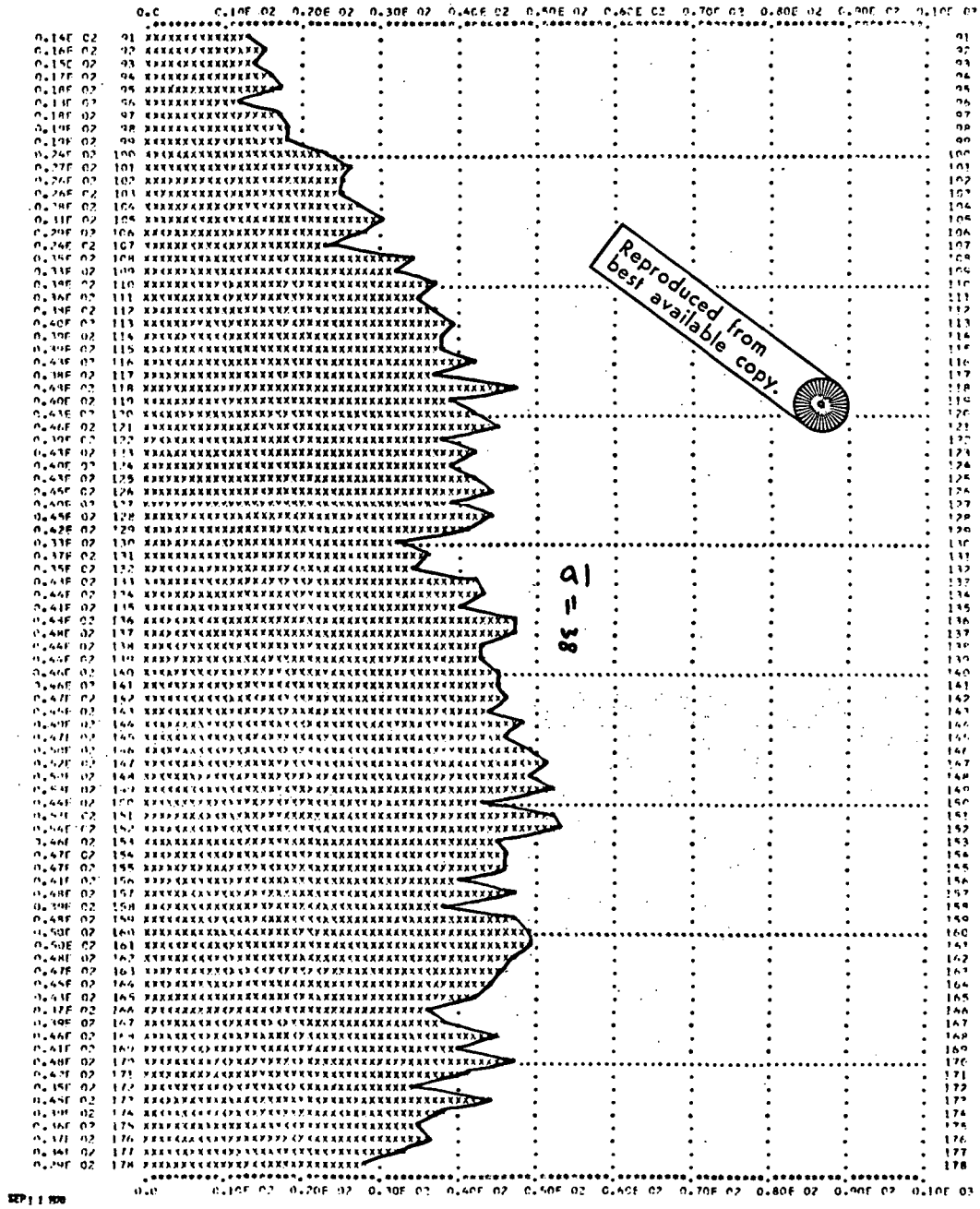

PLOT OF STANDARD DEVIATION A2-74

SLB (A)

UP RAMP SPECTRUM GROUP (18 57 3956 TO 14 57 115423 CALLED -- "#169 SUNSHINE LAVA B

NUMBER OF SPECTRA IN GROUP: 25

COUNTERS RANGE FROM 6.8 TO 13.4 MICRONS

XMIN IS 0.59E 03 XMAX IS 0.87E 03 DELTA IS 0.29E 01

0.58E 03 0.61E 03 0.64E 03 0.67E 03 0.70E 03 0.73E 03 0.75E 03 0.78E 03 0.81E 03 0.84E 03 0.87E 03

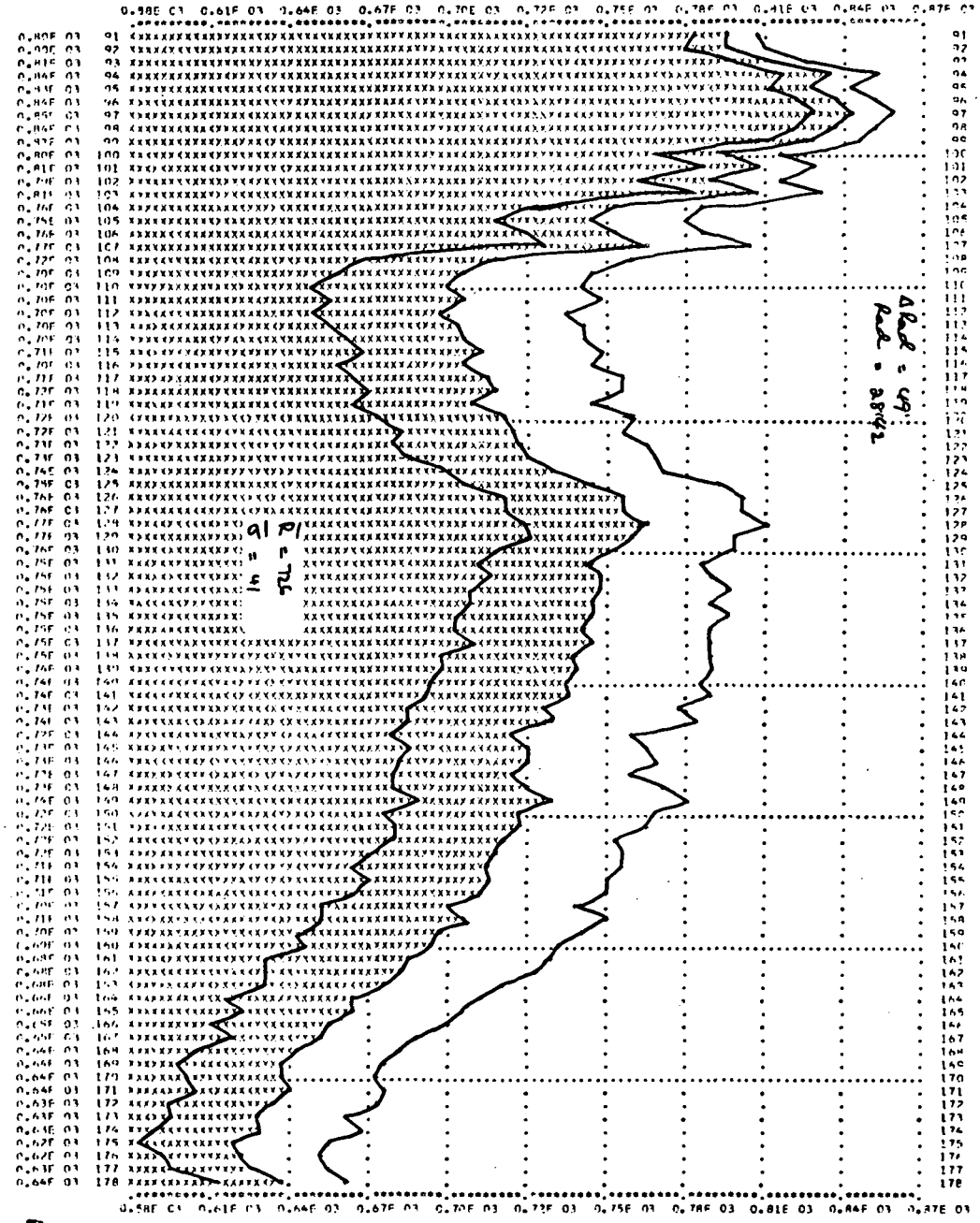

0.58E 03 0.61E 03 0.64E 03 0.67E 03 0.70E 03 0.73E 03 0.75E 03 0.78E 03 0.81E 03 0.84E 03 0.87E 03

SUNSHINE LAVA B

N= 25 $\bar{x}$ = 725
al = 41

A2-75

LP RAMP SPECTRUM GROUP (18 57 3456 TO 18 57 11542) CALLED -- MXICA SUNSHINE LAVA B (-)

NUMBER OF SPECTRA IN GROUP: 25

COUNTERS RANGE FROM 6.8 TO 13.4 MICRONS

XMIN IS 0.0 XMAX IS 0.10E 03 DELTA IS 0.10E 01

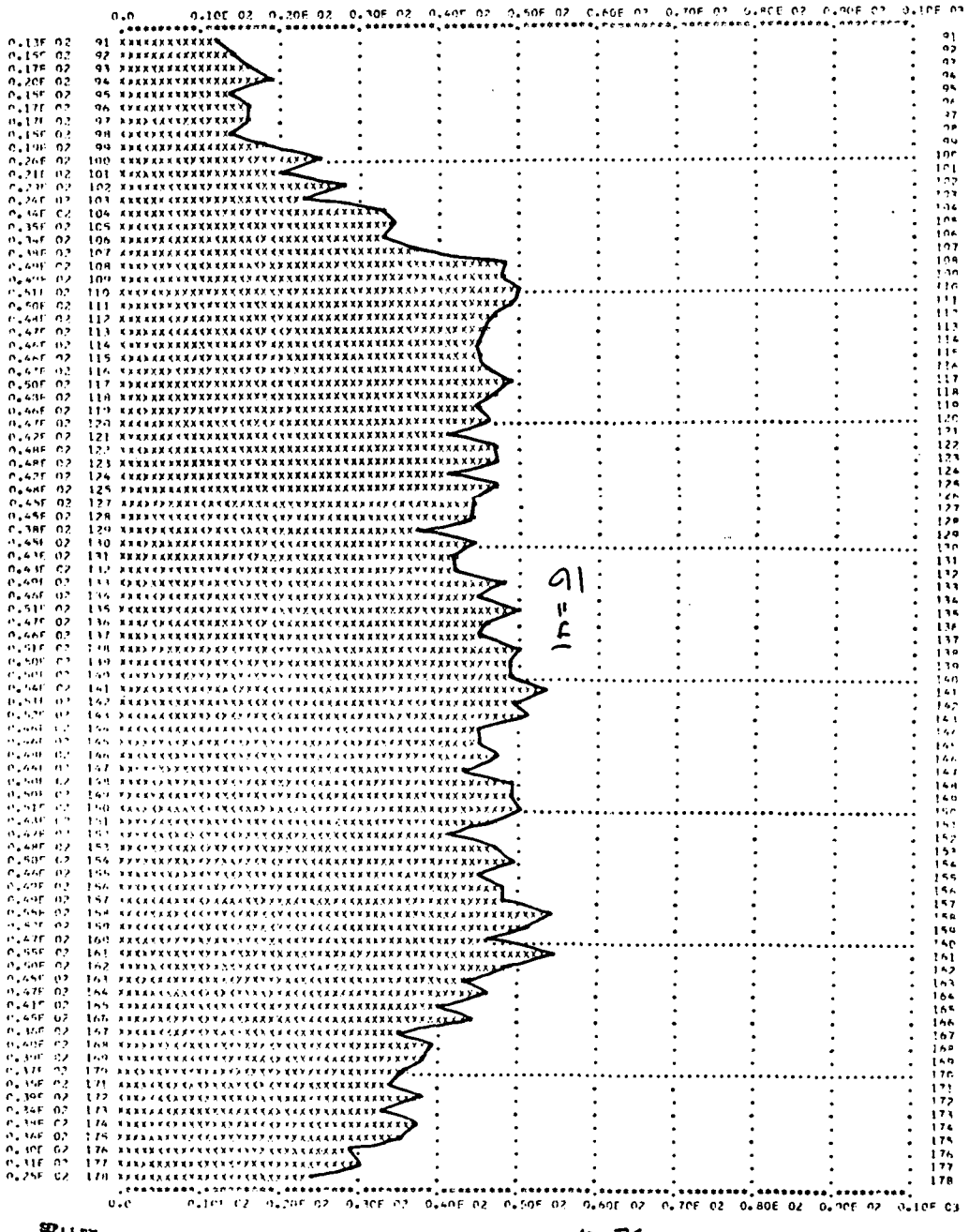

SEP 1 1 870

PLOT OF STANDARD DEVIATION A2-76

UP RAMP SPECTRUM GROUP (18 56 54548 TO 18 56 59706) CALLED -- MX16R SUNSHINE CINDERS C (-) SCC (A)

NUMBER OF SPECTRA IN GROUP: 17

COUNTERS RANGE FROM 6.8 TO 13.4 MICRONS

XMIN IS 0.62E 03 XMAX IS 0.91E 03 DELTA IS 0.10E 01

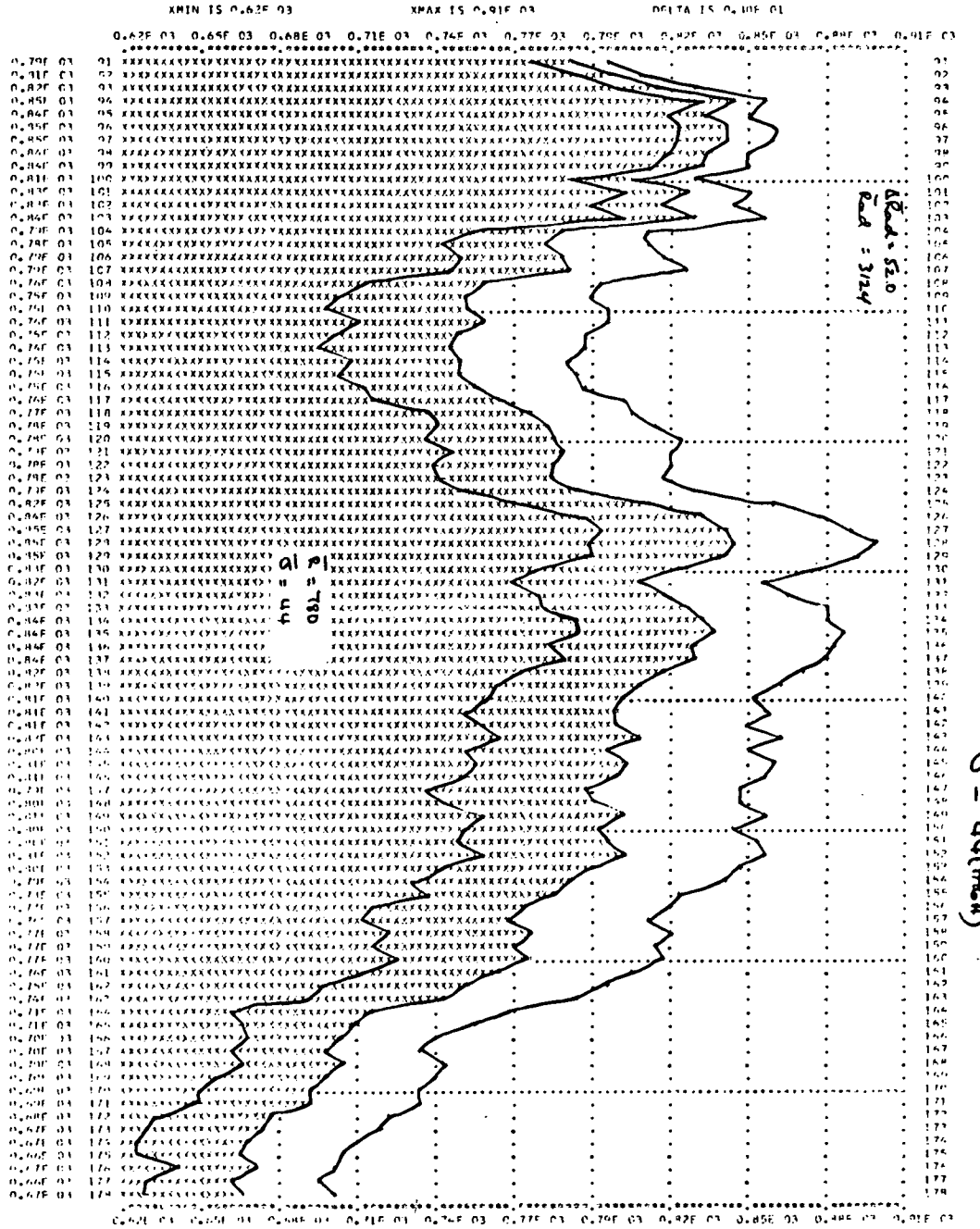

SUNSHINE CINDERS "C"

N = 17 $\bar{x}$ = 780 $\bar{\sigma}$ = 44 (HIGH)

SEP 1 1970

A2-77

Reproduced from best available copy.

GP RAMP SPECTRUM GROUP (18 56 54548 TO 18 55 597061 CALLED -- MX108 SUNSHINE CINDERS C (-)

NUMBER OF SPECTRA IN GROUP: 17

COUNTERS RANGE FROM 6.8 TO 13.4 MICRONS

XMIN IS 0.0 XMAX IS 0.10E 03 DELTA IS 0.10E 01

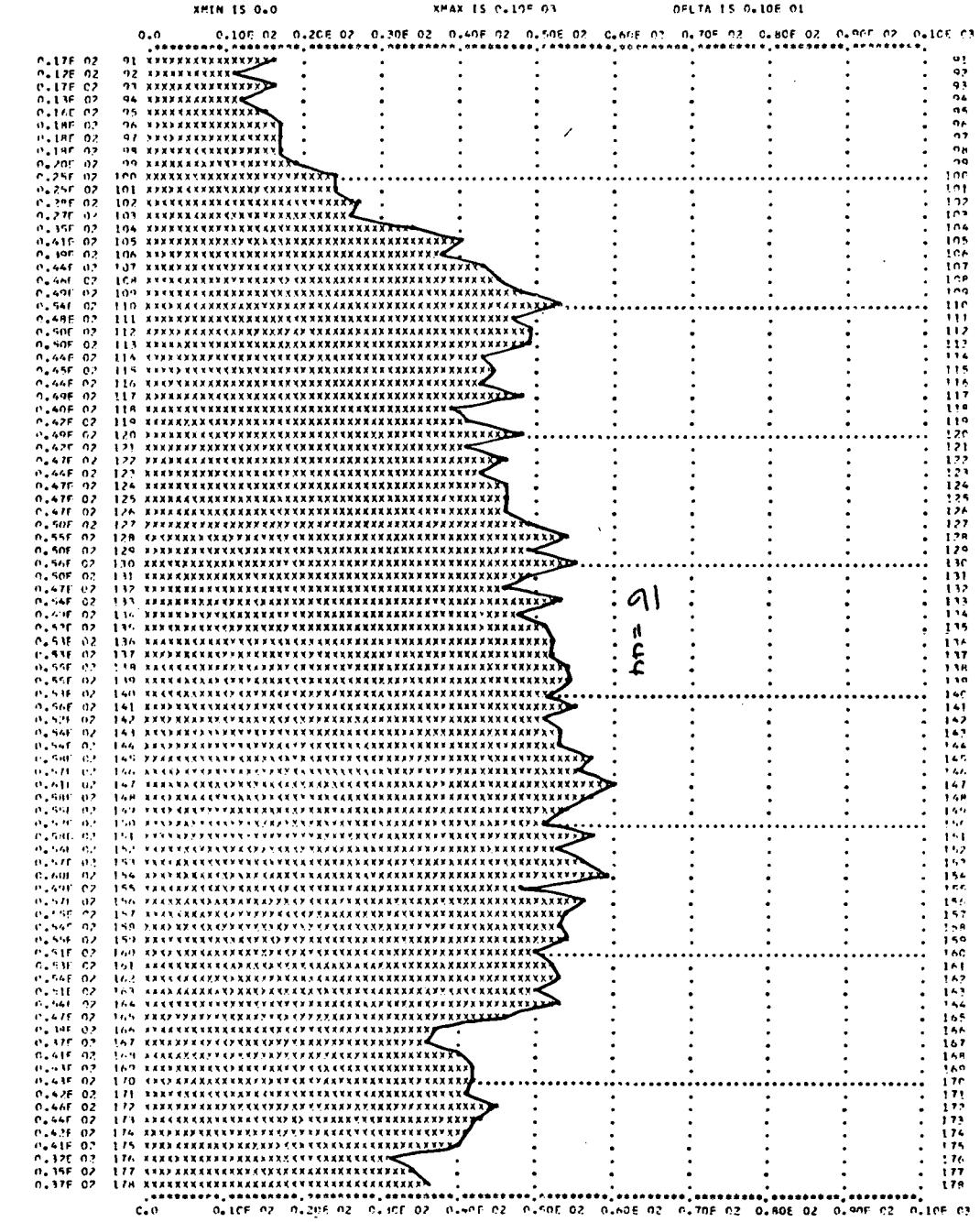

SEP 1 1 1970

PLOT OF STANDARD DEVIATION 42-78

SCD (A)

UP RAMP SPECTRUM GROUP (18 56 47563 TO 18 55 53637) CALLED -- [illegible] SUNSHINE CINDERS D

(-)

NUMBER OF SPECTRA IN GROUP: 20

COUNTERS RANGE FROM 6.8 TO 13.4 MICRONS

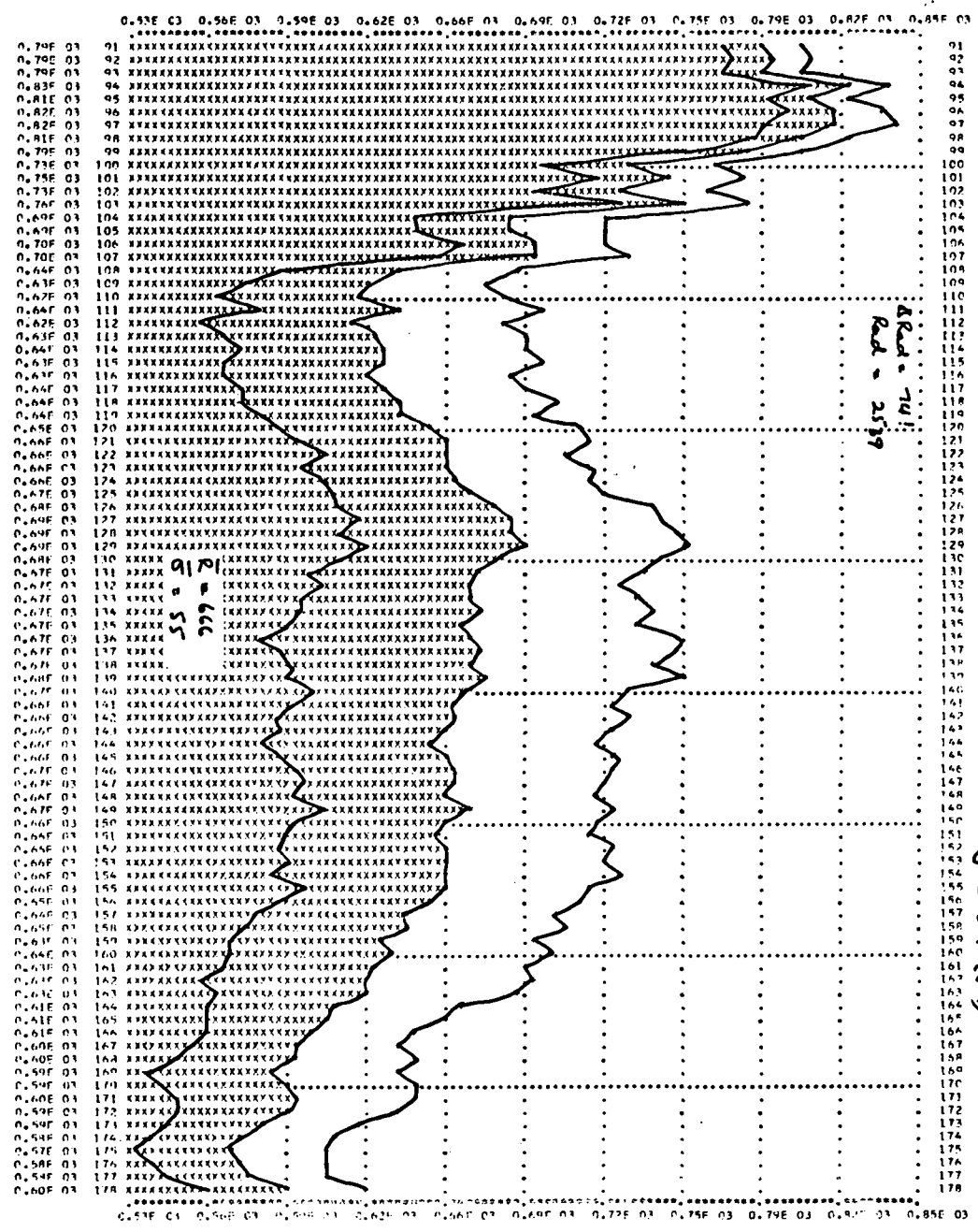

SUNSHINE CINDERS "D"

N=20

$\bar{X}$ = 666

$\bar{\sigma}$ = 54 (UH)

A2-79

UP RAMP SPECTRUM GROUP [illegible] (-)

NUMBER OF SPECTRA IN GROUP: 20

COUNTERS RANGE FROM 4.3 TO 13.4 MICRONS

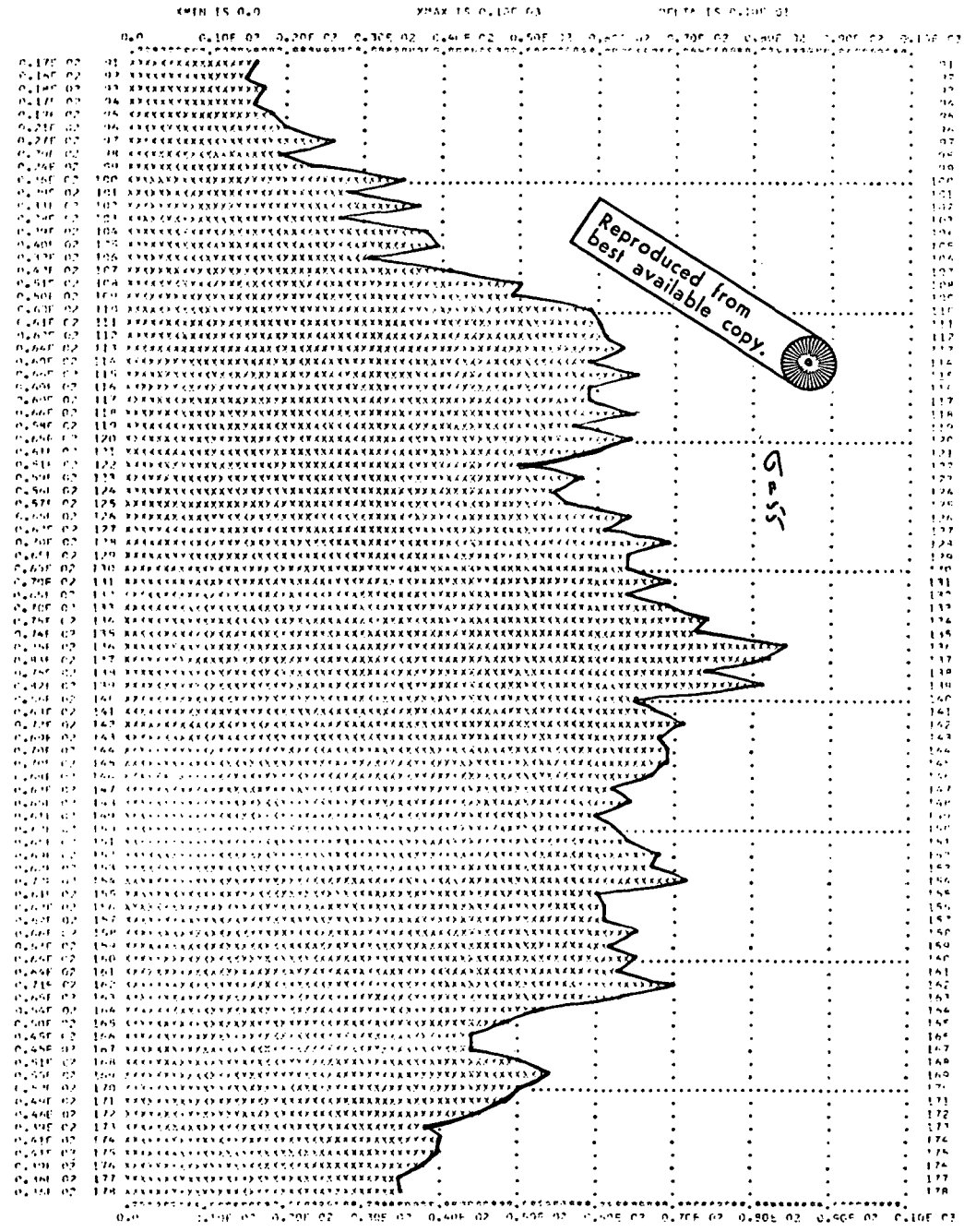

PLOT OF STANDARD DEVIATION A2-80

MONO LK 401

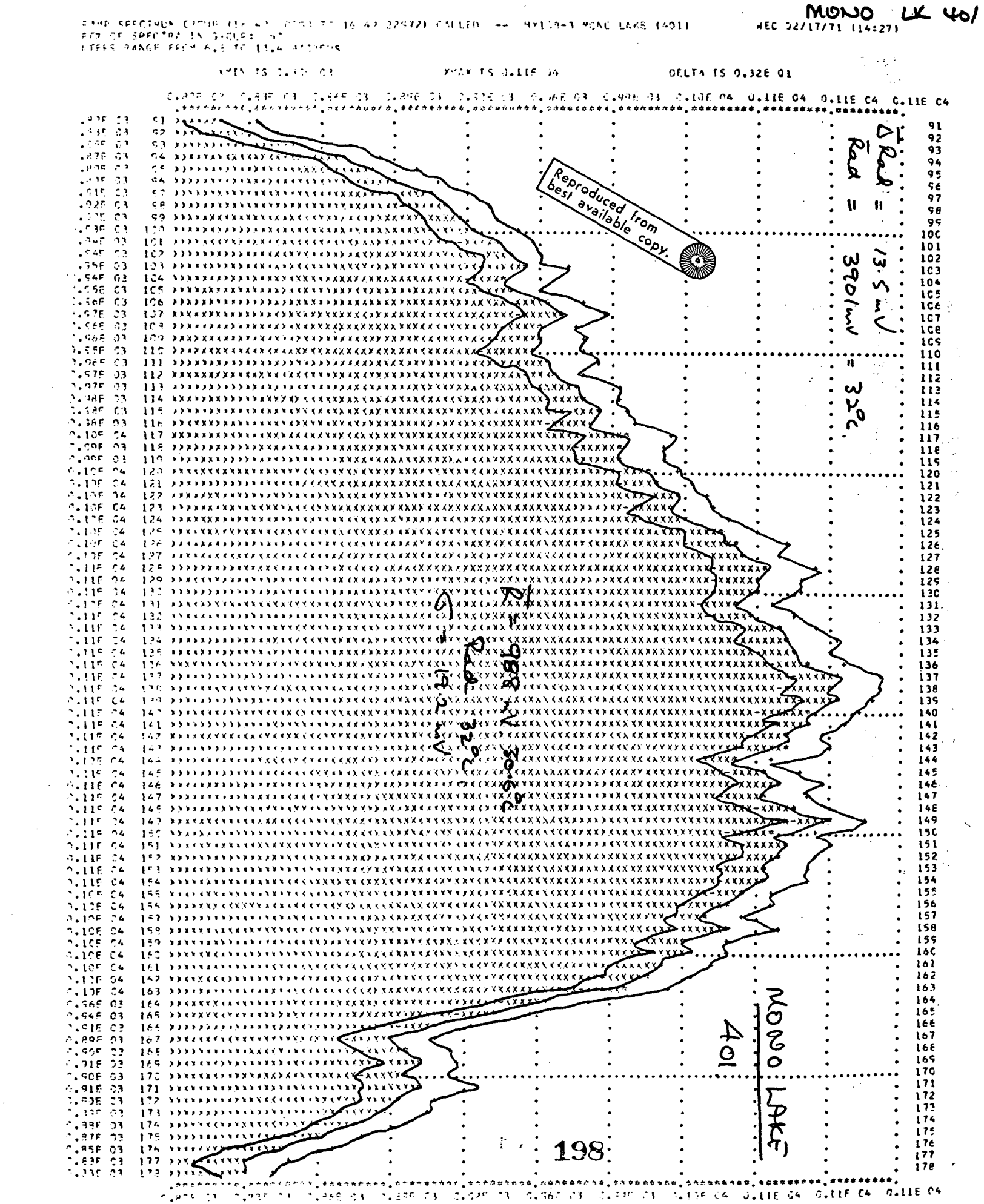
Reproduced from best available copy.
ΔRad = 13.5 mV
R̄ad = 390 mV
= 32°C
MONO LAKE
401

MONO LK 4

XMIN IS 0.0 XMAX IS 0.10E 03 DELTA IS 0.10E 01

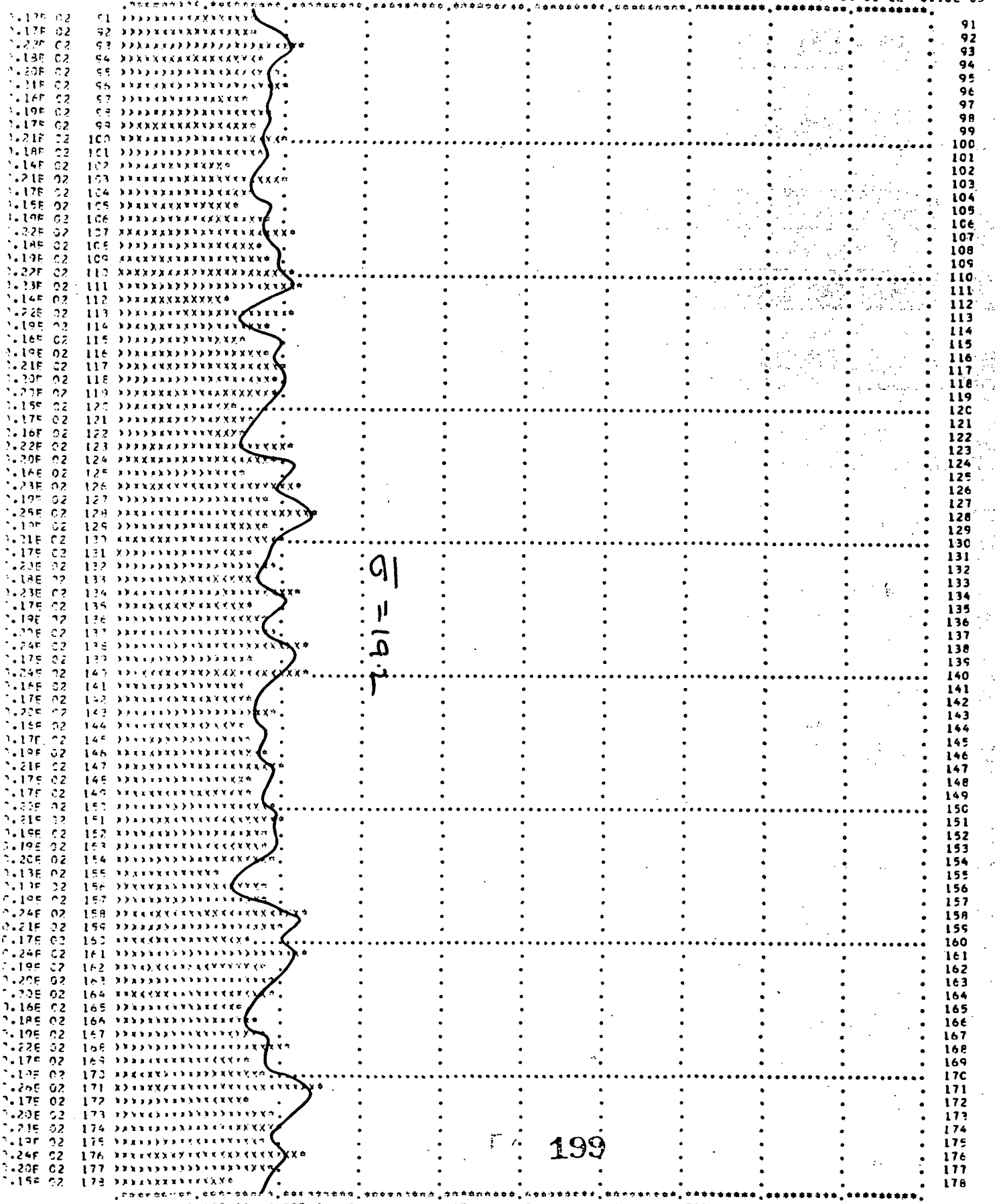

PLOT OF STANDARD DEVIATION A2-82

MONO LK. (402)

WED 02/17/71 (14:27)

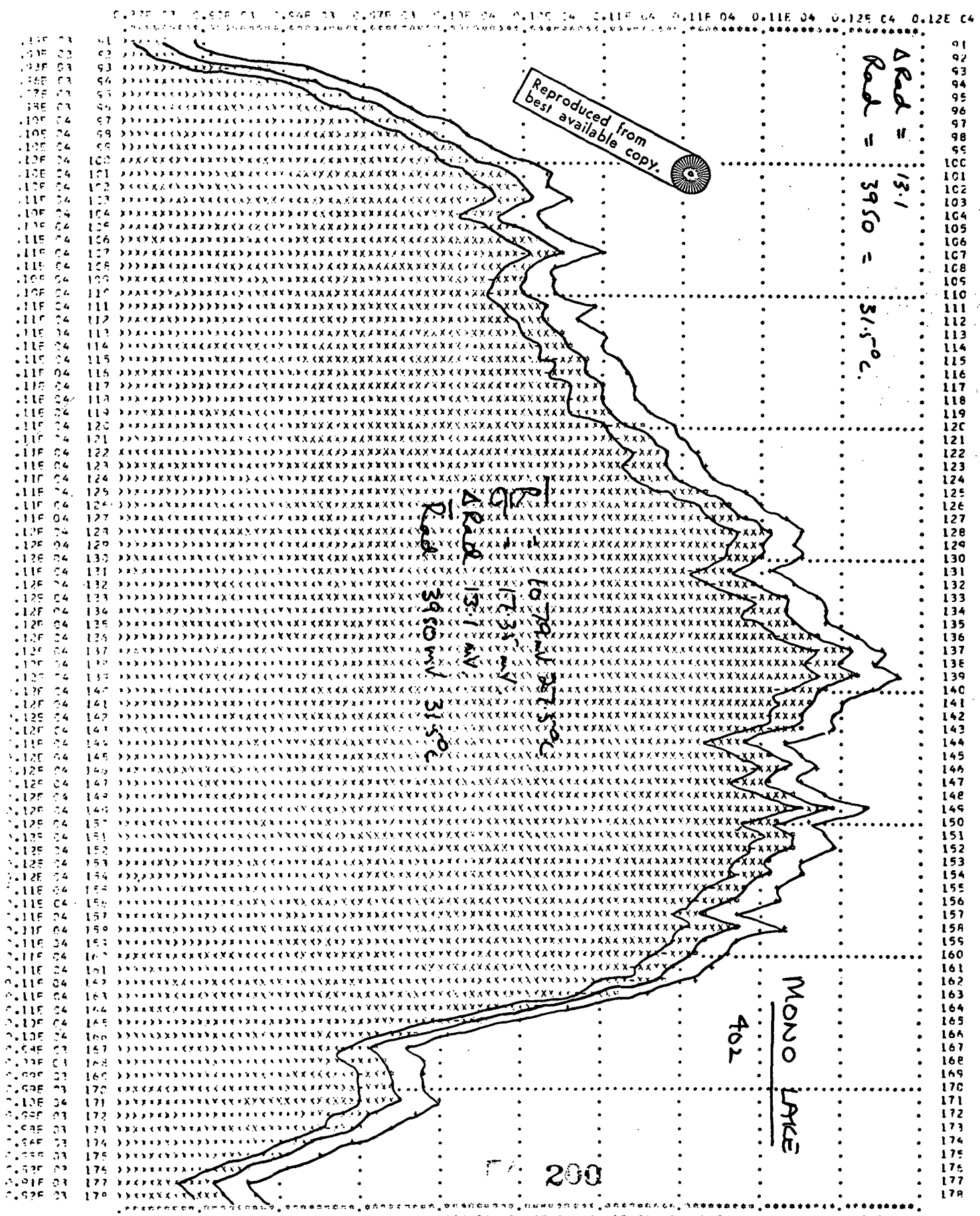

MONO LK. (402

RAMP SPECTRUM GROUP (1[illegible] TO 1[illegible] 44 1-313) CALLED -- MX108-3 MONO LAKE (402) WED 02/17/71 (14:27)
[illegible] OF SPECTRA IN GROUP: [illegible]
[illegible]TERS RANGE FROM [illegible] TO 17.4 MICRONS

XMIN IS 0.0 XMAX IS 0.10E 03 DELTA IS 0.10E 01

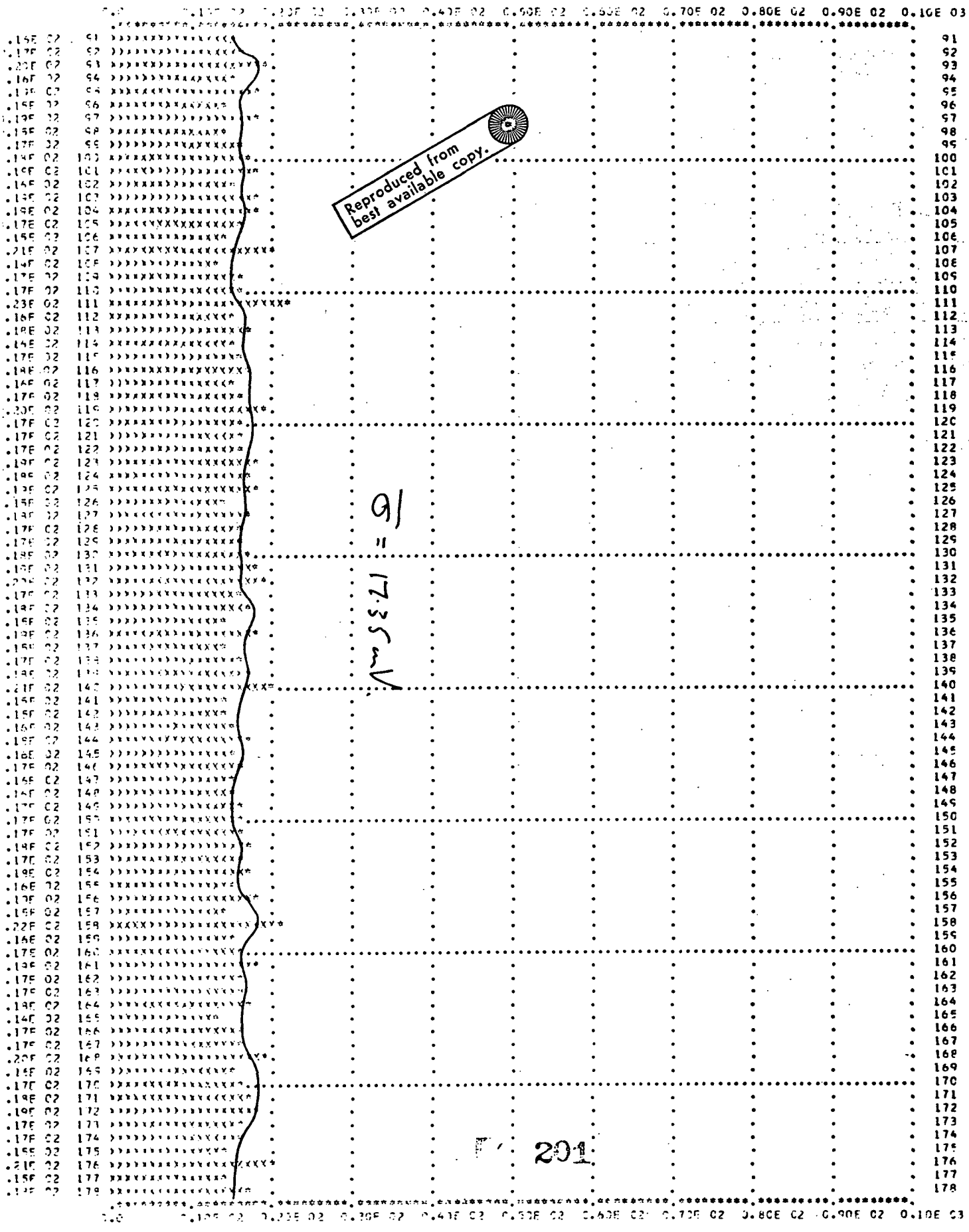

201

PLOT OF STANDARD DEVIATION A2-84

UP RAMP SPECTRUM GROUP (17 13 57900 TO 17 14 5400) CALLED -- MX108-3 QMP I WED 03/17/71 (17:32) QMP

NUMBER OF SPECTRA IN GROUP: 23

COUNTERS RANGE FROM 6.8 TO 13.4 MICRONS

XMIN IS 0.79E 03 XMAX IS 0.11E 04 DELTA IS 0.31E 01

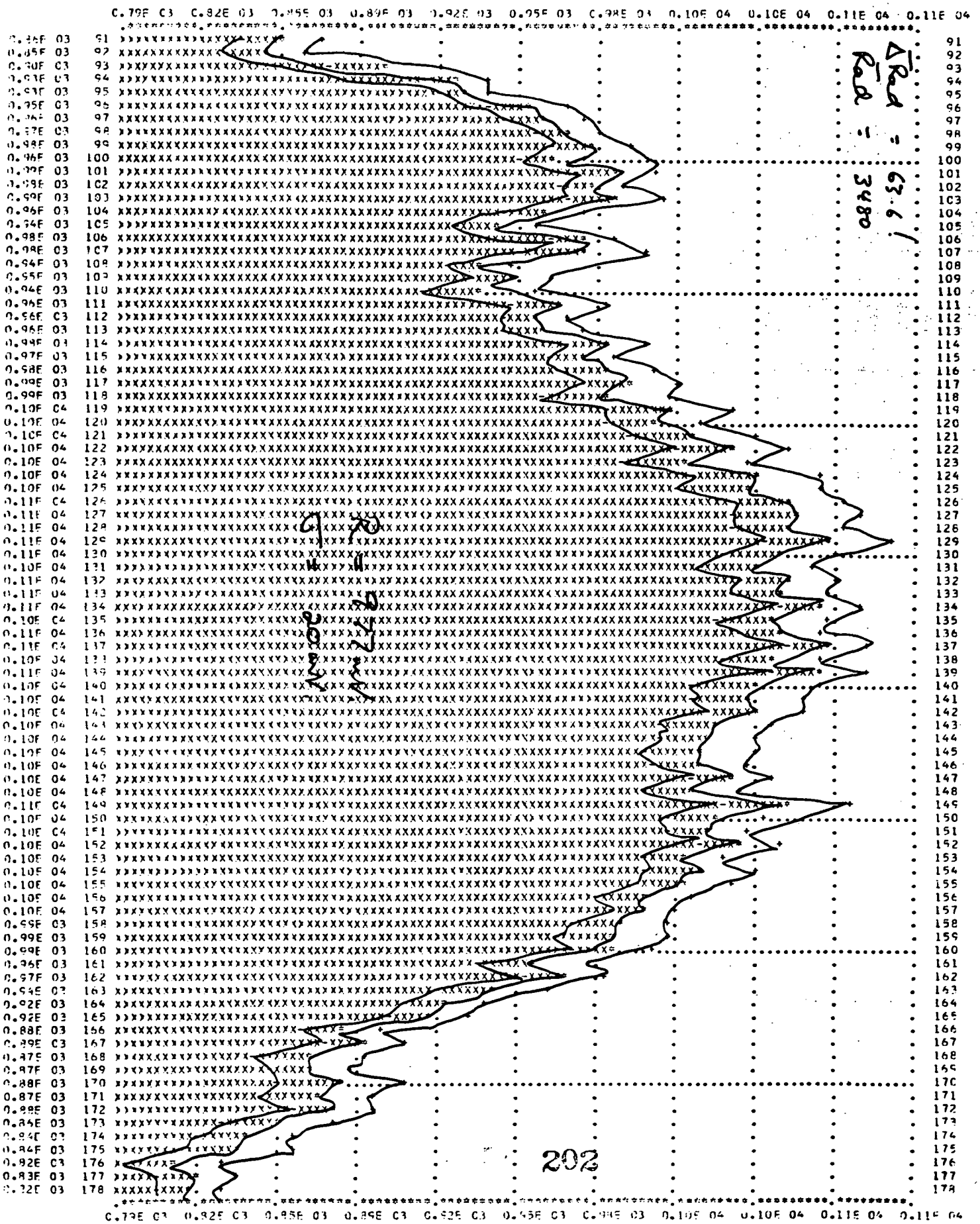

PLOT OF GROUP MEAN Δ2 – 0.5

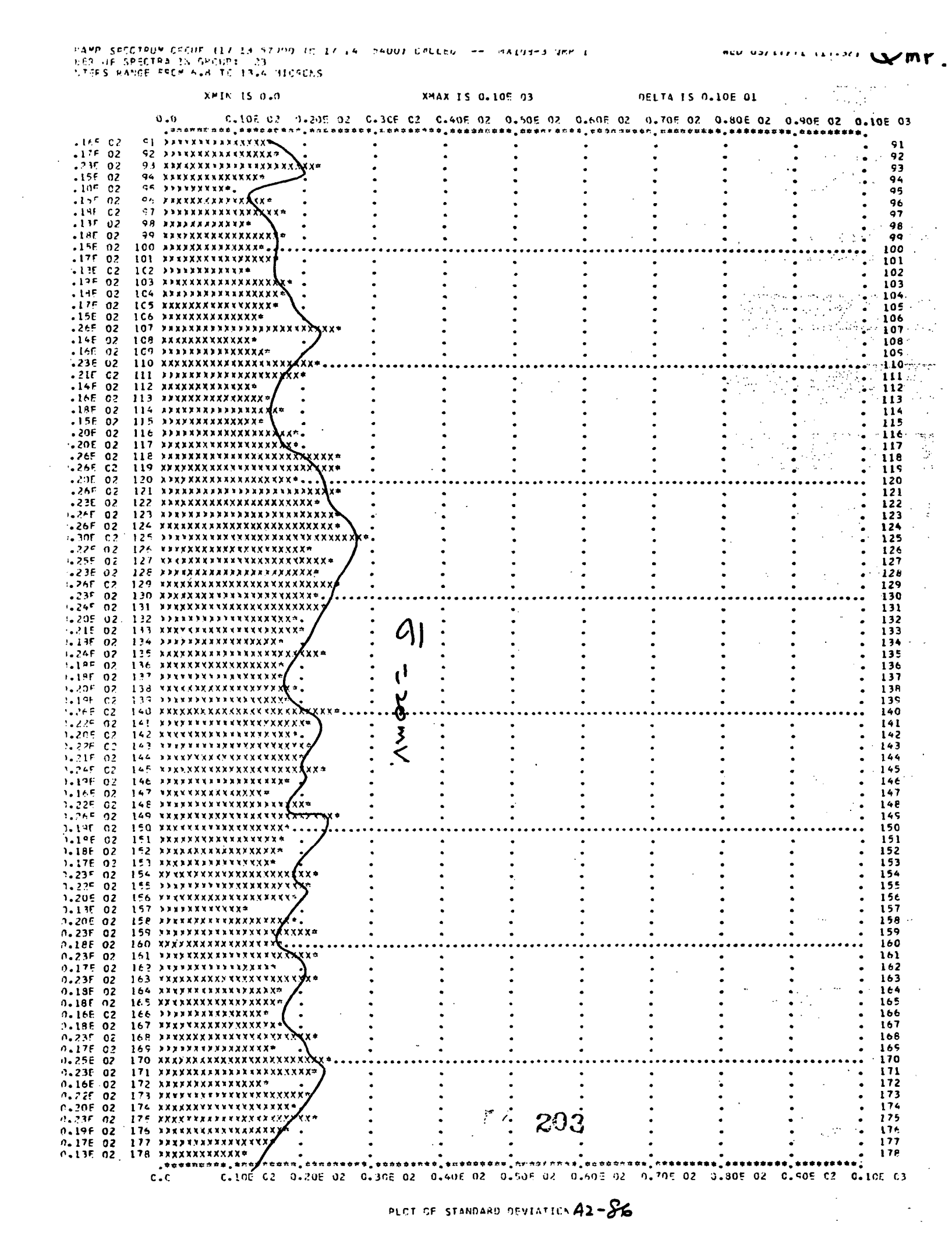

PLOT OF STANDARD DEVIATION 42-86

QMP II

RAMP SPECTRUM GROUP (17 22 4/400 TO 17 22 51400) CALLED -- MX108-3 QMP II WED 03/17/71 (17:32)
NUMBER OF SPECTRA IN GROUP: 23
WATERS RANGE FROM 6.5 TO 13.4 MICRONS

XMIN IS 0.30E 03 XMAX IS 0.11E 04 DELTA IS 0.29E 01

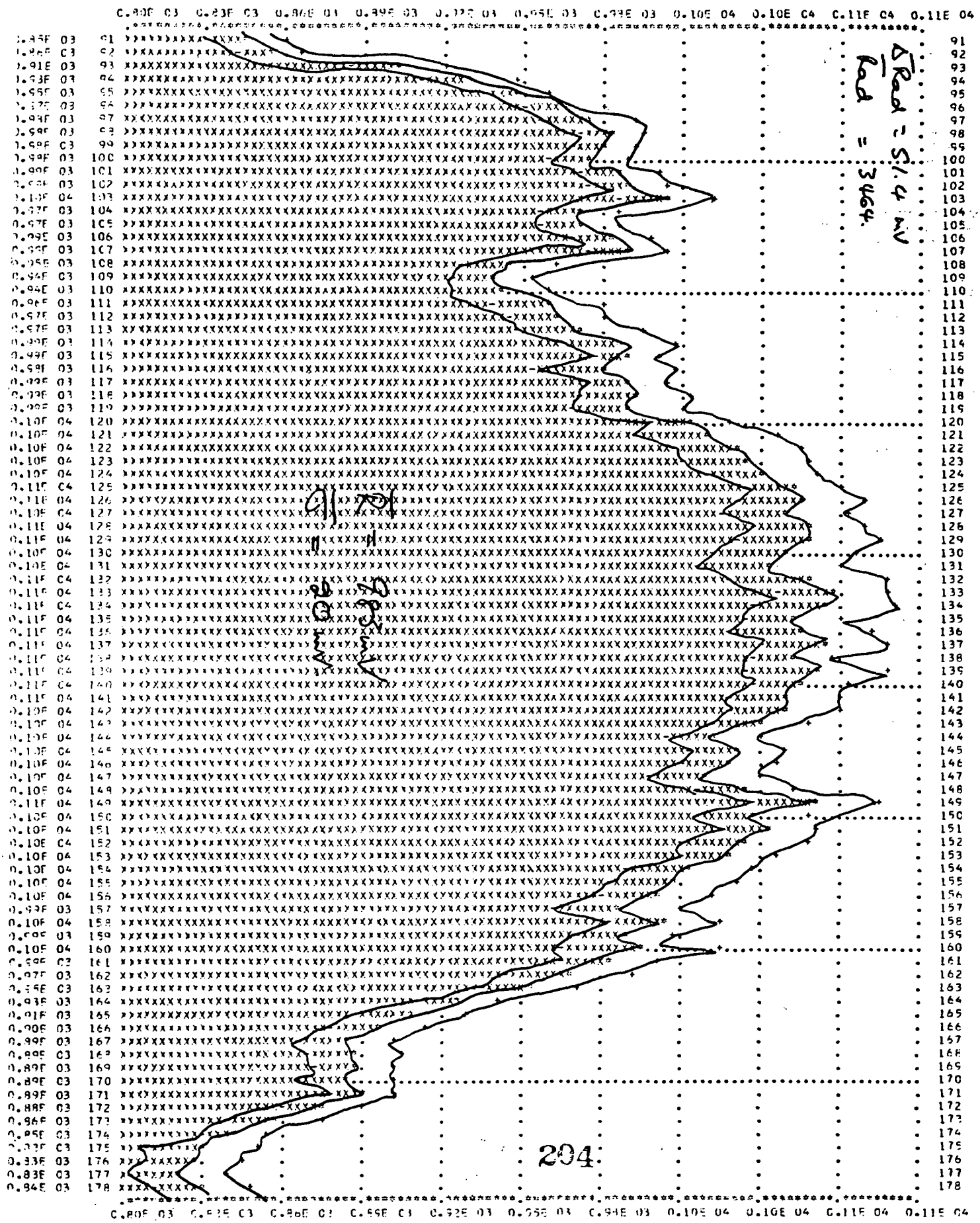

SHOT OF GROUP MEAN A2-87

QMP II

P SPECTRUM GROUP (17 22 44400 TO 17 22 51400) CALLED -- MX109-3 QMP II WED 03/17/71 (17:32)
OF SPECTRA IN GROUP: 23
RS RANGE FROM 6.8 TO 13.4 MICRONS

XMIN IS 0.0 XMAX IS 0.10E 03 DELTA IS 0.10E 01

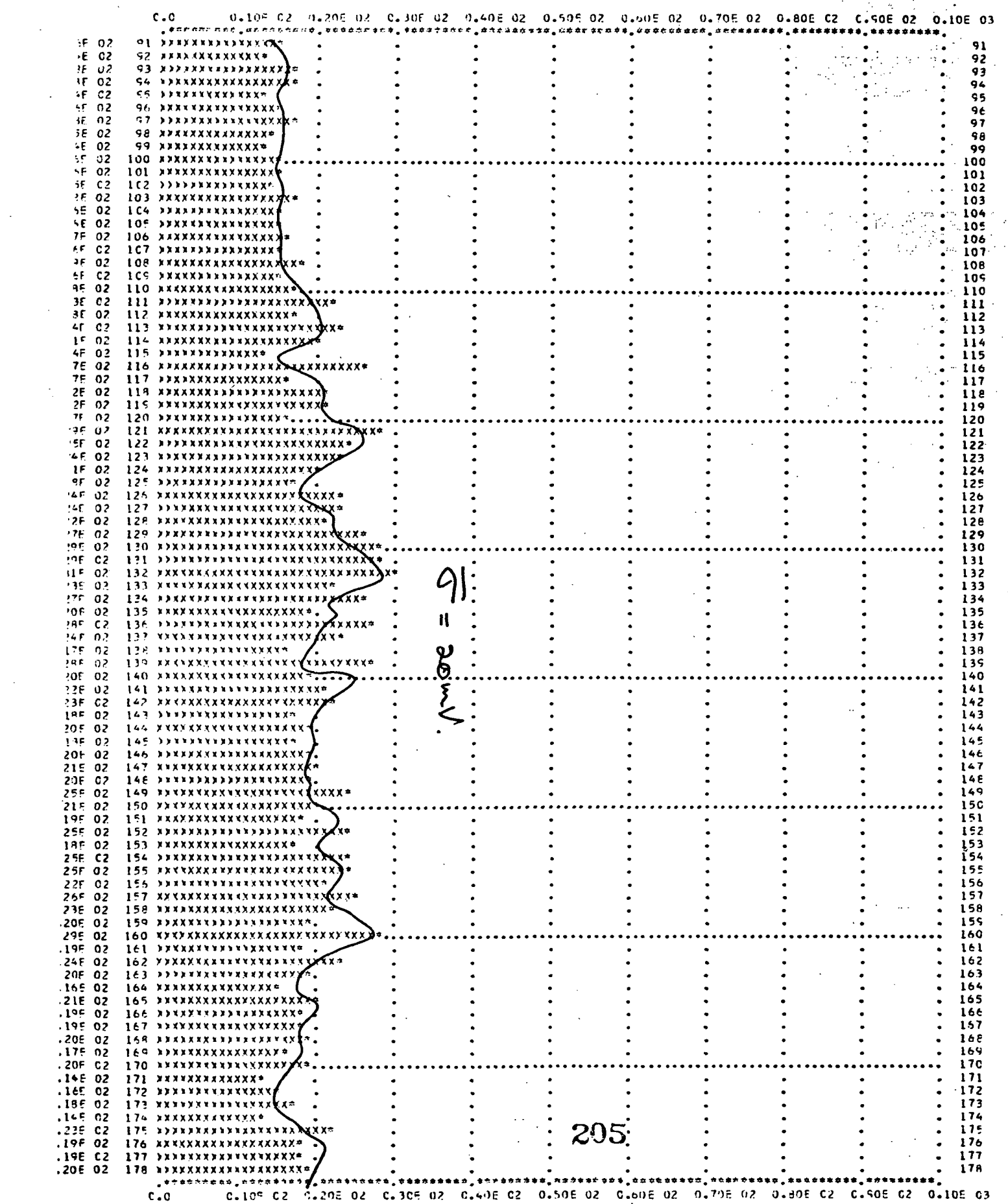

205

PEBBLES I

[illegible] SPECTRUM GROUP (17 13 7200 TO 17 13 15400) CALLED -- MX103-3 PEBBLES I WED 03/17/71 (17:32)
[illegible] OF SPECTRA IN GROUP: 27
[illegible] RANGE FROM [illegible] TO 1[illegible].4 MICRONS

XMIN IS 0.78E 03 XMAX IS 0.11E 04 DELTA IS 0.31E 01

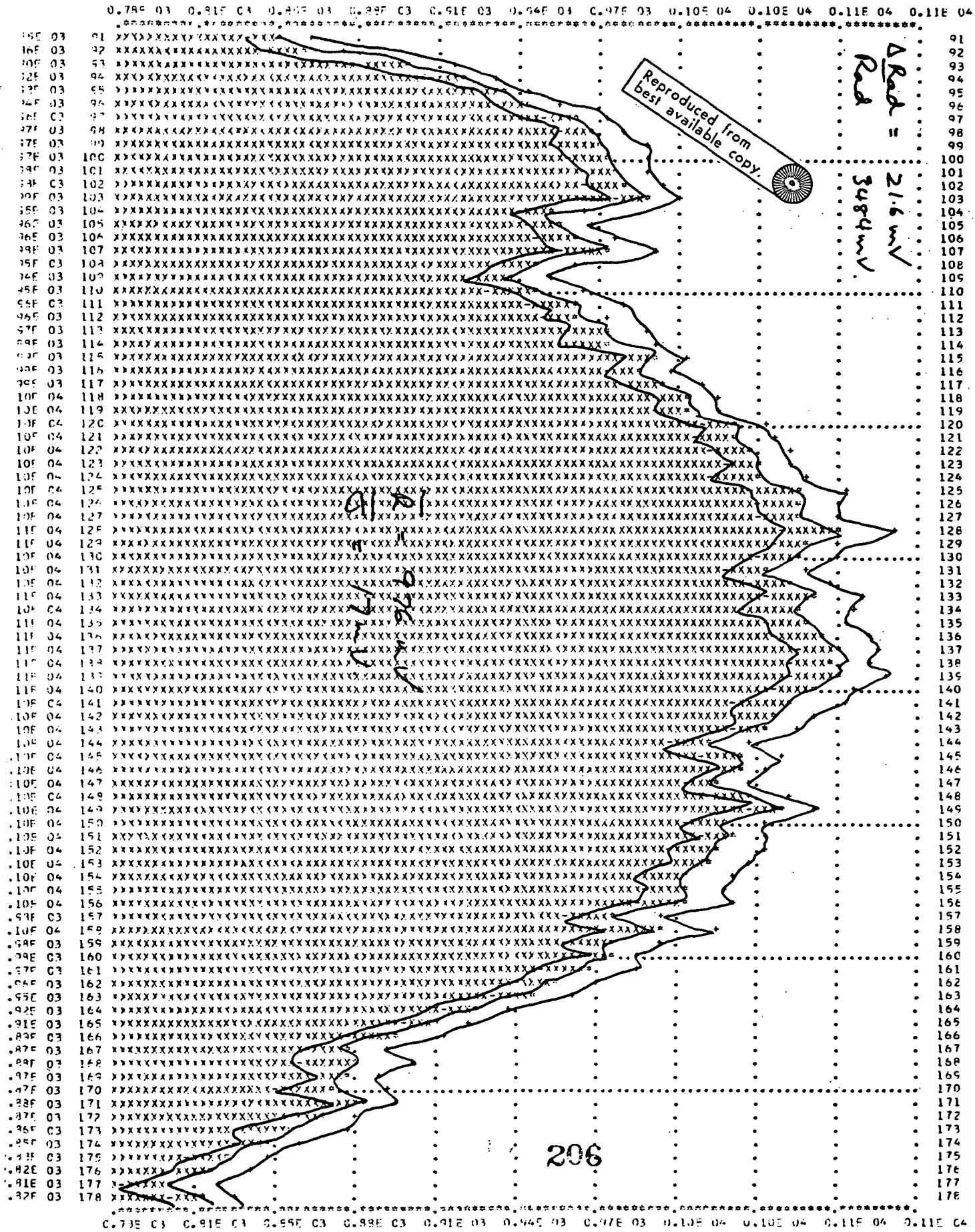

PLOT OF GROUP MEAN A2 - 89

AP SPECTRUM GROUP (17 13 7200) TO 17 13 15400) CALLED -- MX109-3 PEBBLES I WED 03/17/71 (17:32)

OF SPECTRA IN GROUP= 27

TPS PULSE FROM 6.8 TO 13.4 MICROS

XMIN IS 0.0 XMAX IS 0.10E 03 DELTA IS 0.10E 01

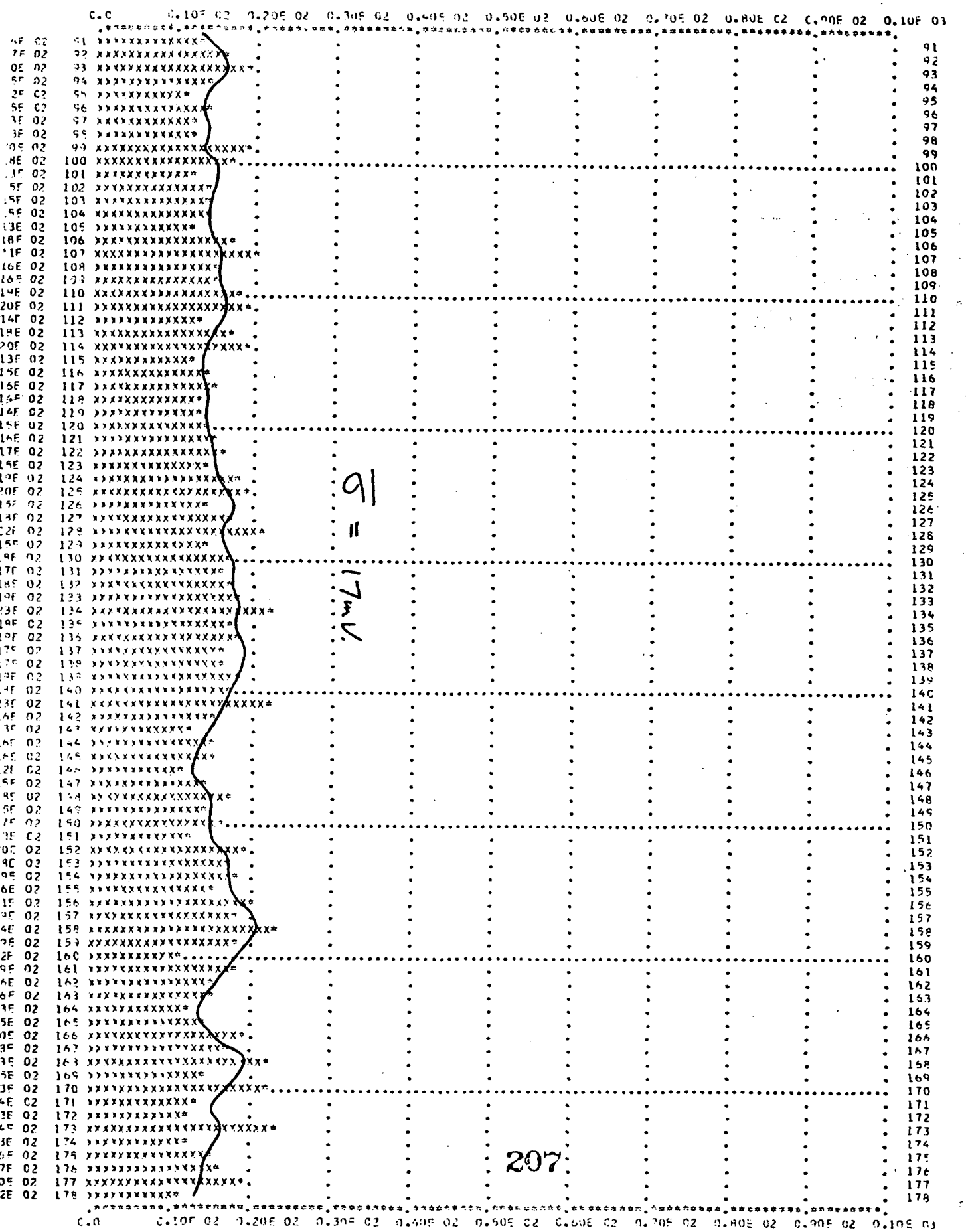

P RAMP SPECTRUM GROUP (17 21 67200 TO 17 22 44001 CALLED -- MX108-3 PEBBLES II WED 03/17/71 (17:32)
UMBER OF SPECTRA IN GROUP: 27
UNTERS RANGE FROM 6.8 TO 13.4 MICRONS

XMIN IS 0.80E 03 XMAX IS 0.11E 04 DELTA IS 0.29E 01

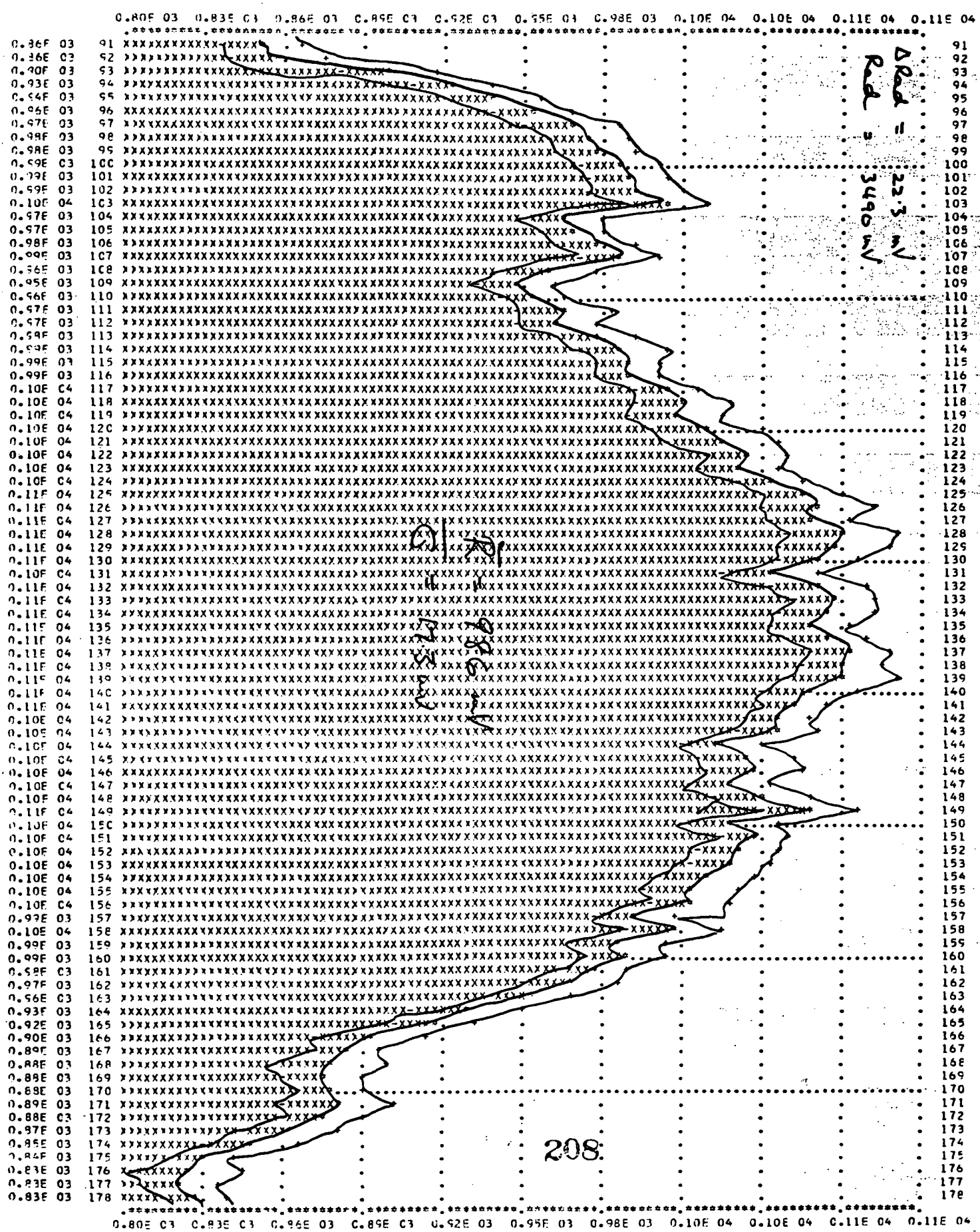

[illegible] TO 17 32 [illegible] CALLED -- [illegible] PEBBLES II WED 03/17/71 (17:32)
[illegible] SPECTRA IN [illegible]
COUNTERS RANGE FROM 6.8 TO 13.4 MICRONS

XMIN IS 0.0 XMAX IS 0.10E 03 DELTA IS 0.10E 01

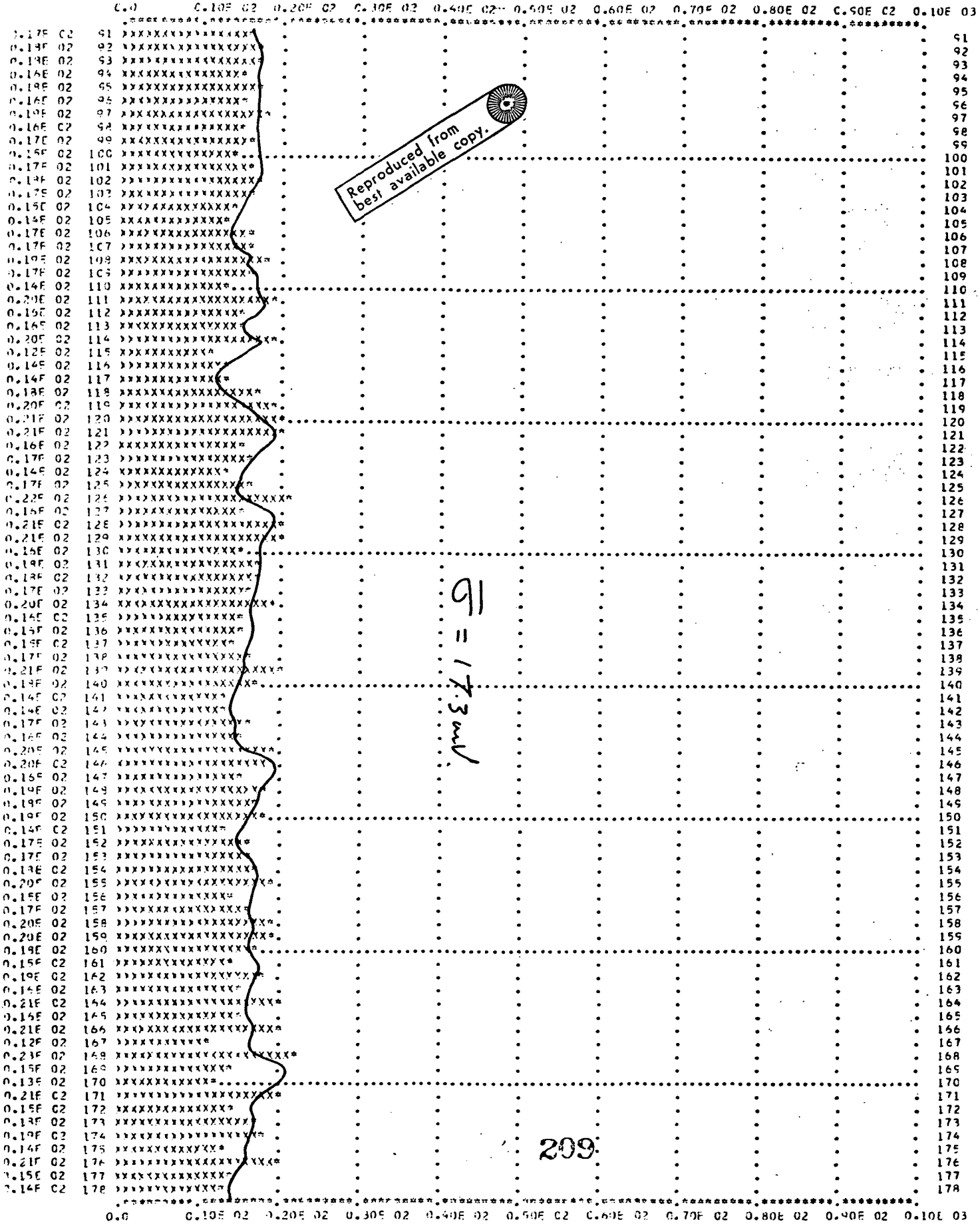

Reproduced from best available copy.

$\bar{\sigma}$ = 17.3 mV

209

PLOT OF STANDARD DEVIATION A2-92

OUTWASH I

UP RAMP SPECTRUM GROUP (17 13 3570) TO 17 (3 46300) CALLED -- MX109-3 OUT 1 WED 03/17/71 (17:32)
NO. OF SPECTRA IN GROUP: 35
COUNTERS RANGE FROM 6.3 TO 13.4 MISSIONS

XMIN IS 0.79E 03 XMAX IS 0.11E 04 DELTA IS 0.29E 01

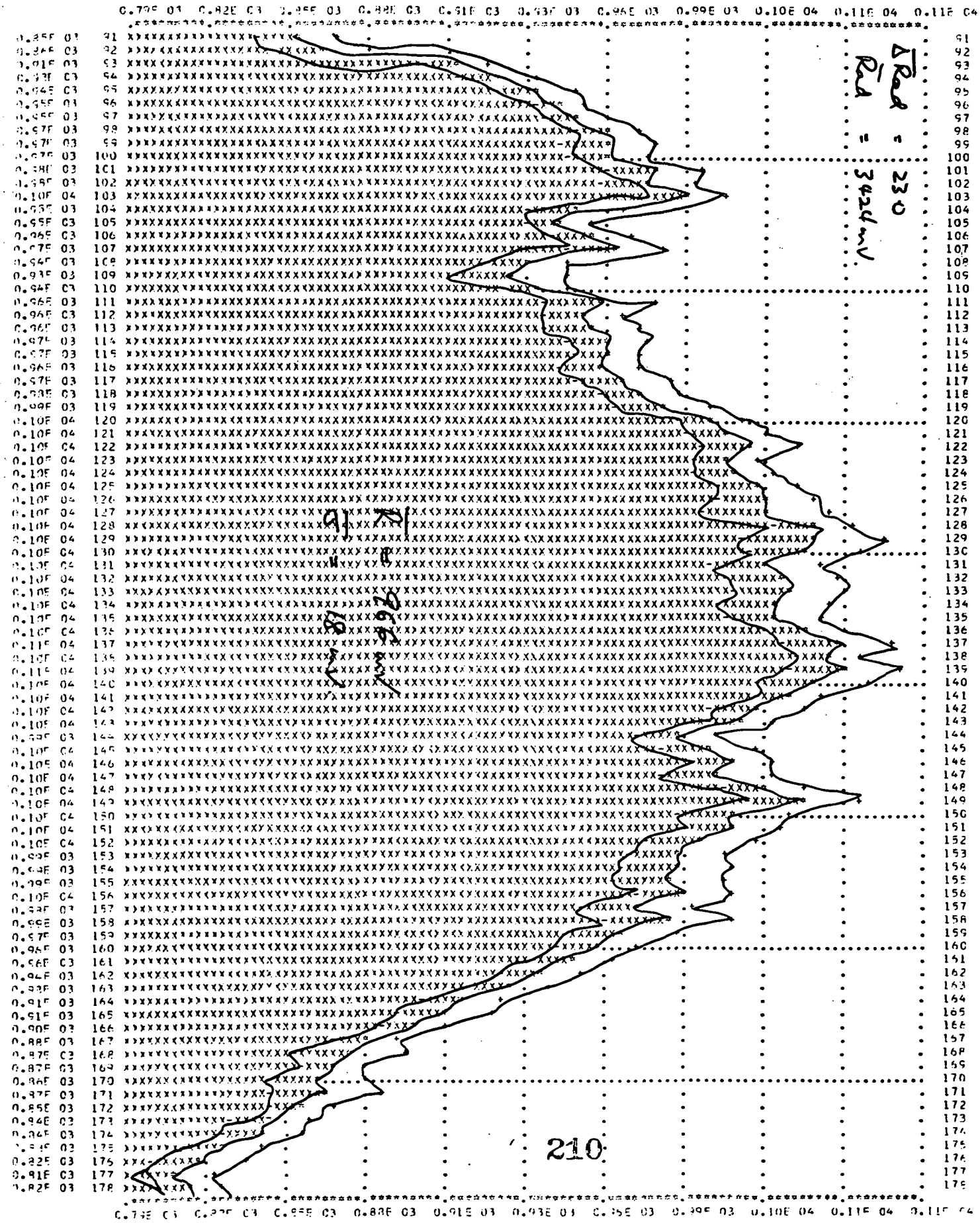

PLOT OF GROUP MEAN Δ>_92

QUTWASH 1

[illegible] CALLED -- XX103-3 CUT I WED 03/17/71 (17:32)

[illegible]

[illegible] RANGE FROM [illegible] TO 10.4 MICRONS

XMIN IS 0.0 XMAX IS 0.10E 03 DELTA IS 0.10E 01

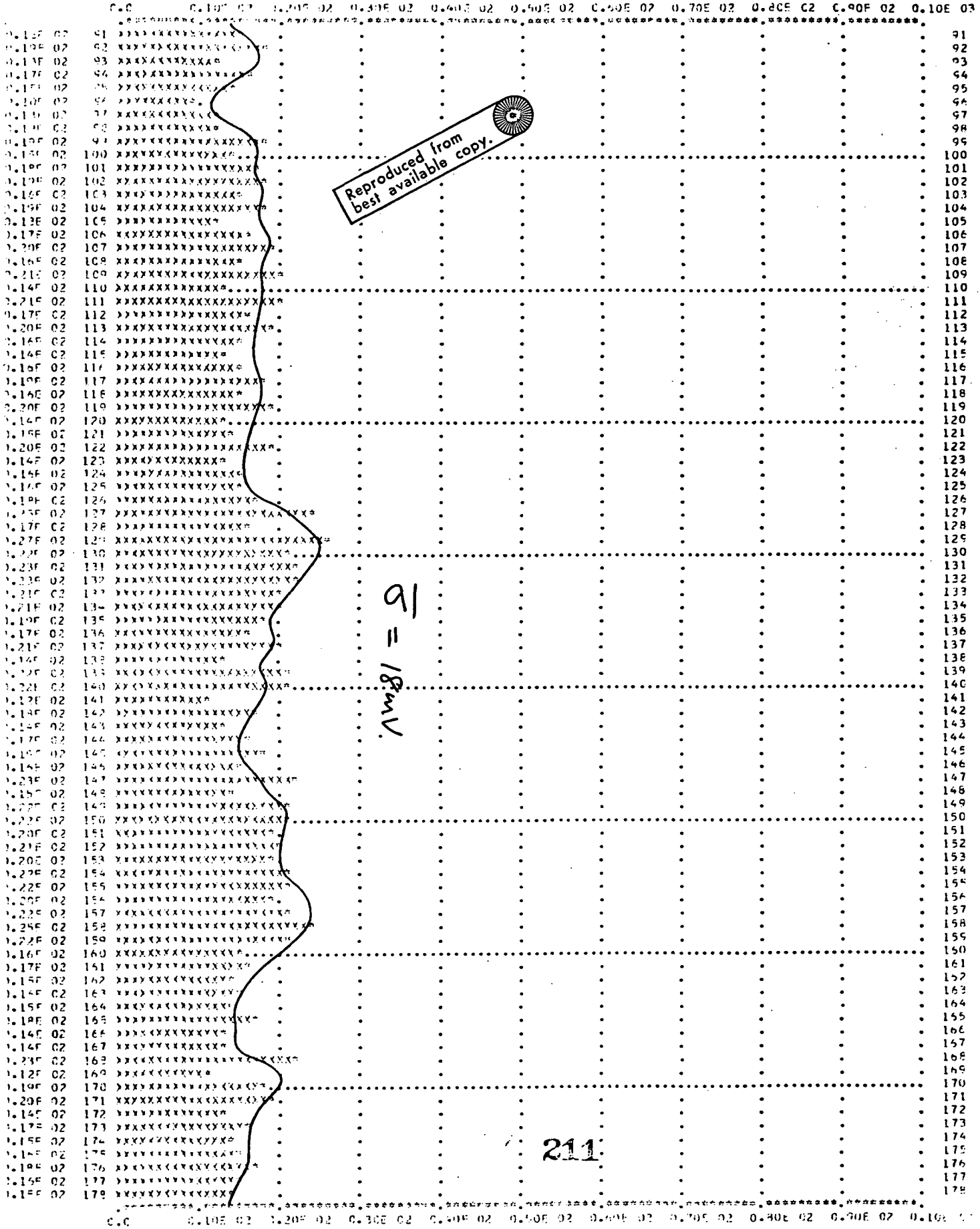

Reproduced from best available copy.

91 = 18mV.

211

PLOT OF STANDARD DEVIATION A2-94

TVA I

AMP SPECTRUM GROUP (17 13 16000 TO 17 13 35400) CALLED -- MX108-3 TVA I WED 03/17/71 (17:32)
BER OF SPECTRA IN GROUP: 64
STEPS RANGE FROM 6.8 TO 13.4 MICRONS

XMIN IS 0.79E 03 XMAX IS 0.11E 04 DELTA IS 0.29E 01

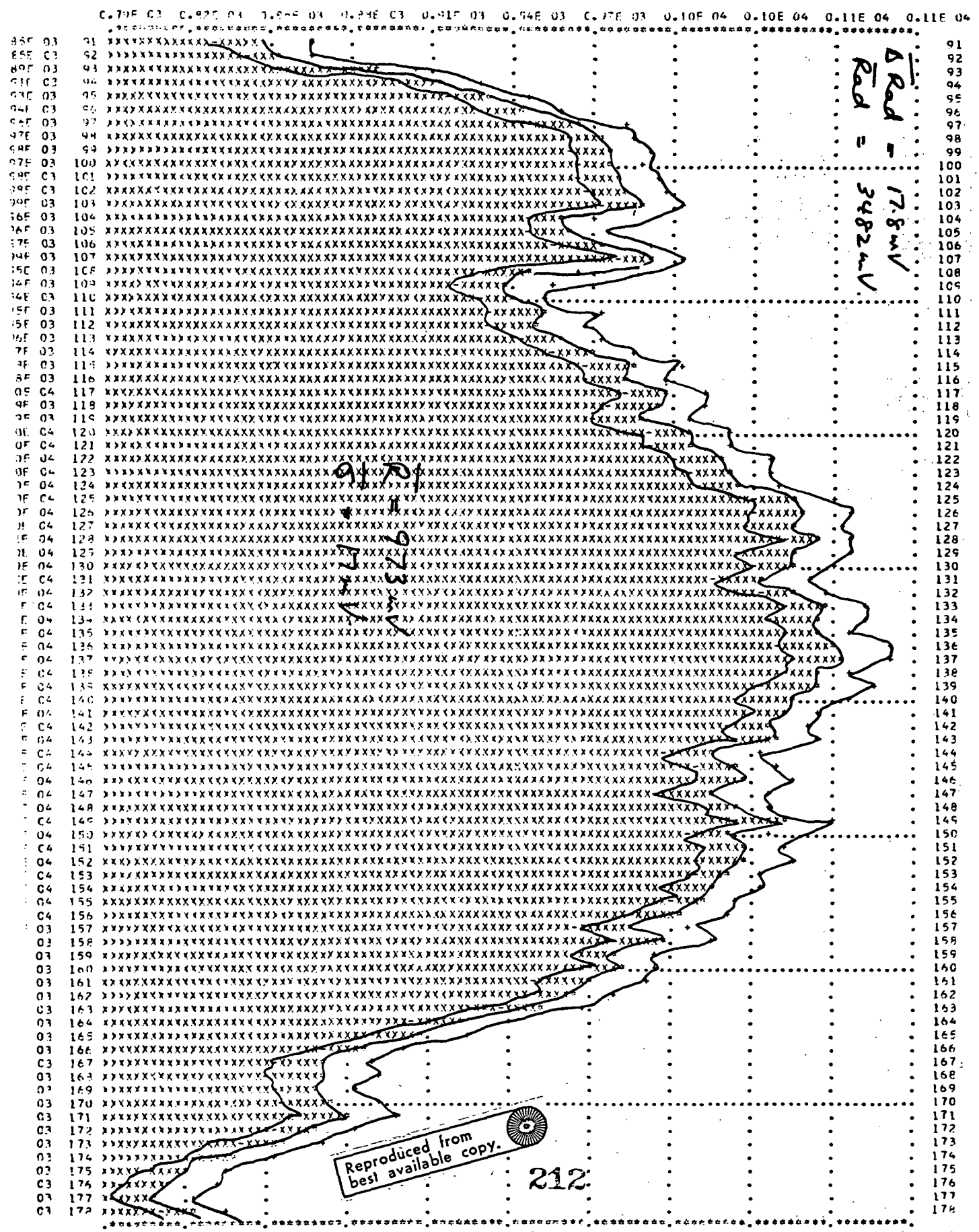

Reproduced from best available copy.

212

PLOT OF GROUP MEAN A2-95

[illegible] SPECTRUM [illegible] (17 13 [illegible]) TO 17 13 35400) CALLED -- MX109-3 TVA I WED 03/17/71 (17:32) TVA I
[illegible] OF SPECTRA [illegible]
[illegible] RANGE FROM 6.8 TO 13.4 MICRONS

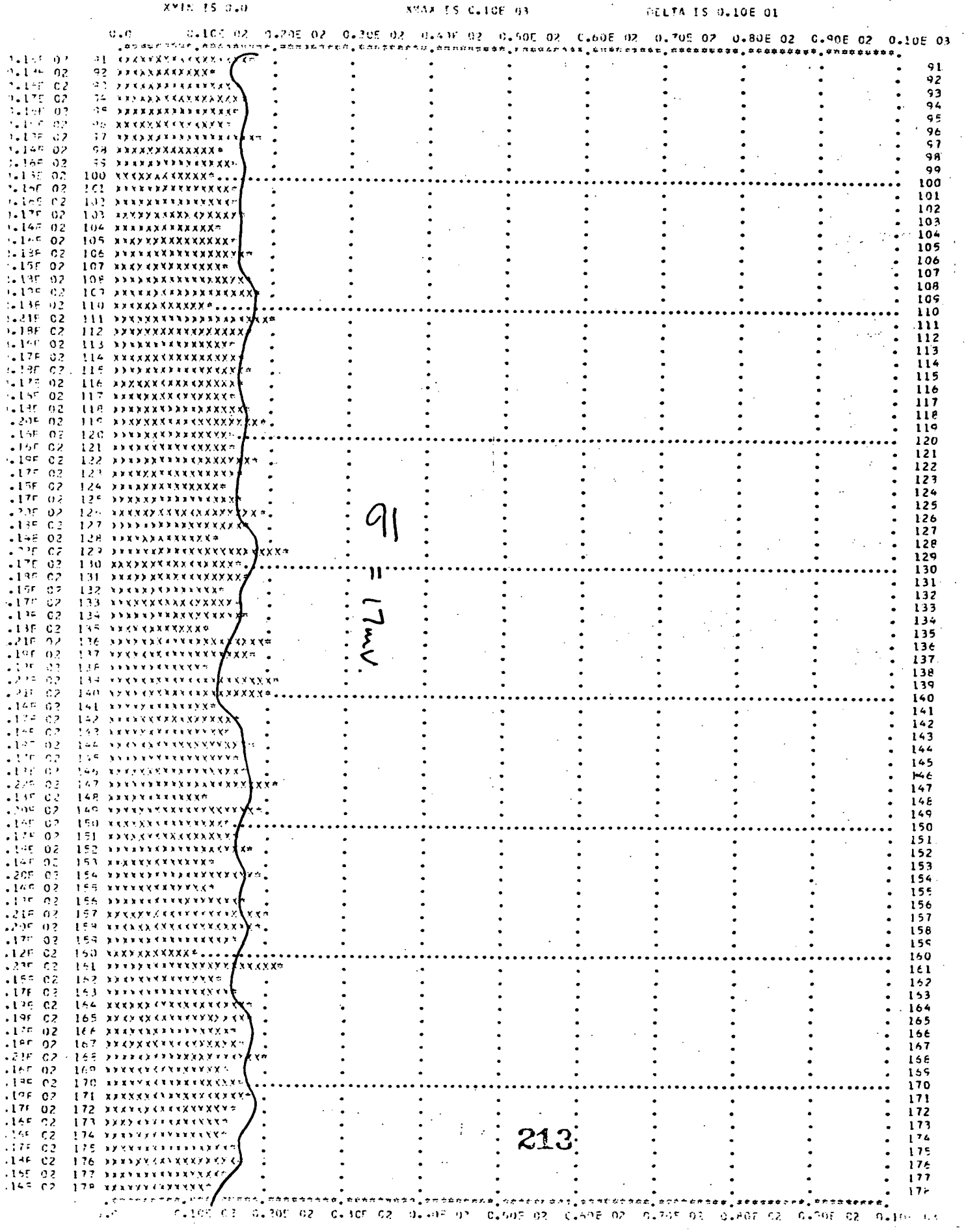

PLOT OF STANDARD DEVIATION A2-96

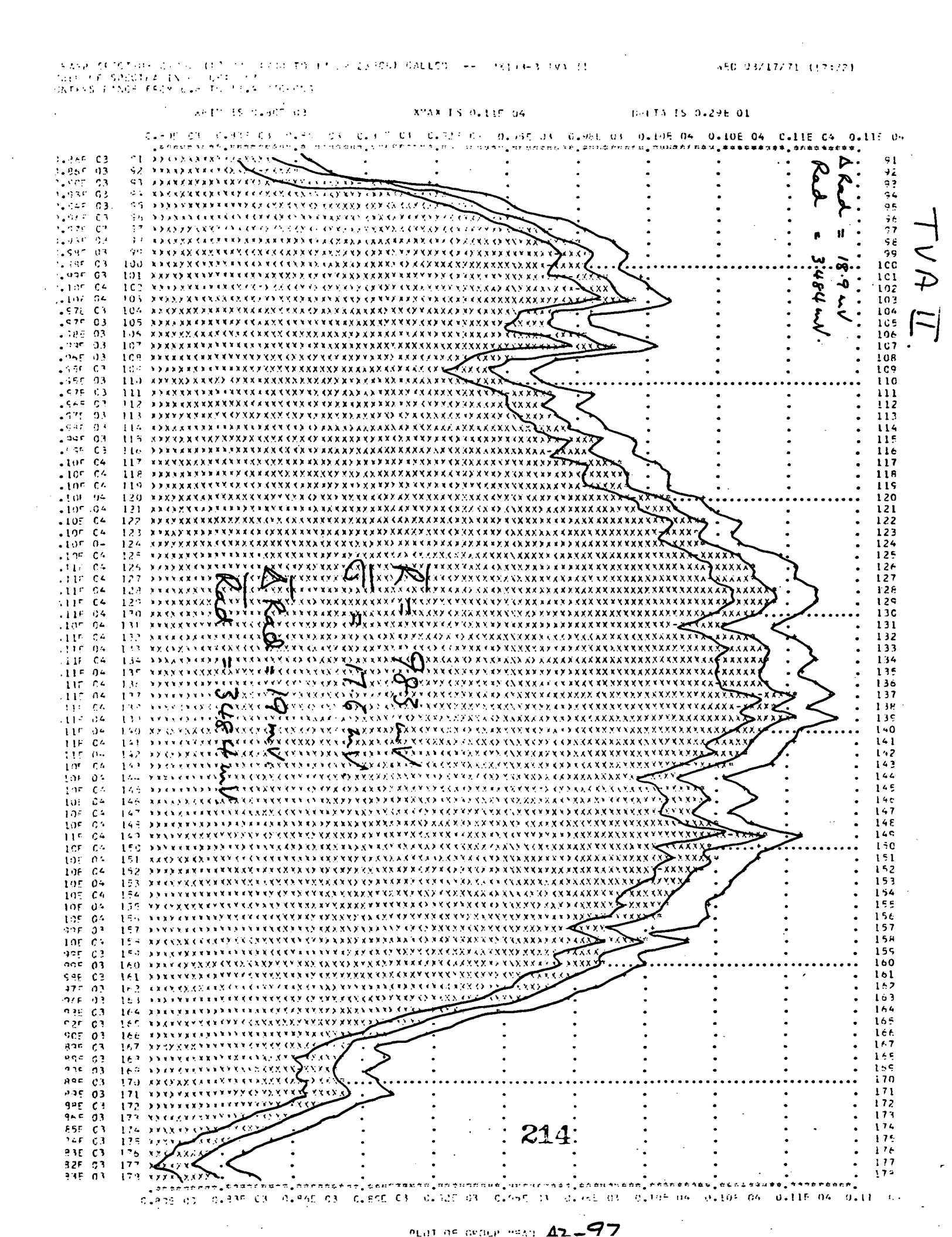

PLOT OF GROUP MEAN 42-97

AMP SPECTRUM GROUP (17 22 4700 TO 17 02 23800) CALLED -- MX108-3 TVA II WED 03/17/71 (17:32)
CR IF SPECTRA IN GROUP: 61
FREQ RANGE FROM 6.8 TO 13.4 MICRONS

XMIN IS 0.0 XMAX IS 0.10E 03 DELTA IS 0.10E 01

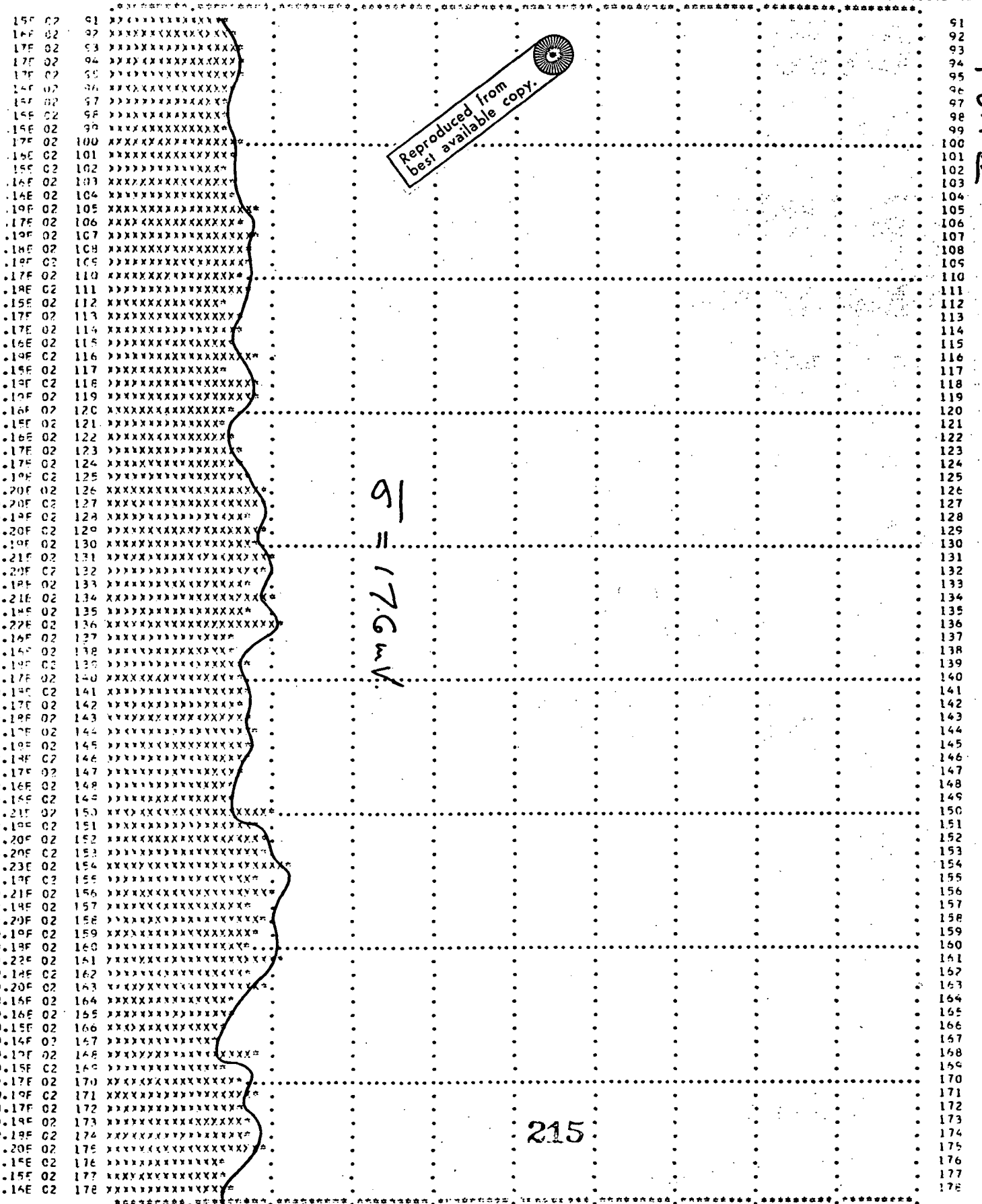

Reproduced from best available copy.

TVA II

91 = 17.6 mV.

215

PLOT OF STANDARD DEVIATION A2-98

RAMP SPECTRUM GROUP (17 22 32500 TO 17 22 53800) CALLED -- MX108-3 TAV II WED 03/17/71 (17:32)
NUMBER OF SPECTRA IN GROUP: 3
HUNTERS RANGE FROM 6.9 TO 13.4 MICRONS

XMIN IS 0.76E 03 XMAX IS 0.11E 04 DELTA IS 0.37E 01

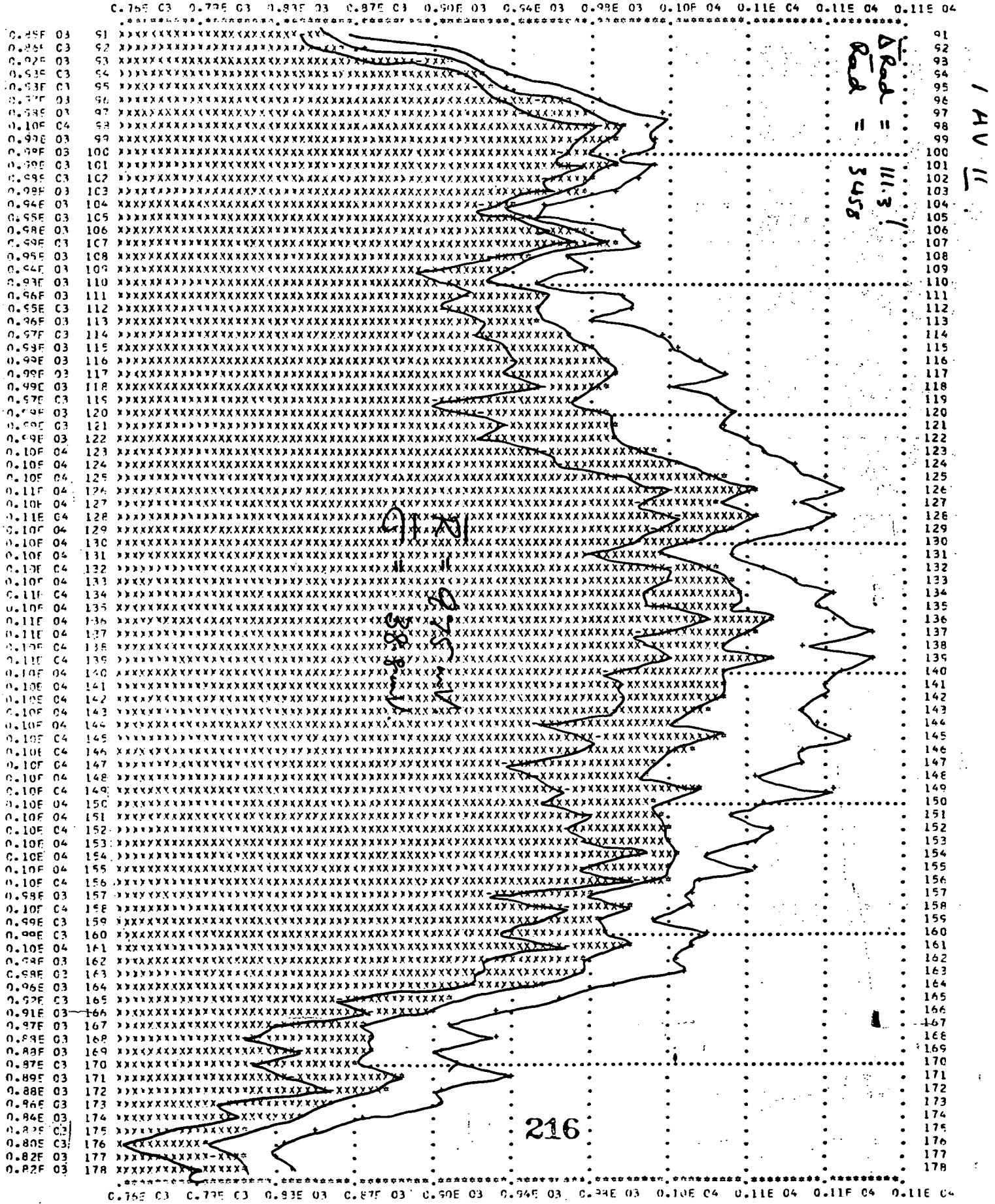

PLOT OF GROUP MEAN 4) 99

[illegible] (17 22 53800 TO 17 22 53800) CALLED -- MX109-3 TAV II WED 03/17/71 (17:32)
[illegible] OF SPECTRA IN GROUP: 3
[illegible] RANGE FROM 0.8 TO 13.4 MICRONS

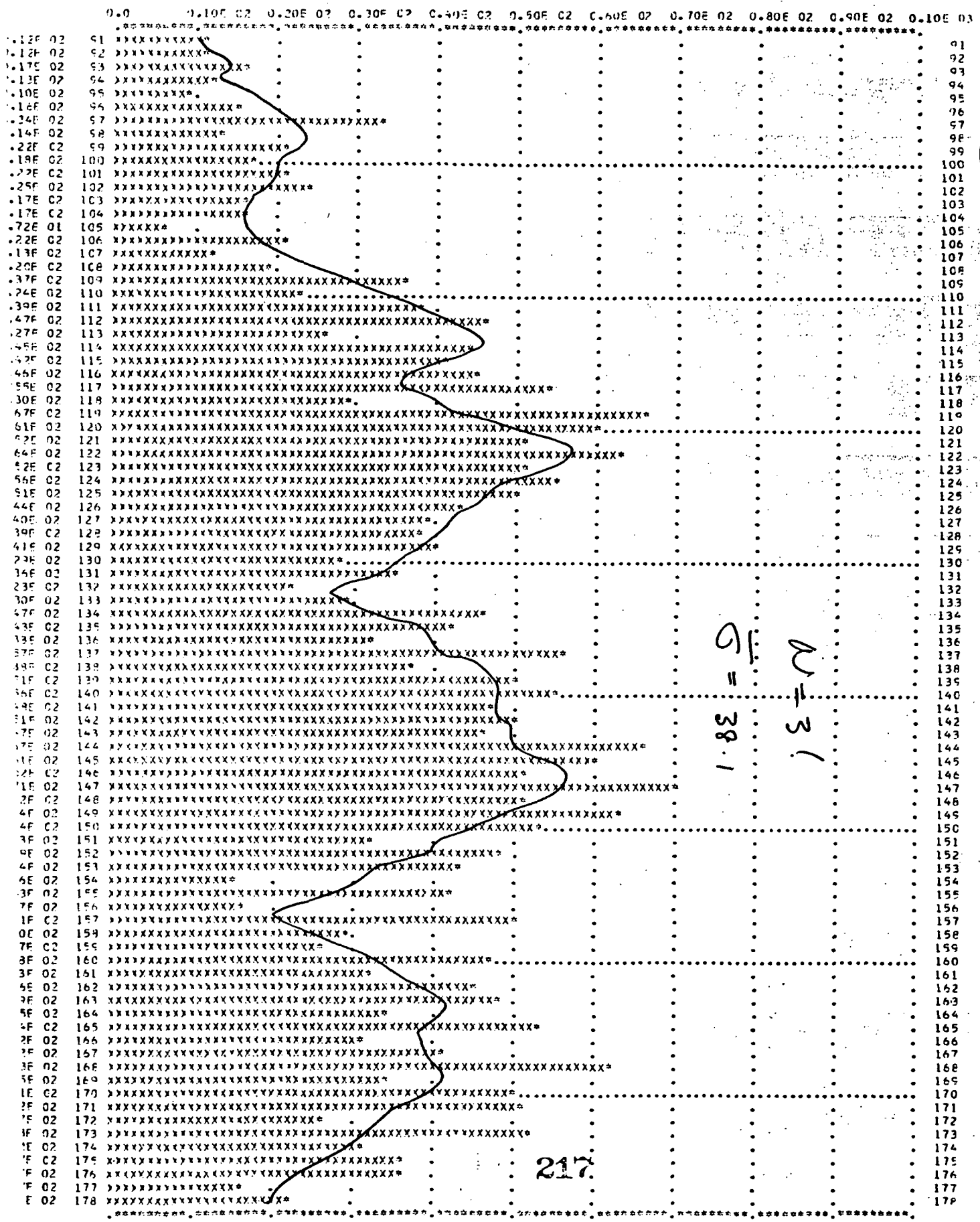

PLOT OF STANDARD DEVIATION A2-100

SAMP SPECTRUM GROUP (17 14 10300) TO 17 14 13600) CALLED -- MX109-3 RE I WED 03/17/71 (17:32)
NUMBER OF SPECTRA IN GROUP: 11
WAVELENGTHS RANGE FROM 6.9 TO 13.4 MICRONS

XMIN IS 0.79E 03 XMAX IS 0.11E 04 DELTA IS 0.34E 01

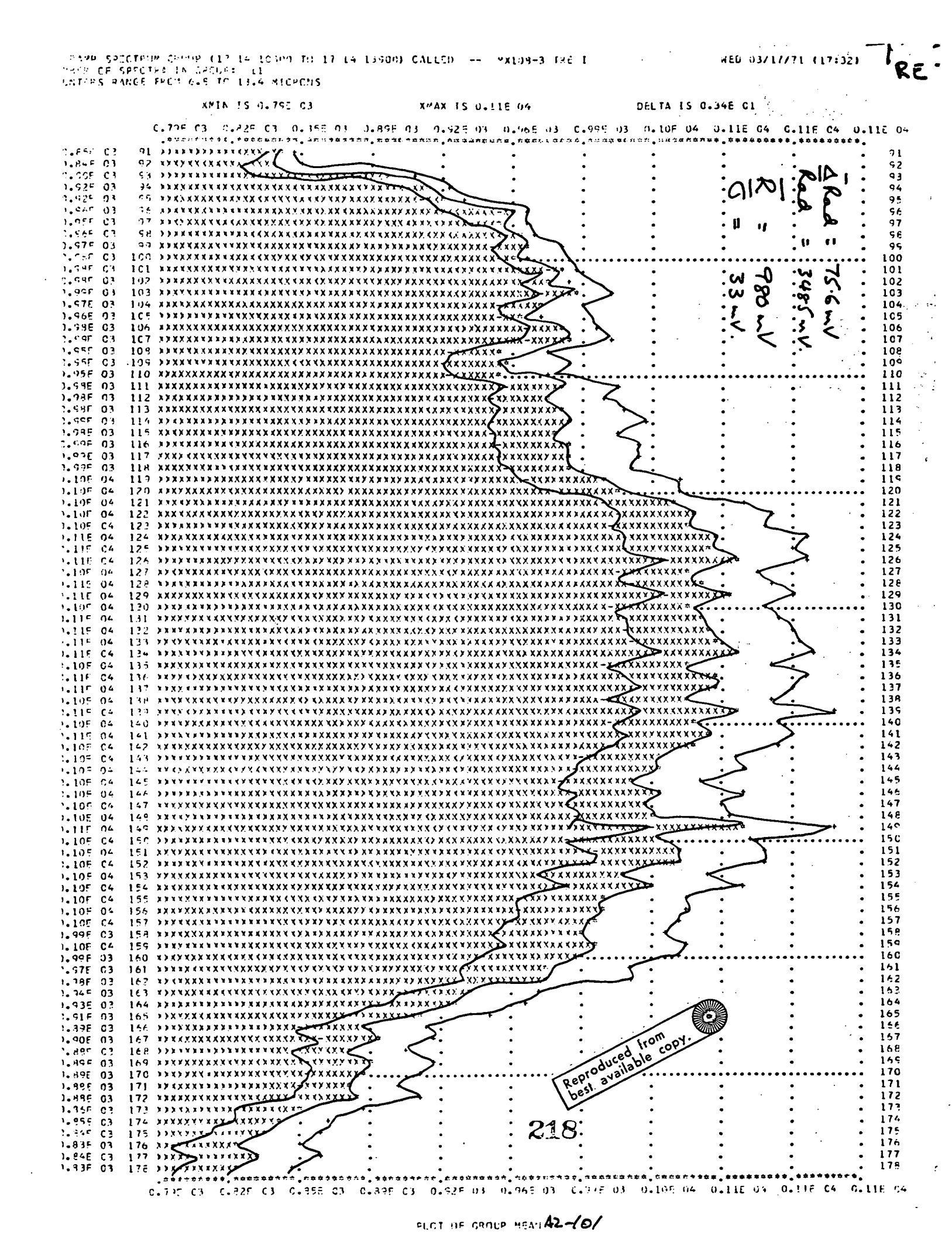

Reproduced from best available copy.

PLOT OF GROUP MEAN 42-101

AMP SPECTRUM GROUP (17 14 10300) TO 17 14 13900) CALLED -- MX108-3 TRE I WED 03/17/71 (17:32)

ER OF SPECTRA IN GROUP: 11

TERS RANGE FROM 9.9 TO 13.4 MICRONS

XMIN IS 0.0 XMAX IS 0.10E 03 DELTA IS 0.10E 01

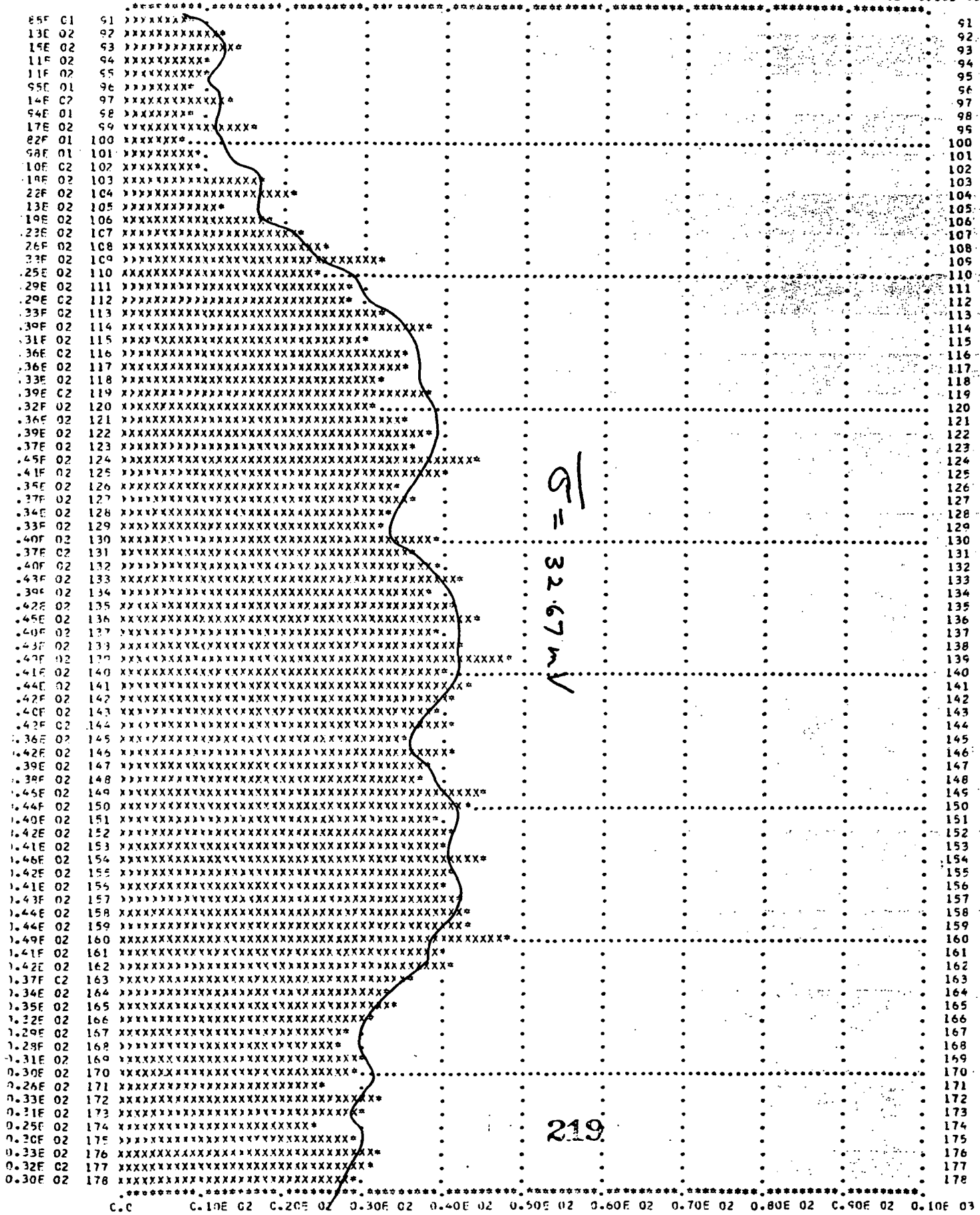

PLOT OF STANDARD DEVIATION

A2-102

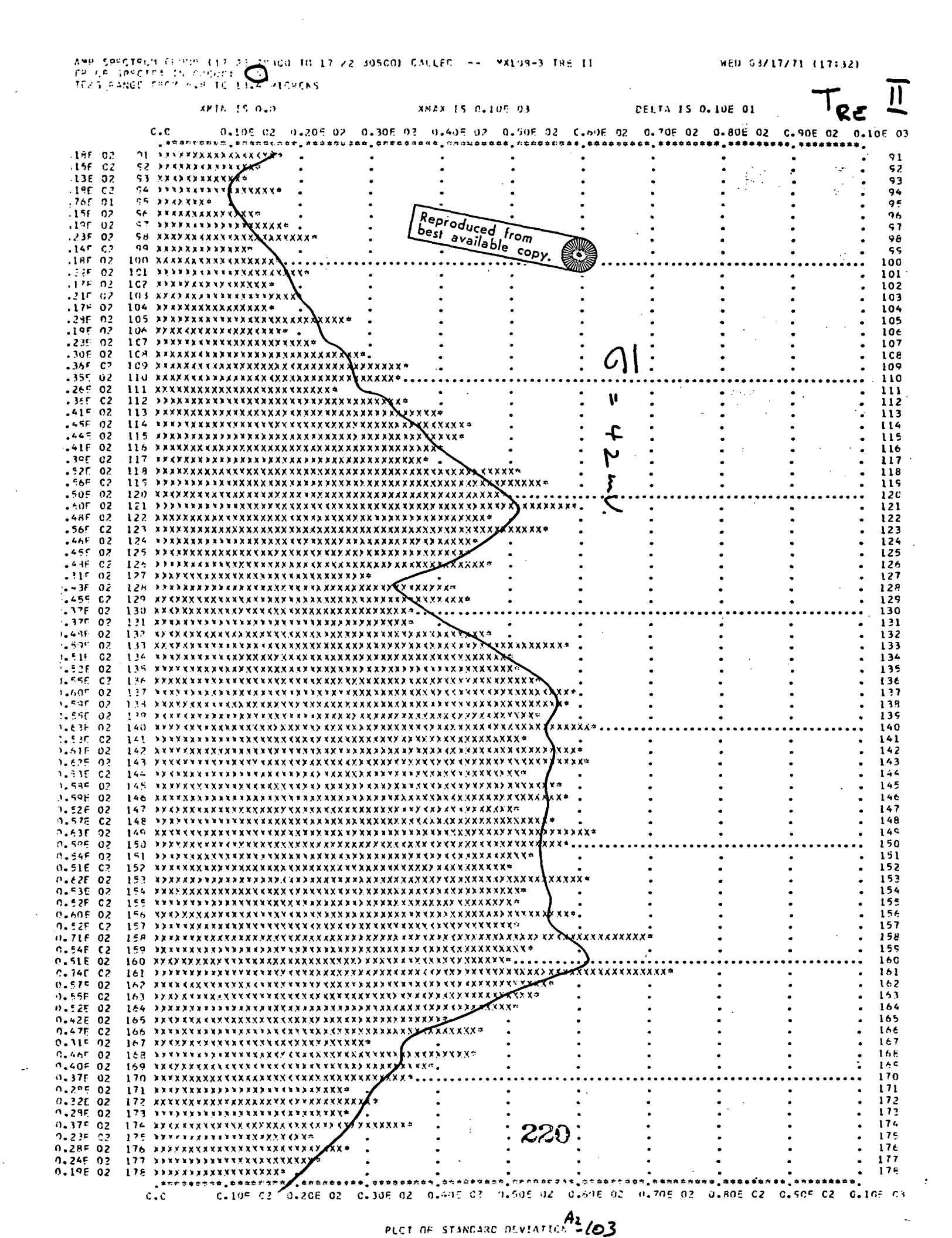

PLOT OF STANDARD DEVIATION A2-103

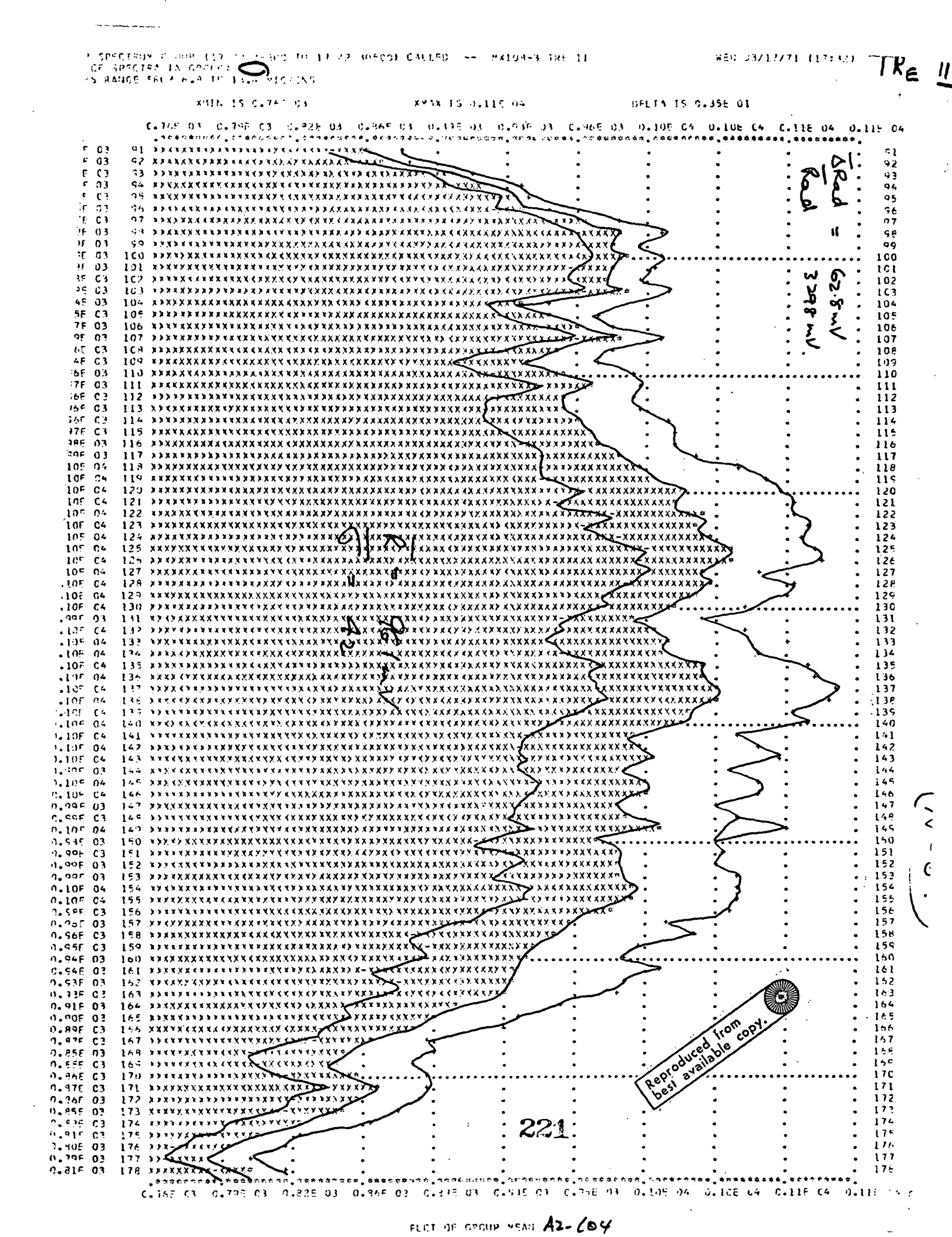

PLOT OF GROUP MEAN A2-C04

Appendix B1:

Abstract of a

Paper presented at the

Seventh Symposium on Remote Sensing of Environment

by

R. J. P. Lyon, Dept. of Mineral Engineering
Stanford University, Stanford, Calif. 94035

Comparison of Airborne Infrared Spectral Emittance and Radar Scatterometer Data from Pisgah Crater Lava Flows

The olivine basalt lava fields of Pisgah Crater, 35 miles ESE of Barstow, Calif., are one of the very few areas which have been studied by more than one sensor. In fact, a big problem in evaluating various remote sensing systems is that so rarely have they been viewing the same targets, let alone from the same attitude and look angles.

In NASA/MSC Mission 108 the infrared spectrometer/radiometer instrumentation was flown twice down the same three-mile long flight line, as was used for the 2 cm-band radar scatterometer in Mission 21, and reported upon at the Fifth Symposium on Remote Sensing of Environment. These two, non-imaging systems measure different parameters - spectral emittance for the infrared, and goniometric radar backscatter for the scatterometer. In addition, cross-track width of the "ground patch" (or footprint) of the IR units is 7 milliradians and the radar is 44 milliradians. Despite these obvious differences, data from both units can be used to arrive at similar classifications for the geological materials at this site - lava flows of three types, lava cinders of Pisgah Crater, dry sediments of Lavic Lake, and several types of Older and Younger alluviums in the desert outwash fans surrounding the crater and flows.

Appendix B 2

Operational Calibration of an Airborne Infrared Spectrometer Over Geologically Significant Terrains

R. J. P. LYON AND A. A. MARSHALL

(RSL 71-1)

Abstract—A three-instrument infrared spectral emittance experiment, comprising a rapid-scan spectrometer (6.7–13.3 μm), radiometer (10.375–12.1 μm), and boresight camera, has been flight tested over selected geological terrain in central and southern California and Nevada. Pre- and post-flight calibrations of the infrared spectrometer were performed both by using polished samples of "standard" rocks (quartz diorite and gabbro) as well as the more familiar blackbody radiance standards. From these latter spectra the instrument transfer function ($A\tau_\lambda$) was derived. In-flight calibrations of wavelength were achieved by the rapid insertion and removal of a polystyrene film in the optical train of the spectrometer, as polystyrene is a material whose transmission spectrum is constant and well known. By flying over a body of water ($\epsilon_{6.7-13.3\mu m} = 0.98$) and recording the radiance spectrum of that target one can determine the transmission spectrum of the atmospheric path between the aircraft and the water (at least to a first approximation) as both the spectral emittance of lake water and the optical transfer functions of the instrument are known or can be calculated. So far, flights have been made only at low altitudes (2000 ft above the lake), with the lake surface at 2000 ft (near Pisgah Crater, S. Calif.) or 6000 ft (Mono Lake, E. Calif.) above sea level. The lake should be in the area to be studied geologically. If the flight altitudes over the study areas are consistent with those over the lake, then the effect of the airpath can be evaluated relative to the spectral information from the geological targets.

Introduction

TO ACCURATELY deduce the surface temperature of terrain from its infrared brightness temperature, the surface emittance as well as the background radiant emittance must be known. Generally when such measurements are made around 8–14 μm a simplifying assumption is used that $\epsilon_{8-11\mu m} \equiv 1.00$, i.e., the target is a blackbody. Sometimes a *graybody* emittance of 0.9 or similar factor is assumed to ease the conscience of the researcher involved. One method of arriving at the emittance integrated across a given passband is to measure the spectral emittance and then integrate for an averaged value. This experiment describes equipment and analytical techniques by which this may be achieved.

A geologically significant more sophisticated experiment which relies upon the nonblackbody behavior of silicate rock materials typically making up planetary terrain, is to use the *spectral* emittance in this band to derive the chemical composition of the terrain being overflown [1]–[3]. Subsequently, one can integrate the spectral data to obtain a suitable wide-band value. The background information on this method is detailed in several references, and the method has been reduced to practice both in the field and in airborne measurements [3].

In the airborne mode, infrared radiance spectra (with a resolution $\lambda/\Delta\lambda = 100$) were taken six times a second over the bandpass 6.7 to 13.3 μm. With every second spectrum a 35-mm boresight photograph was taken to locate the precise ground-track of the sensor system after the data flight. Table I lists the equipment characteristics.

Also included as the third instrument in the infrared "pallet" was an infrared radiometer, a relatively broadband sensor (10.375 to 12.1 μm), which has its bandpass centered in a region of high atmospheric transmittance. This band exhibits consistently high terrain emittance and does not show the spectral departures from a blackbody on which the geological experiment is based [3]. The radiometer served as a monitor to ensure that there were no marked temperature changes over the target which might be mistaken for spectral emittance changes. Within a given spectrum, temperature changes of less than 1°C were allowed—if higher than that level the spectrum was rejected.

Calibration Concepts

The operational calibration was of three main types, pre-flight, inflight, and post-flight; the pre- and post-flight sets being performed immediately prior to take-off and after landing.[1] The aircraft engines usually were not running and the internal systems were connected to ground power (sometimes the auxiliary power unit (APU) was used). There could be differences between the two ground power sources (and with the aircraft engine sources themselves) but the most significant "noise" problem at this stage is the degree of mechanical vibration generated by the APU, and the engines which induces microphonic signals into the infrared detectors.

The in-flight calibrations are more simple, being restricted to a wavelength check performed by inserting

Manuscript received February 26, 1971; revised March 24, 1971. This work was supported by NASA, under Contract NAS9-7313.

The authors are with the Remote Sensing Laboratory, School of Earth Science, Stanford University, Stanford, Calif. 94305.

[1] Cryogenic hold-times were in excess of eight hours; thus long flights could be made and post-flight calibrations obtained without refilling the cryogenic supplies.

TABLE I
INFRARED PALLET

Airborne Rapid Scan Spectrometer	
Scan wavelength	6.76-13.30 μm with 100 elements per spectrum. The CVF[a] wheel has 2 similar spectral octaves—one from 0° to 180°, and one from 180° to 360°
Scan period	0.150 s (6 spectra/s)
Field of view	0.4 degree square (7 mrad)
Detector	Hg-doped germanium, time constant less than 1 μs, cooled by liquid helium
Essential output signals (four)	a) spectral radiance output (analog) b) wavelength ramp (analog, not presently used) c) wavelength (peripheral-edge coding) pulses, every 2°, or 90 per spectrum, 180 per rotation of the CVF (See Table II) d) a spike pulse, (at 0°) was used to fire the boresight camera (used for location purposes)
Accuracy required	10-bit, i.e., better than 0.1 percent
Infrared Radiometer	
Filter bandpass; sampling frequency	10.375 to 12.1 μm approximately 60 temperature measurements per second, i.e., ten to every spectrum (or 1 every 9 spectral elements)
Field of view	0.4 degree, circular (7 mrad)
Detector	Hg-doped germanium, time constant less than 1 μs, liquid helium cooled
Essential output signals (one)	radiance signal sampled 60 times/s (analog)
Accuracy required	10 bit, i.e., better than 0.1 percent
Boresight Camera	
Type	35-mm framing camera, with film-recorded clock and frame counter, electrically pulsed by output command from spectrometer (at approximate rate 3 s)
Field of view	approximately 5° to yield telescopic view of the target. Camera pulse originates 5 ms before the no. 1 *data* pulse, i.e., just past the 0° position

[a] CVF: circular variable filter, a circular dispersive element.

a polystyrene film into the spectrometer optical train. The known spectral transmission of polystyrene provides a characteristic signal readily observed on the data tapes. It was also used as a signal for "line-start" and "line-stop" in the later data analysis steps. Fig. 1 shows a group ($N=5$) of airborne polystyrene spectra. From this, Table II was verified.

A more fundamental type of in-flight calibration was performed by flying the infrared system over a body of water. Water has a well-known spectral emittance varying only slightly from a graybody value of 0.98 [6] over this bandpass. Thus a radiometric check between spectrometer and radiometer may be made in the data analysis steps and brightness temperatures compared. As will be seen later, the AIRPATH spectral transmittance between the water and the aircraft may be defined by this aspect of the flight program.

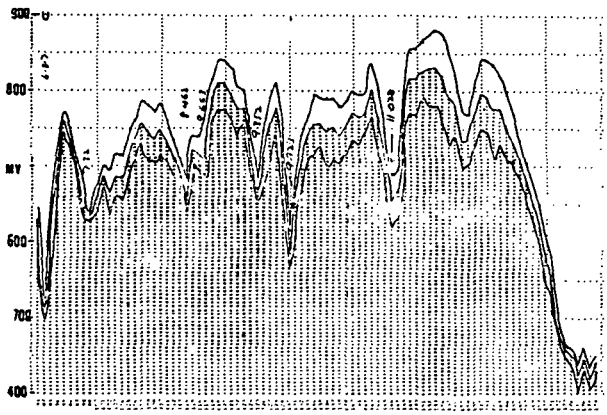

Fig. 1. Average and $\pm\sigma$ of $N=5$ polystyrene transmission spectra airborne over Pisgah target. $N=5$. Times from 17:13:14.442-17:13:16.000 GMT (local time PST=GMT−8 h). Handwritten figures refer to the precisely known absorption lines for polystyrene.

TABLE II
COUNTER POINT (CP) VERSUS WAVELENGTH[a]

CP	λ (μm)	CP	λ (μm)	CP	λ (μm)
91	6.760	121	8.965	151	11.380
92	6.825	122	9.045	152	11.445
93	6.890	123	9.135	153	11.525
94	6.960	124	9.205	154	11.600
95	7.035	125	9.270	155	11.680
96	7.085	126	9.370	156	11.750
97	7.160	127	9.455	157	11.835
98	7.225	128	9.530	158	11.895
99	7.290	129	9.615	159	11.970
100	7.365	130	9.690	160	12.040
101	7.445	131	9.775	161	12.120
102	7.510	132	9.865	162	12.190
103	7.585	133	9.960	163	12.260
104	7.660	134	10.010	164	12.330
105	7.750	135	10.100	165	12.405
106	7.810	136	10.170	166	12.470
107	7.880	137	10.255	167	12.540
108	7.955	138	10.340	168	12.605
109	8.025	139	10.420	169	12.670
110	8.105	140	10.490	170	12.745
111	8.185	141	10.580	171	12.815
112	8.265	142	10.660	172	12.895
113	8.325	143	10.740	173	12.955
114	8.410	144	10.810	174	13.020
115	8.485	145	10.900	175	13.085
116	8.565	146	10.970	176	13.150
117	8.640	147	11.070	177	13.220
118	8.720	148	11.150	178	13.285
119	8.800	149	11.220		
120	8.885	150	11.305		

[a] Original data sheet for points 0–90 and 91–180 for the 1968–1970 ARSS CVF wheel, provided by NASA/MSC by letter TF2/LE 120-68, March 25, 1968. To make the data covered by both halves of the wheel more equal 1 CP is dropped from the leading data set for each side. Thus MSC CP 92 becomes Stanford CP 91, 179 becomes 178, etc. Operational verification of these values may be made by the spectrum of polystyrene in Fig. 1.

PRE- AND POST-FLIGHT CALIBRATIONS

In addition to the above, there were normal engineering-type calibrations of tape recorder channels, etc., of the type usually performed in all high quality data gathering operations [4]. The calibrations described here refer to *geological and meteorological calibrations* which are designed to recover *known* spectral charac-

teristics from the data tapes as an overall check of the system. In detail these are the following.

1) Observation of an external blackbody source lying on the runway beneath the stationary aircraft. This blackbody was temperature controlled at 40°C (313°K), and is called 40°C BB-EXT.[2]

2) Sequential observation of a pair of "standardized" rock specimens (rock A, and rock B), lying on the runway beneath the stationary aircraft. Those were heated in an oven to approximately 40°C (313°K). The specimens were 20 by 20 cm across and 2.5 cm thick, thus having considerable thermal inertia.[3] Rock A was a dark gray to medium gray gabbro, and rock B was a light silver-gray granodiorite, two chemically, and mineralogically, distinct igneous rocks. The front surfaces of these "standards" were highly polished to decrease scattering effects from their front surface making it a more precise spectral emissivity standard.

In order to obtain high contrast in the spectral signature data, i.e., a large signal differential for small spectral emissivity variations, the background radiation *reflected* by the sample into the instrument must be small compared to the emitted radiation. This criterion was achieved by positioning the highly polished sample sufficiently below the aircraft and angled appropriately to ensure that "cold" sky was the effective background.[4] Since all pre- and post-flight calibration measurements were performed under moderately low humidity and cloudless conditions, the sky radiation (between 8 μm and 13.5 μm) was infinitesimal compared to that of the 40°C rock specimen and was neglected from further consideration. Identical procedures were followed during pre- and post-flight calibrations.

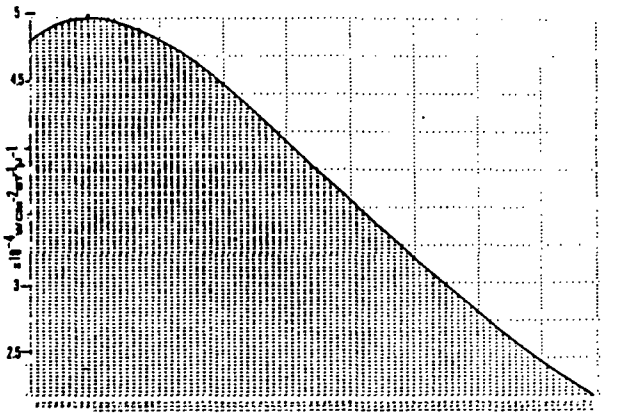

Fig. 2. *Calculated* radiance difference ($W \cdot cm^{-2}\ sr^{-1}\ \mu m^{-1}$) for a blackbody exterior target at 40°C (313°K) and an internal blackbody reference at 60°C (333°K). Wavelength counter points appear as the abscissa, from 91 to 178 (from 6.8 to 13.3 μm), and are common to all graphs.

Transfer Function ($A\tau_\lambda$) Calculation

The optical spectral transfer function (τ_λ) for the spectrometer may be derived jointly with the system gain A as a product form, which we simply call the spectral "transfer function" ($A\tau_\lambda$). The data processing steps outlined in what follows agree closely with those published for the Purdue (LARS) procedures originally performed for field calibration of Block-Michelson interferometer spectra [5].

Calculate for each wavelength step the radiance spectrum (Planck Law) for the 60°C internal blackbody reference (BB-INT). Calculate the radiance spectrum for the temperature controlled external blackbody (BB-EXT). Derive the radiance difference spectrum (TRUE).

Fig. 2 shows this calculated difference

$$N\lambda_{\text{TRUE}} = N\lambda_{\text{BB-INT}} - N\lambda_{\text{BB-EXT}} \qquad (1)$$

where $N\lambda$ = radiance at wavelength λ (μm).

This difference $N\lambda_{\text{TRUE}}$ can be related to the actual signal observed from the spectrometer (proportional to the difference between the two blackbodies, but modified by the spectral transfer function). Figs. 3 and 4 show the actual signal (OBSERVED) from an external blackbody at 40°C (313°K); an average of 22 spectra with $\pm 1\sigma$ limits indicated. The standard deviation levels are a measure of the "noise" riding on the signal. From these data (Figs. 3 and 4) the spectral transfer function ($A\tau_\lambda$) was calculated (Fig. 5)

$$\text{SPECTRAN}\,(A\tau_\lambda) = \frac{\text{OBSERVED}}{\text{TRUE}}. \qquad (2)$$

[2] Extended Source Blackbody, Barnes Engineering, Inc., temperature controlled to ± 0.5°C.

[3] The rocks were selected by a geologist from tombstone material (because of the overall high polish readily available across large slab areas). Thin sections were made and the correct rock type defined by optical means. The slabs were cut into two, and one half of each retained by Stanford University Infrared Lab. to calibrate our other spectrometer and data recording systems. Rock A: Gabbro, contains plagioclase (An_{60}), augite, and little biotite. Rock B: Granodiorite, contains biotite, quartz, epidote, and plagioclase, with orthoclase.

[4] The spectrometer measures $W_{\lambda(\text{eff})}$. Assume a target which entirely fills the instrument field of view.

$$W_{\lambda(\text{eff})} = W_{\lambda a}(1 - \tau_{\lambda a}) + \tau_{\lambda a}[\Sigma_\Omega W_\Omega + H_{\lambda B}(1 - \Sigma_\Omega)]$$

where

- $W_{\lambda(\text{eff})}$ effective radiant emittance seen by the radiometer at wavelength λ;
- $W_{\lambda a}$ radiant emittance of the air at wavelength λ;
- $\tau_{\lambda a}$ atmospheric transmission at λ;
- Σ_Ω target emissivity at λ;
- W_Ω radiant emittance of the target at λ;
- $H_{\lambda B}$ irradiance from the background (sky, terrain, room walls, or ceiling, etc.) incident on the target at wavelength λ.

Note the following:

1) $W_{\lambda a}$, $\tau_{\lambda a}$, Σ_Ω, W_Ω, and $H_{\lambda B}$ are integrated over the spectral bandpass of the instrument. The difference between the integrated values and monochromatic values at wavelength λ depends on the spectral bandwidths of the atmospheric absorption/emission bands, the bandwidth of the spectral features on the target, and similar considerations for the background relative to the instantaneous spectral bandwidth of the instrument. In the 7-14-μm region these differences are generally small for $\Delta\lambda/\lambda < 0.02$.

2) $H_{\lambda B}$ depends upon $\tau_{\lambda a}$, $W_{\lambda a}$, sky conditions, terrain temperature, the target angular aspect, and instrument view angle relative to the zenith. If $W_\lambda = H_{\lambda B}$ no spectral signature of the target is discernible. $H_{\lambda B}$ can be better controlled or minimized with a polished (specular) sample.

3) $\tau_{\lambda a}$ has practical limits between zero and one and has both fine and coarse spectral features.

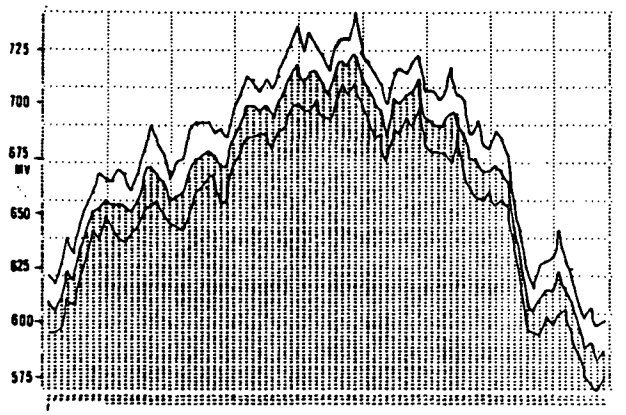

Fig. 3. *Observed* radiance difference (millivolts) for the same 40°C target and 60°C reference. $N=22$ spectra for the average calculation, $\pm 1\sigma$ limits shown, $\bar{X}=668$ mV. Noise (mean sigma, $\bar{\sigma}$) $=13.5$ mV. *Pre-flight* data, mission 108, day 1, times from 15:17:53.647–15:18:00.759 GMT.

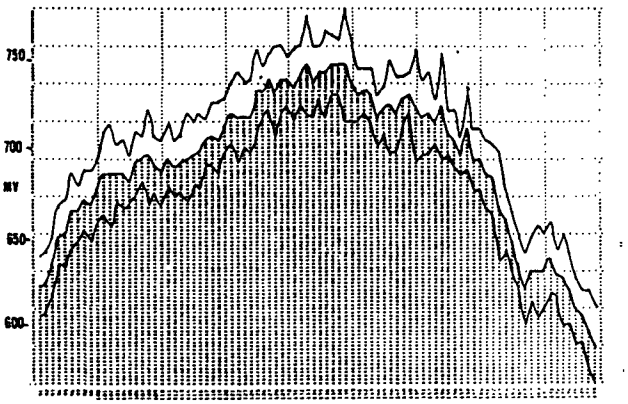

Fig. 4. Comparable *post*-flight data after return. $N=25$, $\bar{\sigma}=19.1$ mV, $\bar{X}=692$ mV (i.e., temperatures were *not* exactly at 40°C). Times from 21:21:23.167–21:21:30.766 GMT.

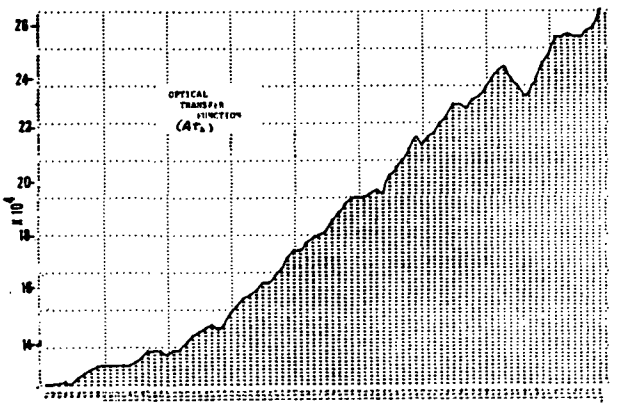

Fig. 5. Optical transfer function ($A\tau_\lambda$), from pre-flight 40°C BB-EXT data. Ratio calculated from Figs. 2 and 3.

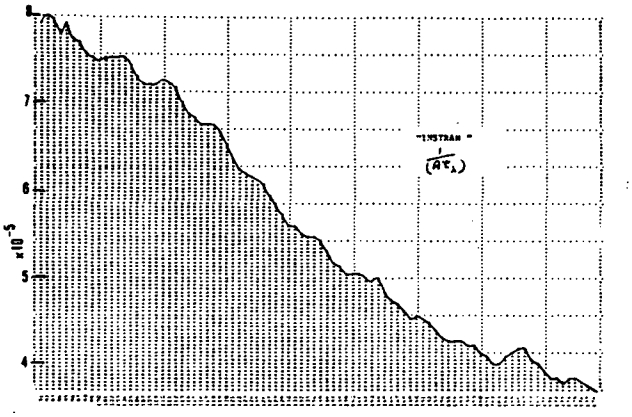

Fig. 6. INSTRAN, or inverse of optical transfer function $(=1/A\tau_\lambda)$.

The inverse of the transfer function $1/A\tau_\lambda$ or INSTRAN was more useful in the calculations and this function was stored for data processing (Fig. 6). The principal straight-line component of the gradient is related to the wavelength sensitivity of the Ge:Hg detector, the system gain (A), and the optical transmittance (τ_λ). Higher frequencies in the function are caused by the variations in τ_λ exhibited by the CVF. Additional small effects of microphonic noise and interference may account for some of the observed high frequency variations.

AIRPATH Calculation

When airborne spectra are collected while flying over a water body (Figs. 7 and 8) a mean spectrum can be calculated which closely resembles the blackbody difference spectrum, OBSERVED (Fig. 3). Absolute levels (in volts) are higher, as most water bodies are cooler than the 40°C external blackbody used in the pre-flight ground calibrations. Standard deviation levels of 17–20 mV rms (Table III) again represent noise levels but are *not* significantly higher than on the ground, a marked change from earlier flights with this system which showed large microphonic noise. (Missions 56, 78, flown in 1967 and 1968.)[5]

The atmospheric transmittance was determined over the two lakes observed in this flight (Palmdale Lake, 96 mi west, and Shallow Lake, 25 mi north of the Pisgah lava field test site, which is at latitude 34.7°N, longitude 116.4°W). They are a considerable distance apart, and somewhat distant from the test site, but it is difficult to find water bodies in the southern Californian deserts! One is forced, therefore, to rely upon the assumption that the airmass over the test site is the same as that over the lakes. In most areas where water bodies are more common and hence closer to the site this is a quite reasonable assumption. Here one may argue otherwise, but no simple operational alternative exists.

AIRPATH is calculated from the airborne data over the lake by the following steps.

1) Calculate the mean and $\pm 1\sigma$ spectra for the (LAKE) airborne data. Calculate lake brightness tem-

[5] Operational rms voltage measurements ("noise") were made on the IR spectrometer output (with the CVF wheel stopped), as follows. MX 108, flight 1. Pre-flight—on ground 20 mV. 1915 GMT—over water 25 mV. MX 108, flight 3. Over Mono Lake, 1641 GMT 24 mV. Over Mono Lake, 1940 GMT 24 mV.

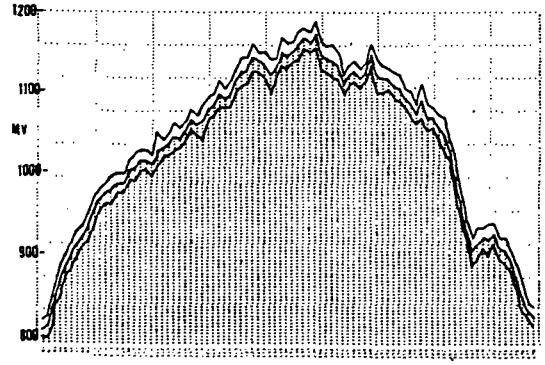

Fig. 7. Observed radiance spectrum from Palmdale Lake, $N=30$, $\sigma=14.7$ mV, $\bar{X}=1010$ mV. Brightness temperature of the lake is expressed as $T_L=30°C$, calculated from $\bar{X}$. Mean spectrum radiance, $\pm 1\sigma$ limits shown. Times from 17:12:38.495–17:12:52.400 GMT, mission 108, flight 1. Dewpoint −6°C; air temperature 23°C; RH 14 percent; radiometer $T_L(R)=30.5°C$.

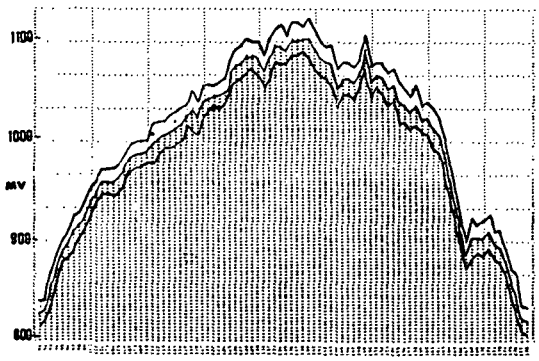

Fig. 8. Observed radiance spectrum from Shallow Lake, $N=26$, $\sigma=17.7$ mV, $\bar{X}=1000$ mV. Brightness temperature of lake $T_L=30°C$. Times from 19:16:20.898–19:16:28.470 GMT, mission 108, flight 1. Dewpoint −6°C; air temperature 27°C; RH 10 percent; radiometer $T_L(R)=33°C$.

TABLE III
TABULATED REDUCED DATA

GMT Time		N	Signal Mean (mV)	Std. Deviation[a] (mV)	Rel. Error[b]	Temperature by Spectrometer
Stanford/MSC Mission-108, Flight 1 (Pisgah, Site 2), Oct. 8, 1969						
	Pre-Flight					
1518	40°C BB-EXT	22	669	13	0.0043	40°C[c]
1516	rock A	30	569	15	0.0048	43
1517	rock B	30	595	15(20)[f]	0.0046	42
	In-Flight					
1712	Palmdale lake	30	1010	15	0.0027	30°C
1915	Shallow lake	30	1000	18(25)[f]	0.0033	30
	Post-Flight					
2121	40°C BB-EXT	25	693	19	0.0055	39°C
2120	rock A	36	512	22	0.0072	45
2120	rock B	28	568	24	0.0080	43
Stanford/MSC Mission-108, Flight 3 (Mono, Site 3), Oct 10, 1969						
GMT Time		N	Signal Mean (mV)	Std. Deviation (mV)	Rel. Error	Temperature by Spectrometer
	Pre-flight					
1423	40°C BB-EXT	30	664	16	0.0042	40°C[c]
1422	rock A	30	569	15	0.0048	43
1424	rock B	30	593	15	0.0046	42
	In-Flight					
1642	Mono Lake run 401	30	987	19(24)[f]	0.0034	30°C[d]
1943	Mono Lake run 402	30	1080	17(24)[f]	0.0029	27[e]

[a] Standard Deviation (σ) is defined as

$$\sigma = \sqrt{\frac{(X-\bar{X})^2}{N-1}}.$$

[b] Relative error is defined as

$$E = \frac{\sigma}{\bar{X}\cdot\sqrt{N}}.$$

[c] By definition, and used as a calibration point for temperature.
[d] West side.
[e] East side.
[f] Actual measured rms values in parentheses. See footnote 5.

perature (T_L), using the radiometer data, i.e., with broader bandpass. This unit was also recalibrated during the pre-flight period [4].

2) Correct the mean lake spectrum for the known spectral emittance for water (ϵ_λ) [6].

3) Divide the correct (observed) lake spectrum by the product of a calculated blackbody radiance spectrum for that temperature (T_L) and SPECTRAN ($A\tau_\lambda$). This modifies the blackbody radiance as though it had been observed through the instrument. If the lake had been at 40°C one could use the observed spectrum from the external 40°C blackbody. Generally, however, the lake temperatures are much lower (27–30°C), and hence their radiance must be calculated.

$$\text{AIRPATH} = \frac{\text{expected radiance}}{\text{actual radiance}} = \frac{\text{LAKE calculated}}{\text{LAKE observed}}$$

then

$$\text{AIRPATH} = \frac{(N_{BB\lambda}, \text{ at } T°_L) \times A\tau_\lambda \times \epsilon_\lambda}{\text{LAKE}_\lambda}. \quad (3)$$

AIRPATH is an absorbance-like ratio which ranges from 0.84 to 0.96 with 10 to 12 sharp maxima. These are

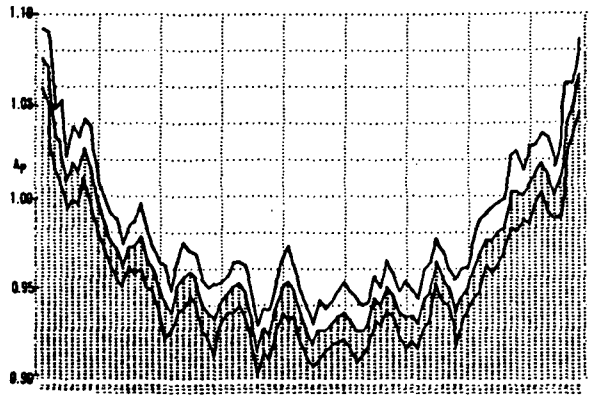

Fig. 9. AIRPATH, or atmospheric absorption ratio spectrum, from Palmdale Lake spectra, after removal of the optical transfer function. Mean airpath $(\overline{Ap}) = 0.96$, $\bar{\sigma}_{Ap} = 0.014$

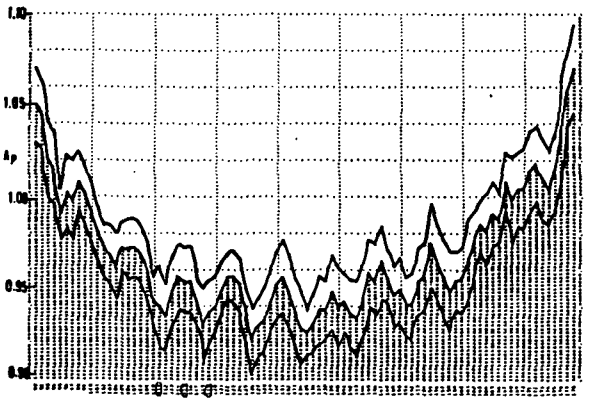

Fig. 10. AIRPATH, from Shallow Lake. Mean airpath $(\overline{Ap}) = 0.96$, $\bar{\sigma}_{Ap} = 0.017$.

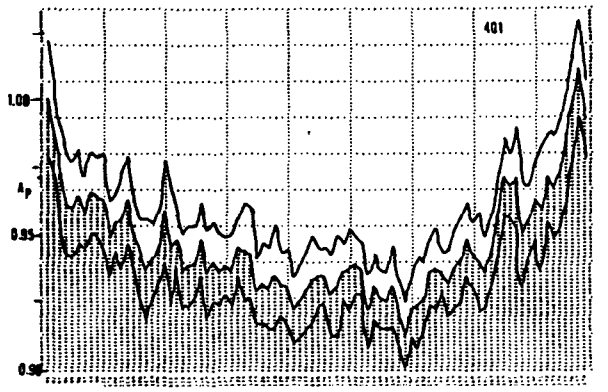

Fig. 11. AIRPATH, from Mono Lake 401 (site 3), flight 3, mean airpath $(\overline{Ap}) = 0.962$, $\bar{\sigma}_{Ap} = 0.018$, $N = 30$, $T_L = 30°C$, times from 16:42:08.098-16:42:22.972 GMT. Dewpoint −15°C; air temperature +11°C; RH 15 percent.

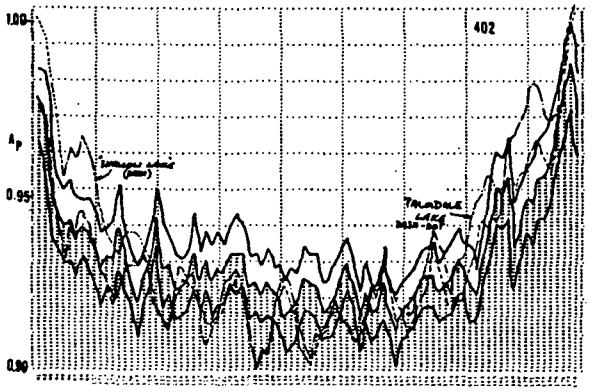

Fig. 12. AIRPATH, from Mono Lake 402 (site 3), flight 3, mean airpath $(\overline{Ap}) = 0.950$, $\bar{\sigma}_{Ap} = 0.015$, $N = 30$, $T_L = 27°C$, times from 19:43:55.112-19:44:14.813 GMT, first 30 spectra used. Dewpoint −19°C; air temperature 10°C; RH 12 percent.

generally in the positions of the atmospheric absorption/emission bands, but may be more exactly caused by the high frequency components in the pre-flight calibration spectra which were ratioed to the lake spectra (Figs. 9–12). As might be expected, for a 2000-ft path in a low[6] humidity (desert) area, these absorptions are not strong between 7.5 and 13 μm. It is significant that both lakes surveyed this day showed very similar patterns with maxima at the same data points. On a subsequent flight (day 3) over Mono Lake several hundred miles to the north, both patterns for AIRPATH were again similar (Figs. 11 and 12), but differences exist between the flight 1 and flight 3 pairs.

Rock Standards—Operational Format

The pre-flight spectra from the two polished rock standards are shown in Figs. 13 and 14 with the mean and 1σ limits plotted. Immediate inspection reveals that they have different shapes as expected; rock A having two maxima at longer wavelengths than the more pronounced single peak for rock B.

At first glance the curves appear to be the inverse of what one would expect from emittance data. A moment's reflection, however, will show that if ϵ_λ is lower at a given point it will appear to have a lower (*colder*) brightness temperature. As we are using a hot internal reference blackbody (60°C) these regions will show a greater radiance difference, and hence a higher millivolt level, for low ϵ_λ regions. In effect, the raw plots are reflectance not emittance spectra.

For rapid checking of the data either this form of presentation or its exact inverse (FLIPPED) will suffice. For most operational use we do not go through the calculations for absolute emittance detailed below, but merely "flip" the data sets. All airborne spectra of the terrain are presented in this inverted form for subsequent statistical processing [7].

Rock Standards—Absolute Emittance

The absolute emittance from rocks A and B may be calculated by the following steps.

1) Prepare a mean and $\pm 1\sigma$ average rock A spectrum from the pre- and/or post-flight data (usually $N = 30$). Determine the average brightness temperature from these spectral levels, e.g., $\overline{X} = 593$ mV. Therefore, target brightness temperature was $T_A = 42°C$.

2) Using the spectral transfer function $(A\tau_\lambda)$, transform the mean spectrum, wavelength interval by wave-

[6] Dewpoint −6°C, aircraft air temperature +23°C.

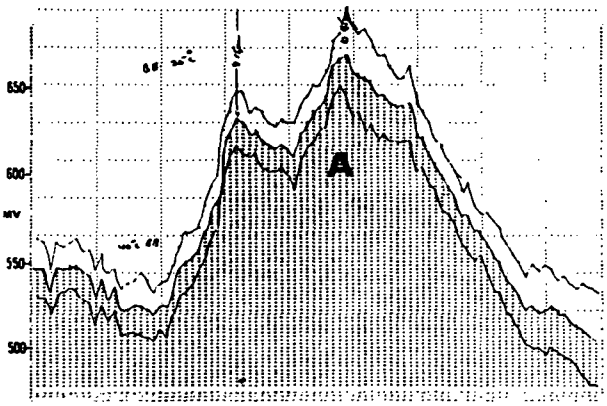

Fig. 13. Rock A mean spectrum for the gabbro slab at $T=43°C$, $N=56$, from raw (i.e., unsmoothed) *pre-flight* data, flight 1. Times are from 15:16:42.190–15:17:00.963 GMT. Peaks are seen at 122 (626 mV) and 139 (660 mV) data points. Radiance levels at data point 108 would approximate that from a 40°C blackbody target, at 139 would be that of a 25°C blackbody. This is indicative of the changing spectral emittance.

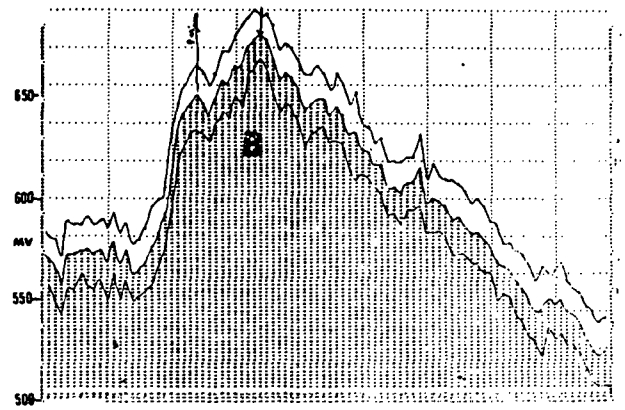

Fig. 14. Rock B mean spectrum for the granodiorite slab at $T=42°C$, $N=43$, from raw *pre-flight* data, flight 1. Times are from 15:17:10.651–15:17:23.674 GMT. Peaks are now at 114 (643 mV) and 124 (673 mV), much shorter wavelengths than for rock A.

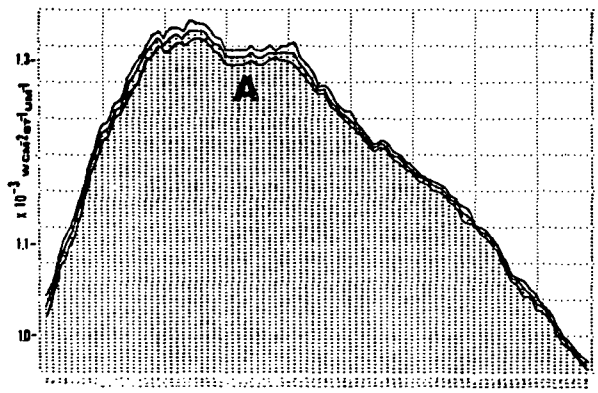

Fig. 15. Radiance mean spectrum ($\pm 1\sigma$) for rock A, pre-flight data, flight 1, for the above times (Fig. 13). Ordinate is now in $W \cdot cm^{-2}\ sr^{-1}\ \mu m^{-1}$, after conversion from millivolts using optical transfer function ($\pm 1\sigma_A$). $T_A=43°C$, spectrometer.

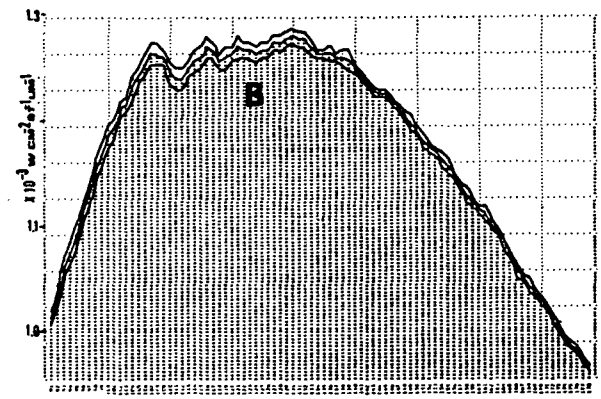

Fig. 16. Radiance mean spectrum ($\pm 1\sigma$) for rock B, pre-flight data, flight 1, for the above times (Fig. 14). Ordinate is now in $W \cdot cm^{-2}\ sr^{-1}\ \mu m^{-1}$. $T_B=42°C$, spectrometer.

length interval, into a radiance spectrum, i.e., transform millivolts to $W \cdot cm^{-2}\ sr^{-1}\ \mu m^{-1}$. In a similar manner one can transform the standard deviation spectra as well. This is plotted in Figs. 15 and 16 for rock A and B as *radiance* spectra.

3) Using the observed target brightness temperature (as above, of 42°C) calculate from the Planck Law, again one wavelength interval at a time, the expected radiance for the target, assuming now that it is a blackbody.

4) Divide the "observed" radiance spectrum by the calculated blackbody radiance spectrum to generate an emittance spectrum, Figs. 17 and 18. By the initial assumption of $\overline{X} \propto$ average brightness temperature this yields emittance values above 1.0. These then can be normalized to unity and the average "absolute" emittance recalculated.

Two items should be noted here. Inspection of Figs. 15 and 16 reveals the very small departures from blackbody behavior on which this geological experiment is based. Figs. 17 and 18 are therefore magnifications of the ϵ_λ ratios, and in this light the $\pm 1\sigma$ variations in the airborne data are strikingly small. As geologists rather than physicists we are not as concerned with the absolute levels in our data as with the homogeneity of the spectral data and its variability from one rock type to another. The strictly geological problems with this experiment are many and real, and added refinements in computational technique are premature at this stage.

Conclusions

1) Optical transfer functions for a spectrometer have been calculated from operational field-type measurements.

2) Standardized rock slabs with known spectral emittance below 1.0 have been used in the pre- and post-flight calibrational steps in a routine manner. From these data one may ascertain if the spectrometer and data system are functioning correctly, i.e., that a known spectrum can be recovered from the taped data record.

3) In-flight calibrations of wavelength can be readily obtained by inserting polystyrene into the optical train.

4) Atmospheric "absorption spectra" can be obtained in the airborne mode by flying over lakes within

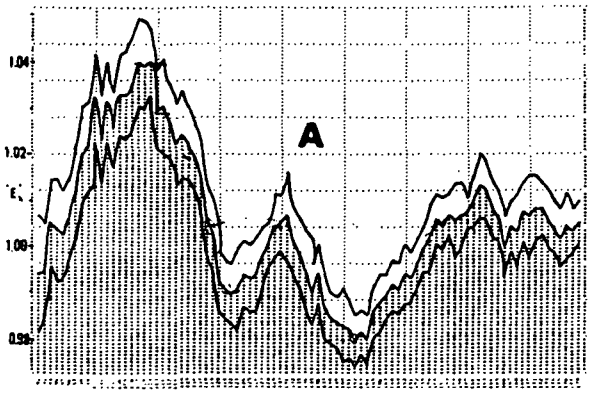

Fig. 17. Calculated "emittance" ratio for rock A target relative to a blackbody at the same *average* brightness temperature. Mean and $\pm 1\sigma$ limits shown. Average emittance = 1.00 by assumption, $\epsilon_{max} = 1.04$ (108), $\epsilon_{min} = 0.98$ (144). When normalized so that the $\epsilon_{max} = 1.00$, then $\epsilon_{min} = 0.94$.

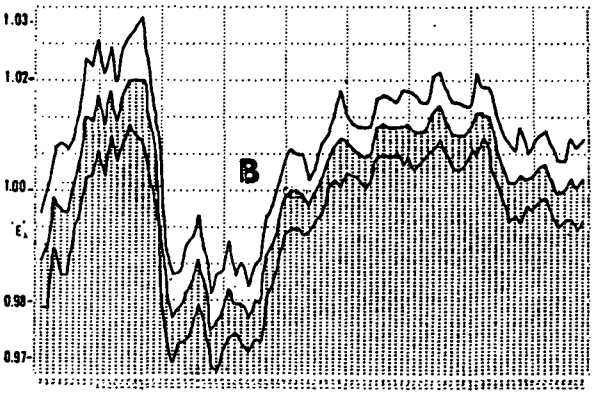

Fig. 18. Calculated "emittance" ratio for rock B. Mean and $\pm 1\sigma$ limits shown. Average emittance = 1.00 by assumption, $\epsilon_{max} = 1.02$ (106), $\epsilon_{min} = 0.97$ (118). When normalized so that $\epsilon_{max} = 1.00$, then $\epsilon_{min} = 0.95$.

or nearby the geological test site. These spectra have many of the characteristics of true atmospheric spectra of a short airpath (around 2000 ft) in a low humidity area. Additional work is necessary to confirm this interpretation or to support the possibility that they are artifacts of the ratioing of airborne data (which appear somewhat smoothed) to those of ground-based data which are more spiked.

5) In-flight spectral data over geological targets are being analyzed, and will be reported elsewhere [7]. Considerable careful study needs to be made, both of the airborne data as well as spectral emittance variabilities within a single rock type in the field. This should be tackled by ground-based mobile instrumentation as well as airborne to define the inhomogeneity of the basic target and separate this effect from artifacts of airborne measurements. Only then can we assess the "noise" uncertainties we presently perceive.

Acknowledgment

Without the careful attention to the many details of calibration, before and after the flights and during the airborne data-gathering, shown by the flight crews of NASA 927 P3A aircraft and especially during mission 108, these data could not have been given meaningful analysis. We would like to specifically mention O. Smistad, Manager, and J. Mitchell, Mission Manager, respectively, Aircraft Project Office, MSC. The infrared pallet operator H. Coppedge was most closely concerned with the calibration and data collection and his consistent attention to the experiment, specifically in the pre- and post-flight periods, is gratefully acknowledged. The contributions of J. Cobb, pilot of the P3A aircraft, and of T. Barnett, MSC Cognizant Scientist for this experiment, are greatly appreciated. A. Marshall developed the computer programs for the computations and the plotting aspects. D. Fain critically reviewed the manuscript and made several important remarks which have been incorporated into this text.

References

[1] R. J. P. Lyon, "Evaluation of infrared spectrophotometry for compositional analysis of lunar and planetary soils," NASA Tech. Note TN-D-1871, 1963, pp. 1–118.
[2] R. J. P. Lyon and J. Patterson, "Infrared spectral signatures—A field geological tool," *Proc. 4th Symp. Remote Sensing of Environment* (University of Michigan, Ann Arbor), Apr. 1966, p. 215–230.
[3] ——, "Airborne geological mapping using infrared emission spectra: I," *Proc. 6th Symp. Remote Sensing of Environment* (University of Michigan, Ann Arbor), Apr. 1970, p. 527–552.
[4] "Operation, calibration and maintenance procedures for the infrared pallet," NASA MSC/IESD Doc. 9-16, Nov. 12, 1968, pp. 1–65.
[5] *Remote Multispectral Sensing in Agriculture*, Res. Bull. 844, ch. III—"Measurement (field spectroscopy)," Sept., 1968, Lab. Agricultural Remote Sensing (LARS), Purdue University, Lafayette, Ind., p. 68–71.
[6] E. D. McAlister, unpublished data, 1951–1952, now reproduced as Figure 5-89 in *Handbook of Military Infrared Technology*, W. L. Wolfe, Ed., Supt. of Pub. Documents, U. S. Govt. Printing Office, 1965, pp. 1–905.
[7] R. J. P. Lyon, "Comparison of airborne infrared spectral emittance and radar scatterometer data from Pisgah Crater lava flows," to be presented at the 7th Symp. on Remote Sensing of Environment, Ann Arbor, Mich., May 17–21, 1971.

Reprinted from IEEE TRANSACTIONS
ON *GEOSCIENCE ELECTRONICS*
Volume GE-9, Number 3, July, 1971
pp. 131-138
COPYRIGHT © 1971—THE INSTITUTE OF ELECTRICAL AND ELECTRONICS ENGINEERS, INC.
PRINTED IN THE U.S.A.

Appendix B3

INFRARED SPECTRAL EMITTANCE IN GEOLOGICAL MAPPING: AIRBORNE SPECTROMETER DATA FROM PISGAH CRATER, CALIFORNIA

(Submitted to SCIENCE for consideration as a Report)

by

R.J.P. Lyon

School of Earth Sciences, Stanford, Calif., 94305

August 28, 1971

231

(STANFORD REMOTE SENSING LABORATORY TECHNICAL REPORT #71-5)

ABSTRACT.

Airborne spectral measurements in the 6.8 to 13.3 μm infrared region were taken at a rate of 6 spectra/sec. while flying at 700 m. over the olivine basalt flows at Pisgah Crater in the southern Californian desert. The rock radiance spectra are considered as emittance spectra when ratioed to similar data over a nearby lake. Spectra show chemical and mineralogical differences which can be related to terrain differences below the aircraft. A companion paper shows pictorial imagery of the same type of remotely sensed information obtained in a single flight over the same area. The images are ratios of the infrared radiances seen in two wide bands within the spectral range of the spectrometer data. The images may be simply interpreted, because they closely resemble a photograph, but the more detailed spectral curves, which are more complex to interpret, verify the geological analysis of the ratio imagery. Considered together the two papers show a convergence of evidence establishing the ratio-imagery as a valid rapid reconnaissance mapping technique.

At a recent symposium (1) two presentations of independantly performed airborne geological mapping techniques over the same terrain were given. Since it was obvious that they were mutually supportive, it was decided to publish them together. This paper emphasizes the non-imaging technique using airborne spectral measurements in the 6.8 to 13.3 μm infrared wavelength, taken while flying at 700 m. (2000') above the olivine basalt flows, alluvial soils and dry lake beds (Lavic Lake) at Pisgah Crater, near Barstow, California. The instrumentation, described in detail elsewhere (1, 2), includes a boresight camera by which one can relocate the ground track of the 7 mrad (0.4°) circular field of view of the spectrometer. Spectra have 100 data points and are taken in the 150 msec. period, representing the integrated spectral radiance from a 5 m.-wide patch smeared out for 15 m. (3).

A total of 514 of the 4300 spectra collected (3) in four flight lines, totalling 28 km. (4) were separated into 31 geologically-selected groupings based upon field knowledge of the area. These are located as black and white bands on the large-scale photographs (Fig. 1) taken at the same time along the flight line (5).

The raw radiance spectra from the rock and soil surfaces were ratioed by an average spectrum (N = 50) obtained by flying at the same altitude, speed, etc., over a nearby lake or other body of water. As water has an average emittance (ε av.) of approximately 0.98 over the bands of interest, it can be considered almost a blackbody (6), thus converting the raw radiance spectra into emittance spectra. The spectra are then inverted (7) and normalized for statistical studies, by setting their means $\bar{\varepsilon} = 0.0$ and their standard deviations S.D. (σ) = 1.0. By this transform all spectra have the same amplitude range, permitting more precise com-

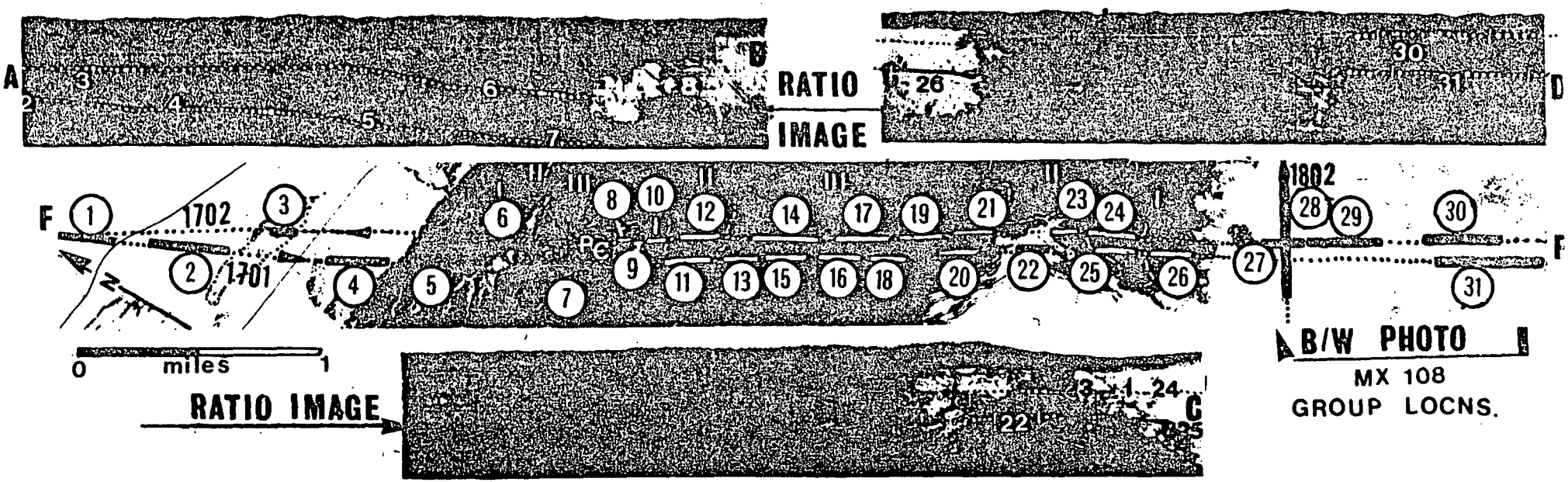

Fig. 1. Composite illustration from Pisgah Crater (PC) and associated flows (black areas), with alluvium (gray) and Lavic Lake (white). The central strip (F-F') is a section of the black and white photography, with the MX-108 flight lines (1701, 1702, 1802) as dotted lines. Spectral sub-group locations (#1-31) are indicated as bars along the flight lines. The three image strips (A-B, B'-C, C"-D) are consecutive sections of the ratio-imagery examples from (1a), with the group localities indicated for easy reference. The imagery tones are darker, when the ratio of radiance in the two channels (8.2 to 10.9/9.4 to 12.0 μm) is less than unity, medium gray if equal, and lighter if the ratio is greater than unity. See Ref. (1a) for details.

Reproduced from best available copy.

parison of their information content. Care should be used in using these normalized spectra, as they are no longer numerically the same as absolute emittance (used for calculating temperatures from radiance levels).

For use as a geological mapping method, several types of spectral comparison methods have been tried, (a) clustering, i.e. "untutored" collection of closely similar spectra, and (b) pre-processing, involving manual segregation into groups of consecutive spectra. At the moment (b), the a priori segregation, based upon geological evidence, has been found to be most effective, but more analysis of clustering techniques is underway.

These geologically-selected spectral groupings, are then prepared for initial (visual) analysis, in two separate formats, firstly with mean and $\pm$ 1σspectra, and secondly as a plot of S.D. (σ) alone, each for 10-50 spectra (8). Both plots use wavelength as the abscissa. The S.D. plot enables a rapid estimate of the data variability to be made. In most groups, this S.D. plot takes one of two shapes, low and flat, if little variability in radiance exists in that terrain patch (Fig. 2A), or higher and bulging, if considerable variability is present (Fig. 2B). An interesting S.D. plot for the dry lake sediments of Lavic Lake (locality 28) shows a third type (2C) with a pronounced upward bulge but only where the restrahlen effect (1, 2) indicated a chemical and mineralogical variation in an otherwise constant lake floor terrain, clearly of geologic significance. Full wavelength spectra have been smoothed before being shown in this figure.

The spectral group means (or "mean spectra") may be compared by visual inspection, using direct overlay of tracings, combined tracings, etc., in the manner of Fig. 3, or group populations may be further studied by

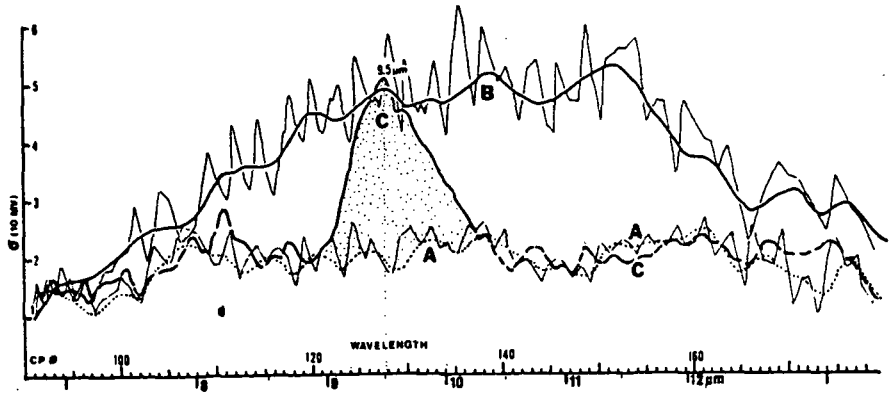

Fig.2 A one-sided, smoothed plot of standard deviation of a sub-group spectrum, with wavelength as the abscissa, in mv. as the ordinate. Curve 2A is sand over basalt, sub-group IIC, N = 11, $\bar{\sigma}$ = 21 mv.; 2B is basalt lava flow, sub-group IIB, N = 10, $\bar{\sigma}$ = 39 mv.; 2C is dry lake sediment, sub-group A, N = 53, $\bar{\sigma}$ = 23 mv. Note that 2C shows an average, flat curve with a single sharp peak at 9.5 μm, indicative of variable mineralogy within that terrain area. Ordinate is in 10 mv. units, Counter points (CP#) are from Ref.6, Table II.

5 (7)

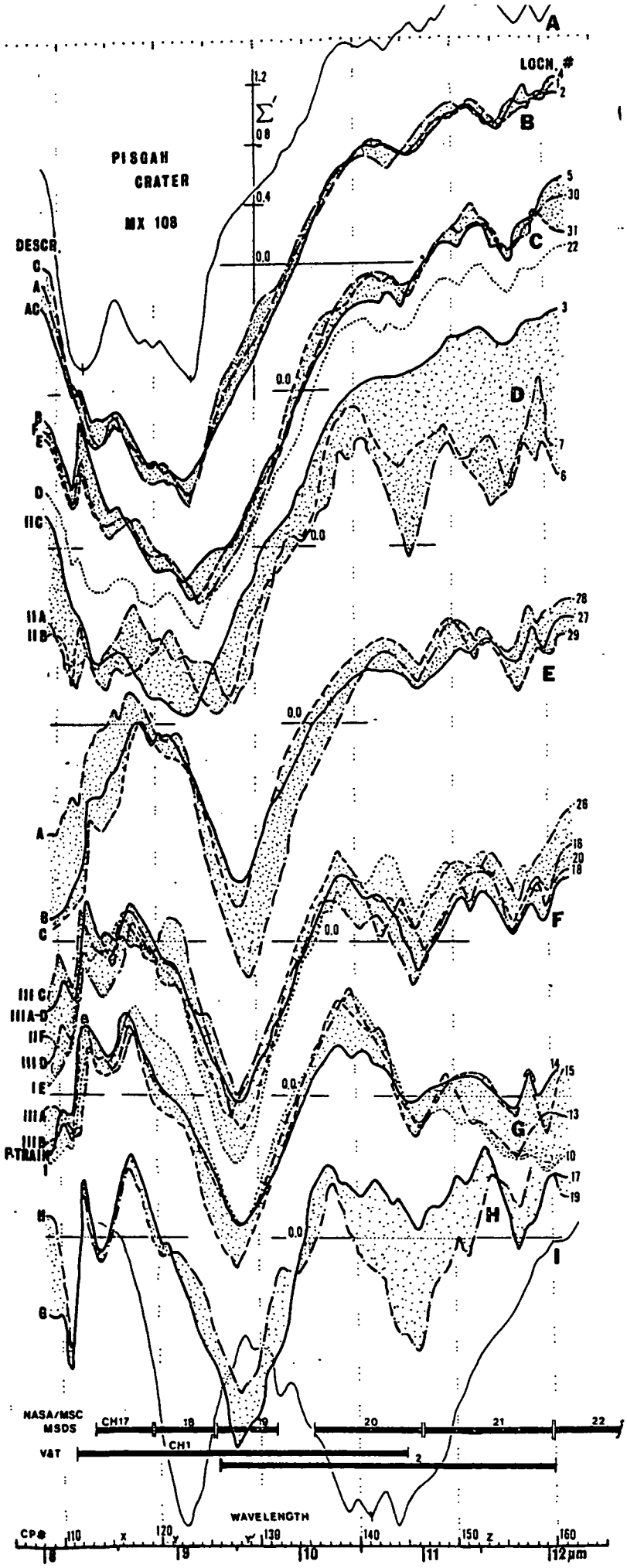

Fig. 3 Nine sets of normalized group mean spectral emittance curves, all with the same horizontal scale (wavelength from 8.0 to 12.0 μm). The vertical scale in all sets is constant, but the sets have been displaced vert--ically for ease in viewing. Normalized spectral emittance is plotted as the ordinate, with the mean = 0.0 as the central line om each spectrum. Spectral shapes thus may be directly compared. Key for the spectral groups appears in the References and Notes as (9). Channel widths for the two imaging systems under discussion, MSDS (Ref. 13 #16-21) and Vincent and Thomson's (Ref. 1a, #1-2) are also shown as the numbered horiz--ontal bars. Counter points (CP#) are from Ref. 6, Table II.

using discriminant functions (9). Within each broader class of geological rock and soil types, several sub-groups have been selected, based upon more subtle features (weathering, surface chemical variability, etc.). In Fig. 3 the mean spectra of these sub-groups are plotted as single curves, showing their similarities within a geological class. Thus each spectrum shown represents the average of N individuals (see margin notation on Fig. 3) sequentially observed along the flight line, over the distance indicated by the bars on Fig. 3 F-F' (which is a portion of the black and white aerial photocoverage of the area).

The geology of the Recent lavas and surrounding rocks and soils have been described in detail elsewhere (10, 11). What is significant to this report is that the infrared emittance spectra are correlatable with the geology, and that meaningful systematic variations appear in the flight data. The spectra of the "younger" alluvium (3B) and "older" alluvium (3C) groups show close similarities, characterised by a single, strong sloping minimum peaking at 9.1 to 9.2 μm. Detailed examination shows further that the 3B pattern is displaced to shorter wavelengths, and that the 9.5 μm shoulder is absent, indicative of a higher quartz (sand) content in the younger materials (10). Comparable similarities in a group are shown by the three olivine basalt flow types (3F, 3G, 3H) which all show a single sharp minimum at 9.45 to 9.55 μm. Differences between the spectral types were emphasized by separating those sub-groups which showed a weak minimum at 10.97 μm (3F, 3G) from those which had a pronounced feature there (3H). A further separation was made using the broad spectral pattern around 11.5 to 12.0 μm (3F is flatter there than 3G, which slopes to lower emittance values). Comparable spectra of (polished) grandiorite (3A) and gabbro (3I) specimens have been included to show the closer similarity of the basalt to

the gabbro spectrum (12).

The interesting group (3D) represent spectra from areas (localities 3, 6, 7, Fig. 3) where sand has been blown across the surface of the basalt flows, and now rests (patchily) in depths greater than the optical depth (for radiation of 10 μm wavelengths) in these silicates. Thus where cover is complete the spectrum of sand (here equivalent to the younger alluvium, 3B), should appear; if not complete, then the basalt spectrum should be evident. Within group 3D, spectral mean II-C (locality 3) shows the younger alluvium pattern, while II-A (locality 7) is most like the basalt spectra (3F, type 2), establishing the ability of the airborne system to discern rock material variations. This variability is also very clearly shown on Fig. 3 (A-B') section of the ratio-imagery (1a).

The spectra of dry lake sediments, from the surface of Lavic Lake, represent an enigma. Although creamy-white in color these fine-grained clays (10) consistently yield almost the same spectra (3E) as the type 2 basalt flows (3F), localities 27, 28, 29, Fig. 3. We found this to be true initially in 1965 during ground measurements of infrared emittance along the same line. The new airborne data now support the earlier (still unexplained) findings. Similar support is gained from the ratio-imagery of the same area on the flight line in Vincent and Thomson's recent work (1a). Three pieces of evidence point to the similarity of the clay spectra to those of the nearby olivint basalt.

In summary, (1) airborne infrared emittance spectra from geologically-selected areas across the Pisgah Crater lavas flows show similarities within (and contrasts between) the areas. The spectral differences can be used to separate the flows. In addition, (2) within the lava flows themselves spectral types may be defined which (at the moment) do not relate clearly

to the mapped flow stages (Flows I, II, and III), i.e. the spectra are subtly depicting some other parameter than that used by the geologist who differentiated the three flows in the field. Extra field work is clearly needed to relate the spectral types to the precise rock types along the exact flight line trace. Again, (3) the dry lake sediments of argillic silts show average spectra which superficially resemble those of the basalt flows, but internal variability in chemical and mineralogical composition is shown by the shapes of the S.D. plots (Fig. 2C). Also, (4) thin layers of wind-blown sand overlying the basalt show the spectra of the sand, but where the sand patchily covers the flow in one resolution cell both the spectra of the sand and the basalt appear in a composite pattern. Finally (5), each of these spectral similarities and differences may be observed also in the imagery prepared by ratioing concurrent radiance levels in two adjacent, 3 μm-wide wavelength channels (1a). This is a most significant discovery, as imagery is so much more practical to use than spectral curves. It is amazing, however that this occured with overlapping bandpass filters of such width (8.1 to 10.9, and 9.4 to 12.0 μm). These bands, indicated on Fig. 3, must represent the integration of all the spectral information within their bounds, expressing it as an average value, rather than showing all the finer points of spectral differences evident on the curves. Clearly a more precise separation of rock types can be effected using non-overlapping and/or narrower bands, even with the lowered signal-to-noise ratio incurred by the lessened energy throughput. Such a system as that being built for the NASA aircraft program (13) truly can become a geological mapping tool.

R.J.P. Lyon

School of Earth Sciences

Stanford University

Stanford, California, 94305

REFERENCES AND NOTES.

1. 7th International Symposium of Remote Sensing of Environment, Ann Arbor, Michigan, May 17-21, 1971. Papers were given in Concurrent Sessions, (a) #1, paper 2 (Vincent, R.K. and F. Thomson) and (b) #8 paper 3 (R.J.P. Lyon).

2. R.J.P. Lyon and J. Patterson, Proc. 6th International Symposium of Remote Sensing of Environment, University of Michigan, Ann Arbor, Michigan, 527 (1970); also Proc. 4th Sym., 213 (1966); R.J.P. Lyon Economic Geology, 60, 715 (1965).

3. Spectra are taken 6/sec. During that interval the aircraft has moved 15 m. The field of view of the spectrometer is small (0.4° or 7 mrad = 7 m./km. altitude). Thus at 700 m. above the terrain the spectra are taken from patches 15 m. long by 5 m. wide.

4. Stanford/NASA(MSC) Mission # 108, Flight 2, October 8, 1968 over NASA Test site #2, Pisgah Crater, California, about 61 km. (35 mi.) SE of Barstow, San Bernardino Co. The spectrometer uses a circular variable filter (CVF) as the dispersive element, with spectral resolution $\frac{\lambda}{\Delta\lambda} = 100$. These filters are made with a left-hand, right-hand mode, such that from 0° to 179° the 6.8 to 13.3 μm range is traversed, and from 180° to 359° the bands from 13.3 to 6.8 μm are traversed. A voltage "ramp" is output proportional to the degrees of rotation, up-ramp = 6.8 to 13.3 μm, down-ramp is 13.3 to 6.8 μm. To ease the data reversal problem in data reduction steps, only the up-ramps are used, i.e. every second spectrum is omitted in the tape processing.

5. Self-organizing ("clustering") programs were extensively used with the older (pre-MX-108) data, and were not found very useful, probably due to the high noise content of the data. The step-wise discriminant

program BMD07M (UCLA Biomedical Series) was the most suitable, both for early grouping into "training" groups and in the subsequent processing of other "unknown" spectral data.

6. In the processing steps the true spectral emittance of water is used and the radiance of a blackbody at T_L = temperature of lake (from the onboard infrared radiometer, $\Delta\lambda$ = 10.375 to 12.1 μm, sampled 60 times/sec.), modified by this factor, wavelength by wavelength, until a "waterbody" spectrum is obtained. See R.J.P. Lyon and A. Marshall, Inst. Elec. Electr. Eng., Trans., GE-9 (3), 131-138 (1971) for details. The wavelength bands from 6.8 to 7.9 μm and from 12.0 to 13.3 μm are clipped off the ratioed spectra as it has been found that these bands contain spectral information mainly from the atmospheric constituents (H_2O vap. and CO_2 variations) and not geological (silicate) data (1).
7. Both the spectrometer and the radiometer utilize chopping of the incoming radiance against that from internal blackbody references. In each case the references are set at "higher than ambient" levels, i.e. at 60°C for the spectrometer, and 50° or 60°C for the radiometer. Accordingly output voltages increase as the target temperatures decrease, e.g. 150 mv. for each 1°C drop seen by the radiometer. Because a non-blackbody radiator has lower brightness temperatures ($\varepsilon_\lambda \neq 1.0$) at wavelengths of chemical interest ("reststrahlen bands") the raw spectral data have <u>maxima</u> of output voltage in these bands. Inverting the emittance data corrects this problem, at least to a first approximation. (For further details see Ref. 6 above).
8. It is presumed, but not yet proven that the distribution of $\varepsilon_{\lambda i}$ values about their mean $\bar{\varepsilon}$ follows a normal distribution curve, and hence the calculation of σ is allowed. Other data from Purdue University (LARS) would support this assumption, see R. Hoffer in <u>Lab for Agric. Res. (LARS) Bull. 844</u>, Chapter III, 68-71 (1968).

9. Key for the spectral groups in Fig. 3 is as follows; Group #, name [descriptor(N =), locality #], for A(27)#4, read group A, N = 27, locality #4.

3B, younger alluvium [A(27)#4: AC(30)#2: C(25)#1].

3C, older alluvium [B(30)#5: D(21)#22: E(37)#31: F(42)#30].

3D, sand over basalt [IIA(9)#7: IIB(21)#6: IIC(11)#3];

3E, dry lake sediments [A(53)#28: B(23)#27: C(25)#29].

3F, olivine basalt flow, spectral type 2 [IE(21)#26: IIF(21)#20: IIIA-D(53)#13, 15, 16, 18: IIIC(18)#16: IIID(12)#18].

3H, olivine basalt flow spectral type 3 [IIIG(10)#17: IIIH(8)#19].

3G, olivine basalt flow spectral type 1 [P-flow I(15)#10: III P-Train(31)#14: IIIA(19)#13: IIIB(17)#15].

(3A, rock standard, granodiorite, and 3I, rock standard, gabbro are included for comparison. N = 43 and 56, respectively.)

Spectral populations may be examined for homogeneity and also for "Between-group differences" by the use of several discriminant programs. One we have used operated in a step-wise manner seeking the most powerful discriminant in X=dimensional space, where X = number of spectral emittance values (vectors) as sequentially selected by the BMD07M program, (2). A similar function (b), called NEIGHBOR can be used to search in X-dimensional space for the M-closest neighbors, and then to take a majority-vote on the classification. Both have worked well in "automated" rock type determination.

10. S.J. Gawarecki (1964), unpubl. report, quoted in detail as Appendix 1, in L.F. Dellwig, Modern Geol., 1, 63 (1969), with further comments by Dellwig, on page 72-3. Specific details are (a) ". . . playa surface (dry lake sediments) is a hard dense compact argillic crust con-

sisting of approximately 79% clay, 20% granular components, 0.2% accessory minerals and a trace of saline minerals (Neal 1965). . .". Another is (b) . . . "two ages of alluvial fans in the area. The older fan is . . . composed of copious amounts of basaltic fragments derived from older flows, felsite, quartzite and quartz . . . main out-crop area is the dark-toned material just west of the crater access road. Wind blown sand covers much of its surface area . . . The younger alluvial fan material . . . is yellowish gray color because of its higher content of sand-sized fraction."

11. J.D. Friedman, U.S.G.S., Tech. Letter (NASA-20), unpubl. (1966). Significant points on the composition of the basalt flows at Pisgah Crater, California, are (a) Flow II, (sample P-2, aa type) olivine 5.7%, plag. 14.7%, clinopyrx 3.7%, alk. fldsp. 0.7%, glass 41.9%, voids 34.0%, and (b) Flow III (Sample P-1, pahoehoe type), olivine 4.3%, plag, 16.6%, clinopyrx 0.8%, alk. fldsp. 12.2%, glass 48.4%, voids 30.0%. In summary, Flow II, total feldspar 15.4%, total ferromag. 9.4%; Flow III, total feldspar 38.8%, total ferromag. 5.1%. (Data from eight 2000-point counts on thin sections of each rock, by W.S. Wise). Flow III is thus more feldspathic than Flow II, at least at the points sampled near the Crater base. Therein lies one of the major problems in relating regionally-variable composition data, such as that collected by these airborne techniques, to those of more classically geological studies, usually from selected points within the whole area.

12. See footnote #3, Ref. 6. Standard rock A: gabbro, contains plagioclase (An_{60}), augite, and litle biotite; Standard rock B, grandiorite, contains biotite, quartz, epidote, and plagioclase with orthoclase.

Spectra taken while the aircraft was still on the ground prior to take-off. Instrumental and data processing steps are those exactly similar except a true blackbody ratio is made.

13. The 24-channel multichannel scanner (MSDS), E.M. Zaitzeff, C.L. Korb, and C.L. Wilson, Inst. Elec. Electron. Eng. Trans., GE-9 (3), (1971), 114-120, has six (6) channels selected within the thermal (6.0 to 13.0 μm) band, using Hg-doped germanium detectors, filtered for the following channels, #16, (6.0 to 7.0), #17, (8.3 to 8.8), #18 (8.8 to 9.3), #19, (9.3 to 9.8), #20, (10.1 to 11.0), #21, (11.0 to 12.0), #22, (12.0 to 13.0 μm). The data shown in Ref. 1a, would represent the combination of the channela #17-20, ratioed with the combined channels #19-21. My spectral data, shown on Fig. 3, indicate that the Pisgah Crater flight line would be more clearly defined using channels #17, 18, and 19 (either singly or combined) ratioed to #20. Channel 21 would show some effect of chemical compositions still (particularly in femic rocks), but would be the best channel for determining the "true" surface temperature, without applying emittance corrections, if that is what is desired.

14. This research was supported in its entirety by NASA Contract NAS9-7313, with NASA/MSC, Houston. This financial support is gratefully acknowledged. The author is also deeply indebted to the crew of the NASA aircraft NP3(927), for the quality of their data collection in Mission 108. This is Technical Report #71-5 , Remote Sensing Laboratory, Stanford University.